

COORDINATED REGULATION OF THE FLAGELLAR, SALMONELLA PATHOGENICITY ISLAND 1, AND
THE TYPE I FIMBRIAE GENE NETWORKS IN SALMONELLA TYPHIMURIUM

BY

SUPREET SAINI

DISSERTATION

Submitted in partial fulfillment of the requirements
for the degree of Doctor of Philosophy in Chemical Engineering
in the Graduate College of the
University of Illinois at Urbana-Champaign, 2010

Urbana, Illinois

Doctoral Committee:

Assistant Professor Christopher V. Rao, Chair
Professor Richard D. Braatz
Assistant Professor Charles M. Schroeder
Professor James M. Slauch

Abstract

Micro-organisms are constantly monitoring their surrounding environment and making important lifestyle decisions. This decision process is governed by large genetic networks that process the information leading to a phenotypic response from the cell. Using the food-borne pathogen, *Salmonella*, as a model organism, we try to investigate how cells encode strategies in networks to optimally control cellular behavior. *Salmonella*, on ingestion with contaminated food, swims in small intestine using propeller-like structures, flagella, on its surface. On reaching the site of infection, it assembles a hypodermic needle on its surface using which it injects proteins into host cells. These proteins cause a change in the host-cell shape leading to internalization of the bacterium. If the bacterium fails to get internalized, it assembles finger-like projections, fimbriae, on its surface to adhere to and persist in the intestine. How *Salmonella* dynamically regulates gene expression and assembly of these organelles is the focus of this study. Our results demonstrate that the networks controlling genes necessary for flagella, needle, and fimbriae are designed so as to encode logic gates and limit expression to conditions optimum for infection. In addition, there is cross-talk between these three systems which serves to dynamically control the timing of activation and de-activation of these networks. Collectively, we demonstrate that cells dynamically process information in genetic networks which ensures that the encoded products are produced at the correct locales, at the appropriate levels, and for the appropriate amount of time.

Acknowledgements

The past five years in graduate school have been thoroughly enriching and an enjoyable experience for me, and I owe a big thanks to a lot of people for all their help during that time. I want to thank my advisor, Prof. Christopher Rao, for all his help in my time in his lab. His technical inputs and research ideas were a massive help in all my research efforts. I am especially grateful to him for having a very fluid environment in the lab where I enjoyed the freedom to pursue all my other crazy ideas and passions. All these experiences in Chris's lab enriched my learning experience at UIUC and made me a more educated and aware human being.

Constant discussions with Prof. James Slauch were an invaluable input in all my research work. I want to especially thank him for all his technical inputs and also help from his lab and him with materials and methods. Working with Prof. Phillip Aldridge was another enjoyable collaboration. I want to extend a sincere thanks to him for all his help and inputs on the flagellar work. I also want to thank Prof. Richard Braatz and Prof. Charles Schroeder for agreeing to be on my doctoral committee. Inputs from Prof. Braatz about graduate school and academic career in general from time to time were really useful for me in planning life after graduate school. I want to thank Prof. George Ordal and his lab, especially, Vince Cannistraro, Hanna Rao, and George Glekas, for their infinite patience while helping me with experiments in their lab. I also want to thank Patrick Mears for his help with the TEM experiments.

My research work and time in lab was made much more enjoyable and fruitful by presence of super-enthusiastic undergraduate students working with me. Doing research with them was as much a learning experience for me as for them. For their time, commitment, and friendship – I want to thank Jeffrey Pearl, Emily Floess, Raed Zuhour, and Siri Chakka. I wish Jeff the very best in Medical School at Northwestern, Emily in Liberia with Peace Corps, and Siri and Raed in their remaining time at UIUC. I hope all their dreams come true.

Teaching undergraduates was a big part of my experience in graduate school. Being a Teaching Assistant gave me an opportunity to interact with and get to know lots of undergraduate students. Discussions with them about courses, problems, sports, India, and education were thoroughly enjoyable. For this opportunity, I want to thank the faculty members - Prof. Rao, Prof. Braatz, Prof. Pack, Prof. Hammack, Prof. Price, and Prof. Kenis – and all the students I interacted with.

I also want to thank all my labmates. Lon Chubiz, Gautam Nistala, Khushnuma Koita, Santosh Koirala, Kang Wu, Shuyan Zhang, and Tasha Desai – were all great fun to work around with. Apart from people at work, I would like to thank Kunal Srivastava, Jagannathan Rajagopalan, Anil Kumar, and Ashish Kapoor for sharing their time, advice, and food with me. I wish them the very best in all their future endeavors.

I owe a special thanks to Mukta Tripathy. She has been a huge influence in how I view, analyze, and understand the world. Her unique and delightful views and opinions have had a motivating and humbling effect on me.

When I needed them, I never had to look beyond friends in India for insane stories and adventures. For this and for all their support, I want to thank Abhinav Gupta, Ankur Kundan Bansal, Lokesh Malik, and Manish Sahai. Last, I want to thank my parents and everyone else in my large family. Their love and support all these years made this journey possible. I owe them a big thank you for this opportunity.

Table of contents

CHAPTER 1. BACKGROUND AND SIGNIFICANCE.....	1
CHAPTER 2. MATERIALS AND METHODS	9
CHAPTER 3. FLAGELLAR GENE NETWORK	27
CHAPTER 4. SALMONELLA PATHOGENICITY ISLAND 1 (SPI1).....	53
CHAPTER 5. SALMONELLA PATHOGENICITY ISLAND 4 (SPI4).....	101
CHAPTER 6. TYPE I FIMBRIAE GENE NETWORK.....	113
CHAPTER 7. COORDINATED REGULATION OF THE FLAGELLAR, SPI1, AND TYPE I FIMBRIAE GENE NETWORKS	134
CHAPTER 8. OTHER RESULTS.....	163
CHAPTER 9. CONCLUSIONS AND FUTURE DIRECTIONS.....	180
CHAPTER 9. CONCLUSIONS AND FUTURE DIRECTIONS.....	180
APPENDIX A: STRAINS USED IN THIS STUDY	184
APPENDIX B: PLASMIDS USED IN THIS STUDY.....	192
APPENDIX C: MATLAB CODE FOR FLAGELLA GENE NETWORK MODEL.....	198
APPENDIX D: MATLAB CODE FOR SPI1 GENE NETWORK MODEL.....	201
REFERENCES	219
CURRICULUM VITAE	232

Chapter 1. Background And Significance

Salmonella enterica is the causative agent for a wide range of diseases in humans, ranging from self-limiting gastroenteritis to life-threatening systemic infections and typhoid fever (Ellermeier, 2006, Miller & Sulavik, 1996). Worldwide, *Salmonella* is estimated to cause over sixteen million cases of typhoid fever, resulting in approximately six hundred thousand deaths, and over one billion cases of acute gastroenteritis, resulting in approximately three million deaths (Pang *et al.*, 1995). *Salmonella* infections constitute a major public health burden and represents a significant cost to society. Very few countries report data on the number of infections annually or the economic cost of *Salmonella*-related infections. In the United States, an estimated 1.4 million non-typhoidal *Salmonella* infections, resulting in 168,000 visits to physicians, 15,000 hospitalizations and 580 deaths take place annually (WHO, 2005).

The clinical course of human infection is usually characterized by acute onset of fever, abdominal pain, diarrhoea, nausea and sometimes vomiting. In some cases, particularly in the very young and in the elderly, the associated dehydration can become severe and life-threatening. In such cases, as well as in cases where *Salmonella* causes bloodstream infection, effective antimicrobials are essential drugs for treatment. Serious complications occur in a small proportion of cases. Although outbreaks usually attract media attention, studies indicate that more than 80% of all infections cases occur individually rather than as outbreaks (WHO, 2005).

While standard fluoroquinolone antibiotic can be used to treat most *Salmonella* infections, the emergence of multi-drug resistant strains in the food chain indicates that these therapeutic options may not be viable in the near future (Fabrega *et al.*, 2008). Significant effort, therefore, has been devoted towards identifying new antibiotic targets and chemical compounds to deal with this emerging threat. However, solving this problem has proven to be extremely difficult. For example, in a recent genome-wide investigation of *Salmonella* metabolism, over 800 enzymes were evaluated as potential antibiotic targets (Becker *et al.*, 2006). Remarkably, no new targets were found in this study despite the large number of enzymes investigated. The reason is that many critical metabolic processes in *Salmonella* involve redundant enzymes and pathways, enabling cells to grow even when key enzymes and pathways are disrupted. Because of these redundancies, the authors of this study concluded that no new targets for antibiotics would be forthcoming in *Salmonella*.

Clearly, new approaches other than simply targeting metabolic genes must be considered. One approach is to target the *Salmonella* virulence machinery. About two hundred genes are virulence factors in *Salmonella* (Bowe *et al.*, 1998). Invasion and systemic infection require the coordinated expression of these genes in response to multiple environmental cues. The process is mediated by a number of interacting gene circuits. By understanding the dynamics and regulation of these circuits, we can identify new drug targets that will potentially attenuate *Salmonella's* ability to infect humans

and livestock. To better understand this dynamic regulation between multiple systems is the motivation for this study.

Previous studies have identified multiple factors, including motility, adhesion, invasion, and intestinal persistence, that are involved in *Salmonella* pathogenesis. Key among them is a type 3 secretion system (T3SS) encoded within a 40 kilobase region of the chromosome called *Salmonella* Pathogenicity Island 1 (SPI1) (Mills *et al.*, 1995, Lee *et al.*, 1992, Kimbrough & Miller, 2000, Kubori *et al.*, 1998, Kimbrough & Miller, 2002, Sukhan *et al.*, 2001). The SPI1 T3SS functions as a molecular hypodermic needle, enabling *Salmonella* to inject proteins into host cells. These injected proteins then commandeer the actin cytoskeleton and facilitate the invasion of host cells.

In addition to the SPI1 T3SS, two other systems, flagella and type I fimbriae, have been implicated in *Salmonella* pathogenesis. Briefly, flagella are long helical filaments attached to rotary motors embedded within the membrane that enable the bacterium to swim in liquids and swarm over surfaces. Flagella are thought to facilitate invasion by enabling *Salmonella* to swim to sites of invasion. In addition to motility, flagellin is a potent activator of the immune system as it binds TLR5 and activates the expression of proinflammatory cytokines, both outside and within host cells. Type I fimbriae, on the other hand, are hair-like appendages that carry adhesions specific for mannosylated glycoproteins on eukaryotic cell surfaces. They are thought to be involved in pathogenesis by facilitating the binding of intestinal epithelial cells. As with the flagella,

type I fimbriae do not appear to play a direct role in intestinal invasion but are rather thought to contribute to intestinal colonization and persistent infections in some mammals.

Infection requires that expression of the SPI1 TTSS is coordinated with other physiological processes (Baxter & Jones, 2005, Lucas *et al.*, 2000, Ellermeier & Schlauch, 2003, Teplitski *et al.*, 2003). The current physiological picture of the infection process is as follows. After ingestion with contaminated food, *Salmonella* survives the harsh acidic environment in the stomach. From there, the bacterium reaches its preferred site of infection, the lumen of the small intestine. In the lumen, *Salmonella* specifically target microfold cells (or M-cells) lining the intestine (Wallis & Galyov, 2000, Santos *et al.*, 2003, Zhou & Galan, 2001). The purpose of the M-cells in the intestine is to sample the antigenic content in the lumen and pass it to the underlying Peyer's Patch. *Salmonella* invades M-cells using the SPI1-encoded T3SS and SPI4-encoded adhesion system (Main-Hester *et al.*, 2008, Gerlach *et al.*, 2007a, Lawley *et al.*, 2006). As described above, the injection of effector proteins into the host cell results in engulfment of the bacterium. If the bacterium is successfully internalized, *Salmonella* encodes and assembles another T3SS encoded on *Salmonella* Pathogenicity island 2 (SPI2)(Hensel, 2000). However, if internalization fails, the bacterium then assembles another appendage, Type I fimbriae, on its surface, to presumably attach itself to the host cells and persist in the intestine for a more favorable time for invasion (**Figure 1**).

Multiple studies have shown that extensive transcriptional crosstalk exists between these three systems. While the molecular details have been studied extensively, the role and significance of these interactions are still relatively unknown. All three systems play unique and potentially mutually exclusive roles during the infection cycle (Baxter & Jones, 2005, Ellermeier & Slauch, 2003, De Keersmaecker *et al.*, 2005, Main-Hester *et al.*, 2008). Presumably, the crosstalk between the circuits is used to time the various steps involved in infection. How this crosstalk mediates coordination is still not known nor is it clear that the infection process necessarily follows this simplistic model.

The goal of this research effort is to understand how *Salmonella* coordinates the regulation of the motility (flagella), SPI1 (T3SS), and type I fimbriae (*fim*) gene circuits. Each of these three gene circuits control expression and assembly of a surface appendage that serves a mutually exclusive purpose and for a successful infection process, it is important that the bacterium switches these systems “on” and “off” at precise times. As a first step, we experimentally investigated how each one of these circuits is dynamically regulated in isolation. As this regulation is dynamic and involves multiple interacting feedback loops, we utilized mathematical modeling to facilitate data analysis and to test specific aspects of our hypothesis. Next, we investigated the coordinated regulation of these three circuits. In particular, we hypothesize and then demonstrate that regulatory crosstalk between these circuits controls the timing of their activation and ensures that they do not interfere with one another. This study enables

us to extract the general regulatory mechanisms and principles utilized by the *Salmonella* during invasion. By understanding this complex regulation, we will likely be able to identify new drug targets, not just by targeting virulence genes but also by targeting others involved in interacting processes such as motility and adhesion. In addition to their medical significance, these results will provide new insight into the regulation of interacting gene circuits. Few cellular processes act in isolation. Therefore, to understand how a given process is regulated, we must also investigate how it interacts with other processes.

Figures – Background And Significance

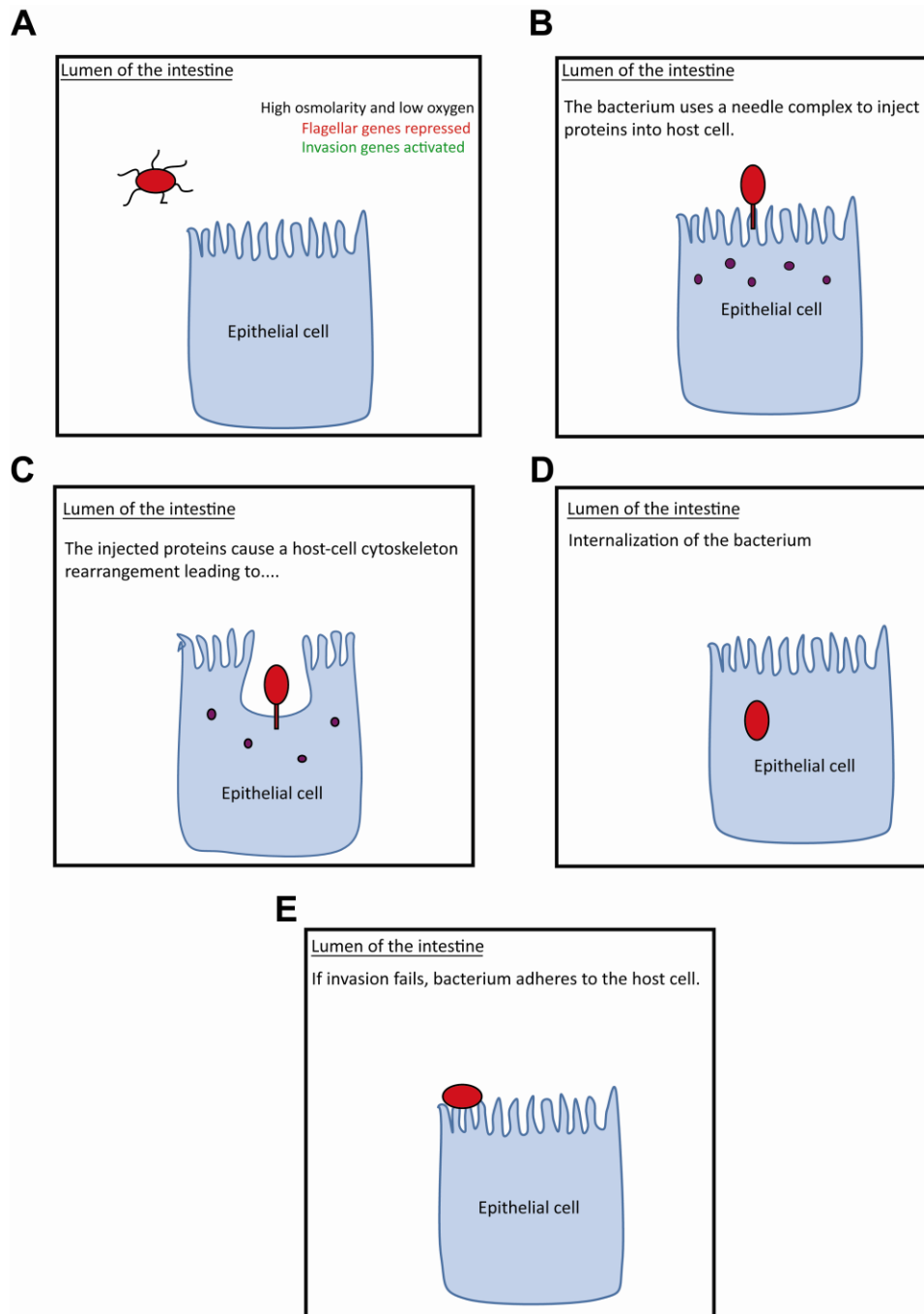


Figure 1. Cartoon depicting steps in the Salmonella infection process. (A) Bacteria utilizes the flagella system to swim in the liquid medium to the site of infection. (B) At the site of infection, it sheds flagella and encodes a non-fimbrial adhesion system and a Type 3 Secretion System (T3SS) (C) The injected proteins via the T3SS lead to actin cytoskeletal rearrangement (D) Cytoskeletal rearrangement leads to internalization of

the bacterium. (E) If the bacterium is not internalized, it encodes Type I fimbriae on its surface to adhere to the epithelial cells and persist in the intestine.

Chapter 2. Materials And Methods

General Techniques And Growth Conditions

All culture experiments were performed in Luria-Bertani (LB) broth at 37°C unless noted otherwise. Antibiotics were used at the following concentrations: ampicillin at 100 ug/ml, chloramphenicol at 20 ug/ml, kanamycin at 40 ug/ml, and tetracycline at 15 ug/ml. All experiments involving the growth of strains containing plasmid pKD46 were performed at 30°C as previously described (Datsenko & Wanner, 2000). Loss of pKD46 from strains was achieved by growth at 42°C on non-selective media after electroporation of the PCR products. Removal of the antibiotic from the FRT-Cm/Kan-FRT insert was achieved by passing pCP20 through the isolated mutants (Cherepanov & Wackernagel, 1995). The plasmid pCP20 was removed after growth on non-selective media at 42°C. Enzymes were purchased from Fermentas or New England Biolabs and used according to the manufacturer's recommendations. Primers were purchased from IDT Inc.

Plasmid Miniprep

5 ml of a LB culture was grown overnight at 37°C with the appropriate antibiotic. The cells in the culture were spun down by centrifuging for 5 minutes at 4000 rpm. The supernatant was discarded and the plasmid was recovered from the pellet of cells using

the Zymo Plasmid Miniprep kit (D4036). Briefly, the cell pellet was resuspended in 0.25 ml of the Resuspension buffer. The resuspended culture was then transferred to a micro-centrifuge tube. The cells were then lysed by adding 0.25 ml of the lysis buffer. After addition of the lysis buffer, the tube was shaken for about 30 seconds to ensure complete lysis of the cells. This was followed by adding 0.35 ml of the neutralization buffer to the tube and shaking the tube for about 30-45 seconds. The sample tube was then spun down at 14000 rpm for 5 minutes.

The supernatant from the spin was transferred to a plasmid miniprep column and spun for 1 minute at 14000 rpm. The flow-through was discarded and 0.5 ml of the wash buffer was added to the column. The column was again spun for 1 minute at 14000 rpm followed by discarding the flow-through and another spin of 1 minute. The column top was then transferred to a micro-centrifuge tube and the plasmid recovered by addition of 50 ul of water and spinning at 14000 rpm for 1 minute. To improve the plasmid recovery, the column was allowed to stand for 1 minute after addition of water and before the centrifuge step for plasmid recovery.

Polymerase Chain Reaction (PCR)

DNA fragments were amplified using PCR. For cloning purposes, the Phusion High-Fidelity DNA Polymerase enzyme was used (Finnzymes). For checking DNA fragment size, the Green Taq Green Master Mix kit from Promega was used. Primers

were ordered from IDT Inc. and their stock solution prepared by adding water to a final concentration of 30 nM. For each reaction, 1 ul of each primer and 1 ul of the DNA template were added in a total reaction volume of 50 ul.

Checking PCR Products (High Melt Electrophoresis Gels)

To check DNA fragment sizes, the PCR products were run on a 0.8% high melt gel (0.8% agarose (Fermentas) in TAE buffer). One liter of 50x TAE buffer was prepared using the following recipe: 242 grams of Tris Base, 57.1 ml of glacial acetic acid, and 100 ml of 0.5M EDTA were mixed and water added to make the total volume 1 liter. Gels were cast after adding 1 μ l Ethidium Bromide (5.25 mg/ml in water) per 10 ml of the gel solution for DNA detection. After the gel was poured, it was allowed to solidify and run in a TAE buffer solution. Biorad DNA electrophoresis gel boxes were used to run the DNA gels. Gels were run at a constant voltage of 130 volts. To check the band size of the PCR product, the samples were run against an appropriate DNA-standard from New England Biolabs (N3231 for 100 bp ladder or N3232 for 1 kb ladder). To load the samples in the gel wells, 6X Gel Loading Dye (NEB, B7021) was added to the sample before loading them on the gel. The gel picture was taken under UV-transilluminator.

Restriction Digest

The plasmid and the PCR DNA fragments were digested using restriction enzymes from New England Biolabs (NEB). A sample was digested with 30 ul of the

plasmid/PCR, 5 ul of the digestion buffer, 0.5 ul BSA, and 1 ul each of the restriction enzymes. De-ionized water was then added to the samples to make the total volume of the sample 50 ul. The digest was carried out at 37°C for 4-6 hours, unless otherwise specified by the manufacturer.

DNA Recovery After Double Digest (Low melt Electrophoresis Gels)

To recover the digested DNA fragments, 8 ul of the 6x DNA dye was added to the 50 ul digests. The dye-DNA mix was then loaded on 1% low melt agarose gels and run at 130V for 20-30 minutes. To dissolve the gel fragments carrying the DNA, 0.6ml of Agarose Dissolving Buffer (ADB) (Zymo) was added to per 0.2 grams of the gel fragment and the mixture heated at 55-60°C. Upon dissolving, the solution was transferred to a gel-recovery column (Zymo) and the column spun for 15 seconds at 14000 rpm. The flow-through was discarded and the column was spun for 15 seconds after addition of 0.2 ml of DNA wash buffer. The flow-through was discarded again and the column spun for another 30 seconds after addition of 0.2ml of DNA wash buffer. The column top was then transferred to a micro-centrifuge tube and DNA recovered by elution using 8-20 ul of de-ionized water and spinning the column for 1 minute at 14000 rpm. The gel-purified products were mixed in a ratio so as to ensure that the plasmid and PCR product in the ligation mix were in the ratio 1:2.

DNA Ligation

After recovery of the DNA fragments, ligations were carried in the following manner. The cut insert and the plasmid were added roughly in the ratio 2:1 in a microcentrifuge tube. The appropriate amount of the ligation buffer (T4 DNA Ligase Buffer from NEB or Quick T4 DNA Ligase from Finnzymes) was added to the tube followed by addition of water to make the total reaction volume 20 ul. After that, 1 ul of DNA ligase was added to the tube and allowed to sit at room temperature (25°C) for a 2-3 hours. Controls such as ligating the cut plasmid were also prepared in the same manner. When using the Quick T4 Ligase, ligations were kept on bench for 30-40 minutes prior to transformations. For T4 DNA Ligase from NEB, the ligation mixture was kept at 4°C for at least 2-3 hours before transforming.

Chemical Transformations – Cell Preparation And Plasmid Transformations

The cloned plasmids were transferred to *E. coli* Dh5α strain using chemical transformation. Briefly, the protocol followed was as follows. The cells were thawed and 50 ul of the cells was transferred to glass test-tubes (which were already sitting on ice). 5 ul of the ligation mix was added to the cells. The ligation mix-cell mixture was allowed to sit on ice for approximately 30 minutes and then transferred to a 42°C for 2 minutes. The test-tube was then transferred again to ice for 8 minutes after which 1 ml of LB was added to the test-tube and the cells allowed to recover for 1 hour at 37°C. 50-100 ul of

the cells were then plated on an agar-plate (12.5 grams LB/lt. and 15 grams agar/lt.) carrying the appropriate antibiotic. The plate was then kept at 37°C overnight and colonies checked the next morning. The plates were kept at 37°C two hours before the plating step. Using warm plates for transformation increased ease of spreading and also reduces the time it takes for colonies to appear on the plates.

Electroporation And Electro-Competent Cells

Electroporation was used to transform plasmids into *Salmonella* strains. The cells were prepared as follows. Overnight culture was diluted 1:100 and grown at 37°C till mid-log phase. After that, cells were quickly transferred to ice and then, spun at 4000 rpm for 10 minutes. The culture was discarded and the pellet of cells resuspended in 10 ml of 10% glycerol. The resuspended culture was again spun at 4000 rpm for 10 minutes and the pellet resuspended in 10 ml 10% glycerol. This was repeated 3 times. After the final spin, the liquid was discarded and the cells resuspended in 0.5 ml of 10% glycerol. The cells were stored at -80°C.

To transform, cells were thawed on ice. 50 ul of the cells were taken out and mixed with 1 ul of the plasmid. The mixture was then transferred to an electroporation cuvette and cells and plasmid electroporated. Immediately after electroporation, 1 ml of LB was added to the cells in the cuvette. The mix was then transferred to a test tube and cells allowed to recover at 37°C for 1 hour. 100 ul of the liquid was then plated on plates

with the appropriate antibiotic. Electroporation, in general, is a lot more efficient than chemical transformations described above. Therefore, plate less to get individual colonies and avoid a lawn.

Gene Knockouts

Chromosomal gene knockouts were done as follows. Cells were first transformed with the temperature sensitive plasmid, pKD46, with ampicillin resistance gene. pKD46 has a temperature sensitive replication of origin, therefore, all experiments dealing with it were done at 30°C. After transforming pKD46 in the cell, a colony was selected and grown in liquid media with ampicillin at 30°C. The overnight culture was then diluted 1:100 in LB media with 0.2% arabinose. Cells were grown to mid-log phase to prepare electro-competent cells. The electro-competent cells were transferred with 5 ul of the PCR product from the plasmids pKD3 or pKD4 or from the strain TH8094. After transformation with the PCR product, the cells were allowed to recover at 37°C for 2 hours and then plated on plates with the appropriate antibiotic.

Note: Plate 100 ul on each plate and not more than that to avoid background colonies.

Note: after the PCR product from the plasmids pKD3, pKD4, pKD13 – digest the product with 1 ul DpnI to digest the template plasmid from the PCR product.

Note: The PCR product from pKD3/pKD4/TH8094 was only eluted with 20µl water instead of standard 50µl for PCR clean ups. This concentrated the PCR fragment needed for the knock out and was found to increase the efficiency of the knockout.

The colonies obtained on the plates the next day were restreaked on plates with the antibiotic to get “clean” colonies. These restreaked colonies were then checked using primers that bound outside the deleted region to ensure that the correct mutation was introduced. After the check PCR, the colonies were grown on LB plates at 42°C. Next, the colonies were checked for the loss of the temperature sensitive plasmid, pKD46, by growth on LB plates and also on LB plates with ampicillin.

To remove the antibiotic resistance marker from the mutated strains, the cells were transformed with the temperature sensitive plasmid, pCP20. The colonies on the ampicillin plates at 30°C were streaked on non-selective plate agar at 42°C and then checked for the loss of antibiotics kanamycin/chloramphenicol and ampicillin. Prior to removal of the antibiotic marker, all mutations were moved into a wild-type background using P22 transduction.

Tetracycline Counter Selection

Chromosomal tetracycline counter-selection was done using the method described previously (Karlinsky, 2007). Briefly, the method consists of two steps. In the

first step, the region of interest to be mutated was first replaced with a *tetRA* element from the transposon Tn10. This was done using λ -Red recombination using the plasmid pKD46. The resultant strain is resistant to tetracycline and was selected for on tetracycline plates. In the second step, the tetracycline resistance marker on the plates was replaced by the desired mutation. This was again done using λ -Red recombination and selecting for colonies on Tetracycline sensitive plates.

For counter-selections, after the transformation of the PCR product, the cells were allowed to recover at 42°C (instead of 37°C) for 2 hours. After recovery, the cells were plated on plates which were pre-heated to 42°C (J. E. Karlinsey, Personal communication). Cellular growth on the counter-selection media was extremely slow and small colonies were only visible on the plates after growth for 24 hours at 42°C. The colonies were then streaked on LB plates and checked for loss of tetracycline and ampicillin resistance. Individual colonies on the LB plate were then PCR checked for introduction of the correct mutation. Prior to using the strain in the experiments, the PCR product was sequenced.

P22 Transduction

Prior to use in experiments, all mutations were moved (except the mutations introduced by counter-selectios) into clean wild-type background (14028) using P22 transductions (Davis, 1980). The lysate was prepared as follows. The strain carrying the

mutation of interest was grown overnight at 37°C. 100 ul of the overnight culture was added to 5 ml of LB and 100 ul of wild-type lysate and the mix allowed to grow at 37°C overnight. The next morning, cell debris should be visible in the media. Spin the overnight culture down at 14000 rpm for 5 minutes. Carefully remove the supernatant (the lysate) and store at 4°C. The lysate is good for years.

To move the mutation into wild-type, a wild-type culture grown overnight in LB media at 37°C. One hundred microliters of the overnight was then mixed with a hundred microliters of 1:10 and 1:100 dilution of the lysate of interest and allowed to sit stationary at 37°C for 30-45 minutes. 100 ul of the solution was then plated on plates with the appropriate antibiotic. Colonies were re-streaked on LB plates twice before selection of a colony for use in experiments.

Note: Prior to use, 3-4 drops of chloroform was added to the wild-type lysate to activate the phage. The lysate was then allowed to sit for a few minutes to allow the chloroform to settle down.

Note: all phage related work was done with glass pipettes.

Note: Respective controls (recipient strain only or phage lysate only) were also plated to check if any colonies were obtained.

Transcriptional Fusions

Transcriptional fusions with *gfp*, *venus*, *luxCDABE*, or *mCherry* for promoter activity measurements were made by amplifying the promoter of interest and cloning it in the multiple-cloning site of pPROBE. The size of the promoter fragment was decided by looking at the inter-genic distance and the previously characterized regulatory elements for a particular promoter. While amplifying, we typically, also went 15-20 base pairs into the gene to amplify the promoter fragment.

Ectopic Gene Expression

Genes of interest were cloned in the multiple cloning site of the vector pPROTet.E *tetR*. If introducing a synthetic RBS to the gene, the one on pPROBE was used and the one on pPROTet.E was removed. The 6x-His tag was also removed from the plasmid when cloning the gene of interest.

Motility And Swarm Plates

Motility Plates: Motility plates for swimming assays had the following recipe: Tryptone Broth (10 g/lit), NaCl (8 g/lit), and agar (0.3%). After autoclave, the plates were poured and allowed to solidify at room temperature. 1 ul of the overnight culture of the strain of interest was then pipette on to the plate. The plate was then transferred to 37°C and left there for a few hours for the rings to develop.

Swarm Plates: Swarming plates contained either LB broth with 0.6% Difco agar and 0.5% glucose (Kim & Surette, 2004) or 0.6% Bacto agar, 1% tryptone, 0.8% NaCl, and 0.02% Tween 80.

Note: motility media left on bench continuously loses water to evaporation. So, after a while, the agar percent in the media goes above 0.3% and the cells are no longer able to swim. Therefore, always use fresh motility media.

Flagella Kinetic Experiments

All mutants were combined with $P_{flhDC}::tetRA$ by phage-mediated transduction. Prior to the assays, the necessary strains were grown overnight at 30°C in LB broth. The overnight cultures were diluted to a starting OD₆₀₀ of 0.02 and incubated with shaking at 30°C to an OD₆₀₀ of approximately 0.15, in a method similar to Kalir and co-workers (Kalir *et al.*, 2001). The cultures were then pipetted (200 µl) into a 96-well microplate with each well containing 5 µl of tetracycline (2.5 µg ml⁻¹). To allow for aerobic growth and reduce desiccation, the plates were overlaid with a Breathe-Easy sealing membrane (Sigma, Z380059). The sealed microplates were then incubated at 30°C with intermittent shaking, light detection and absorbance readings in a TECAN Safire microplate reader for 50 cycles. A cycle was defined as: (i) measure light production, (ii) measure absorbance, (iii) shake for 5 min and (iv) pause for 25 s. All microplate assays were repeated at least

three times (i.e. three independent plates) allowing for the average promoter activity of $n \geq 9$ to be calculated, unless otherwise stated.

SPI1 Kinetic Experiments

Fluorescence assays: One milliliter cultures were first grown overnight in 16mm borosilicate test-tubes in LB medium lacking salt under vigorous shaking at 37°C (SPI1 repressing conditions) and then subcultured 1:1000 into fresh LB medium (with salt) and grown statically in test tubes at 37°C for 12 hours (Ellermeier & Slauch, 2003). A 100 μ L aliquot of each culture was then transferred to a 96-well microplate, and fluorescence and absorbance (OD600) were measured using a Tecan Safire2 microplate reader. The fluorescence readings, given in terms of relative fluorescence units (RFU), were normalized to the OD600 absorbance to account for cell density.

For single-cell fluorescence measurements, overnight cultures were first grown under SPI1-repressing conditions at 37°C. The cells were then sub-cultured to an OD of 0.05 into fresh LB medium (with salt) and grown statically at 37°C. Samples were collected at different time points by resuspending them in phosphate buffered saline (PBS) with 34 μ g/mL chloramphenicol in order to arrest translation and then storing on ice. All fluorescent-activated cell sorting (FACS) experiments were performed on a BD LRS II system from BD Biosciences. Data extraction and analysis for the FACS

experiments was done using FCS Express Version 3 (De Novo Software). For all FACS experiments, fluorescence values of 30,000 events was recorded and reported.

In the flow cytometry experiments involving the P_{hilC} and P_{hilD} promoters, we used destabilized GFP transcriptional fusions where the sequence AANDENYAASV was appended to the C-terminus of the protein. This tag reduces the half life of GFP from approximately 24 hours to 110 minutes (Miller *et al.*, 2000). The reason that we needed to employ destabilized GFP is that P_{hilC} and P_{hilD} promoters are partially active even when the cells are grown in SPI1-repressing conditions. As a consequence, we were unable to observe the “off” to the “on” transition using “tagless” GFP. We did not run into similar problems with the P_{hilA} and P_{rtsA} promoters and consequently used transcriptional fusions to “tagless” GFP.

Fimbriae End-Point And Kinetic Experiments

As an indirect measure of gene expression, end-point and dynamic measurements of the fluorescent reporter system were made using a Tecan Safire2 microplate reader. For fluorescence end-point measurements, 1 ml culture was grown at 37°C overnight and then subcultured 1:1,000 in fresh medium and grown in static conditions for 24 h at 37°C. A total of 100 ul of the culture was then transferred to a 96-well microplate, and the relative fluorescence and optical density at 600 nm (OD600) measured. The fluorescence readings were normalized with the OD600 to account for

cell density. For time course measurements, overnight cultures at 37°C were subcultured to an OD of 0.05 in fresh medium and allowed to grow to an OD of 0.15. A total of 100 ul of the culture was then transferred to a 96-well microplate and overlaid with 25 ul of oil to prevent evaporation. The temperature was maintained at 37°C, and fluorescence and OD readings were taken every 5 min. All experiments were done in triplicate and average values with the standard deviations reported. Single-cell measurements were done similarly by growing the cells in noninducing conditions with vigorous shaking at 37°C. Overnight cultures were subcultured to an OD of 0.05 in fresh medium (LB) and grown in inducing conditions of high oxygen and no shaking at 37°C. Samples were collected at different time points by spinning the cells down, resuspending them in phosphate-buffered saline supplemented with chloramphenicol (20 ug/ml) to stop all translation and arrest the cells in their respective state, and finally storing on ice. All flow cytometry experiments were performed on a BD LRS II system (BD Biosciences). The data extraction and analysis for the flow cytometry experiments were done using FCS Express version 3 (De Novo Software).

Western Assay

Cells from overnight cultures were subcultured 1:1,000 in fresh medium and grown at 37°C for 6 h. Prior to lysis, OD₆₀₀ measurements were taken to ensure that there were equivalent numbers of cells between samples. To lyse the cells, cultures were spun down, resuspended 3:1 in 4x sodium dodecyl sulfate solubilizer, and boiled at

95°C for 10 minutes. Lysates were run on a 4 to 20% Tris-HCl precast gel (Bio-Rad) for 50 min at 150 V. Transfer to the membrane was done using Immobilon transfer membranes with 0.2-um pore size (Millipore). 3x FLAG-tagged FlhC was detected with an anti-FLAG M2 monoclonal antibody (Sigma) and an anti-mouse horseradish peroxidase-conjugated antibody (Jackson Laboratories) using the ECL Plus Western blotting detection system (Amersham). In order to quantify the relative protein levels, the membrane was scanned using a STORM 840 PhosphorImager (Amersham) and then analyzed using the LabWorks software package (UVP). The relative amount of protein in each lane was estimated by measuring the integrated OD for each band. All measurements were performed in triplicate.

Co-Immunoprecipitation

We followed the basic protocol outlined by Shin and Groisman (Shin & Groisman, 2005). Briefly, cells from overnight growth were sub-cultured 1/100 in 200ml LB and grown for 8 hours at 37°C. Formaldehyde (1%) was then added to the cultures, and the reaction was incubated at room temperature for 15 minutes. The cross-linking reaction was quenched by addition of 125 mM glycine. The cells were then washed twice with ice-cold phosphate-buffered saline (PBS). The cells were lysed in 0.5 ml of lysis solution (10 mM Tris, pH 8.0, 50 mM NaCl, 10 mM EDTA, 20% sucrose, 10 mg/ml lysozyme) and 0.5 ml of 2xRIPA solution (100 mM Tris, pH 8.0, 300 mM NaCl, 2% Nonidet P-40, 1%

sodium deoxycholate, 0.2% SDS). The cell extract was sonicated so that the average fragment DNA had an average size of 500 bp.

The Ni-NTA resin and the lysate were mixed in equal volumes and allowed to sit at 4°C for 60 minutes. The lysate/Ni-NTA mixture was then loaded on a column and the flow through discarded. The column was then washed thrice with the wash buffer (50mM NaH₂PO₄, 300mM NaCl, 20mM imidazole, and pH adjusted to 8.0 using NaOH) and the flow-through discarded. The protein and the bound DNA were eluted with one-eighth volume of the elution buffer (50mM NaH₂PO₄, 300mM NaCl, 250mM imidazole, and pH adjusted to 8.0 using NaOH). Reversal of cross-linking and DNA purification was done as described by Kuo and Allis (Kuo & Allis, 1999). The isolated DNA was checked for the presence of the promoter region of interest by PCR.

DNA Mobility Shift Assay

DNA mobility shift assays were performed using the approach previously described by Ellermeier and Slauch (Ellermeier & Slauch, 2003). Briefly, whole-cell extracts were prepared by subculturing overnight cultures 1/100 in LB medium and growing them to an OD₆₀₀ of 0.5, at which time 0.2% L-arabinose was added and cultures were grown for an additional 4 h at 37°C. The cells were then harvested by centrifugation at 5,000 x *g* for 10 min. The pellet of cells was resuspended in 10 ml of 50 mM Tris-HCl (pH 7.9) with 30 μM dithiothreitol (DTT), and the solution was then

sonicated to lyse the cells. Lysates were then centrifuged at 16,000 x *g* for 30 min at 4°C. The protein concentration in each sample was determined by using a bicinchoninic acid (BCA) protein assay reagent (Pierce Protein Research Products).

The binding reaction mixture contained approximately 0.1 ng of ³²P-labeled DNA (*xyIA* promoter; genomic region, nucleotides 3726575 to 3727102), 50 µg of herring sperm DNA per ml, 10 mM Tris-Cl (pH 8), 50 mM KCl, 100 µg of bovine serum albumin per ml, 10% glycerol, 1 mM DTT, 0.5 mM EDTA, and 2 µg whole-cell extract in a final volume of 20 µl. In the experiments where the I1-I1 binding site was included as a competitor, 10 ng of the double-stranded sequence (5'-ATG CG T AGC ATT TTT ATC CAT AAG ATT AGC ATT TTT ATC CAT AAG CCA-3') was added to the mixture. The binding reaction mixtures were incubated for 30 min at room temperature and then subjected to electrophoresis on a 5% native polyacrylamide gel in 0.5x Tris-borate-EDTA (TBE) at room temperature. Gels were dried on filter paper in a vacuum drier and were scanned using a Storm 840 PhosphorImager (Amersham).

Chapter 3. Flagellar Gene Network

Introduction

The bacterial flagellum is a rotary motor that enables cells to swim in liquid environments and drift along surfaces (Berg, 2003, Harshey & Matsuyama, 1994). In *Salmonella enterica* serovar Typhimurium, over 50 genes divided among at least 17 operons are involved in motility (Chilcott & Hughes, 2000). These genes encode not only the flagellar subunits and chemotaxis proteins but also a number of regulators that synchronize gene expression with the assembly process.

The flagellum consists of three structural elements: the basal body, the hook, and the filament (Macnab, 1999) (**Figure 2**). The basal body, embedded in the membrane, anchors the flagellum to the cell. It also houses the rotary motor necessary for swimming and the type III secretion apparatus, which is involved in assembly. The hook, a flexible joint, transmits torque produced by the motor to the filament, a rigid helical structure approximately 5 to 15 μm in length that functions as the propeller (Yonekura *et al.*, 2003). In *S. enterica* serovar Typhimurium, there are approximately four to six flagella per cell (Karlinsky *et al.*, 2000b). When the motors spin counterclockwise, the filaments form a helical bundle that propels the cell forward in a corkscrew-like manner.

Flagellar assembly proceeds in a sequential manner beginning at the base along the inner membrane and concluding with the filament (Macnab, 2003). The type III secretion apparatus, located at the cytoplasmic interface of the flagellum, delivers the majority of the protein subunits through a central channel within the growing flagellar structure. The process concludes with the nucleation and elongation of the flagellar filament, driven by the secretion of flagellin monomers into the hollow interior of the filament and subsequent incorporation at the distal tip (Asakura *et al.*, 1968, Homma & Iino, 1985, Morgan *et al.*, 1995, Yonekura *et al.*, 2000).

A critical feature of flagellar biogenesis is that gene expression is coupled to assembly. Upon initiation, where cells transition from a non-flagellated to a flagellated state, gene expression proceeds in a sequential manner: first, genes encoding the basal body and hook proteins are expressed, and then, only after these structures are assembled, the late genes encoding the filament, motor, and chemotaxis proteins are expressed (Kalir *et al.*, 2001, Karlinsey *et al.*, 2000a). If hook or basal body assembly is unsuccessful, then the late genes are not expressed. This checkpoint enables cells to coordinate assembly and is the main regulatory mechanism observed during initiation. The way that cells enforce this checkpoint is to use late protein secretion as a proxy signal for hook-basal body (HBB) completion (Hughes *et al.*, 1993).

Coordinated expression of more than 50 genes is required for assembly of a functional flagella (**Figure 3A**). The flagellar promoters can be divided into three classes

(Chilcott & Hughes, 2000) **(Figure 3)**. A single P_{class1} promoter controls the expression of the *flhDC* master operon involved in initiating assembly **(Figure 3B,C)**. This promoter integrates environmental signals through the combinatorial action of multiple global transcriptional regulators, thus allowing cells to determine whether or not to be motile (Pruss *et al.*, 2001, Yanagihara *et al.*, 1999). When motility is induced, the FlhD₄C₂ complex activates the P_{class2} promoters (Ikebe *et al.*, 1999, Wang *et al.*, 2006). These promoters control the expression of the genes encoding the HBB and two regulatory proteins, σ^{28} (or FliA) and FlgM. The σ^{28} alternate sigma factor, also known as FliA, is required for activating the P_{class3} promoters, which control the expression of the late genes (Ohnishi *et al.*, 1992). However, prior to HBB completion, FlgM binds to σ^{28} and prevents it from activating the P_{class3} promoters (Chadsey & Hughes, 2001, Chadsey *et al.*, 1998, Gillen & Hughes, 1991). This inhibition, however, is relieved when the HBB is assembled, as the completed structure can secrete FlgM along with other late proteins involved in assembly (Hughes *et al.*, 1993). Thus, the cell is able to use protein secretion as a cue for HBB completion.

Recently, a number of additional flagellar proteins have been shown to regulate gene expression. These proteins include two chaperones, FlgN and FliT, and a flagellar protein, FliZ (Fraser *et al.*, 1999, Kutsukake *et al.*, 1999, Karlinsey *et al.*, 2000a, Lanois *et al.*, 2008). FlgN facilitates the secretion of two hook-associated proteins (HAPs), FlgK and FlgL, which form the junction between the hook and filament (Bennett *et al.*, 2001, Fraser *et al.*, 1999). FlgN also enhances *flgM* translation with a specific preference for

class 3 transcripts (Karlinsky et al., 2000a). In a manner similar to the σ^{28} -FlgM checkpoint, both FlgK and FlgL bind to and inhibit FlgN's regulatory activity, suggesting that FlgN too is involved in a checkpoint coupled to the completion of HBB (Aldridge *et al.*, 2003). Interestingly, however, FlgN's effect on gene expression is most pronounced in strains defective for secretion, contrary to what we would expect from a HBB-dependent checkpoint.

FliT has previously been shown to negatively regulate FlhD₄C₂ activity (Kutsukake et al., 1999, Yamamoto & Kutsukake, 2006). FliT is the T3S chaperone for the filament cap protein, FliD (Fraser et al., 1999). Yamamoto and Kutsukake (2006) showed that FliT binds to FlhD₄C₂ and prevents it from activating P_{class2} promoters (Yamamoto & Kutsukake, 2006). Because it affects FlhD₄C₂, FliT can potentially inhibit both P_{class2} and P_{class3} promoters, unlike FlgM or FlgN. Furthermore, it can potentially activate the P_{class1} promoter by preventing FlhD₄C₂ from inhibiting its own expression. Deletion mutants of *fliT* are still motile but show increased flagellar gene expression and numbers consistent with it being a transcriptional inhibitor (Yokoseki *et al.*, 1995). Because it is a chaperone, FliT's activity is likely coupled to HBB completion and secretion in a manner similar to σ^{28} and FlgN. Lastly, FliZ is a positive regulator of P_{class2} activity (Kutsukake et al., 1999). While FliZ is not known to be a chaperone, it is expressed on the same mRNA transcript as σ^{28} and therefore responsive to secretion as it is expressed from both P_{class2} and P_{class3} promoters.

The flagellum is interesting from various points of view. Research efforts in understanding the bacterial flagellum have focused on characterizing the energy efficiency of the flagella as a motor-operated organelle; the hydrodynamics of the flagellar function; and the evolutionary history of a complex organelle such as the flagellum. Our research focus has been to study the role of regulatory interactions in the flagellar cascade of genes leading to timely assembly of the flagellar subunits. This chapter deals with the following two ideas:

To investigate the role of FliZ in regulating flagellar assembly. FliZ has been reported as a flagellar gene expression activator (Bischoff *et al.*, 1992, Kutsukake *et al.*, 1999, Saini *et al.*, 2008). However, the precise mechanism of FliZ-dependent activation of the flagellar genes is not known. In this section, we try and elucidate the mechanistic details of FliZ-regulation of the flagellar genes. We also study the impact of *fliZ* deletion on gene expression dynamics and the role of FliZ in controlling flagellar abundance per cell.

Role of FliA-FlgM in dictating gene expression dynamics. The second idea we explore in this chapter deals with the σ^{28} -FlgM regulatory system in the flagellar network. This interaction has previously been thought to function as a binary checkpoint, activating expression from the class 3 promoters only when the HBB complex is complete and repressing expression when not. However, in recent work from our and Phillip Aldridge's laboratory at the University of Newcastle, we characterized a

number a secretion and regulatory mutants where the relative timing of class 2 and class 3 promoter activities was altered (Brown *et al.*, 2008). In particular, we found that gene expression dynamics were determined by the rate of protein secretion. These results led us to hypothesize that the σ^{28} -FlgM regulatory system functions not only as a developmental checkpoint but also as a rheostat that serves to dynamically fine tune gene expression in response to flagellar abundance using protein secretion as a proxy signal. In this work, we investigated the role of the σ^{28} -FlgM regulatory system in controlling the dynamics of flagellar gene expression in *S. enterica*. To explore the different elements of this regulatory system, we first developed a mathematical model of the flagellar regulon. Analysis of the model predicted that the temporal ordering in the activation of the class 2 and class 3 promoters is not a direct consequence of the transcriptional hierarchy but rather due to the σ^{28} -FlgM regulatory system. In particular, this system serves to control the dynamics of gene expression from both the class 2 and class 3 promoters in response to the rate of protein secretion. Based on our results, we conclude that the primary function of the σ^{28} -FlgM regulatory system is not to enforce a developmental checkpoint as previously thought but rather to ensure robust, homeostatic control.

Flagella Results

FliZ Regulates the FlhD₄C₂ Level in the Cell to Control Flagellar Abundance.

FliZ is a protein of no known homology with regulatory proteins. FliZ is encoded in the flagellar network along with the flagellar specific sigma factor, FliA. FliZ has also been shown to act as a positive regulator of the SPI1 encoded T3SS used by the bacterium *S. typhimurium* in the intestinal phase of infection. We previously reported that FliZ-dependent activation of the flagellar cascade is via post-translation activation of the flagellar master regulator, FlhD₄C₂ (Saini et al., 2008). With these results, we hypothesized if FliZ acts via negatively regulating proteases in the cell which are known to negatively regulate flagellar gene expression. In particular, we tested the proteases Lon and ClpXP. However, against our prediction, our results show that FliZ-dependent regulation of the flagellar system is independent of both Lon and ClpXP (**Figure 4**).

Although, we do not as yet know the mechanism of FliZ-dependent activation of the flagellar genes, we wanted to learn impact of a *fliZ* mutation on the dynamics of flagellar gene expression in wild type. Our results indicate that FliZ controls the activation kinetics of class 2 promoters in the flagellar cascade. In a $\Delta fliZ$ mutant, class 2 promoters exhibit a delay in activation as compared to the wild type. In addition, maximal levels of class 2 promoter activity is also decreased in the $\Delta fliZ$ mutant as compared to the wild type. On the other hand, loss of FliZ only had an effect on the

absolute value of class 3 promoter levels and the dynamics of activation was the same as that in the wild type (**Figure 5**).

Since class 2 gene products are structural components of the HBB of the flagellum, we hypothesized that class 2 expression controls the flagella number per cell and that a $\Delta fliZ$ mutant would be less flagellated as compared to the wild type. To test this hypothesis, we performed electron microscopy experiments to count the flagellar numbers per cell in wild type and the $\Delta fliZ$ mutant. Our results demonstrate that a $\Delta fliZ$ mutant assembles less flagella per cell as compared to the wild type (**Figure 6**). Therefore, our results suggest that during flagellar assembly FliZ acts to control the flagellar abundance per cell.

Flagellar Model for FliA-FlgM Interaction

Following initiation, flagellar gene expression occurs in a sequential manner. The class 1 promoter is first induced, then the class 2 promoters, and finally the class 3 promoters. A characteristic feature of this temporal program is that there is a delay between the induction times of these different promoter classes (**Figure 7**). We previously characterized a number of mutants with altered delays between the induction of the class 2 and class 3 promoters (Brown et al., 2008). To understand the mechanistic origin of these changes in the timing of gene expression, we constructed a mathematical model of the flagellar gene circuit.

Our initial goal in constructing this model was to understand why there is a delay. In particular, the transcriptional hierarchy, where the class 1 gene products are necessary for the activation of the class 2 promoters and the class 2 gene products are necessary for the activation of the class 3 gene promoters, alone does not explain the delays. As simple experimental proof for this ascertain, both the class 2 and class 3 promoters are activated at roughly the same time in a $\Delta flgM$ mutant. These results indicate that FlgM somehow plays a role in generating these delays. In further support of such a mechanism involving FlgM, many of the timing mutants that we previously identified were associated with a secretion defect. In particular, in mutants where the secretion rate was increased, the delay between the activation of the class 2 and class 3 promoters decreased. Likewise, when the secretion rate was decreased, the delay increased.

Based on these data, we hypothesized that the rate of FlgM secretion determines the magnitude of the delay. A key element of this hypothesis is that the secretion rate is a variable quantity and determined by the number of functional HBB's in the cell.

We did not attempt to model expression of FlhD₄C₂. The P_{class1} promoter, P_{flhDC} is regulated by a large number of global regulators in response to various external and intracellular signals. The precise role of these global regulators is not known and therefore, was not included in the analysis. However, motility is induced in *S.*

typhimurium in the early exponential phase and therefore, the class 1 promoter activity was represented by an incomplete gamma function.

Structural components of the HBB are encoded from a number of FlhD₄C₂-dependent class 2 promoters and therefore, were lumped together and treated as one entity in our model.

Protein secretion takes place from the cells through discrete number of HBB structures assembled. However, in absence of an estimate of the HBB structures assembled in the cell we assume that protein secretion is proportional to class 2 gene expression.

Flagellar gene circuit is known to be regulated at the translational level (FliC/FlgN-FlgM). We, however, ignore the regulatory interactions at the mRNA level in the circuit and only study transcription and protein-protein interaction at the FliA-FlgM level in our model.

Promoter activity was modeled using equilibrium thermodynamics expressions (i.e. Michaelis-Menten type expressions).

FliA is a chaperone for its anti-sigma factor, FlgM. We assume that only FlgM bound to FliA is recognized by the export apparatus to be secreted from the cell. Free

cellular FlgM will not get secreted from the HBB structure. In addition, we also assume that FliA does not affect FlgM stability but only regulates its secretion. Also, we ignore the FlgM-dependent stabilization of FliA.

Based on the assumptions enumerated above, we can model the FliA-FlgM interaction in the flagellar network with the following set of ordinary differential equations:

$$\frac{dA}{dt} = \frac{K_{2a}fK_a + K_{3a}A}{K_a + A} - d_a A - k_{on}A \cdot M + k_{off}C + \frac{k_e X \cdot C}{k_e + C} \quad (1)$$

$$\frac{dM}{dt} = k_{2m}f + \frac{k_{3m}A}{K_{3m} + A} - d_m M - k_{on}A \cdot M + k_{off}C \quad (2)$$

$$\frac{dC}{dt} = k_{on}A \cdot M - \frac{k_e X \cdot C}{k_e + C} - d_c C - k_{off}C \quad (3)$$

$$\frac{dX}{dt} = f - d_x X \quad (4)$$

$$\frac{dY}{dt} = \frac{k_y f \cdot A}{K_m + A} - d_y Y \quad (5)$$

Where, A denotes the concentration of FliA, M the total concentration of FlgM, C the total concentration of the FliA-FlgM complex, X the concentration of class 2 genes, Y the concentration of class 3 genes, and f the total concentration of the FlhD4C2 complex. The parameter values used for all our modeling results are as follows: $K_a = 1$,

$K_m = 1$, $K_{am} = 3$, $k_{2m} = 1.5$; $k_{3m} = 3$, $k_{2a} = 0.2$, $k_{3a} = 1.8$, $K_{on} = 30$, $K_{off} = 0.006$, $dx = 1$, $dy = 1$, $da = dm = dc = 0.4 + \log(2)/30$, and $K_e = 2$.

To validate our model, we first observed the dynamics of class 2 and class 3 promoters in a wild type mutant. Consistent with our experimental observations, we observed that there exists a delay between induction of class 2 and class 3 promoters. We hypothesize that the FliA-FlgM interaction in conjunction with protein secretion from the growing flagellum is responsible for tuning the gene expression dynamics. To further validate our model, we tested our model output for a $\Delta flgM$ mutant. To generate the gene expression profiles for the mutant, we put the FlgM generation rate equal to zero in our model. Loss of FlgM, consistent with our experimental observation, eliminates the hierarchy of class 2 and class 3 promoter activation as both classes were induced at the same time (**Figure 8**).

Next, we tested the model output in a mutant where we reduce the secretion rate from the flagellum. Experimentally, we did this by fusing FlgM with β -lactamase, and we observe that reducing the secretion rate delays induction of class 3 promoters, therefore, further increasing the time delay between class 2 and class 3 promoter activation. Our mathematical model was able to capture this effect when we decrease the FlgM secretion rate from the growing flagellum (**Figure 9**). These results suggest that the FliA-FlgM interaction does not encode a hard-checkpoint in the flagellar assembly

but it serves the role of a gene expression tuning agent in response to the assembly status of the growing flagellum.

In this regard, our model predicted that FliA-auto-regulation plays an important role in gene expression regulation. FliA expression is under a hybrid class 2 and class 3 promoter, and by setting the auto-activation term equal to zero, our model predicted that this auto-activation is essential for faster activation of the class 3 promoters. In other words, our model predicts that in the absence of FliA-autoactivation, the delay between class 2 and class 3 promoter induction would increase (**Figure 10**). To test this prediction experimentally, we replaced the hybrid P_{fliA} promoter with pure class 2, P_{flhB} promoter. The P_{flhB} promoter is not regulated by FliA and is solely under the control of FlhD₄C₂ complex for activation. Under physiological conditions, the two promoters, P_{fliA} and P_{flhB} , are of approximately equal strength. Consistent with our model prediction, we observe that replacing the native P_{fliA} promoter by a pure class 2, P_{flhB} promoter, increases the delay between inductions of class 2 and class 3 promoters (**Figure 10**).

The fact that the delay in class 2 and class 3 promoter induction during flagellar assembly is not rigid but is tunable in response to assembly status and protein secretion rate was also predicted by our model when we ectopically expressed FliA. By replacing the FlhDC- and FliA-dependent activation of FliA by a constant term our model predicted that the induction of class 3 promoters with respect to class 2 promoters is tunable. To test this prediction, we first replaced the P_{fliA} promoter with a *tetRA* element on its

chromosomal locus. The resulting strain was called $P_{fliA}::tetRA$. The *tetRA* element in this strain was then replaced by the *lacI*^q P_{tac} element from the CRIM plasmid pAH55 (Haldimann & Wanner, 2001). The resulting strain was called $P_{fliA}::P_{tac}$ where *FliA* expression could be induced by addition of IPTG to the medium (**Figure 11**). The results of gene expression dynamics experiments in this strain validated our hypothesis that *FliA*-*FlgM* interaction is not a hard-checkpoint in the flagellar assembly but a tunable interaction that links gene expression to assembly status (protein secretion).

Our model, however, suffers from some important limitations. Flagellar gene expression is controlled by a large number of feedback loops. Important among those are *FliZ*-*FlhD₄C₂* positive feedback loop and the *FliT*-*FlhD₄C₂* negative feedback loop. Where, in response to high-secretion rates (high flagellar abundance) *FliT* binds to *FlhD₄C₂* and prevents activation of class 2 promoters, we do not understand the mechanism of *FliZ*-dependent activation of *FlhD₄C₂* amounts inside the cell. Both these feedback loops are not accounted for in our model. Other regulatory interactions, *FliS* and *FlgN*, are also not included in our model. Thus, the next step in this direction is incorporation of more interactions in the model to develop a more comprehensive understanding of the link between gene expression, assembly process, and control over flagellar abundance.

Discussion

The FliA-FlgM interaction enforces a critical check point when cells transition from a non-flagellated to a flagellated state. This check point includes allowing class 3 expression to start only when a functional HBB has been assembled. As we have shown, it also causes a delay in class 3 gene expression. Our results indicate that in the architecture of the flagellar cascade, the *fliAZ* operon tunes the delay in class 2 and class 3 gene expression. In a $\Delta fliZ$ mutant, the delay between class 2 and class 3 expression is reduced as a mutation in *fliZ* leads to a delay in class 2 gene expression. Eliminating the FliA feedback on its promoter resulted in elimination of the positive feedback driving class 3 gene expression. Loss of FliA feedback led to a big delay in class 3 expression in $P_{fliA}::P_{flhB}$ strain resulting in increase in the delay between class 2 and class 3 gene expression. Eliminating the FliA feedback, however, weakened the FliZ-dependent feedback on FlhD₄C₂ as well. Weakening this positive feedback resulted in lower than wild type levels of class 2 promoter activity in $P_{fliA}::P_{flhB}$ though the dynamics of gene expression were the same as wild type.

Conversely, we can also enhance the positive feedback loops driving class 2 and class 3 gene expression by deleting *flgM*. In this case, FliA is free to activate P_{fliA} resulting in enhanced FliA and FliZ levels, resulting in stronger feedback loops driving class 2 and class 3 expression. Enhancing the positive feedback by eliminating *flgM*

though comes at a cost that the cells no longer check the status of the flagellar assembly before initiating with class 3 gene expression.

Based on our experimental and modeling results, we hypothesize that the role of the FliZ and FliA dependent positive feedback loops in the flagellar circuit is to tune the dynamics of expression of class 2 and class 3 genes. FliA-FlgM interaction ensures that the feedback loops does not start before the assembly of a functional HBB. This checkpoint leads to a natural delay in class 3 and class 3 gene expression. We demonstrate here that we can tune the delay in gene expression by breaking, weakening or strengthening these positive feedback loops dictating flagellar gene expression and assembly. Thus, we propose that the role of the feedback loops in the *fliAZ* operon is to tune class 2 and class 3 gene expression timing.

Figures – Flagella Gene Network

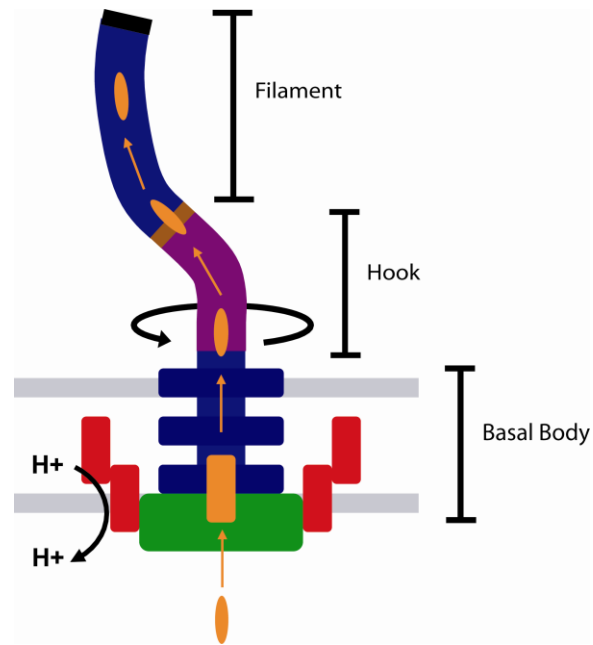


Figure 2. Structure of flagellum in *S. typhimurium*. The flagellum is divided into three distinct parts (a) the basal body which anchors the flagellum to the cell, (b) hook, which is a flexible joint that transmits torque from the motor to the filament, and (c) filament, which is a long rigid structure.

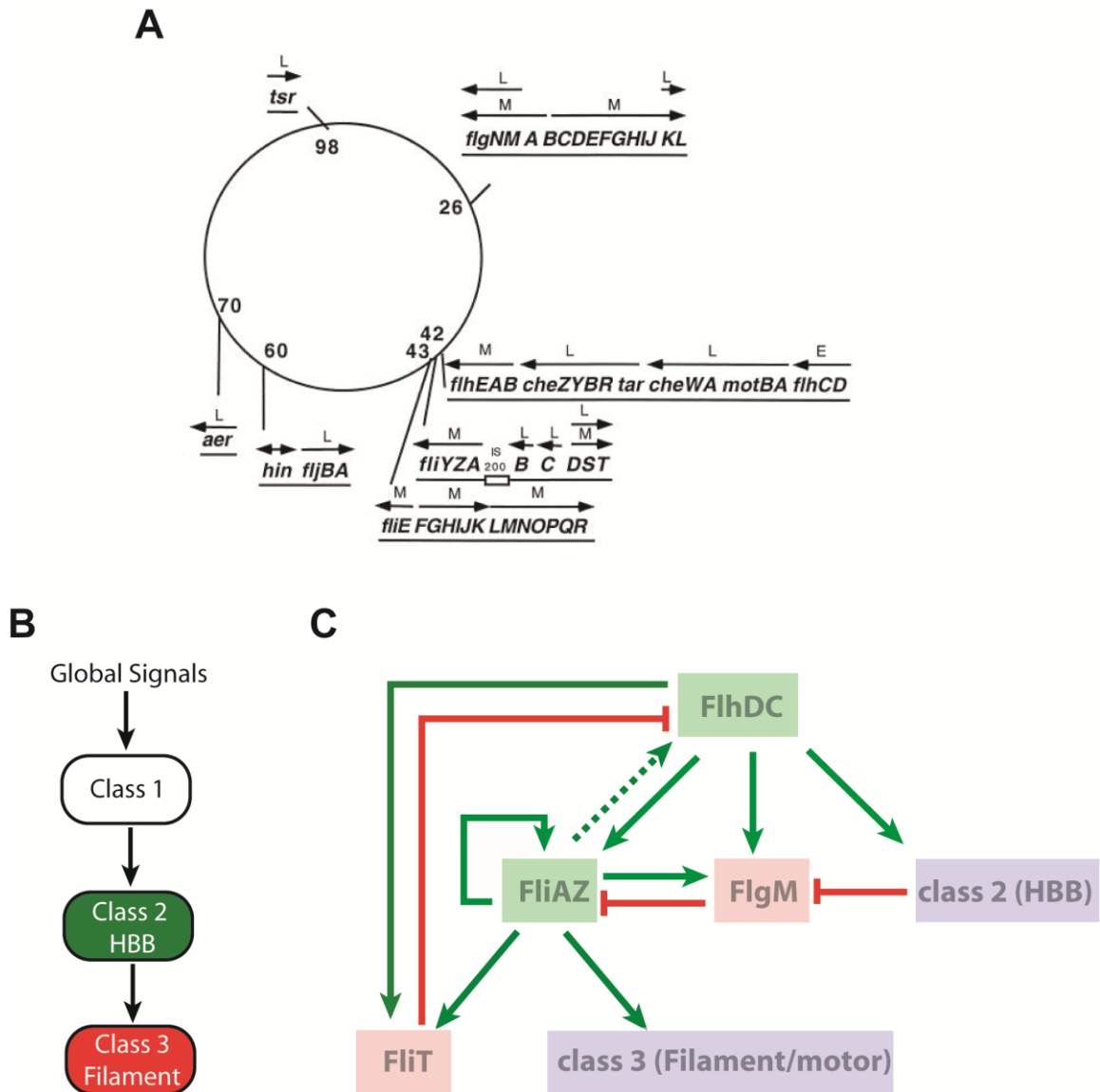


Figure 3. The regulatory network for the flagellar assembly. (A) Chromosomal locations of the operons that make up the flagellar regulon of *S. enterica* serovar Typhimurium. The operons are labeled E, M, or L depending on whether they are expressed early, middle, or late in the temporal induction pathway (Chilcott & Hughes, 2000). **(B)** Global signals feed into the class 1 promoter. Class 1 products activate the class 2 promoters leading to assembly of the hook basal body (HBB). Class 2 products also activate class 3 promoters, which encode for the filament, motor, and chemotaxis proteins. **(C)** FliA, FliM, FliZ, and FliT, all encode feedback loops in the flagellar network.

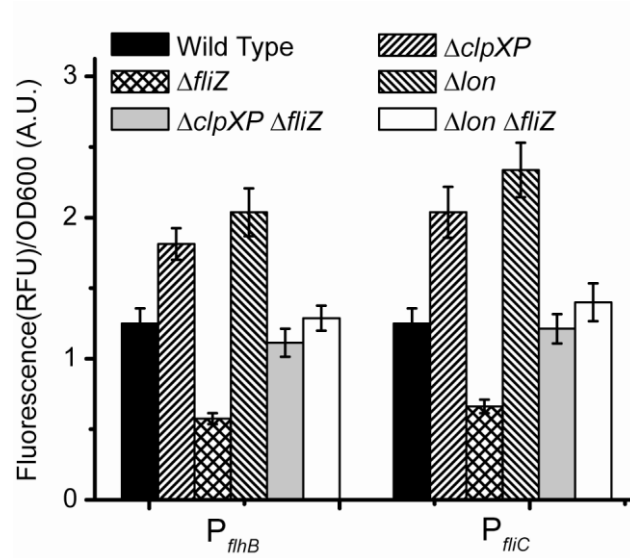


Figure 4. FliZ does not regulate flagellar gene expression via proteases, ClpPX and Lon. Class 2 and class 3 promoter activity in wild type, $\Delta fliZ$, $\Delta clpXP$, and Δlon mutants. P_{flhB} and P_{fliC} promoters were fused with $gfp[tagless]$ and fluorescence and OD600 were measured 8 hours after sub-culturing an overnight culture 1:500. Experiments were performed in triplicate at 30°C.

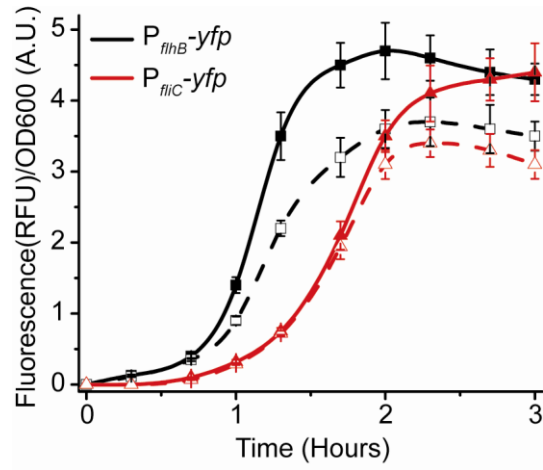


Figure 5. FlhZ leads to a faster and stronger induction of class 2 promoters. Class 2 (P_{fliB}) and class 3 (P_{fliC}) promoter dynamics in wild type (solid) and $\Delta fliZ$ mutant. Overnight culture was sub-cultured to an OD of 0.05 in fresh media and allowed to grow to an OD of 0.15 at 30°C. 100 μ l of the culture was then transferred to a 96-well plate. Fluorescence and Optical Density (OD600) readings were taken every 20 minutes with shaking in between. The temperature was maintained at 30°C. All experiments were performed in triplicate with average values and standard deviations reported.

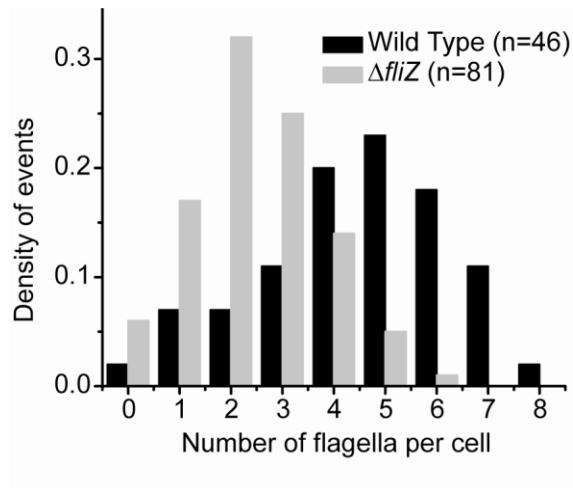


Figure 6. *FliZ* positively regulates the flagellar number per cell. Histogram of flagellar abundance per cell in wild type and a Δ *fliZ* mutant. Cells were grown to late exponential stage at 30°C and then arrested in their respective state by transferring to PBS with 34 μ g/ml chloramphenicol. The cells were then laid on a grid and images taken on a Tunneling Electron Microscope (TEM).

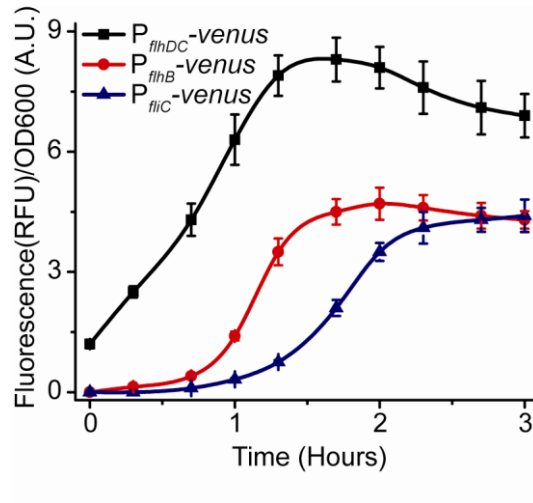


Figure 7. Flagellar gene expression is hierarchical in nature. Class 1, class 2, and class 3 promoter activities in wild type cells. All experiments were performed as described in Figure 5.

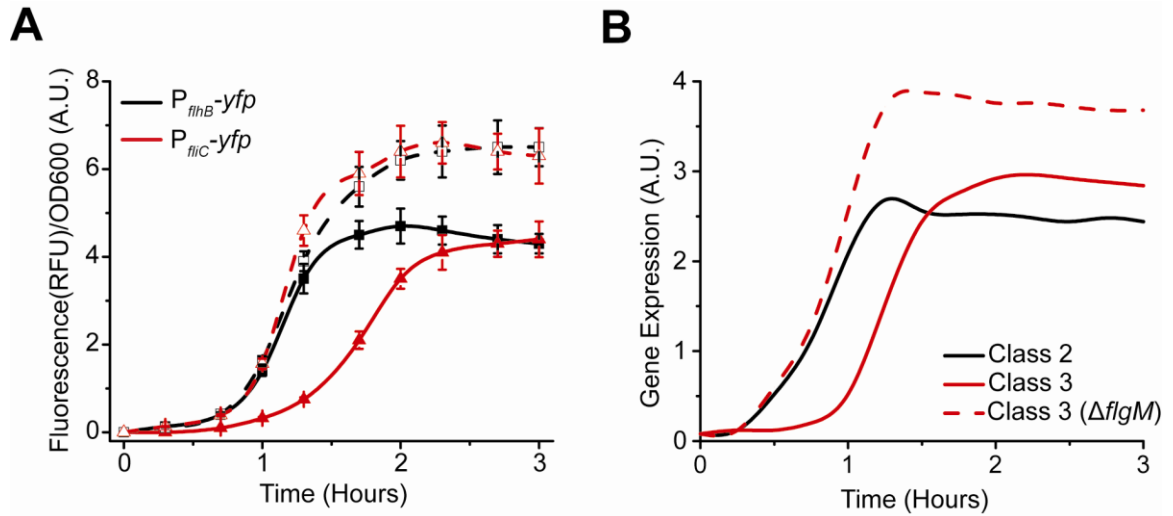


Figure 8. (A) FlgM delays class 3 promoter activation. Class 2 and class 3 promoter activities in wild type (solid) and $\Delta flgM$ mutant (dashed). Experiments were performed in triplicate with average value and standard deviations reported. All experiments were performed as described in Figure 5. **(B) Class 2 and class 3 promoter dynamics in wild type (solid) and $\Delta flgM$ (dashed) from our mathematical model.**

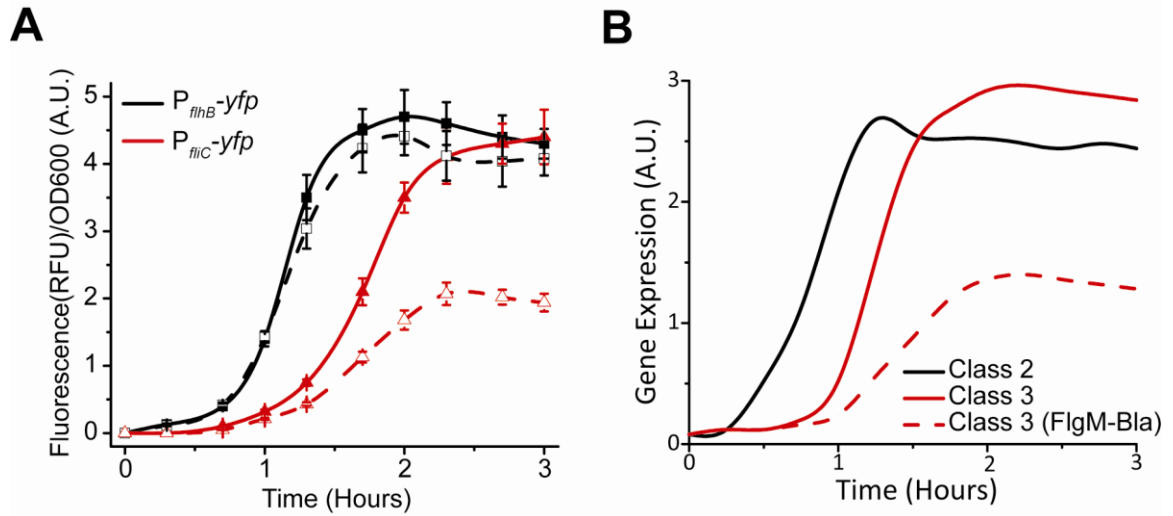


Figure 9. (A) Class 3 promoter activation is delayed in a FlgM-Bla mutant. Class 2 and class 3 promoter activities in wild type (solid) and an FlgM-Bla (dashed). Experiments were performed in triplicate with average value and standard deviations reported. All experiments were performed as described in Figure 5. **(B) Class 2 and class 3 promoter dynamics in wild type (solid) and FlgM-Bla (dashed) from our mathematical model.**

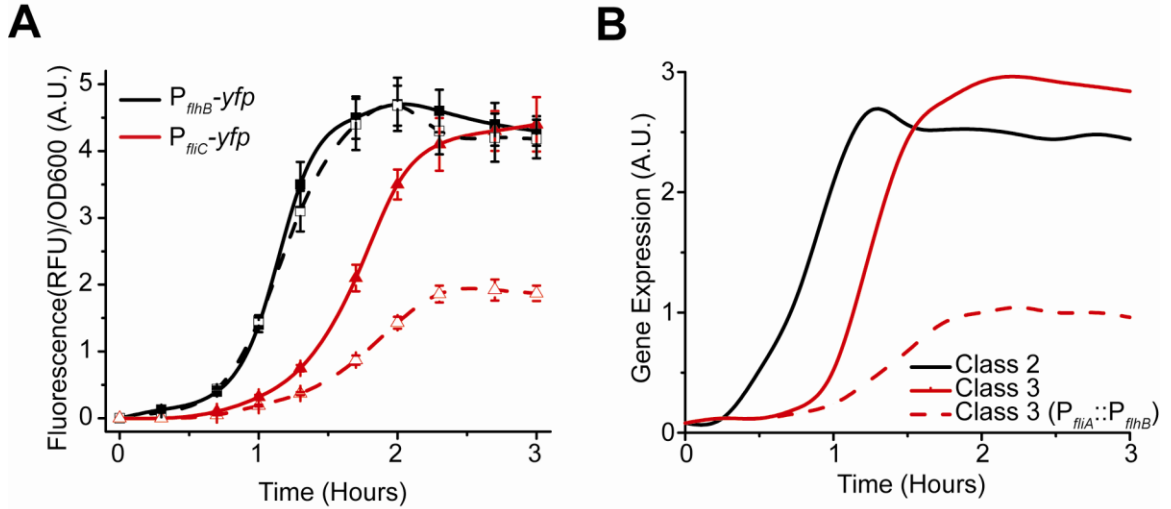


Figure 10. (A) Class 3 promoter activation is delayed in a $\Delta P_{fliA}::P_{fliB}$ promoter mutant. Class 2 and class 3 promoter activities in wild type (solid) and a $\Delta P_{fliA}::P_{fliB}$ promoter mutant (dashed). Experiments were performed in triplicate with average value and standard deviations reported. All experiments were performed as described in Figure 5. **(B) Class 2 and class 3 promoter dynamics in wild type (solid) and a $\Delta P_{fliA}::P_{fliB}$ promoter mutant (dashed) from our mathematical model.**

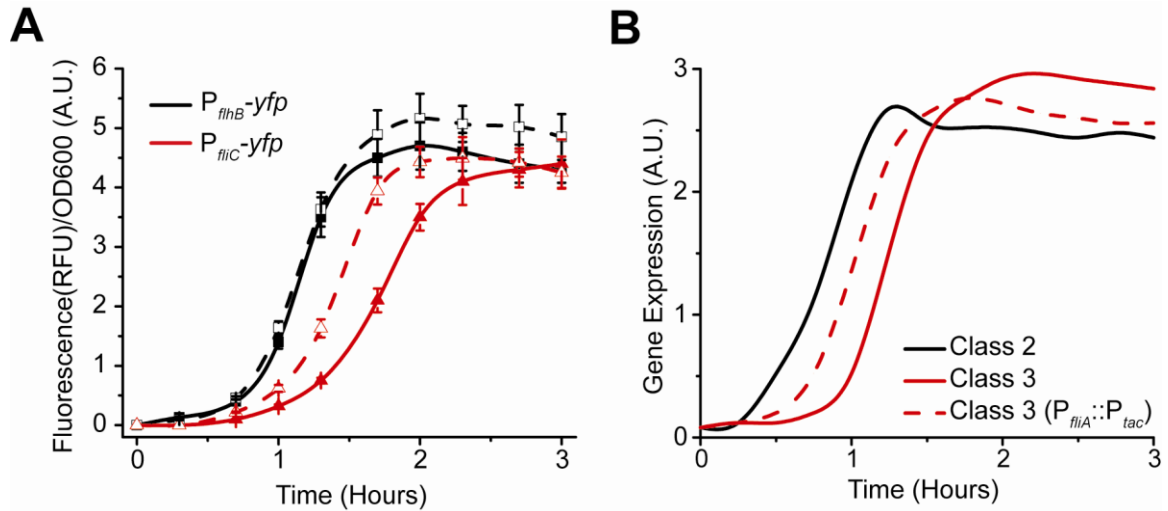


Figure 11. (A) Class 3 promoter activation is delayed in a $\Delta P_{fliA}::P_{tac}$ promoter mutant. Class 2 and class 3 promoter activities in wild type (solid) and a $\Delta P_{fliA}::P_{tac}$ promoter mutant (dashed). Experiments were performed in triplicate with average value and standard deviations reported. All experiments were performed as described in Figure 5. **(B) Class 2 and class 3 promoter dynamics in wild type (solid) and a $\Delta P_{fliA}::P_{tac}$ promoter mutant (dashed) from our mathematical model.**

Chapter 4. Salmonella Pathogenicity Island 1 (SPI1)

Introduction

Salmonella enterica is a common food-borne pathogen that causes a wide array of diseases in humans, ranging from self-limiting gastroenteritis to life-threatening systemic infections (Zhou & Galan, 2001). The bacterium initiates infection by invading intestinal epithelial cells using a type 3 secretion system (T3SS) encoded within a forty kilobase region of the chromosome called *Salmonella* Pathogenicity Island 1 (SPI1) (Lee et al., 1992, Ginocchio *et al.*, 1994, Mills et al., 1995) (**Figure 12A**). The bacterium uses this T3SS to inject proteins into the cytoplasm of host cells (Kimbrough & Miller, 2000, Kimbrough & Miller, 2002, Sukhan et al., 2001). The secreted proteins are then able to commandeer the host cells' actin-cytoskeleton machinery and promote the uptake of the bacterium into these otherwise non-phagocytic cells (Zhou & Galan, 2001, Hayward & Koronakis, 2002). These secreted effector proteins mediate engulfment by collectively altering the regulation of the actin cytoskeleton (Cain *et al.*, 2008, Galan & Zhou, 2000, Zhou & Galan, 2001). Two *Salmonella* actin-binding proteins – SipA and SipC – are used to directly control cytoskeleton dynamics (Zhou *et al.*, 1999a, Zhou *et al.*, 1999b). In addition, further cytoskeleton control is achieved by the guanine exchange factors (GEF) mimics SopE and SopE2 and the inositol polyphosphatase mimic SopB that, together, activate Cdc42 and Rac1 Rho-family GTPases (Hardt *et al.*, 1998, Stender *et al.*, 2000,

Zhou *et al.*, 2001). After engulfment, the ATPase activating protein (GAP) mimic SptP is used to reverse these changes to the actin cytoskeleton and return the cell to its original state (Fu & Galan, 1999). Remarkably, these proteins achieve this regulation by mimicking the function of the host regulatory proteins even though they share no amino acid sequence similarity (Stebbins & Galan, 2001). Note that *Salmonella* also utilizes a second TTSS, encoded within *Salmonella* Pathogenicity Island 2 (SPI2), to persist and replicate within host cells (Ochman *et al.*, 1996, Shea *et al.*, 1996). In addition to the SPI1 T3SS, *Salmonella* also utilizes a second T3SS, encoded within *Salmonella* Pathogenicity Island 2 (SPI2), to survive and replicate within host cells during systemic infection (Hensel, 2000, Shea *et al.*, 1996).

The genes encoding for the SPI1 T3SS are tightly regulated by a network of interacting transcriptional regulators that are responsive to a combination of environmental and intracellular signals (Ellermeier *et al.*, 2005). These signals are presumably used by *Salmonella* as anatomical cues for initiating invasion and also for coordinating SPI1 gene expression with other cellular processes, most notably adhesion and motility (Iyoda *et al.*, 2001, Kovaleva, 1976, Ellermeier & Slauch, 2003, Baxter & Jones, 2005).

The master regulator for the SPI1 gene circuit is HilA, a transcription factor that contains a DNA binding motif belonging to the OmpR/ToxR family (Lee *et al.*, 1992) and a large C-terminal domain of unknown function (Daly & Lostroh, 2008). HilA activates

the expression of the genes encoding for the structural components of the SPI1 T3SS (Lee et al., 1992, Bajaj *et al.*, 1995, Ahmer *et al.*, 1999, Bajaj *et al.*, 1996). In addition, HilA also activates the expression of an AraC-like transcription factor, InvF, involved in regulating the expression of the SPI1 secreted effector proteins and their cognate chaperones (Darwin & Miller, 2000, Darwin & Miller, 2001). HilA expression, in turn, is regulated by three homologous, AraC-like transcription factors: HilC, HilD, and RtsA (Schechter & Lee, 2001, Olekhovich & Kadner, 2002, Ellermeier & Slauch, 2003). Both the *hilC* and *hilD* genes are encoded within SPI1 whereas *rtsA* is encoded elsewhere on the chromosome. These three transcription factors can independently activate HilA expression. They can also activate each others' and their own expression (Ellermeier et al., 2005). Specifically, HilC, HilD, and RtsA are all capable of individually activating expression from the P_{hilA} , P_{hilC} , P_{hilD} , and P_{rtsA} promoters. These auto-regulatory interactions result in three coupled positive feedback loops comprising HilC, HilD, and RtsA, the output of each capable of activating HilA expression. Of the three, HilD is dominant, as there is no HilA expression in its absence (Schechter *et al.*, 1999). This reflects that fact that many activating signals, both environmental and intracellular, affect SPI1 gene expression by modifying the activity of HilD protein (Behlau & Miller, 1993, Pegues *et al.*, 1995, Baxter *et al.*, 2003, Baxter & Jones, 2005, Ellermeier et al., 2005, Lim *et al.*, 2007, Ellermeier & Slauch, 2008, Lin *et al.*, 2008a).

In addition to positive regulation, SPI1 gene expression is also subject to negative regulation. HilA negatively regulates its own production, apparently by binding to the

P_{hilA} promoter and repressing transcription (De Keersmaecker et al., 2005). HilE, a protein of unknown structure encoded outside of SPI1, binds HilD (Baxter et al., 2003) and prevents it from activating the P_{hilD} , P_{hilC} , P_{rtsA} , and P_{hilA} promoters.

While the core architecture has been determined, the function of all of these interacting regulators and associated feedback loops comprising the circuit is still unknown (**Figure 12B**). Therefore, to understand their function, we measured gene expression dynamics at both population and a single-cell resolution in a number of SPI1 regulatory mutants. The results from these experiments show that a pulse in P_{hilD} promoter activity activates the SPI1 gene circuit. This pulse is then amplified by the positive feedback loops in the circuit, resulting in the rapid transition from the “off” to the “on” state. Differences in the timing of this activating signal among individual cells result in transient heterogeneity within the population, as some cells are induced more rapidly than others. Based on these experimental results, we constructed a simple mathematical model of the SPI1 gene circuit. Analysis of the model predicted that HilC and RtsA play a secondary role in SPI1 gene expression, serving to amplify the HilD signal. Our analysis also predicted that HilE sets a variable threshold for SPI1 activation. To experimentally test these two predictions, we remodeled the SPI1 network by swapping the promoters for *hilC* and *hilD*. Consistent with both predictions of our model, we find that HilC and HilD are not interchangeable due to differences in relative activity, and that only HilD is sufficiently strong to initiate activation of the SPI1 gene circuit. We also find that when HilD is expressed from the weak P_{hilC} promoter, it can

activate the circuit only in the absence of HilE. Interestingly, HilA expression dynamics are no longer switch-like but rather continuous in this mutant. Collectively, these results enable us to deconstruct this complex circuit and determine the role of its individual components in regulating SPI1 gene expression dynamics.

Results

Dynamics of SPI1 Gene Expression

To investigate the dynamics of SPI1 gene expression, we grew cells statically in Luria-Bertani (LB) medium using 1% NaCl as the inducing signal. Growth in low-oxygen and high-salt conditions has previously been shown to induce SPI1 gene expression *in vitro* (Bajaj et al., 1996, Lee et al., 1992). In these experiments, we grew the cells overnight in LB/no salt and then sub-cultured them into fresh LB/1% NaCl medium, thus inducing a transition from SPI1 repressing to SPI1 inducing conditions. We employed two different reporter systems to measure gene expression. In our bulk, population-level experiments, we measured gene expression using plasmid-based promoter fusions to the luciferase operon, *luxCDABE*, from *Photobacterium luminescens* (Winson et al., 1998, Saini et al., 2008). In our single-cell experiments, we employed promoter fusions to the green fluorescent protein (GFP) using an otherwise identical plasmid-based system (Miller & Lindow, 1997).

The advantage of using the luciferase reporter system is that it is sensitive to dynamic changes in promoter activity, particularly at low levels of expression (Hakkila et al., 2002). However, bacterial luciferase produces insufficient light for single-cell studies, hence the need for fluorescent reporters. We also note that the bacterial luciferase reporter system imposes a metabolic burden due to the production of the luciferase substrate, tetradecanal, by LuxC, LuxD, and LuxE (Meighen, 1991). To account for any

potential biases associated with bacterial luciferase, we repeated a number of population-level experiments using the GFP reporters with similar results (results not shown).

We measured gene expression dynamics in wild-type cells using the luciferase reporter system. After a brief lag following subculture, we found that the P_{hilD} and P_{hilA} promoters were activated in a sequential manner, consistent with HilD being necessary for HilA expression (**Figure 12C**). In the case of the P_{hilC} and P_{rtsA} promoters, we found that they were activated at roughly the same time as the P_{hilD} promoter. This hierarchy can also be seen when the expression values are normalized with respect to their maximal value (**Figure 12D**). These results indicate that there is a temporal hierarchy in SPI1 gene expression, with HilC, HilD, and RtsA at the top of the transcriptional cascade and HilA at the bottom. A similar hierarchy has also been observed in the activation of the downstream promoters regulating the expression of the genes encoding the T3SS and secreted effector proteins (Temme *et al.*, 2008).

We also measured wild-type gene expression dynamics using flow cytometry in order to determine how individual cells within the population behave during SPI1 induction. In the case of the P_{hilA} promoter, the dynamics were not continuous; rather, individual cells transitioned from an “off” to the “on” state in a switch-like manner (**Figure 13**). By switch-like, we mean that the individual cells exist in one of two expression states. At intermediate times, transient heterogeneity in the population is

observed, with most cells existing in either the “off” or “on” state. Similar switch-like dynamics were also observed for the P_{hilC} , P_{hilD} , and P_{rtsA} promoters, with a comparable hierarchy in activation times as observed in the population data (**Figure 13**). We note that heterogeneity in SPI1 gene expression has been previously observed by others (Hautefort *et al.*, 2003). As the SPI1 gene circuit involves multiple interacting positive feedback loops, these results are not surprising. In particular, positive feedback is known to be an integral element in many cellular switches (Mitrophanov & Groisman, 2008). To identify the genesis of this behavior, we further investigated the regulation of SPI1 gene expression.

Induction of the SPI1 Gene Circuit Begins with a Step Increase in P_{hilD} Promoter Activity

HilD is necessary for HilA expression. Even though HilC and RtsA can independently activate HilA expression when constitutively expressed from ectopic promoters, these two regulators are incapable of doing so in the absence of HilD when expressed from their native promoters (Ellermeier *et al.*, 2005). Therefore, to understand the role of HilD, we measured gene expression dynamics in a $\Delta hilD$ mutant using the luciferase reporters. In the case of the P_{hilA} promoter, we observed no activity in the absence of HilD (data not shown), consistent with previous results (Schechter *et al.*, 1999, Ellermeier *et al.*, 2005). In the case of the P_{hilD} promoter, we observed a weak, step-like increase in activity in the absence of HilD (**Figure 14A**). When we performed identical experiments using flow cytometry, we found that the P_{hilD} promoter again

transitions from an “off” to the “on” state in a switch-like manner (**Figure 14B**). These results are identical to what is observed in wild-type cells, the only difference being that the magnitude of expression is significantly reduced when HilD is not present. We also performed identical experiments in a Δ SPI1 Δ rtsA mutant and observed an identical response (**Figure 14C**), indicating that the transient switch in P_{hilD} promoter activity is not due to any SPI1 regulator but rather factors external to SPI1.

These results demonstrate that the SPI1 gene circuit is activated by a step input in P_{hilD} promoter activity. This signal is then amplified by a positive feedback loop involving HilD. As discussed below, HilC and RtsA serve to further amplify this signal. Interestingly, the heterogeneity in SPI1 activation is not due to the interacting positive feedback loops within the circuit but rather is intrinsic to the activating signal. The signals activating the P_{hilD} promoter, however, are unknown. While multiple global regulators are known to affect SPI1 gene expression (Ellermeier & Slauch, 2007), these regulators appear to affect the activity of the HilD protein and not its promoter (Ellermeier & Slauch, 2008, Baxter & Jones, 2005, Ellermeier et al., 2005, Lim et al., 2007, Lin et al., 2008b).

With regards to HilC and RtsA, we found that the P_{hilC} promoter was active in absence of HilD, though at a reduced level, whereas the P_{rtsA} promoter was effectively off (**Figure 14D**). However, even though the P_{hilC} promoter is active in the absence of HilD, HilA is not expressed. These results suggest that activation of the P_{hilD} promoter is

the trigger mechanism for induction of SPI1 gene expression. Interestingly, when we assayed P_{hilC} promoter activity in a $\Delta hilD$ mutant using flow cytometry, we found that the dynamics were not switch-like but rather continuous and rheostatic (**Figure 14E**). This homogeneity within the population indicates that the signal activating the P_{hilC} promoter is fundamentally different than the one activating the P_{hilD} promoter.

HilC and RtsA Function as Transcriptional Amplifiers and Accelerators

Unlike HilD, the HilC and RtsA proteins are not absolutely required for HilA expression. Yet, these two proteins can independently induce transcription from the P_{hilA} promoter when constitutively expressed from an ectopic promoter (Ellermeier et al., 2005). To understand the role of these two proteins in regulating SPI1, we compared gene expression in wild type and a $\Delta hilC \Delta rtsA$ mutant using the luciferase reporters (**Figure 15A**). Deleting these two regulators decreases the activity of the P_{hilD} and P_{hilA} promoters. Moreover, in the $\Delta hilC \Delta rtsA$ mutant, there is also a delay in the induction of the P_{hilA} promoter. This delay becomes more apparent when we normalize the luminescence measurements with respect to their maximal values (**Figure 15B**). When we measured gene expression at single-cell resolution using flow cytometry, we again observed a switch-like response in the $\Delta hilC \Delta rtsA$ mutant (**Figure 15C and 15D**). The main difference relative to wild type was that the transition from the “off” to “on” state occurred more slowly in the absence of HilC and RtsA. Also, the activity of the P_{hilA} promoter in the “on” state was lower in the $\Delta hilC \Delta rtsA$ mutant than in wild type. With the P_{hilD} promoter, we did not observe any change in the timing of promoter activation

in the $\Delta hilC \Delta rtsA$ mutant relative to wild type (**Figure 15E and 15F**). Rather, we observed only a decrease in the level of P_{hilD} promoter activity associated with the “on” state. Similar results for both promoters are observed in the single deletion mutants, though the overall effect is less, indicating that HilC and RtsA additively contribute to SPI1 gene expression. Based on these results, we conclude that HilC and RtsA serve two functions in the SPI1 circuit. First, HilC and RtsA amplify HilA and HilD expression. Second, they accelerate the transition of HilA expression from the “off” to the “on” state.

HilE Dampens SPI1 Gene Expression

We next investigated the role of HilE in the SPI1 gene circuit. HilE binds to HilD and prevents it from activating the P_{hilD} , P_{hilC} , P_{rtsA} , and P_{hilA} promoters (Baxter et al., 2003). As HilD is at the top of the SPI1 transcriptional cascade, HilE is able to repress the expression of all SPI1 genes. However, unlike the other regulators, HilE does not participate in a feedback loop, as its expression is not regulated by any SPI1 gene (data not shown). Rather, its expression is regulated by exogenous factors. For example, the type I fimbrial regulator, FimZ, increases HilE expression whereas the phosphoenolpyruvate phosphotransferase system (PTS) regulator, Mlc, represses it (Baxter & Jones, 2005, Lim et al., 2007, Saini *et al.*, 2009).

We compared gene expression using the luciferase assay in wild type and a $\Delta hilE$ mutant (**Figure 16A**). In the case of both the P_{hilD} and P_{hilA} promoters, we observed a

roughly two-fold increase in promoter activity in the absence of HilE. However, we found that HilE did not affect the timing of activation for these two promoters (**Figure 16B**). Similar results were observed in the flow cytometry experiments for the P_{hilD} and P_{hilA} promoters (**Figure 16C and 16D**) and the P_{hilC} and P_{rtsA} promoters (data not shown). These data suggest that HilE serves to dampen SPI1 gene expression by reducing the maximal level of promoter activity.

Computational Analysis of SPI1 Gene Circuit

The defining feature of the SPI1 gene circuit is the presence of three coupled positive feedback loops. An immediate question then is why are multiple loops present when most bacterial circuits have just one. To explore this question in more detail, we constructed a simple mathematical model of the SPI1 gene circuit based on our understanding of how it functions. The major assumptions used in formulating the model are enumerated below.

1. In formulating the model, we focused solely on the interacting SPI1 regulators - HilC, HilD, HilE, and RtsA - and their role in regulating *hilA* expression. In particular, we ignored the effects of additional external regulators (Altier, 2005, Ellermeier & Slauch, 2007). These external factors were accounted for implicitly in the model through our choice of the kinetic parameters. In other words, we assumed that there are no additional feedback loops beyond those detailed in **Figure 12A**. As a consequence, we treated these external regulators as constant inputs into the model. The validity of this

hypothesis is debatable, though there is insufficient evidence at this time to consider any reasonable alternatives. We also did not include the downstream SPI1 regulators – InvF and SicA – in the model. These downstream regulators do not appear to affect HilA expression. Rather, they are thought to regulate the timing of expression of the proteins comprising the SPI1 needle complex and the secreted effectors (Temme et al., 2008, Darwin & Miller, 2000, Darwin & Miller, 1999a). In these regards, the model focuses only on initiation and ignores assembly and secretion. It also does not account for the decrease in SPI1 gene expression seen when cells enter stationary phase (**Figure 12B**).

2. The model does not account for negative regulation by HilA and SprB. HilA, in particular, negatively regulates its own expression by apparently binding to the P_{hilA} promoter and repressing transcription (De Keersmaecker et al., 2005). Likewise, SprB, a transcription factor from the LuxR/UhaP family that is positively regulated by HilA, appears to bind to the HilD promoter and weakly repress its activity (Saini & Rao, 2010). Inclusion of these negative feedback loops does not substantively affect the results from our model and, for simplicity, we chose to ignore them in the model.

3. The model does not distinguish between transcription and translation. Both are lumped together in a single step. As a consequence, the rate of protein synthesis is assumed to be linearly proportional to the concentration of mRNA within the cell. Our justification for this assumption is that based on a number of unpublished observations,

we believe that regulation of HilD occurs primarily either at the transcriptional or the post-translational level (i.e. the level of HilD protein).

4. HilC, HilD, and RtsA are all AraC-like transcription factors and likely function only in the dimeric form. In the model, we assume for simplicity that the dimers form spontaneously and are stable (i.e. the dimerization reaction is irreversible). As a consequence, the model does not distinguish between the monomeric and dimeric forms; all protein is assumed to be in the dimeric form. We also do not account for the possible formation of heterodimers.

5. HilC and RtsA can independently induce HilA expression (Ellermeier et al., 2005). Yet, in the absence of HilD, HilA is not expressed even though *hilC* is transcribed (albeit at reduced levels). To account for HilD dominance (or rather dominant epistasis) in the model, we needed to assume that the SPI1 promoters have two binding sites with occupancy of both required for transcription. We specifically assumed that one site is highly specific for HilD with only weak affinity for HilC and RtsA. This first binding site establishes dominance as it effectively probes for whether HilD is present in the cell. Moreover, because of its high affinity, HilD will occupy this site even when expressed at low levels. Due to their weak affinity, neither HilC nor RtsA will occupy this site under physiological conditions. However, when over expressed, the elevated concentrations of these proteins will compensate for their weak affinity for this site, allowing them to bind. The second site, on the other hand, has moderate affinity for all three regulators

(with the affinity for HilD still the highest) and serves to tune expression in proportion to their aggregate concentration. Other alternatives are possible, though this model for promoter regulation offers perhaps the simplest mechanism to explain HilD dominance consistent with what we already know about SPI1 gene expression. Moreover, others have found that the SPI1 promoters contain multiple binding sites for the HilC, HilD, and RtsA (Schechter & Lee, 2001, Olekhovich & Kadner, 2002), so this assumption is not entirely implausible. Lastly, we note that while HilD dominance has been documented previously only in the case of the P_{hilA} promoter, our data suggests that it also extends to the P_{hilC} , P_{hilD} , and P_{rtsA} promoters as detailed below.

6. The most speculative aspect of the model concerns the mechanism for activation of the SPI1 promoters – P_{hilA} , P_{hilC} , P_{hilD} , and P_{rtsA} - by HilC, HilD, and RtsA. In the model, we assume that all four promoters have the same two binding sites, one highly specific for HilD and the other much less so (see Assumption 5). While there is no mechanistic data to support this hypothesis, we have found that the promoter activities are linearly proportional to one another when we compared them at varying levels of NaCl induction and in different genetic backgrounds (**Figure 17**). The simplest explanation for this linear correlation is that the binding mechanism is the same for all four promoters. As a consequence, we used the same mathematical expressions and parameters to model occupancy of the P_{hilA} , P_{hilC} , P_{hilD} , and P_{rtsA} promoters by the SPI1 regulators. Aside from our supporting data, we significantly reduce the number of free parameters in the model by invoking this assumption.

7. The model assumes that HilE not only binds and inhibits HilD but also promotes its degradation. While there is no experimental data to support such a mechanism, we found it necessary to match our experimental results for the $\Delta hilE$ mutant. In the absence of such a mechanism, we found that the steady-state concentrations of HilD and HilA were not affected by HilE, a result contrary to experimental observations.

8. The model assumes that the transient heterogeneity observed in the gene expression data is due solely to asynchrony in the timing of the activation signal. To model this behavior, we assumed that the P_{hilD} promoter is activated at random times in individual cells, where the activation times are exponentially distributed. Likewise, we assumed that the P_{hilC} promoter is activated in a deterministic manner. For simplicity, we assumed that both promoters have, on average, the same activation kinetics. Beyond asynchrony in the timing of activation, we do not believe that noise arising from any number of possible sources plays a critical role in SPI1 gene expression beyond introducing variability in the gene expression measurements (see below).

9. To qualitatively compare the simulation results with our flow cytometry data, we employed density estimation using a Gaussian kernel with fixed bandwidth. This method replaces each data point with a Gaussian basis function of constant variance. While this method is typically used to smooth data, namely to approximate a discrete

histogram with a continuous function, we employed it to artificially introduce noise into our model. Our motivation was simply to obtain a better qualitative fit to the flow cytometry data where, aside from the heterogeneity, we observed variable gene expression in individual cells. While we do not believe this variability is significant for understanding how the circuit functions, we nonetheless attempted to capture it in our model. As do not know the origins of this variability (e.g. stochastic gene expression, measurement error, etc), we simply assumed that there was an additive Gaussian noise term in the model, effectively what density estimation does.

We note that Mande and coworkers previously published a mathematical model of the SPI1 gene circuit (Maithreye & Mande, 2007, Ganesh *et al.*, 2009). While there is substantial overlap between their model and ours, the Mande model does not account for the critical role of positive feedback on HILF expression, a key finding in our experimental investigations. More significantly, their model does not include HILF. As a consequence, the major conclusion drawn from the analysis of our model regarding the activation threshold cannot be obtained from theirs.

Model Equations.

The governing equations for the model are the following:

$$\frac{dD}{dt} = \alpha_D H(t - t_\lambda) + k_D O_1 O_2 - \delta_D D - a_E D \times E + d_E ED, \quad (6)$$

$$\frac{dE}{dt} = \alpha_E - \delta_E E - a_E D \times E + d_E ED, \quad (7)$$

$$\frac{dC}{dt} = \alpha_C \left(1 - e^{-t/\lambda}\right) + k_C O_1 O_2 - \delta_C C, \quad (8)$$

$$\frac{dR}{dt} = k_R O_1 O_2 - \delta_R R, \quad (9)$$

$$\frac{dA}{dt} = k_A O_1 O_2 - \delta_A A, \quad (10)$$

$$\frac{dED}{dt} = a_E D \times E - d_E ED - \delta_E ED, \quad (11)$$

$$\frac{dG}{dt} = \alpha_D + k_D O_1 O_2 - \delta_G G, \quad (12)$$

where t denotes time and the state variable D denotes the concentration of HilD, E the concentration of HilE, C the concentration of HilC, R the concentration of RtsA, A the concentration of HilA, ED the concentration of the HilE-HilD complex, and G the concentration of the luciferase reporter for the P_{hilD} promoter. We included this last state variable, G , to better match the model to our experimental data. Otherwise, we needed to account for the fraction of HilD bound to HilE (ED) and the associated differences in the stabilities of the respective moieties. The variable t_λ is used to denote an exponentially random distributed with a rate parameter λ and $H(\bullet)$ the Heaviside step function. The occupancy state of the two respective binding sites within the SPI1 promoters are given by the following equilibrium expressions

$$O_1 = \left(\frac{K_{O1}^D D + K_{O1}^C C + K_{O1}^R R}{1 + K_{O1}^D D + K_{O1}^C C + K_{O1}^R R} \right) \quad (13)$$

and

$$O_2 = \left(\frac{K_{O_2}^D D + K_{O_2}^C C + K_{O_2}^R R}{1 + K_{O_2}^D D + K_{O_2}^C C + K_{O_2}^R R} \right) \quad (14)$$

With regards to the model parameters, insufficient data are available to accurately and uniquely estimate them. However, as our goal was simply to construct a model that captured the general trends observed in the data, we simply choose numerical values for the parameters that provided a good qualitative fit. In these regards, the model is only semi-quantitative given the subjective basis of our parameterization. That said, the model captures our current understanding of the SPI1 gene circuit and provides a reasonable fit to the data as documented in the main text.

The model is qualitatively consistent with our experimental results, both with respect to the relative timing of HilD, HilC, RtsA, and HilA induction (**Figure 18A-C**) as well as the effects of mutations on HilD and HilA expression (**Figure 18D-E**) at both population and single-cell resolution.

In constructing this model, we assumed that asynchronous activation of the P_{hilD} promoter in individual cells causes the transient heterogeneity observed in SPI1 gene expression. We specifically assumed that the P_{hilD} promoter is activated at random times in individual cells, where the times are exponentially distributed. Otherwise, the model is entirely deterministic. To capture the heterogeneous response, we also needed to

assume that the switch from the “off” to “on” state occurs very rapidly. Otherwise, the population will respond homogeneously as differences in the timing of the activating signal in individual cells would be smoothed out due to the slow kinetics of the circuit. As our results demonstrate, this mechanism is sufficient for generating transient heterogeneity. In fact, if the P_{hilD} promoter is activated in all cells at the same time or the kinetics of the switch are too slow, then the population behaves homogeneously (**Figure 19A and 19B**). In the case of the P_{hilC} promoter, we assumed that it was activated at the same time in all cells. While transient heterogeneity is observed in wild type cells, the P_{hilC} promoter behaves homogeneously in a $\Delta hilD$ mutant. Our model is also able to capture this behavior (**Figure 19C and 19D**).

Our goal in constructing this model was not simply to recapitulate our experimental results but rather to explore the behavior of the circuit by simulating it over a range of different parameter values. When performing this parametric analysis, we found it most informative to focus on the steady-state behavior of the SPI1 gene circuit as this enabled us to explore the effect of two model parameters at the same time. We also confined our analysis to the parameters characterizing the regulatory topology of the circuit and not those defining the dynamics (e.g. degradation and protein-protein association/disassociation rates).

We first considered the role of positive feedback on HilD expression, given the central role of this SPI1 regulator. To perform this analysis, we varied the degree by

which the SPI1 regulators - HilC, HilD, and RtsA - could activate HilD expression by simulating the model at different values for the parameter k_D . When interpreting these results, we found it informative to also vary the strength of the activating signal in our simulations, given by the parameter α_D in the model. As shown in **Figure 20A**, HilD expression increases as the value of the parameter k_D increases, equivalent to increasing the strength of the feedback on HilD expression. When this feedback is sufficiently strong, the response to the activating signal becomes discontinuous and switch-like, the result of a supercritical pitchfork bifurcation (Strogatz, 2001). These results suggest that, in addition to amplifying the response, positive feedback may serve, along with HilE as described below, to endow the SPI1 circuit with an activation threshold. This threshold would ensure that SPI1 gene expression occurs only when a sufficiently strong activating signal is present. Moreover, the threshold decreases as the strength of the feedback increases, indicating that there is tradeoff between the degree of amplification and size of the threshold.

Next, we explored the role of HilC and RtsA on SPI1 gene expression by varying the strength of their connectivity within the circuit. Specifically, we varied the degree by which the SPI1 regulators – HilD, HilC and RtsA - could enhance both HilC and RtsA gene expression, given respectively by the parameters k_C and k_R in the model. As HilC and RtsA both have a weaker effect on SPI1 gene expression than HilD, the degree of amplification is also less strong though the overall trend is the same (**Figure 20B**). Similar results are also obtained when the expression of only one protein is varied,

though the effect then is even weaker (data not shown). These results suggest that HilC and RtsA serve to fine tune SPI1 gene expression. A useful analogy here is to consider the fine and coarse focusing knobs on a microscope, where HilC and RtsA provide the fine-tune control and HilD the coarse control. This may explain why HilC and RtsA have a significantly weaker effect on SPI1 gene expression than HilD as the circuit is more robust than one with three strong regulators in the sense that only a single regulator defines the behavior of the circuit whereas the others simply tune the output.

Last, we explored the effect of HilE on SPI1 gene expression. Unlike the other SPI1 regulators, HilE is not known to be involved in any feedback loops with the other SPI1 regulators. Rather, its expression is controlled by exogenous factors. In our simulations, we varied the rate of HilE expression, given by the parameter α_E in the model. Consistent with its role as a negative regulator, HilE decreased both HilD and HilA expression in a dose-dependent manner (**Figures 20C and 21C**). In addition, when expressed at a sufficiently high rate, HilE effectively shuts off the expression of HilD and HilA, a result that we also observe experimentally (data not shown). Most notably, our model predicts that HilE sets the threshold for SPI1 activation - as the rate of HilE expression increases so does the threshold for activation and vice versa. The exogenous factors regulating HilE expression, therefore, may serve to tune this activation threshold. However, we note that HilE alone does not endow the SPI1 circuit with a threshold. Rather, the threshold results from the complex interplay between HilE and the HilD positive feedback loop (**Figure 21D**).

Taken together, these results allow us to assign putative function to the interacting regulators and associated feedback loops comprising the SPI1 gene circuit. When viewed as a whole, the circuit appears to serve two functions. The first is to place a threshold on SPI1 activation, ensuring that the assembly of the needle complex is initiated only in response to the appropriate combination of environmental and cellular cues. The second is to amplify SPI1 gene expression.

Rewiring the SPI1 Gene Circuit

Our computational analysis predicts that SPI1 gene circuit functions as a gene expression amplifier with a variable activation threshold. While our experimental results directly support the conclusion regarding gene amplification, the one concerning the activation threshold is not evident from our experimental results, and thus derives solely from analysis of the model. Therefore, to test this prediction regarding the threshold experimentally, we rewired the SPI1 gene circuit by replacing the P_{hilD} promoter with the weaker P_{hilC} promoter at its native chromosomal locus in an otherwise $\Delta hilC$ background. In this mutant, ($\Delta P_{hilD}::P_{hilC} \Delta hilC$), *hilD* is transcriptionally regulated in a manner similar to *hilC*. If the circuit does indeed function to place a threshold on activation, then we expect that this mutant will be unable to induce HilA expression if the activating signal for the P_{hilC} promoter is too weak to overcome the threshold.

We found the P_{hilA} promoter is not active in this strain (**Figure 22A**), suggesting that the P_{hilC} activating signal is too weak to overcome the threshold as hypothesized. If true, then according to our model, removing HilE should enable HilA expression as it sets the activation threshold. In agreement with our model predictions, we found that if the *hilE* gene is removed then the P_{hilA} promoter is active in a related strain ($\Delta P_{hilD}::P_{hilC} \Delta hilC \Delta hilE$) (**Figure 22A**). In other words, by removing the threshold set by HilE, HilD is capable of inducing HilA expression when expressed from the weaker P_{hilC} promoter. However, when the threshold is present, HilD is not expressed at sufficiently high levels to overcome this threshold.

When we measured gene expression in this strain ($\Delta P_{hilD}::P_{hilC} \Delta hilC \Delta hilE$) using flow cytometry, we no longer observed the transient heterogeneity found in wild type. Rather, we found that the population responded homogeneously (**Figure 22B**). As we have previously noted, the input signal to the P_{hilC} promoter is not switch-like but instead is homogenous and rheostatic in nature. These results further support our hypothesis that the switch-like dynamics observed in wild type is due to asynchronous activation of the P_{hilD} promoter and not intrinsic to the circuit. In particular, when *hilD* is expressed from the P_{hilC} promoter then *hilA* expression is also not switch-like and instead homogenous and rheostatic. Thus, the characteristics of the output of the circuit match the input. In other words, the qualitative dynamics of the input driving *hilD* expression are also observed in the network output, namely *hilA* expression. Collectively, these results support our conclusion that the SPI1 gene circuit functions as

a genetic amplifier with an activation threshold, where the circuit magnifies the activating signal only if this signal exceeds a defined threshold.

A remaining question concerns the uniqueness of the SPI1 regulators given their similarity to one another. Namely, to what degree are HilC, RtsA, and HilD interchangeable? Of the three, HilD is the most important as HilA is not expressed in its absence. In formulating the model, we needed to assume that HilD was dominant in the sense that it was required for activating HilA expression. We also found that we needed to assume that HilD was necessary for establishing connectivity within the network, where it was again required for activating the P_{hilC} , P_{hilD} , and P_{rtsA} promoters by the other SPI1 regulators. HilC and RtsA, on the other hand, appear to play an ancillary role in regulating SPI1 gene expression. These two proteins simply tune gene expression in a HilD-dependent manner. One specific question then is whether this behavior is intrinsic to these proteins, as assumed in the model, or simply due to these proteins not being expressed at sufficiently high levels (as HilC and RtsA can independently activate SPI1 gene expression when over expressed).

To explore this issue in more detail, we rewired the SPI1 gene circuit by placing HilC under the control of the P_{hilD} promoter. In this reciprocal design, we replaced the P_{hilC} promoter with the P_{hilD} promoter at its native chromosomal locus in an otherwise $\Delta hilD$ background ($\Delta P_{hilC}::P_{hilD} \Delta hilD$). The rationale behind this promoter replacement experiment was to see whether HilC alone could induce HilA expression if expressed

from the P_{hilD} promoter. As HilD is capable of inducing HilA expression in absence of HilC or RtsA, we reasoned that HilC may be able to do the same in the absence of HilD if it is transcribed in a manner similar to *hilD*. However, despite trying a number of different designs where different sections of the promoter region were replaced, we were unable to engineer such a strain where the P_{hilA} promoter was active in the absence of HilD (data not shown). These results lend credence to our hypothesis regarding HilD dominance used in formulating the model, namely that HilD is necessary for activating the SPI1 promoter under physiological conditions.

Discussion

Using a combination of experimental and computational approaches, we found that the SPI1 gene circuit functions as a signal amplifier with a variable activation threshold (Saini, 2010). This virulence switch likely ensures that the SPI1 T3SS is assembled only when the bacterium has reached its target site for invasion, the distal small intestine (Carter & Collins, 1974). *Salmonella* is thought to be able to determine its location within the host by sensing a number of environmental factors, key among them oxygen and osmolarity (Bajaj et al., 1996). In addition to these environmental signals, SPI1 gene expression is also coordinated with other cellular processes such as motility and adhesion (Lin et al., 2008b, Lucas et al., 2000, Iyoda et al., 2001, Ellermeier & Slauch, 2003, Baxter & Jones, 2005, Saini et al., 2009). The accumulated evidence to date, including the results from this study, indicates that HilD is the primary site for signal integration. According to our model, these activating signals, both intracellular cellular and environmental, initiate SPI1 gene expression by inducing the expression and activation of HilD through still unknown mechanisms. HilE, however, binds to HilD and inhibits its activity. Only when the strength of the activating signals is sufficiently large is HilD expressed at a high enough level to overcome sequestration by HilE and activate the expression of the other SPI1 regulators – HilC, RtsA, and HilA - and also further induce its own expression. Once induced, HilC and RtsA serve to further amplify and also accelerate SPI1 gene expression. The result is a two-state switch with a defined activation threshold, defined in the sense that the threshold is set by the level of HilE

expression and possibly other systems that function through HilD protein (Ellermeier & Slauch, 2007).

A notable feature of the SPI1 gene circuit is the presence of three, coupled positive feedback loops. At the most fundamental level, positive feedback amplifies the response to an external signal (Becskei *et al.*, 2001, Maeda & Sano, 2006). It is also capable of effectively transforming a continuous input into a digital output when the feedback is sufficiently strong. In the context of bacterial gene circuits, positive feedback has most often been associated with multi-stable switches and cell population heterogeneity (Mitrophanov & Groisman, 2008, Dubnau & Losick, 2006). What makes the SPI1 gene circuit particularly intriguing is that most bacterial systems utilizing positive feedback, at least those documented so far in the literature, possess only a single loop.

We first note that these additional feedback loops, namely the ones regulating the expression of HilC and RtsA, do not add redundancy to the circuit, as the loss of HilD effectively shuts off SPI1 gene expression. Rather, they serve to further amplify and accelerate SPI1 gene expression. *In vivo*, loss of either HilC or RtsA does not significantly attenuate intestinal invasion. Yet, loss of both does (Ellermeier *et al.*, 2005), indicating that the amplification or acceleration provided by these loops plays an important physiological role. Whether this role is simply to ensure that the SPI1 structural genes

are expressed at sufficiently high levels or to provide a sharp activation threshold is still unknown.

Only a few studies to date, mostly focused on eukaryotic systems where this regulation is more common, have explored systems employing coupled positive feedback (Brandman *et al.*, 2005, Cui *et al.*, 2008, Thomas *et al.*, 1995, Tian *et al.*, 2009). In one notable theoretical study, the coupling of a slow and fast positive feedback loop was shown to yield a “dual-time” switch that is capable of being rapidly induced yet still is robust to fluctuations in the activating signal (Brandman *et al.*, 2005). However, these properties are not obtained when two loops of the same type are coupled. While rapid induction is observed in SPI1 gene expression, there is no evidence to suggest that some loops are fast whereas others are slow. Furthermore, these loops do not operate synergistically in the sense that coupling in the SPI1 gene circuit does not engender new functions unattainable with just a single loop.

As the loops involving HilC and RtsA only additively contribute to the response, we imagine that the coupling in SPI1 may result instead from the piecemeal evolution of the circuit. According to this model, HilC and RtsA were acquired to compensate for the inability of HilD alone to mediate a robust response. The motivation for this model comes from a recent study where a synthetic gene circuit coupling two weak positive feedback loops was engineered (Chang *et al.*, 2009). The authors found that their coupled circuit yielded a bistable response that, in the case of a single loop circuit, could

be obtained only with an ultrasensitive activator even though the individual regulators in the coupled circuit lacked this behavior. Based on these results, the authors speculated that natural circuits could evolve using a similar approach - rather than evolve a circuit with a single regulator requiring precise biochemical properties, a more robust and facile solution may be obtained by simply linking together multiple regulators that alone lack the requisite properties. Similarly, others have shown that by changing regulatory architecture of a circuit one can affect its behavior without commensurate changes in the underlying proteins (Wu & Rao, 2010, Mitrophanov *et al.*, 2008, Kato *et al.*, 2007). We hypothesize that a similar process may have occurred with the SPI1 gene circuit. As such, this model provides a possible explanation as to why the circuit involves multiple feedback loops when one alone would suffice.

In a related study, we found that the gene circuit controlling the expression of type I fimbriae in *Salmonella* utilizes two coupled positive feedback loops (Saini *et al.*, 2009). In this system, the expression of the genes encoding the type I fimbriae is controlled by two regulators, FimY and FimZ. These two proteins form two coupled positive feedback loops and encode a logical AND gate or, alternatively, a coincidence circuit. A similar logic may also be encoded within the SPI1 gene circuit. In particular, HilC is expressed in the absence of HilD. Moreover, the signals activating the P_{hilC} promoter appear to be different than the ones activating the P_{hilD} promoter, given their dissimilar dynamics. We are tempted therefore to speculate that, in addition to being an amplifier, the SPI1 gene circuit may also function as some sort of coincidence

circuit, optimally expressing SPI1 genes only when the activating signals for both the P_{hilC} and P_{hilD} promoter are present. Coupled feedback in this case would reinforce the effect of these signals and further link the two. While such a model alone would not explain why multiple feedback loops are present in the SPI1 gene circuit, it may nonetheless provide one possible advantage for such a design.

In conclusion, we have been able to propose an integrated model for the regulation of SPI1 gene expression. While this system has been studied extensively, an integrated model of its regulation was previously lacking. Using a combination of experimental and computational analyses, we have been able to deconstruct this complex circuit and determine how the individual components contribute towards its integrated function. A key element in our analysis involved rewiring the SPI1 genetic circuit. As the kinetic parameters are unavailable and difficult to perturb, direct validation of our model remains an elusive challenge. However, by rewiring the circuit, we were nonetheless able to test a number of predictions from our mathematical model. Such an approach provides a powerful framework for integrating models with experimental data, particularly when parameters values are lacking or difficult to perturb. Finally, our results provide a detailed examination of a natural system employing coupled positive feedback, a mechanism of control that to date has primarily been investigated in eukaryotes.

Figures - Salmonella Pathogenicity Island 1 (SPI1)

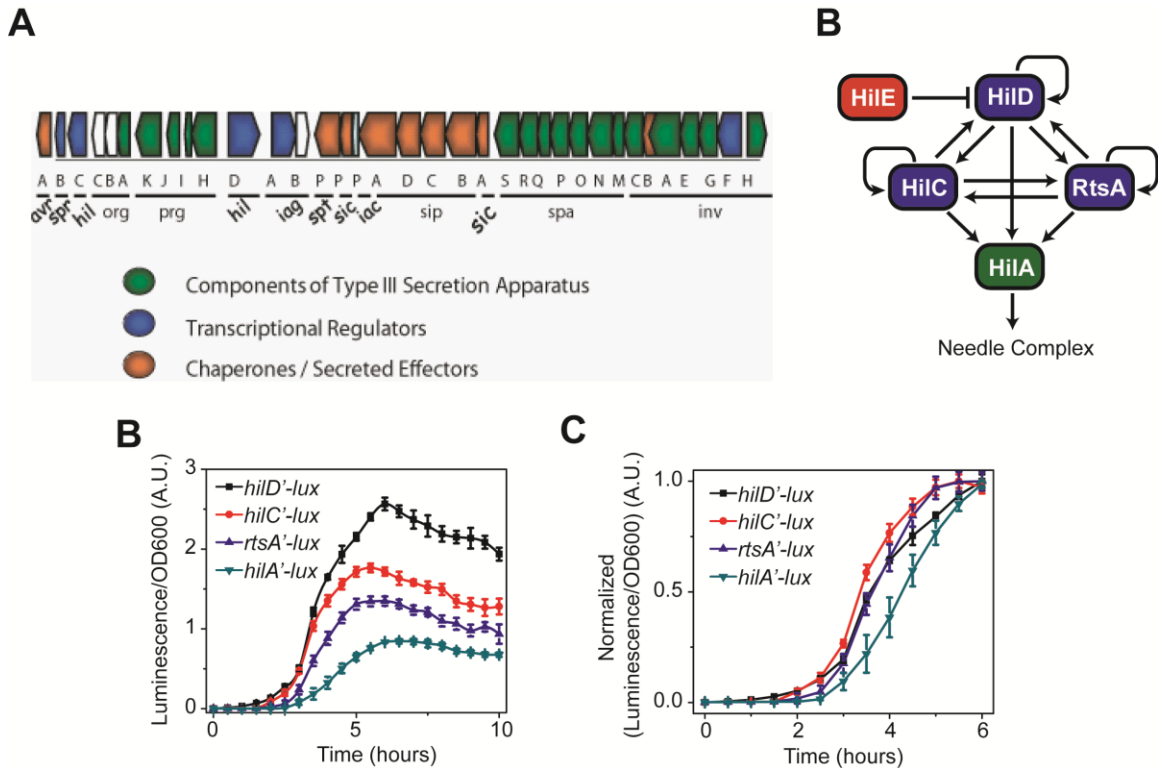


Figure 12. (A) Salmonella Pathogenicity Island-1 (SPI1). SPI1 is a 40kb fragment on the chromosome that encodes all the proteins necessary for assembly of a functional T3SS. Also encoded on SPI1 are transcription factors that control gene expression, and effector proteins and their cognate chaperones. **(B) Diagram of SPI1 gene circuit.** HilA is the master SPI1 regulator as it activates the expression of the genes encoding the TS33. HilA, in turn, is regulated by HilC, HilD, and RtsA. These three regulators can independently activate HilA expression. They can also activate their own expression and that of each other. HilE represses the activity of HilD by binding to it and preventing it from activating to its target promoters. **(C) Time-course dynamics of P_{hilD} (pSS074), P_{hilC} (pSS075), P_{rtsA} (pSS076), and P_{hilA} (pSS077) promoter activities in wild-type cells as determined using luciferase transcriptional reporters.** To induce SPI1 gene expression, cells were first grown overnight in LB/no salt and then sub-cultured into fresh LB/1% NaCl conditions to an OD of 0.05 and grown statically. Luminescence values were normalized with the OD₆₀₀ absorbance to account for cell density. Average promoter activities from three independent experiments on separate days are reported. For each experiment, six samples were tested. Error-bars indicate standard deviation. **(D) Normalized promoter activities (data in the Figure 1A was normalized to one for each promoter)**

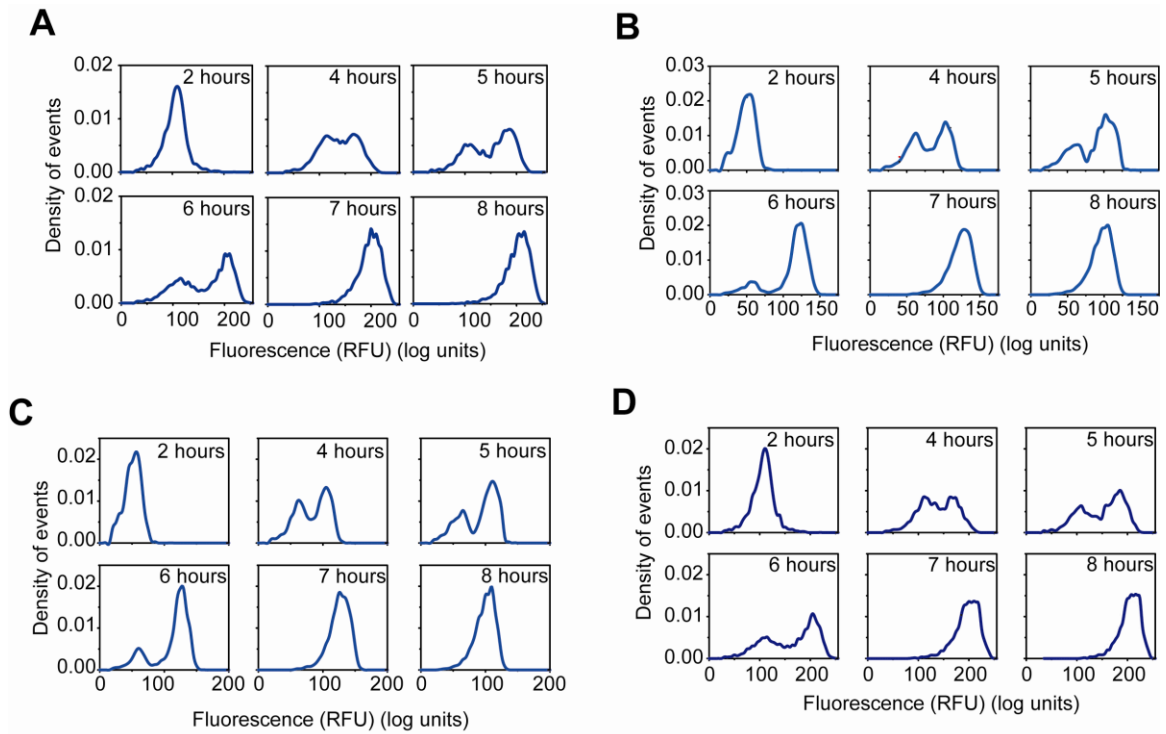


Figure 13. Dynamics of (A) P_{hilA_r} , (B) P_{hilD_r} , (C) P_{hilC_r} and (D) P_{rtsA} promoter activity in wild-type cells as determined using green fluorescent protein (GFP) transcriptional fusions and flow cytometry. The SPI1 gene expression was induced as described above. Samples were collected at the indicated times and arrested in their respective state by addition of chloramphenicol. Approximately 30,000 cell measurements were used to construct each histogram.

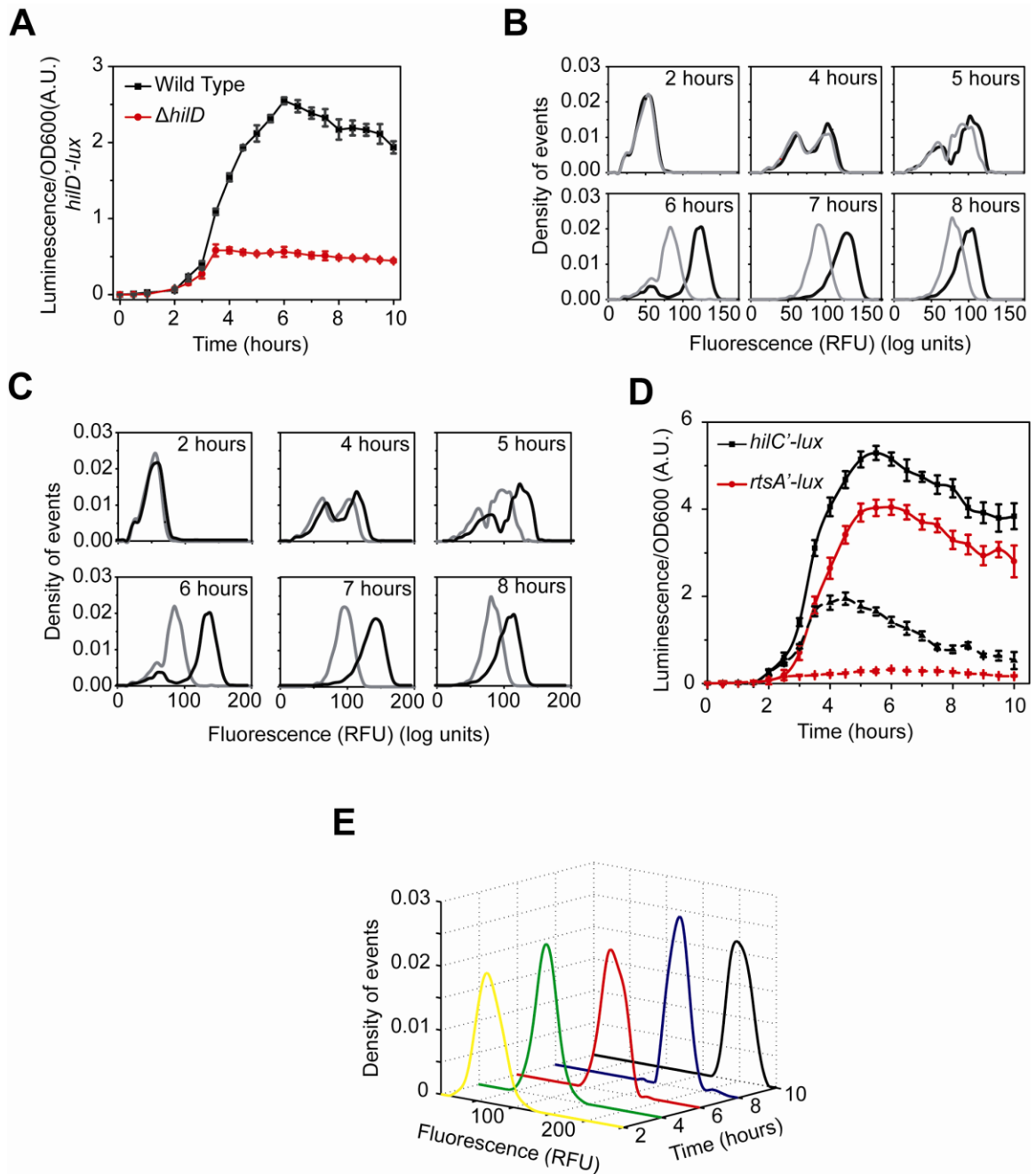


Figure 14. (A) Comparison of time-course dynamics for P_{hilD} (pSS074) promoter activities in wild type (black) and a $\Delta hilD$ mutant (JS253, red) as determined using luciferase transcriptional reporters. (B) Comparison of P_{hilD} (pSS072) promoter activity in wild type (black) and a $\Delta hilD$ mutant (JS253, grey) as determined using GFP transcriptional reporters and flow cytometry. Note that the activation of the P_{hilD} promoter is switch-like both in wild type and the $\Delta hilD$ mutant. (C) Comparison of time-course dynamics of P_{hilD} (pSS072) promoter activities in wild type (black) and a $\Delta SPI1 \Delta rtsA$ mutant (CR349, grey) as determined using green fluorescent protein (GFP) transcriptional fusions and flow cytometry. (D) Comparison of P_{hilC} (pSS075, black) and P_{rtsA} (pSS076, red) promoter

activities in wild type (solid lines) and a $\Delta hilD$ mutant (JS253, dashed lines). Note that the P_{rtsA} promoter is off in the absence of HilD. **(E)** Dynamics of P_{hilC} (pSS073) promoter activities in a $\Delta hilD$ mutant (JS253) as determined using green fluorescent protein (GFP) transcriptional fusions and flow cytometry. Note that, in the absence of HilD, the activation of the P_{hilC} promoter is no longer switch-like but instead continuous.

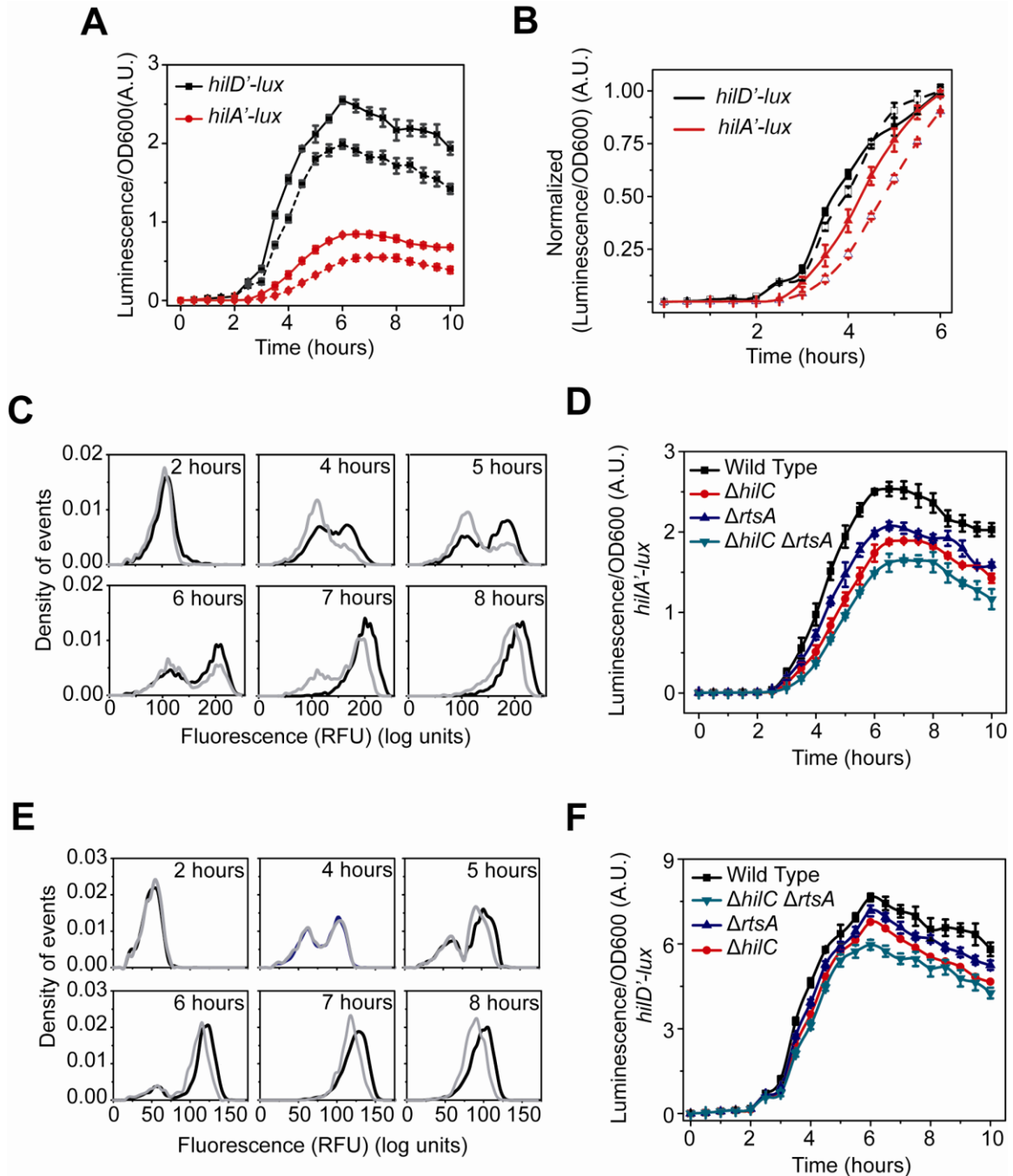


Figure 15. (A) Comparison of time-course dynamics for P_{hilD} (pSS074, black) and P_{hilA} (pSS077, red) promoter activities in wild type (solid lines) and a $hilC \Delta rtsA$ mutant (CR350, dashed lines) as determined using luciferase transcriptional reporters. (B) Normalized P_{hilD} and P_{hilA} promoter activity in wild type (solid) and $\Delta hilC \Delta rtsA$ (dashed) mutant. (C and E) Comparison of P_{hilA} (pSS055, C) and P_{hilD} (pSS072, E) promoter activities in wild type (black) and a $\Delta hilC \Delta rtsA$ mutant (CR350, grey) as determined using GFP transcriptional reporters and flow cytometry. Note that the loss of HilC and RtsA causes a delay and decrease in P_{hilA} promoter activity whereas it causes only a

decrease in activity in the case the P_{hilD} promoter. **(D)** Comparison of time-course dynamics of P_{hilA} (pSS077) promoter activities in wild type and $\Delta rtsA$ (JS248), $\Delta hilC$ (JS252), $\Delta hilC \Delta rtsA$ (CR350), and $\Delta hilD$ (CR253) mutants as determined using luciferase transcriptional reporters. **(F)** Comparison of time-course dynamics of P_{hilD} (pSS074) promoter activities in wild type and $\Delta rtsA$ (JS248), $\Delta hilC$ (JS252), $\Delta hilC \Delta rtsA$ (CR350), and $\Delta hilD$ (CR253) mutants as determined using luciferase transcriptional reporters.

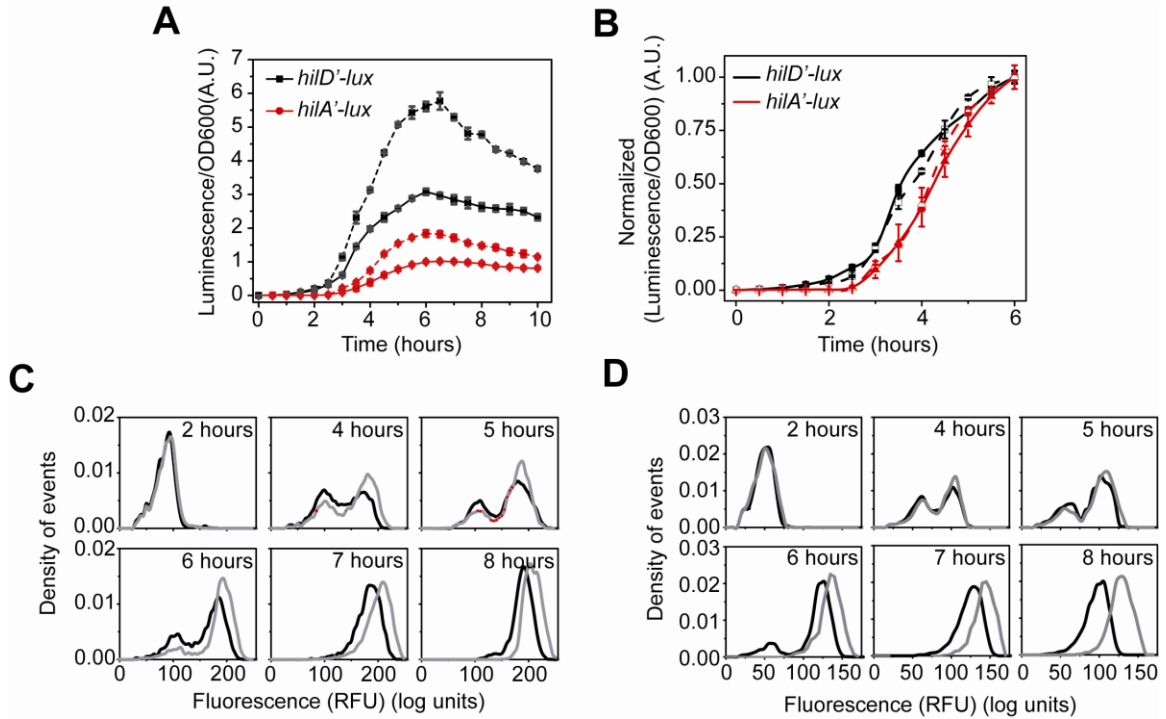


Figure 16. (A) Comparison of time-course dynamics for P_{hilD} (pSS074, black) and P_{hilA} (pSS077, red) promoter activities in wild type (solid lines) and a $\Delta hilE$ mutant (CR361, dashed lines) as determined using luciferase transcriptional reporters. **(B)** Normalized P_{hilD} and P_{hilA} promoter activities in wild type (solid) and $\Delta hilE$ (dashed) mutant. **(C)** Comparison of P_{hilA} (pSS055) promoter activities in wild type (black) and a $\Delta hilE$ mutant (CR361, grey) as determined using GFP transcriptional reporters and flow cytometry. **(D)** Comparison of P_{hilD} (pSS072) promoter activities in wild type (black) and $\Delta hilE$ (CR361, grey) mutant as determined using green fluorescent protein (GFP) transcriptional fusions and flow cytometry.

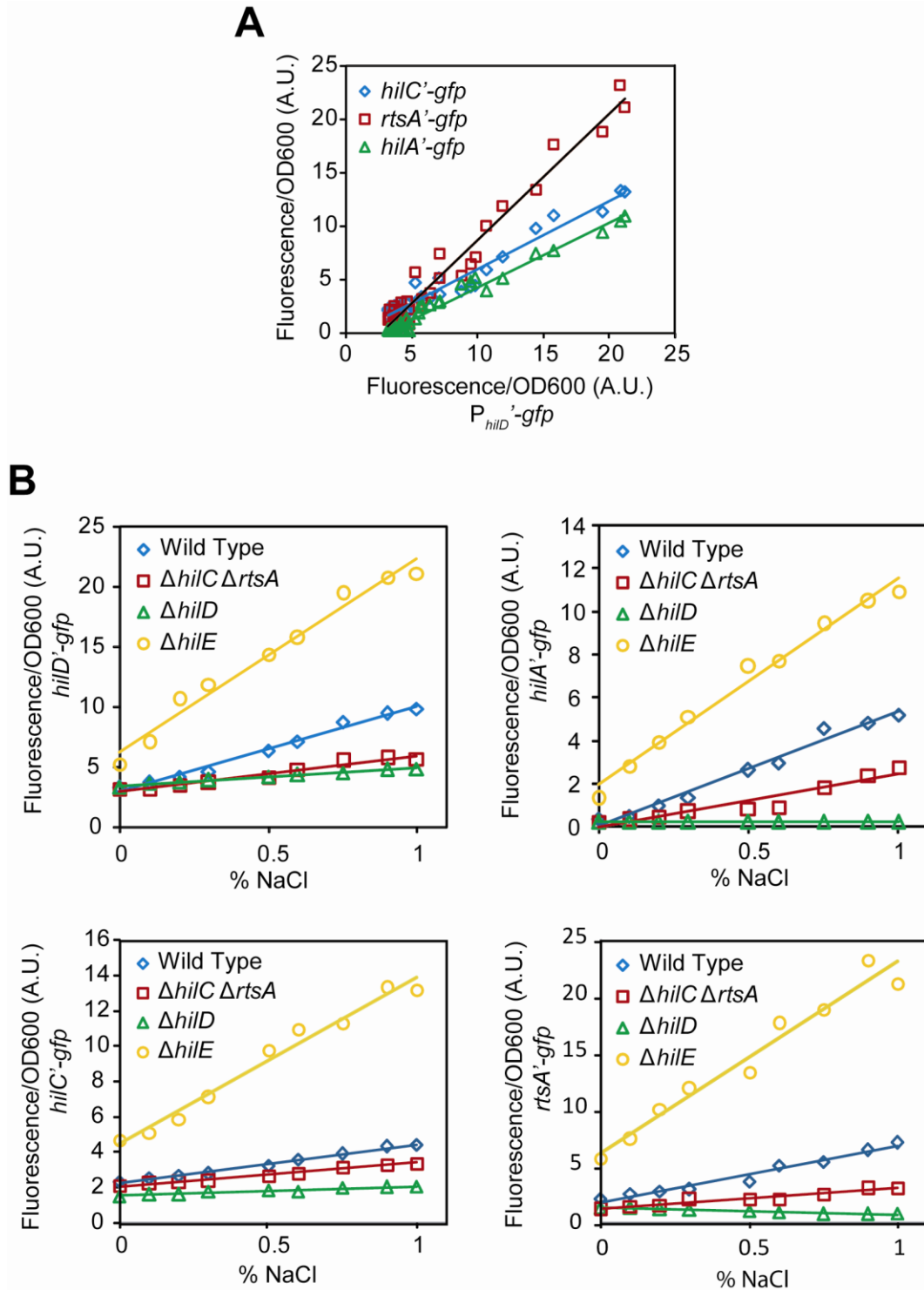


Figure 17. (A) Correlation of P_{hilD} (pSS052) promoter activity with P_{hilA} (pSS055), P_{hilC} (pSS053), and P_{rtsA} (pSS054) promoter activities. To induce SPI1 gene expression, cells were first grown overnight in LB/no salt and then sub-cultured into fresh LB at varying concentrations of NaCl to an OD of 0.05 and grown statically for 15 hours. Individual experiments used to construct correlations are given in Panels B-E. **(B-E)** Comparison of

P_{hilD} (pSS052, B), P_{hilC} (pSS053, C), P_{hilA} (pSS055, D), and P_{rtsA} (pSS054, E) promoter activities at varying concentration of NaCl and in different mutant backgrounds as determined using GFP transcriptional reporters. Fluorescence values were normalized with the OD600 absorbance to account for cell density. Data is the average of three independent experiments.

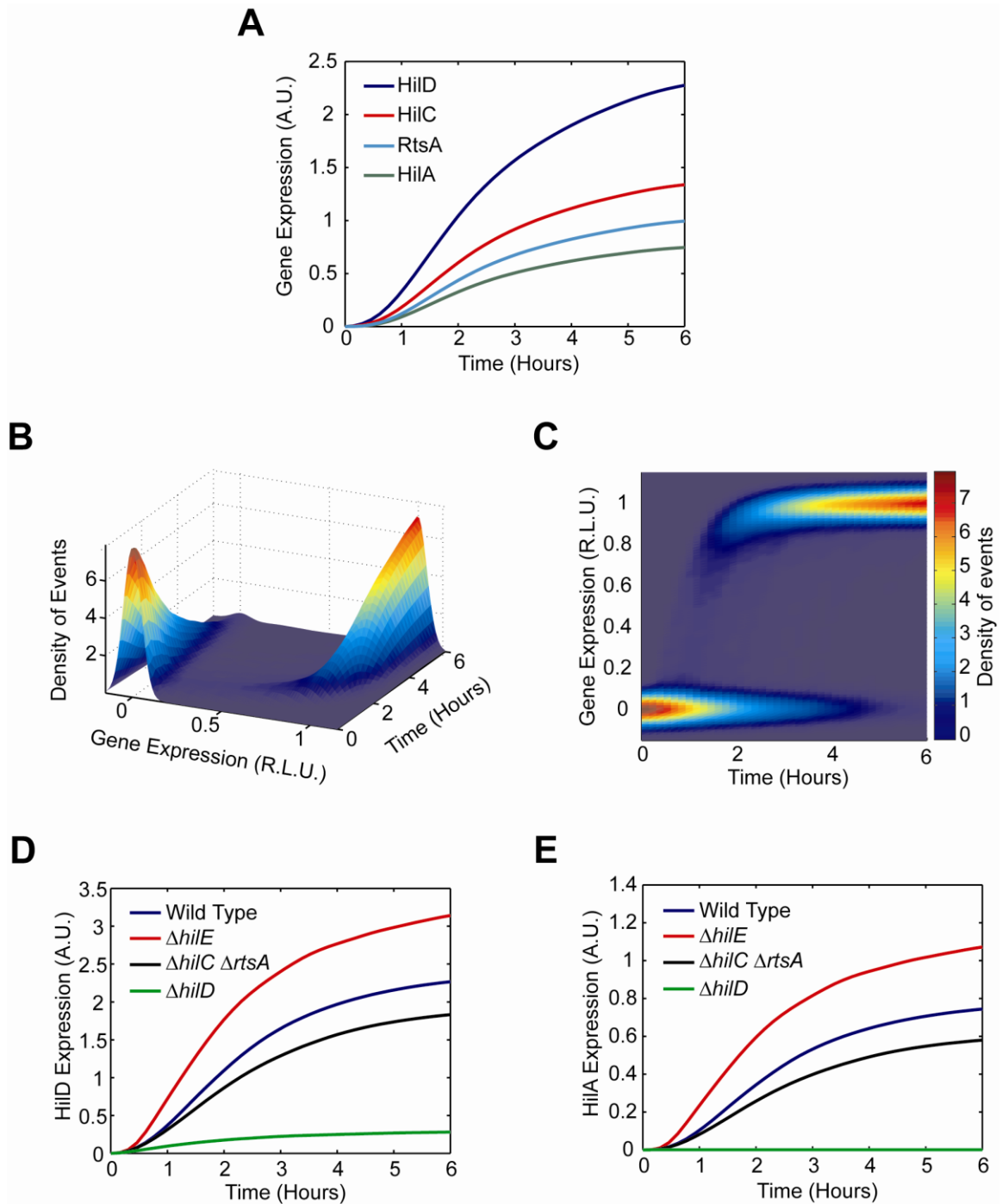


Figure 18. (A) Time-course simulation of HilD, HilC, RtsA, and HilA expression dynamics in wild-type cells. These results are the average of 1000 simulations. These simulations are meant to capture the population-level behavior of the circuit. **(B)** Time-course simulation of HilA expression at single-cell resolution. The expression values are normalized to one and plotted on a log scale. The expression values are given in relative log units (R.L.U.). Similar expression dynamics are also seen for HilD, HilC, and RtsA (see Matlab code provided as supplementary material). **(C)** Same results provided as a two-

dimension heat plot. Note that the model captures the transient heterogeneity observed in our flow cytometry data where cells in both the “off” and “on” states are found at intermediate times. Panels A-C were generated from the same set of simulation runs. **(D and E)** Time-course simulation of HilD (D) and HilA (E) expression dynamics in wild type and $\Delta hilD$, $\Delta hilC \Delta rtsA$, and $\Delta hilD$ mutants at population resolution. The results for each mutant were obtained from the average of 1000 simulations. Similar behavior is also seen at single-cell resolution. Mutants were simulated by setting the activity of the respective gene to zero in the model. A detailed description of the model is provided in the Materials and Methods.

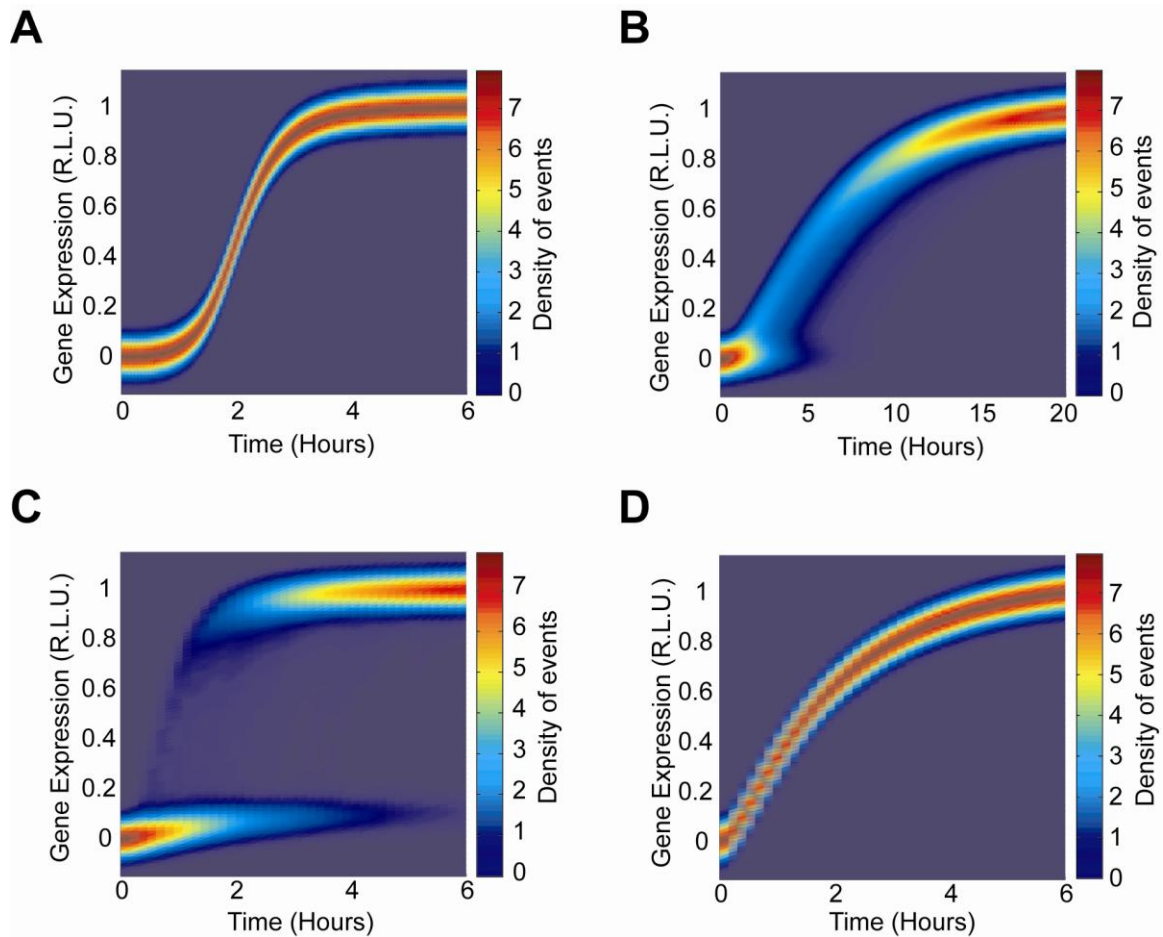


Figure 19. (A) HilA expression at single-cell resolution when activation of the P_{hilD} promoter is deterministic. All other equations in the model are unchanged. (B) HilA expression at single-cell resolution when the kinetic parameters are reduced by a factor of ten. In our simulations, we accomplished this by reducing by a factor of ten and rescaling time by a factor of ten. (C-D) Comparison of HilC expression at single-cell resolution in wild type (C) and $\Delta hilD$ mutant (D). Figures are given as two-dimension heat plots, where the color intensity denotes the density of events. The results for each plot were obtained from 1000 simulations. The expression values are normalized to one and plotted on a log scale. The expression values are given in relative log units (R.L.U.). Mutants were simulated by setting the activity of the respective gene to zero in the model.

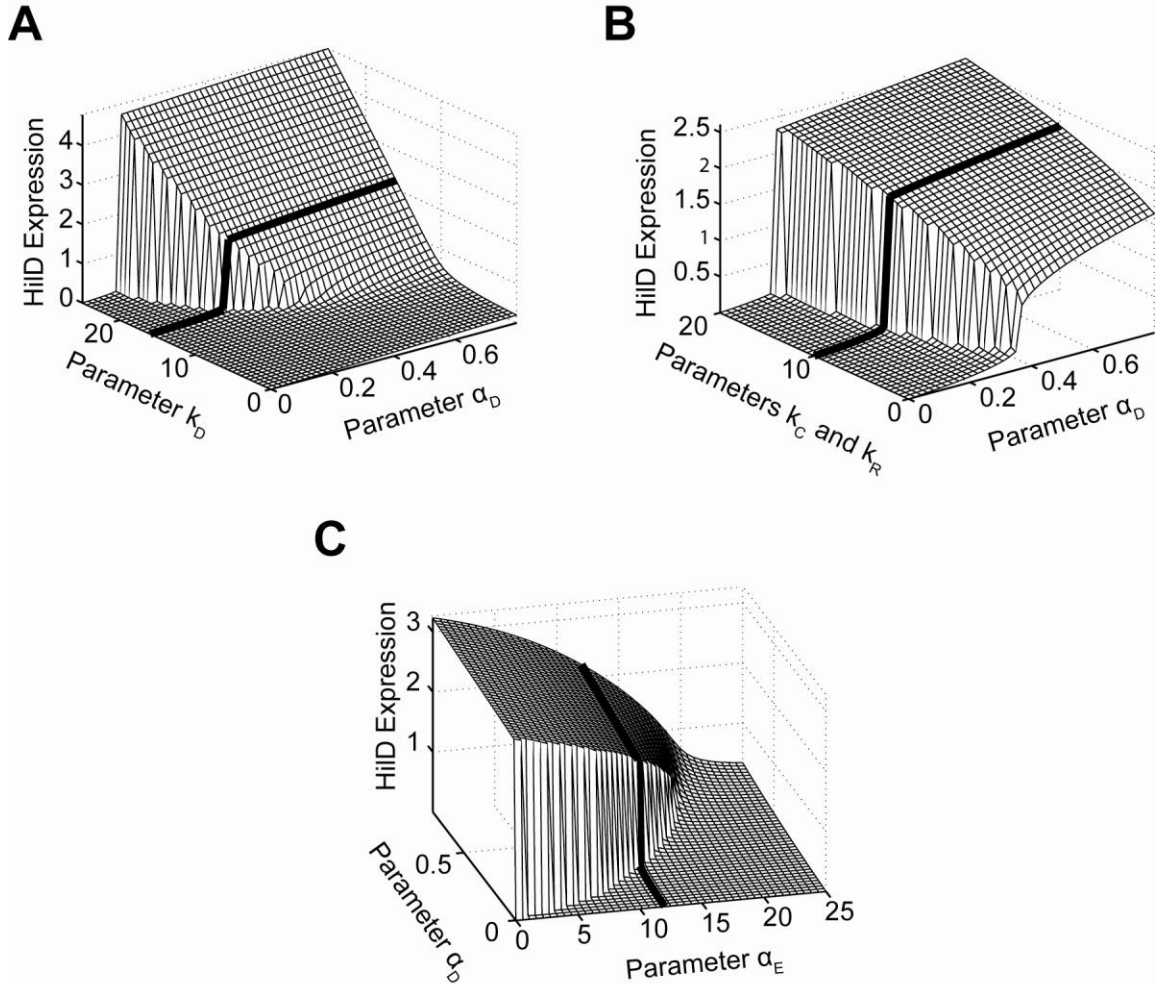


Figure 20. (A) Effect of positive feedback on HilD expression. Plot shows steady-state concentration of HilD as a function of the parameters k_D and α_D . The parameter k_D specifies the degree by which the SPI1 regulators - HilC, HilD, and RtsA - can activate HilD expression, effectively the strength of positive feedback on HilD expression. The parameter α_D specifies the strength of the signal activating HilD expression. **(B) Effect of HilC and RtsA on HilD expression.** Plot shows the steady-state concentration of HilD as a function of the parameters k_C , k_R , and α_D . The parameters k_C and k_R specify the degree by which the SPI1 regulators - HilC, HilD, and RtsA - can activate HilC and RtsA expression, respectively. In other words, these parameters set the strength of feedback on HilC and RtsA expression. In these simulations, the parameters k_C and k_R were both varied in tandem: the numerical values for the two are the same. **(C) Effect of HilE on HilD expression.** Plot shows the steady-state concentration of HilD as a function of the parameters α_E and α_D . The parameter k_E specifies the rate of HilE expression.

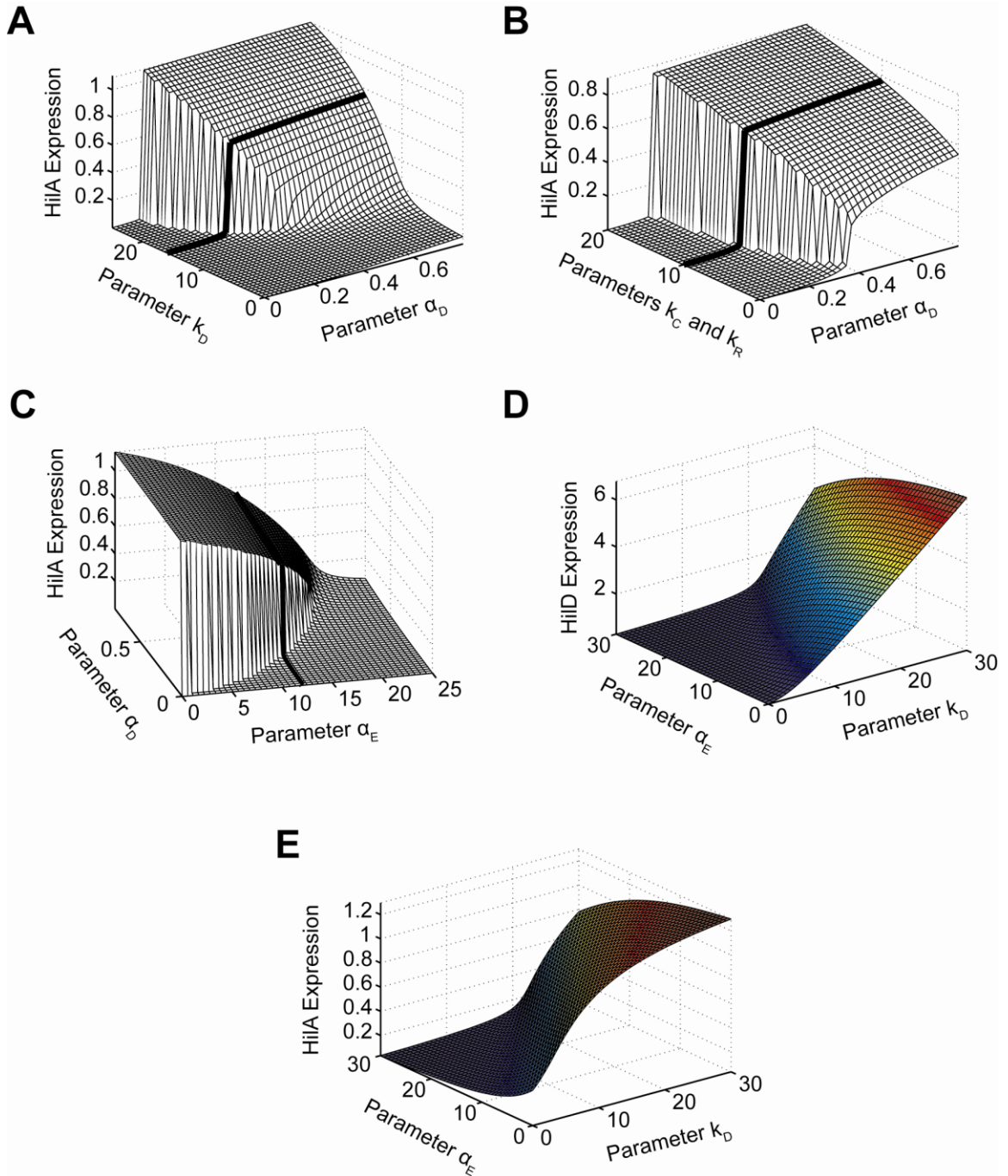


Figure 21. (A) Effect of HiID positive feedback on HiIA expression. Plot shows steady-state concentration of HiID as a function of the parameters k_D and α_D . The parameter k_D specifies the degree by which the SPI1 regulators - HilC, HilD, and RtsA - can activate HiID expression, effectively the strength of positive feedback on HiID expression. The parameter α_D specifies the strength of the signal activating HiID expression. **(B) Effect of HilC and RtsA on HiIA expression.** Plot shows the steady-state concentration of HiID as a

function of the parameters k_C , k_R , and α_D . The parameters k_C and k_R specify the degree by which the SPI1 regulators - HilC, HilD, and RtsA - can activate HilC and RtsA expression, respectively. In other words, these parameters set the strength of feedback on HilC and RtsA expression. In these simulations, the parameters k_C and k_R were both varied in tandem: the numerical values for the two are the same. **(C) Effect of HilE on HilA expression.** Plot shows the steady-state concentration of HilD as a function of the parameters α_E and α_D . **(D-E) Effect of HilE and HilD positive feedback on HilD (D) and HilA (E) expression.** Plots shows the steady-state concentrations of HilD and HilA as a function of the parameters α_E and k_D . The black lines in the plots (A-C) are used to denote the results obtained using the nominal parameters (aside from α_E).

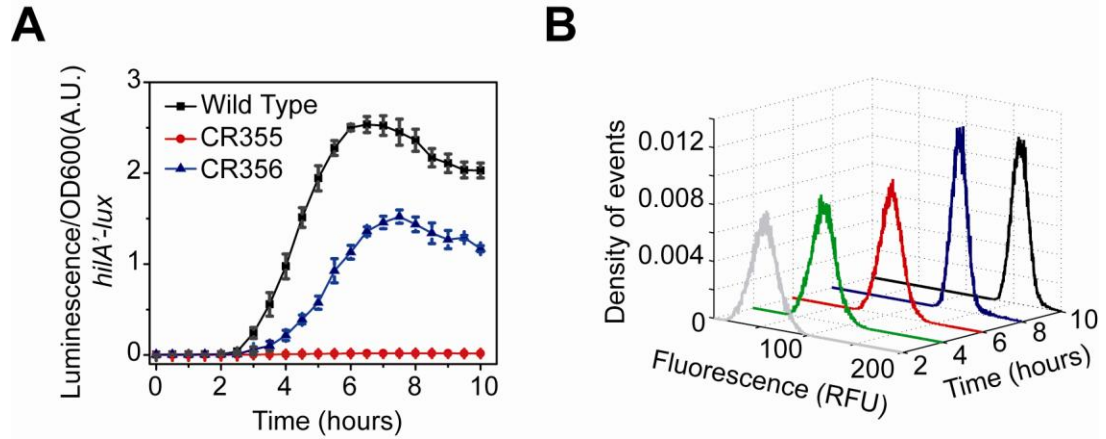


Figure 22. (A) Comparison of time-course dynamics for P_{hilA} (pSS077) promoter activities in wild type (black), CR355 ($\Delta P_{hilD}::P_{hilC} \Delta hilC$, red) and CR356 ($\Delta P_{hilD}::P_{hilC} \Delta hilC \Delta hilE$, blue) as determined using luciferase transcriptional reporters. In strain CR355, the P_{hilD} promoter was replaced with the P_{hilC} promoter in an otherwise $\Delta hilC$ background. In this strain, $hilD$ is transcriptionally regulated in a manner identical to $hilC$. Strain CR356 is the same as CR355 except that it lacks $HilE$. **(B)** Dynamics of P_{hilA} promoter activity in CR356 as determined using green fluorescent protein (GFP) transcriptional fusions and flow cytometry. Note that the activation of the P_{hilA} promoter in CR356 is no longer switch-like but rather rheostat-like in nature.

Table 1. Parameter definitions and nominal values.

Parameter	Description	Value ^a
λ	Initiation rate for P _{hilD} and P _{hilC} promoter	2.0 hr ⁻¹
α_D	Basal activity for P _{hilD} promoter	1.2 N hr ⁻¹
α_E	Basal activity for P _{hilE} promoter	12.0 N hr ⁻¹
α_C	Basal activity for P _{hilC} promoter	0.4 N hr ⁻¹
k_D	Activity for P _{hilD} promoter	16.0 N hr ⁻¹
k_C	Activity for P _{hilC} promoter	10.0 N hr ⁻¹
k_R	Activity for P _{rtsA} promoter	8.0 N hr ⁻¹
k_A	Activity for P _{hilA} promoter	6.0 N hr ⁻¹
δ_D	HilD degradation/dilution rate	4.0 hr ⁻¹
δ_E	HilE degradation/dilution rate	8.0 hr ⁻¹
δ_C	HilC degradation/dilution rate	4.0 hr ⁻¹
δ_R	RtsA degradation/dilution rate	4.0 hr ⁻¹
δ_A	HilA degradation/dilution rate	4.0 hr ⁻¹
δ_{ED}	HilE-HilD degradation/dilution rate	16.0 hr ⁻¹
δ_G	Reporter degradation/dilution rate	4.0 hr ⁻¹
a_E	Association rate of HilD and HilE	8.0 N ⁻¹ hr ⁻¹
d_E	Disassociation rate of HilE-HilD complex	8.0 hr ⁻¹
$K_{O_1}^D$	Equilibrium constant for HilD- O ₁ complex	10.0 N ⁻¹
$K_{O_1}^C$	Equilibrium constant for HilC- O ₁ complex	0.001 N ⁻¹
$K_{O_1}^R$	Equilibrium constant for RtsA- O ₁ complex	0.001 N ⁻¹
$K_{O_2}^D$	Equilibrium constant for HilD- O ₂ complex	1.0 N ⁻¹
$K_{O_2}^C$	Equilibrium constant for HilC- O ₂ complex	0.1 N ⁻¹
$K_{O_2}^R$	Equilibrium constant for RtsA- O ₂ complex	0.1 N ⁻¹
h	Bandwith for density estimation	0.05 N

^a We are unable to assign absolute concentrations units to the parameter values. As a consequence, we report the parameters in terms of dimensionless concentration units, denoted by N.

Chapter 5. Salmonella Pathogenicity Island 4 (SPI4)

Introduction

Along with the regulators that control expression of genes responsible for the SPI1-encoded T3SS, also encoded within SPI1 is a transcription factor, SprB, from the LuxR/UhaP family of transcription factors. Eichelberg and coworkers (Eichelberg *et al.*, 1999) previously found this gene to be expressed in conditions similar to other SPI1-encoded genes. However, they found that it was not involved in regulating the expression of SPI1-encoded genes and speculated that it may instead regulate novel SPI1 T3SS substrates. In this section of the thesis, we demonstrate that SprB regulates the expression of the genes encoded within *Salmonella* Pathogenicity Island 4 (SPI4).

SPI4 encodes a non-fimbrial adhesion (Gerlach *et al.*, 2007b) that is involved in the intestinal phase of infection (Kiss *et al.*, 2007, Lawley *et al.*, 2006, Morgan *et al.*, 2004). Previously, a number of studies have shown that there is a link between SPI1 and SPI4-encoded gene expression (Ahmer *et al.*, 1999, De Keersmaecker *et al.*, 2005, Ellermeier & Slauch, 2003, Gerlach *et al.*, 2007b, Main-Hester *et al.*, 2008). In particular, they demonstrated that SPI4-encoded gene expression is HilA dependent. However, Main-Hester and coworkers showed that, in the absence of the SPI1 locus, HilA is unable to activate SPI4 gene expression (Main-Hester *et al.*, 2008). Their results suggest that

some other HilA-dependent regulator within SPI1 may be involved. Here, we show that this other regulator is SPI1-encoded transcription factor, SprB.

Results

SprB Transcriptionally Regulates SPI4-Encoded Gene Expression

The SPI4 locus encodes six genes within a single operon under the control of the P_{siiA} promoter (Gerlach et al., 2007b). While previous reports have identified that SPI1 and SPI4 gene expression are linked together, the regulator responsible for this is still unknown. In addition to HilC, HilD, and HilA; SPI1 also encodes for a transcriptional regulator, SprB. Previous studies have so far not assigned any role to SprB in regulating SPI1 gene expression. Therefore, we hypothesized that SprB might act as a molecular link between SPI1 and some other systems' gene expression. In particular, we tested whether SprB regulates SPI4 gene expression or not. To test this hypothesis, we measured P_{siiA} promoter activity using a plasmid-based, Venus transcriptional reporter (Nagai *et al.*, 2002) in wild type and a $\Delta sprB$ mutant. As shown in **Figure 23**, deleting *sprB* causes a two-fold decrease in P_{siiA} promoter activity as determined by changes in fluorescence. Moreover, we can complement this mutant by expressing SprB from an anhydrotetracycline (aTc)-inducible promoter on a compatible plasmid.

We next tested how individually expressing the SPI1 regulators – HilA, HilC, HilD, RtsA, and SprB – from a tetracycline-inducible promoter would affect P_{siiA} promoter activity in a $\Delta SPI1 \Delta rtsAB$ mutant. Of the five, only SprB was capable of activating the

P_{siiA} promoter (**Figure 23**). We performed similar experiments in *Escherichia coli* and observed identical results (data not shown).

To test whether SprB directly binds to the P_{siiA} promoter, we used chromatin immunoprecipitation (ChIP). In this experiment, we first expressed 6xHis-tagged SprB from the constitutive $P_{LtetO-1}$ promoter on a plasmid in a $\Delta sprB$ mutant and then passed the cross-linked cell lysate over a Ni^{2+} column (see supplemental material for more details). Upon elution from the column and reverse cross-linking, we found by PCR that SprB directly binds the P_{siiA} promoter region (**Figure 23**). As a negative control, we also tested whether SprB binds to the P_{fimA} promoter region, a promoter whose activity is unaffected by SprB, and found that it did not. Collectively, these results demonstrate that SprB binds to P_{siiA} promoter and activates SPI4-encoded gene expression.

HilA Transcriptionally Regulates SprB Expression

Multiple studies have previously shown that SPI4-encoded gene expression is HilA dependent (Ahmer et al., 1999, De Keersmaecker et al., 2005, Ellermeier & Slauch, 2003, Bode *et al.*, 1980, Main-Hester et al., 2008). We therefore hypothesized that HilA regulates SprB expression, as this would explain the decrease in P_{siiA} promoter activity previously observed when HilA is deleted. It would also explain why other SPI1 regulators - namely HilC, HilD, and RtsA - affect SPI4-encoded gene expression, as they in turn regulate HilA expression.

To test this hypothesis, we measured the effect of individually expressing the SPI1 regulators - HilA, HilC, HilD, and RtsA – from an aTc-inducible promoter in a Δ SPI1 Δ rtsAB mutant on P_{sprB} promoter activity. Similar to the experiments described above, we used a plasmid-based Venus transcriptional reporter to measure P_{sprB} promoter activity. Of the four, only HilA was capable of activating P_{sprB} promoter activity (**Figure 24**). Identical results were obtained when we performed similar experiments in *E. coli* (data not shown). To test whether this effect is direct, we used ChIP and found that HilA does indeed bind the P_{sprB} promoter (**Figure 24**). As respective positive and negative controls, we used the P_{prgH} and P_{fimA} promoter regions. These results demonstrate that HilA transcriptionally regulates SprB expression.

SprB Transcriptionally Represses HilD Expression

We last tested whether SprB regulates SPI1-encoded gene expression. Here, we measured the activity for a number of SPI1 promoters using plasmid-based, Venus transcriptional reporters in wild type, a Δ sprB mutant, and a Δ sprB mutant constitutively expressing *sprB* from the $P_{LtetO-1}$ promoter on a plasmid. Our data show that deleting *sprB* resulted in a mild increase in SPI1 promoter activity (**Figure 25**). However, plasmid expression of SprB caused a two-fold reduction in SPI1 promoter activity in a Δ sprB mutant background. These results suggest that SprB is a weak negative regulator of SPI1-encoded gene expression. The weak level of repression may explain why Eichelberg and coworkers (Eichelberg et al., 1999) previously concluded that SprB does not regulate SPI1-encoded gene expression. Since SPI1-encoded gene expression is known

to be growth dependent, we also checked if expressing SprB from a plasmid in a $\Delta sprB$ mutant caused any growth defect. Our data show that it has no effect (**Figure 25**).

As SprB regulates multiple SPI1 promoters, we hypothesized that it likely represses the transcription of either HilC, HilD, or RtsA. These three regulators are all activators of P_{hilA} promoter activity and each others expression as well (Ellermeier et al., 2005, Ellermeier & Slauch, 2007, Lostroh & Lee, 2001b). To identify the target for repression, we first expressed SprB from an arabinose-inducible promoter on a plasmid (Guzman et al., 1995) in $\Delta hilC \Delta sprB$ and $\Delta rtsA \Delta sprB$ null mutants and found that P_{hilA} promoter activity was still repressed by SprB, as determined using a plasmid-based, Venus transcriptional reporter (**Figure 25**). These results demonstrate that repression is not HilC or RtsA dependent. Next, we investigated if SprB represses the P_{hilD} promoter by measuring P_{hilA} promoter activity in a strain where the P_{hilD} promoter was replaced with the *tetRA* element from transposon *Tn10* (Karlinsky, 2007).

This arrangement decouples *hilD* expression from its native regulation and causes it to be constitutively expressed from its native chromosomal locus in the presence of tetracycline. In the strain, $P_{hilD}::tetRA \Delta sprB$, we found that expressing SprB from an arabinose-inducible promoter plasmid (Guzman et al., 1995) did not affect P_{hilA} promoter activity (**Figure 25**), suggesting that SprB represses HilD expression. To demonstrate that the SprB-dependent repression of SPI1-encoded gene expression is due to the binding of the SprB protein to the P_{hilD} promoter, we used ChIP (**Figure 25**).

These results demonstrate that SprB binds to P_{hilD} promoter region and likely represses SPI1-encoded gene expression by inhibiting *hilD* transcription.

Discussion

Our results demonstrate that SprB functions as a molecular link between SPI1 and SPI4 gene expression. We propose the following model (**Figure 26**). Upon induction of the SPI1 gene circuit, HilA activates SprB expression. SprB plays a dual role in regulating gene expression. First, it weakly represses SPI1-encoded gene expression by binding to the P_{hilD} promoter and likely inhibiting *hilD* transcription. Secondly, it activates the expression of the SPI4-encoded adhesin, presumably helping the bacterium adhere to intestinal epithelial cells during invasion. This mode of regulation links gene expression in two distinct systems in *Salmonella*, enabling the coordinate regulation of adherence to and invasion of the intestinal epithelia.

Figures – Salmonella Pathogenicity Island 4 (SPI4)

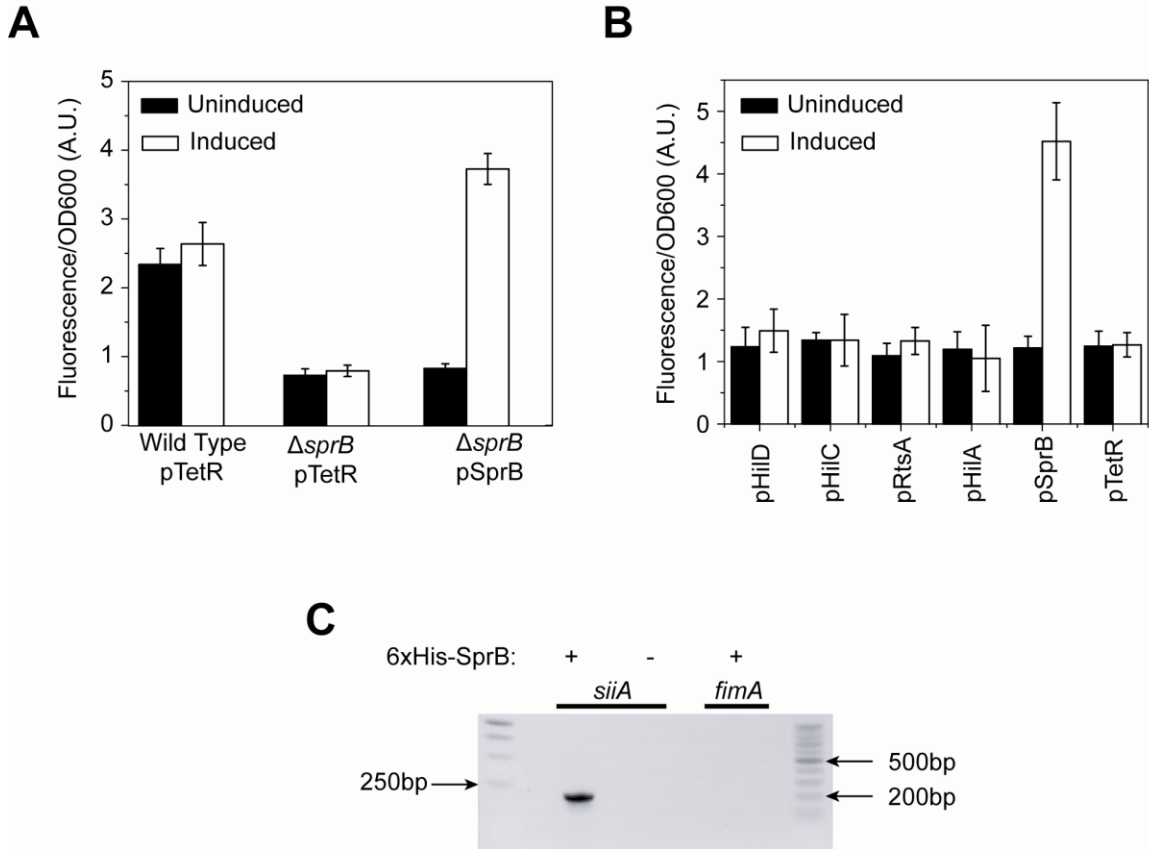


Figure 23. SprB regulates SPI4-encoded gene expression. (A) Comparison of P_{siiA} promoter activity in wild type, a $\Delta sprB$ mutant, and a $\Delta sprB$ mutant expressing SprB from an anhydrotetracycline (aTc)-inducible promoter on a plasmid (pSprB). pTetR denotes the empty plasmid control. Expression was induced with 50 ng/mL of aTc. **(B)** SprB can activate the P_{siiA} promoter in the absence of other SPI1 genes ($\Delta SPI1 \Delta rtsAB$); the other SPI1 regulators – HilA, HilC, HilD, and RtsA – cannot. Activators were expressed from an aTc-inducible promoter on a plasmid. Expression was induced with 50 ng/mL of aTc. Fluorescence values were normalized with the OD_{600} absorbance to account for cell density. Errorbars indicate standard deviations. **C.** SprB binds to the P_{siiA} promoter region as determined by a co-precipitation assay using 6xHis-tagged SprB. PCR was used to determine whether the P_{siiA} promoter region is in the co-precipitated DNA. The P_{fimA} promoter region was included as a negative control. An expanded description of the experimental procedures is provided as supplementary material.

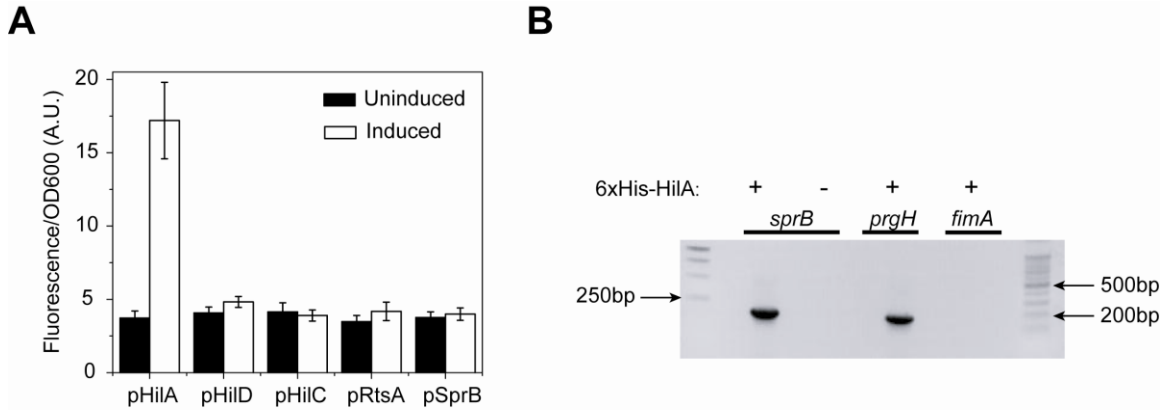


Figure 24. HilA regulates SprB expression. (A) HilA can activate the P_{sprB} promoter in the absence of other SPI1 genes ($\Delta SPI1 \Delta rtsAB$); the other SPI1 regulators – HilC, HilD, and RtsA – cannot. SprB was also found not to regulate its own expression. Activators were expressed from an aTc-inducible promoter on a plasmid. Expression was induced with 50 ng/mL of aTc. Fluorescence values were normalized with the OD_{600} absorbance to account for cell density. Error-bars indicate standard deviations. **(B)** HilA binds to the P_{sprB} promoter region as determined by a co-precipitation assay 6xHis-tagged HilA. PCR was used to determine whether the P_{sprB} promoter region is in the co-precipitated DNA. The P_{prgH} and P_{fimA} promoter regions were included as positive and negative controls, respectively. An expanded description of the experimental procedures is provided as supplementary material.

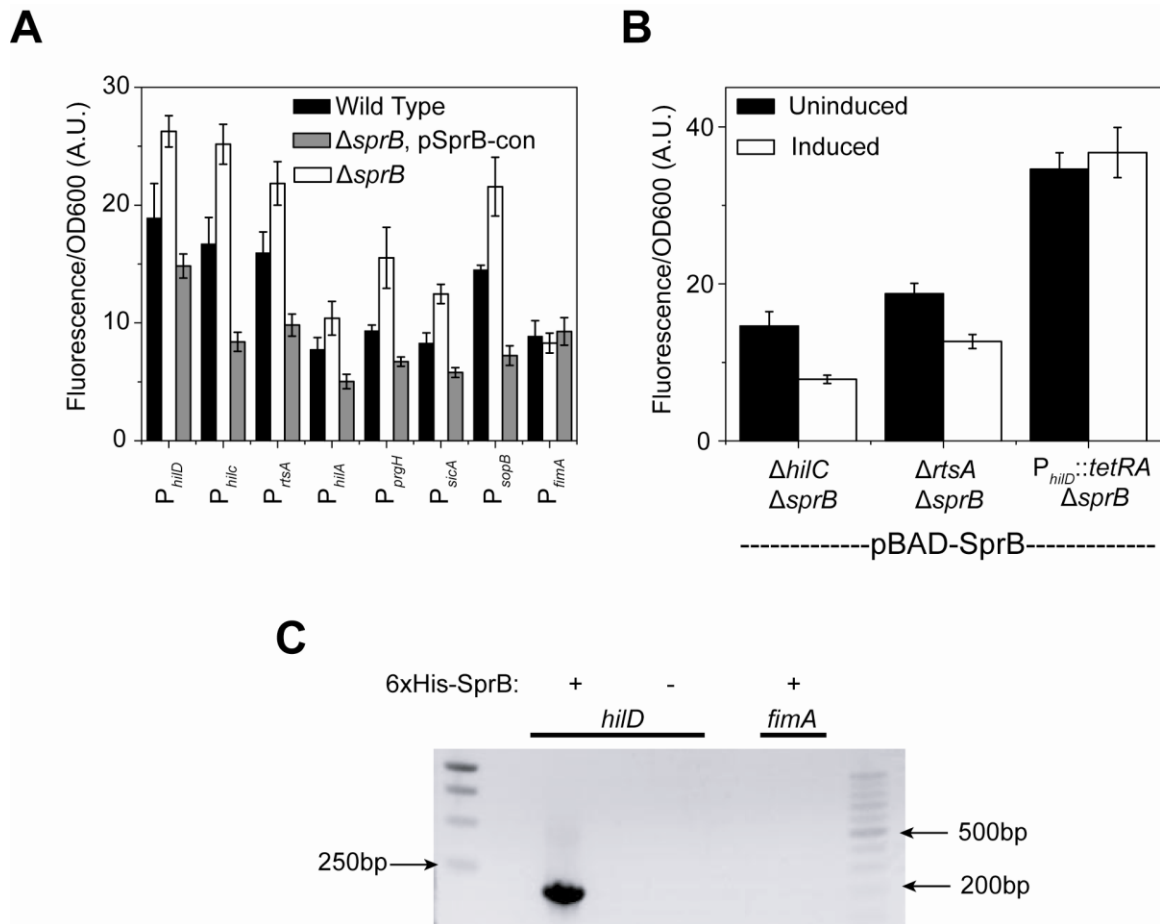


Figure 25. SprB represses SPI1-encoded gene expression through HilD. (A) Comparison of SPI1 promoter activities in wild type, a $\Delta sprB$ mutant, and a $\Delta sprB$ mutant constitutively expressing SprB from a plasmid (pSprB-con). **(B)** SprB repression of SPI1-encoded gene expression is through the P_{hilD} promoter. Comparison of P_{hilA} promoter activity in $\Delta hilC \Delta sprB$, $\Delta hilC \Delta sprB$, and $P_{hilD}::tetRA \Delta sprB$ mutants when SprB is expressed from an arabinose-inducible promoter on a plasmid (pBAD-SprB). SprB expression was induced with 2 mg/mL of arabinose. In the experiments involving the $P_{hilD}::tetRA \Delta sprB$ mutant, 2 μ g/ml tetracycline was added to the growth medium in order to induce HilD expression. Induction in panel B is used to denote the presence or absence of arabinose. Fluorescence values were normalized with the OD₆₀₀ absorbance to account for cell density. Errorbars indicate standard deviations. **(C)** SprB binds to the P_{hilD} promoter region as determined by a co-precipitation assay using 6xHis-tagged SprB. PCR was used to determine whether the P_{hilD} promoter region is in the co-precipitated DNA. The P_{fimA} promoter region was included as a negative control.

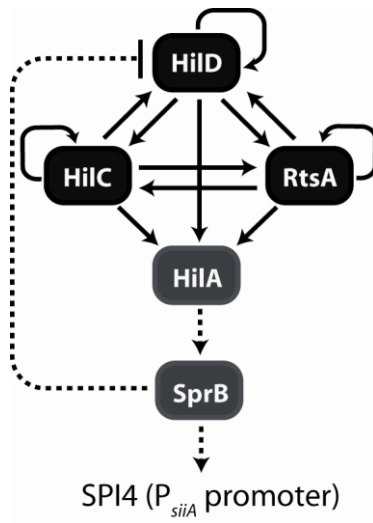


Figure 26. Model for SPI1 and SPI4 regulation. Arrows indicate transcription activation. Blunt-ends represent repression.

Chapter 6. Type I Fimbriae Gene Network

Introduction

Type I fimbriae in *Salmonella enterica* serovar Typhimurium are proteinaceous surface appendages that carry adhesions specific for mannosylated glycoproteins (Buchanan *et al.*, 1985). Type I fimbriae are involved in serovar Typhimurium pathogenicity by facilitating the binding to and invasion of intestinal epithelial cells (Tavendale *et al.*, 1983). In orally inoculated mice, a wild-type strain has been shown to cause more infections and deaths than a *fim* mutant strain (Duguid *et al.*, 1976). A *fim* mutant has also been shown to exhibit severalfold weaker binding to HEp-2 and HeLa cells, and the defect in binding could be restored by complementing the *fim* system on a plasmid (Baumler *et al.*, 1996). Apart from type I fimbriae, mutations in different *Salmonella* fimbrial systems—*lpf*, *pef*, and *agf*— have all also been shown to greatly reduce virulence in mice (van der Velden *et al.*, 1998). These systems appear to work synergistically in order to facilitate colonization of the ileum (Baumler *et al.*, 1997). In serovar Typhimurium, the *fim* gene cluster possesses all of the genes necessary for type I fimbrial production. This gene cluster is composed of six structural genes, three regulators, and a tRNA specific for rare arginine codons (AGA and AGG). The structural genes *fimA*, *fimI*, *fimC*, *fimD*, *fimH*, and *fimF* are all expressed in one transcript from the P_{fimA} promoter (Hancox *et al.*, 1997, Pikhova *et al.*, 2005, Purcell *et al.*, 1987, Rossolini *et al.*, 1993). The regulators *fimZ*, *fimY*, and *fimW* are all expressed from independent

promoters (Tinker & Clegg, 2000, Tinker *et al.*, 2001, Yeh *et al.*, 1995). The tRNA encoded by *fimU* is located at one end of the cluster and is required for the effective translation of the regulatory genes that all carry rare arginine codons (Swenson *et al.*, 1994).

Type I fimbriation is environmentally regulated with *fim* gene expression favored in static liquid medium, whereas growth on solid medium inhibits expression (Duguid *et al.*, 1966a). Moreover, serovar Typhimurium cultures in fimbriae-inducing conditions contain cells in both fimbriated and nonfimbriated states (Old & Duguid, 1970). While the regulation of *fim* gene expression has been studied extensively in *Escherichia coli*, far less is known about the regulation in serovar Typhimurium (Abraham *et al.*, 1985, Klemm, 1984). In particular, despite homology between the structural genes for type I fimbriae in *E. coli* and serovar Typhimurium, their expression is regulated in completely different manners. No homologs of *E. coli* regulators, FimB and FimE, are present in serovar Typhimurium (Gally *et al.*, 1996, Klemm, 1986). Also, the serovar Typhimurium P_{fimA} promoter is inactive in *E. coli*, indicating that the P_{fimA} promoter is regulated by different factors in these two organisms (Yeh *et al.*, 1995).

In serovar Typhimurium, the expression of the structural genes is regulated by three transcription factors, FimY, FimZ, and FimW (Tinker & Clegg, 2000, Tinker *et al.*, 2001, Yeh *et al.*, 1995). Both FimZ and FimY are essential for the expression of the structural genes from the P_{fimA} promoter (Yeh *et al.*, 1995). In particular, the deletion of

either the *fimY* or *fimZ* gene reduces expression from the P_{fimA} promoter and prevents serovar Typhimurium from making type I fimbriae. FimZ has been shown to bind the P_{fimA} promoter and promote transcription (Cotter & Miller, 1994, Yeh et al., 1995). FimY, on the other hand, is thought to facilitate the activation of the P_{fimA} promoter, as direct binding has not been observed (Tinker & Clegg, 2000). FimW is a negative regulator of *fim* gene expression (Tinker & Clegg, 2001). FimW has also been suggested to autoregulate its expression, as enhanced P_{fimW} activity has been observed in the $\Delta fimW$ mutant. In DNA-binding assays, FimW was not observed to bind any of the *fim* promoters. However, FimW was found to interact with FimZ in a LexA-based two-hybrid system in *E. coli* (Tinker & Clegg, 2001). Thus, a possible mechanism for FimW mediated repression may be that it binds FimZ and prevents it from activating transcription. However, an analysis of the FimW amino acid sequence predicts that it has a DNA-binding domain. Moreover, it is related to a broad range of prokaryotic transcription factors, with its closest relatives being BpdT from *Rhodococcus* spp. and an uncharacterized response regulator, TodD, from *Pseudomonas putida* (Labbe et al., 1997, Lau et al., 1997). Thus, FimW may also act by an alternate mechanism involving DNA binding.

In addition to these transcription factors, the *fimU* tRNA also plays a role in *fim* gene expression (Swenson et al., 1994). All three regulators— FimZ, FimY, and FimW— contain a number of the rare arginine codons, AGA and AGG, recognized by the *fimU* tRNA. In the case of FimY, $\Delta fimU$ mutants have been shown to be nonfimbriated due to

the inefficient translation of *fimY* mRNA. This translational regulation results from FimY having three rare arginine codons within its first 14 amino acids. The phenotypic effect of the $\Delta fimU$ mutation could, however, be overcome by expressing *fimU* from a plasmid or by changing these three rare arginine codons in *fimY* to ones more efficiently translated.

As a pathogen, serovar Typhimurium invades host cells by a process in which effector proteins are injected into the target cells with the help of the *Salmonella* pathogenicity island 1 (SPI1) type III secretion system (Collazo & Galan, 1997a, Darwin & Miller, 1999b). SPI1 gene expression is regulated by a number of proteins, with the critical activator being HilA (Bajaj et al., 1995). The expression of *hilA*, in turn, is regulated by three AraC-like transcriptional activators, *hilC*, *hilD*, and *rtsA* (Eichelberg et al., 1999, Ellermeier & Slauch, 2003, Fahlen et al., 2000, Lucas & Lee, 2001, Schechter et al., 1999, Schechter & Lee, 2001). HilD activity is controlled by HilE; this protein binds HilD and is thought to prevent it from activating the P_{hilA} promoter (Baxter et al., 2003, Boddicker et al., 2003). FimY and FimZ have been previously shown to regulate SPI1 gene expression by repressing *hilA* expression through their activation of the P_{hilE} promoter (Baxter & Jones, 2005).

In the work reported in this chapter, we investigated the gene circuit regulating *fim* expression. Using genetic approaches, we found that FimZ and FimY activate each other's expression and that each protein can independently activate the P_{fimA} promoter.

Moreover, FimZ and FimY were found to be weak autoactivators. Our data also suggest that FimW-mediated repression occurs at the level of *fimY* transcription. As the *fim* gene circuit involves a combination of positive and negative feedback, we tested whether induction was bistable. However, we found the cell population responded homogeneously when induced. By reprogramming the genetic circuit we were able to qualitatively change the response of the P*fimA* promoter from a homogeneous rheostat-like response to a heterogeneous switch-like transition from the “off” to the “on” state.

Results

FimZ and FimY are Activators and FimW is a Repressor of *Fim* Gene Expression

FimZ and FimY have previously been reported as activators of *fim* gene expression in serovar Typhimurium (Tinker & Clegg, 2001, Yeh et al., 1995). Both have also been reported as essential for fimbriation, as the deletion of either one results in the loss of expression from the P_{fimA} promoter (Yeh *et al.*, 2002). To understand the roles of FimZ and FimY in the *fim* gene circuit, we measured expression from the P_{fimA} , P_{fimZ} , P_{fimY} , and P_{fimW} promoters in the wild type and the $\Delta fimZ$, $\Delta fimY$, $\Delta fimYZ$, and $\Delta fimW$ mutants (**Figure 27**). Chromosomally integrated Venus transcriptional reporters were employed as indirect measures of promoter activities (Nagai et al., 2002). In the cases of all four promoters, activity levels were found to be about two times less active in the $\Delta fimZ$, $\Delta fimY$, and $\Delta fimYZ$ mutants than in the wild type. For all four promoters, note that no further reduction in promoter activity was observed in the double mutant. In a $\Delta fimW$ mutant, the activities of all four promoters were approximately two times higher than the wild-type levels. While these results agree with previously published data regarding the *fim* system in serovar Typhimurium, they still do not tell us how FimW, FimY, and FimZ individually contribute to P_{fimA} activation.

FimY and FimZ Form a Coupled Positive Feedback Loop

To determine the relative effect of FimY and FimZ on *fim* gene expression, the P_{fimY} and P_{fimZ} promoter activities were measured in a $\Delta fimYZ$ mutant in which either FimZ or FimY was expressed from a strong, aTc-inducible promoter on a plasmid. Using this system, we found that expressing FimZ in the $\Delta fimYZ$ mutant led to a more than 10-fold increase in P_{fimY} activity (**Figure 28A**). Likewise, expressing FimY in the $\Delta fimYZ$ mutant led to about a 10-fold increase in P_{fimZ} levels. In addition to their ability to activate each other's promoters, FimY and FimZ were found to increase expression from their own promoters roughly threefold. Even though *E. coli* makes type I fimbriae, the serovar Typhimurium *fim* promoters by themselves are inactive in this organism. Therefore, we performed an identical set of experiments with *E. coli* using the serovar Typhimurium proteins and promoters. Overall, the results were identical to those for serovar Typhimurium (**Figure 28B**). In particular, FimZ expression led to a more than 10-fold increase in P_{fimY} promoter activity, and FimY expression led to a 10-fold increase in P_{fimZ} activity. Both FimZ and FimY were again found to weakly activate expression from their own promoters. The goal of these experiments was to remove the effect of any serovar Typhimurium specific regulatory mechanisms, thus allowing us to more confidently conclude that the observed results are due to direct interactions. Collectively, these results show that FimY and FimZ strongly activate each other's expression and weakly activate their own expression. This cross-regulation also explains why both FimY and FimZ are required for strong P_{fimA} promoter activity, as the expression of each is dependent on the other. Next, we wanted to investigate to what

extend do FimY and FimZ control the P_{fimA} promoter activity independently of each other.

FimZ and FimY can Independently Activate the P_{fimA} Promoter

Next, we looked at how FimZ and FimY independently affected P_{fimA} expression. To investigate this problem, we measured P_{fimA} promoter activity in a $\Delta fimYZ$ mutant in which either FimY or FimZ was expressed using the aTc-inducible system. FimZ expression was found to strongly (15-fold) activate the P_{fimA} promoter, whereas FimY could only weakly (more than twofold) activate it (**Figure 29**). We also performed these experiments with *E. coli* with similar results (data not shown). Based on these results, we conclude that FimZ and FimY can both independently activate the P_{fimA} promoter. In the case of FimY, the weak activation of the P_{fimA} promoter is likely due to its strong dependence on *fimU* tRNA (see below) (Swenson et al., 1994).

FimY Activates the P_{fimW} Promoter, and FimW Represses the P_{fimY} Promoter

FimW has previously been observed to repress *fim* gene expression (Tinker & Clegg, 2001). Consistent with these results, we observed that P_{fimA} , P_{fimW} , P_{fimY} , and P_{fimZ} promoter activities were all elevated in a $\Delta fimW$ mutant. To understand the mechanism of FimW-mediated repression, we first sought to identify the proteins that regulate expression from the P_{fimW} promoter. To answer this question, we measured the level of

expression from the P_{fimW} promoter in a $\Delta fimYZ$ mutant in which FimW, FimY, and FimZ were independently expressed using the aTc-inducible system. In the case of FimW and FimZ, expression had no effect on P_{fimW} promoter activity (data not shown). However, in the case of FimY, we observed a significant increase in P_{fimW} promoter activity (1,052 +/- 381 relative fluorescence units [RFU]/OD [uninduced] versus 14,718 +/- 1,032 RFU/OD [induced]). Similar results were also obtained when these experiments were performed with *E. coli* (data not shown). To identify the regulatory targets of FimW, we measured the expression of the P_{fimA} , P_{fimZ} , and P_{fimY} promoters in a $\Delta fimW \Delta fimYZ$ mutant in which FimW was expressed using the aTc-inducible system. In the cases of the P_{fimA} and P_{fimZ} promoters, we found that FimW expression had no effect. However, in the case of the P_{fimY} promoter, FimW expression led to about a threefold decrease in P_{fimY} activity (7,462 +/- 319 RFU/OD [uninduced] versus 2,781 +/- 188 RFU/OD [induced]). Based on these results, we conclude that FimY activates expression from the P_{fimW} promoter and that FimW represses expression from the P_{fimY} promoter.

The P_{fimU} Promoter is Not Regulated by FimW, FimY, or FimZ

Both *fimY* and *fimZ* contain rare arginine codons (AGA and AGG) and need *fimU*, a tRNA specific for rare arginine codons, for effective translation. In a $\Delta fimU$ mutant, P_{fimA} activity was less than 10-fold compared to the wild-type levels (wild type, 16,723 +/- 1,173 RFU/OD; the $\Delta fimU$ mutant, 1,389 +/- 261 RFU/OD). The expression of FimY in the $\Delta fimU$ mutant using the aTc-inducible system, however, did not increase P_{fimA} activity (988 +/- 319 [uninduced] versus, 343 +/- 166 [induced]). Replacing the rare

arginine codons in the *fimY* gene with consensus ones did restore P_{fimA} activity to the wild-type levels (817 +/- 73 RFU/OD [uninduced] versus 11,294 +/- 462 RFU/OD [induced]). These experiments are consistent with previously published results (Tinker & Clegg, 2001) and indicate that *fimU* is essential for effective *fimY* translation. As *fimU* has a strong effect on P_{fimA} promoter activity, we hypothesized that it may be subject to regulation by the other proteins within the circuit. To test this hypothesis, we measured P_{fimU} promoter activity in different regulatory mutants. Contrary to our hypothesis, we did not observe any change in P_{fimU} promoter activity in any mutant (wild type, 26,717 +/- 1,381 RFU/OD; the $\Delta fimZ$ mutant, 28,991 +/- 2,164 RFU/OD; the $\Delta fimY$ mutant, 25,884 +/- 1,983 RFU/OD; the $\Delta fimYZ$ mutant, 26,516 +/- 1,772 RFU/OD; and the $\Delta fimW$ mutant, 24,829 +/- 2,073 RFU/OD). Likewise, we did not observe any change in P_{fimU} promoter activity when FimW, FimY, and FimZ were expressed using the aTc-inducible system in wildtype serovar Typhimurium or *E. coli* (data not shown). Based on these results, we conclude that the P_{fimU} promoter is not regulated by any *fim* protein.

FimZ Alone is Able to Regulate SPI1 Gene Expression

Previous studies have shown that both FimY and FimZ regulate SPI1 expression through their activation of the P_{hilE} promoter (Baxter & Jones, 2005). HilE, in turn, is known to bind HilD and repress the HilD-mediated activation of the P_{hilA} , P_{hilC} , P_{rtsA} , and P_{hilD} promoters (Baxter et al., 2003, Ellermeier et al., 2005). To test which protein activates the P_{hilE} promoter, we independently expressed FimY and FimZ in a $\Delta fimYZ$ mutant using the aTc-inducible system and then measured the level of expression from

the P_{hilE} promoter. Of the two, only FimZ was found to affect P_{hilE} expression (1,089 +/- 421 RFU/OD [uninduced] versus 17,654 +/- 2,234 RFU/OD [induced]). Similar results were also observed for *E. coli* (data not shown). We note that these results are contrary to those previously reported, for which it was shown that both FimY and FimZ were necessary for activation of the P_{hilE} promoter (Baxter & Jones, 2005). One possible explanation for the discrepancy involves how the two gene products were selectively expressed. In the original study, a DNA fragment containing the *fimYZ* gene cluster was cloned onto a plasmid and expressed using the tetracycline promoter. To study their relative effects, each gene was selectively inactivated using a universal translational terminator. As part of the P_{fimY} promoter and the whole P_{fimZ} promoter were left intact in their construct, transcriptional interference may have occurred between the various promoters. In our design, we selectively cloned each gene and then expressed it from an inducible promoter, eliminating any potential interfering effects from having the native promoters still present.

Dynamics of *Fim* Gene Expression

Finally, we wished to investigate the dynamics of *fim* gene expression. We first measured P_{fimA} promoter activity in the wild type and the $\Delta fimY$, $\Delta fimZ$, $\Delta fimYZ$, and $\Delta fimW$ mutants using a microplate reader (**Figure 30A**). Consistent with our end-point measurements, we found that the P_{fimA} promoter was weakly expressed in the $\Delta fimY$, $\Delta fimZ$, and $\Delta fimYZ$ mutants. Likewise, expression was enhanced in a $\Delta fimW$ mutant. Note that the microplate experiments tell us only about the average response of the

population and nothing about how individual cells are behaving. To test whether the cells were responding homogeneously, we also performed single-cell measurements of P_{fimA} promoter activity at selected times in the wild type and a $\Delta fimW$ mutant using flow cytometry (**Figure 30B**). Our results indicate that individual wild-type and $\Delta fimW$ mutant cells are responding homogeneously with respect to P_{fimA} promoter activity at all times tested. In other words, we did not observe any phase variation or heterogeneity with regard to P_{fimA} promoter activity in our kinetic experiments.

Discussion

In this work, we investigated the regulatory gene circuit controlling the expression of type I fimbriae in *S. typhimurium*. Using genetic approaches, we demonstrated that FimY and FimZ independently activate the P_{fimA} promoter. Of the two, FimZ was found to be the dominant activator. We also found that FimY and FimZ strongly activate each other's expression and weakly activate their own expression. In addition to these two positive regulators, a third regulator, FimW, is known to repress *fim* gene expression. We found that FimW negatively regulates *fim* gene expression by repressing expression from the P_{fimY} promoter. Furthermore, FimW participates in a negative feedback loop as FimY was found to enhance P_{fimW} expression. Interestingly, these results suggest that FimY is both an activator and repressor of *fim* gene expression, as it can directly activate the P_{fimZ} , P_{fimY} , and P_{fimA} promoters and indirectly repress them by enhancing FimW expression. In addition to these regulators, type I fimbriation is also dependent on expression of rare arginine codon tRNA, *fimU*. However, our results showed that the P_{fimU} promoter is not regulated by FimY, FimZ, or FimW. The results suggest that *fimU* does not play a role in the internal regulation of the circuit. Finally, we demonstrated that the previously observed coordinate regulation of SPI1 gene expression by the *fim* gene circuit (Baxter & Jones, 2005) occurs through the activation of *hilE* expression by FimZ. Based on these results, we are able to propose the following model for the *fim* gene circuit in *S. typhimurium* (**Figure 31**).

According to our model, induction of the *fim* circuit begins with activation of the P_{fimY} and P_{fimZ} promoters, resulting in small amounts of *fimY* and *fimZ* being expressed. FimY and FimZ then rapidly accumulate in the cell due to the positive feedback loop formed by the cross-activation of P_{fimY} and P_{fimZ} promoters by these two proteins. Expression of the type I fimbrial structural genes from the P_{fimA} promoter commences when the concentration of FimY and FimZ accumulates within the cell beyond a critical level. These two regulators can independently activate the P_{fimA} promoter; however, their expression is correlated as each activates the others expression. Moreover, FimY and FimZ protein expression levels are controlled by a negative feedback loop involving FimW. In this loop, FimY activates expression of the P_{fimW} promoter, and FimW represses expression from the P_{fimY} promoter. We hypothesize that this negative feedback loop involving FimW prevents runaway expression of FimY and FimZ arising from their participation in an interacting positive feedback. Specifically, we hypothesize that when FimY and FimZ reach their optimum expression levels, the FimW negative feedback loop is activated and halts expression from the P_{fimY} and P_{fimZ} promoters.

While our model for the *fim* circuit explains internal regulation, it still does not explain how the circuit is activated. In particular, we do not know which factors induce the P_{fimY} and P_{fimZ} promoters. We suspect that these factors activate both promoters as each alone exhibits some activity in a $\Delta fimYZ$ mutant. In addition to these factors, another open question concerns whether *fimU* plays a role in regulating circuit dynamics. While it is tempting to speculate that *fimU* expression is tuned in response to

environmental signals and thus affects circuit dynamics, more likely this gene is constitutively expressed like other tRNAs.

Our results also indicate that FimW-mediated inhibition of *fim* gene expression is through repression of the P_{fimY} promoter. Earlier reports suggested that FimW binds FimZ and somehow inhibits FimZ-dependent activation of *fim* promoters (Tinker & Clegg, 2001). Moreover, FimW was not found to bind to the P_{fimW} promoter. Based on these results, FimW would appear to repress the P_{fimY} promoter by preventing FimZ from activating it. However, we found that FimW is able to repress the P_{fimY} promoter in the absence of FimZ. Our results would suggest that FimW directly binds the P_{fimY} promoter and represses transcription, irrespective of FimZ. Consistent with our model, FimW has a C-terminal LuxR-type helix-turn-helix DNA domain (SM00421) (Letunic *et al.*, 2006). However, at this time we have no direct experimental support for such a mechanism. Moreover, an equally likely hypothesis is that repression by FimW is indirect. Further experiments are clearly required to determine the mechanism of FimW-mediated repression and distinguish between these different putative models.

A final unanswered question concerns the role of the positive and negative feedback loops in the *fim* gene circuit. Our initial hypothesis was that these feedback loops would result in bistability. In particular, interacting positive and negative feedback loops are known to be sufficient ingredients for bistability (Ferrell, 2002). This bistability could potentially explain the phase variation observed in type I fimbriation during

growth in inducing conditions (Old & Duguid, 1970). To test whether the *fim* circuit exhibited bistability, we measured P_{fimA} activity at single-cell resolution as a function of time. Contrary to our initial hypothesis, we did not observe a heterogeneous or switch-like response in induction, the tell tale indicator of bistability. Rather, we observed a continuous or rheostatic-like response in both wild type and a $\Delta fimW$ mutant (Batchelor *et al.*, 2004). One possibility is that there is a lack of correlation between *fim* gene expression and the production of type I fimbriae in *S. typhimurium* (Clegg *et al.*, 1996). Moreover, Duguid and coworkers previously observed distinct subpopulations of cells expressing type I fimbriae indicative of phase variation, though under conditions different from those used in our study (Duguid *et al.*, 1966b). With these in mind, we hypothesize that the bacteria exhibit type I fimbriae phase variation under specific environmental conditions and that the regulation of this process involves post-transcriptional mechanisms as well.

Figures – Type I Fimbriae Gene Network

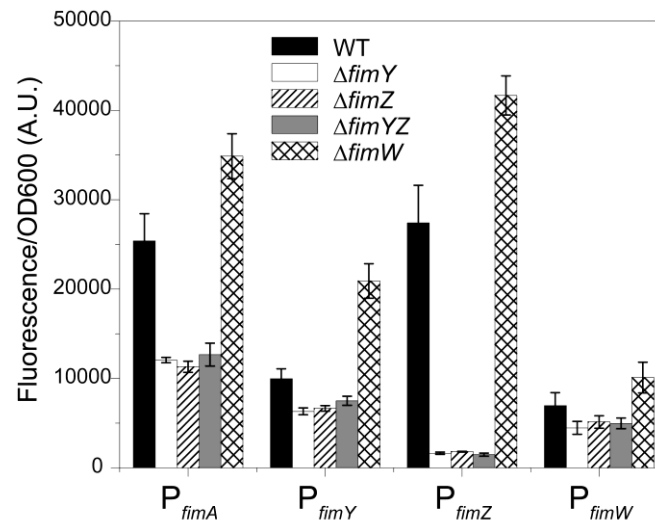


Figure 27. FimY and FimZ are activators and FimW is repressor of *fim* gene expression. Comparison of P_{fimA} , P_{fimY} , P_{fimZ} , and P_{fimW} promoter activities in wild type (WT) and $\Delta fimY$, $\Delta fimZ$, $\Delta fimYZ$, and $\Delta fimW$ mutants. (Data is average of 3 experiments. Each experiment was done in triplicate).

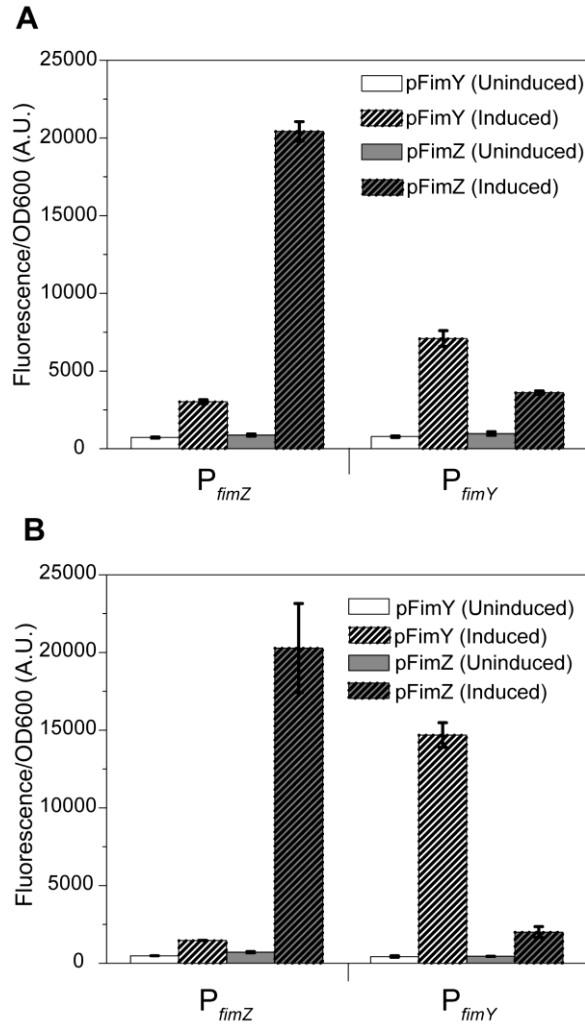


Figure 28. FimY and FimZ are strong activators of each other's expression and also weak auto-activators. Comparison of P_{fimY} and P_{fimZ} promoter activities in a *S. typhimurium* $\Delta fimYZ$ mutant (**A**) and *E. coli* (**B**) where FimY and FimZ are independently expressed from an aTc-inducible promoter on a plasmid. Note that *tetR* is also expressed from this plasmid in order to achieve aTc-inducible expression. (Data is average of 3 experiments. Each experiment was done in triplicate).

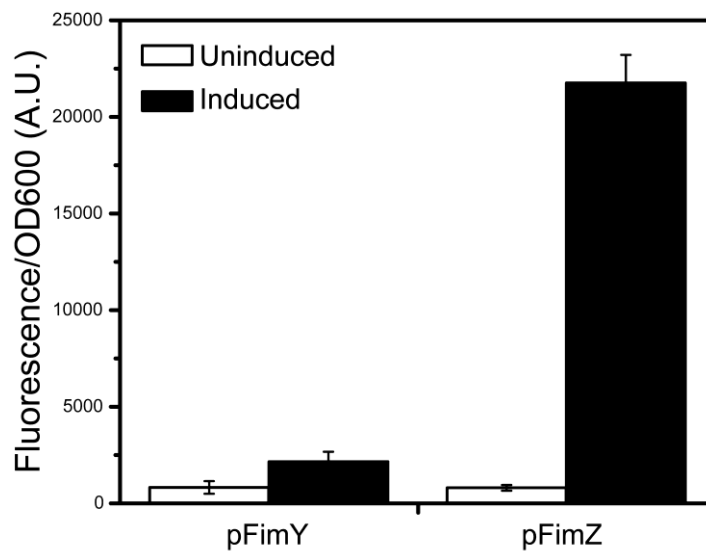


Figure 29. FimY and FimZ can independently activate expression from the P_{fimA} promoter. Comparison of P_{fimA} promoter activity in a $\Delta fimYZ$ mutant where FimY and FimZ are independently expression from an aTc-inducible promoter on a plasmid. (Data is average of 3 experiments. Each experiment was done in triplicate).

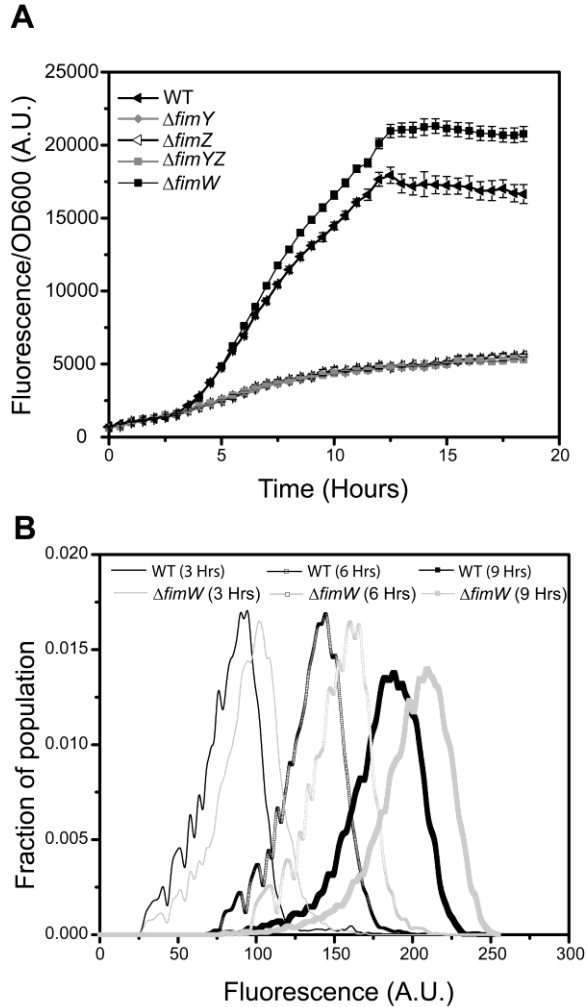


Figure 30. Dynamics of P_{fimA} promoter activity. (A) Population-average P_{fimA} activity as a function of time in wild type (WT) and $\Delta fimY$, $\Delta fimZ$, $\Delta fimYZ$, and $\Delta fimW$ mutants. **(B)** Histogram of single-cell P_{fimA} promoter activity at select times in wild type and a $\Delta fimW$ mutant. Single-cell measurements of promoter activity were obtained using flow cytometry. (Figure 4A: Data is average of single experiment with average of 6 independent cultures. The experiment was repeated thrice and identical results observed. Figure 4B: Population distribution data is from a single experiment. The experiment was repeated thrice and identical results were observed (data not shown)).

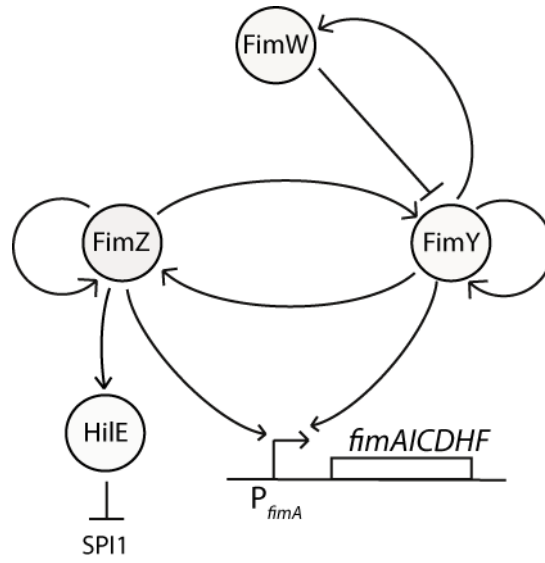


Figure 31. Model for the type I fimbriae gene circuit in *S. typhimurium*.

Chapter 7. Coordinated Regulation of the Flagellar, SPI1, and Type I Fimbriae Gene Networks

Introduction

Salmonella serovars are responsible for a large number of diseases ranging from self-limiting gastroenteritis to life-threatening systemic infection (Ellermeier, 2006, Miller SI, 2000). The complete infection process comprises of a number of steps and for successful infection, the bacterium needs to ensure that the appropriate cellular processes are activated at the right times and in the right amounts. After ingestion, on reaching the preferred site of infection - the ileum of the small intestine – the bacterium utilizes flagella on its surface to swim in the liquid media. In the environmental conditions of the small intestine, the bacterium then assembles a Type 3 Secretion System (T3SS) encoded on a 40 kilobase fragment of the chromosome called *Salmonella* Pathogenicity Island 1 (SPI1) (Mills et al., 1995, Lee et al., 1992, Kimbrough & Miller, 2000, Kubori et al., 1998, Kimbrough & Miller, 2002, Sukhan et al., 2001). The SPI1-encoded T3SS injects effector proteins directly into the host cell cytoplasm (Collazo & Galan, 1997b, Collazo & Galan, 1996). The injected effector proteins elicit a large number of physiological responses from the host cell, including actin rearrangement that promotes invasion, fluid accumulation and transepithelial migration of polymorphonuclear leukocytes, and necrosis of Peyer's patch macrophages (Ginocchio

et al., 1994, Francis *et al.*, 1993, Hayward & Koronakis, 2002, Zhou & Galan, 2001). Regulators encoded on the SPI1 fragment also activate a non-fimbrial adhesin encoded on SPI4 that helps bacteria adhere to epithelial cells during invasion (Gerlach *et al.*, 2007a, Main-Hester *et al.*, 2008, Saini & Rao, 2010). In addition, during stationary phase of growth, *Salmonella* assembles surface appendages, Type I fimbriae, which are finger-like projections that carry adhesins specific for mannosylated glycoproteins. These Type I fimbriae facilitate binding to the epithelial cells and long-term persistence of the bacterium in the small intestine (Lawley *et al.*, 2006, Gerlach *et al.*, 1989, Saini *et al.*, 2009). Therefore, successful invasion and persistence requires successful assembly and function of a number of surface organelles namely – flagella, SPI1-encoded T3SS, SPI4-encoded adhesin, and Type I fimbriae. All these appendages serve distinct cellular functions of motility, injection, and adhesion.

In *Salmonella enterica* serovar Typhimurium (*S. typhimurium*), more than 50 genes arranged in at least 17 operons are involved in gene-regulation, assembly and function of flagella. Structurally, the flagellum is composed of three parts – the basal body, hook, and the filament. Basal body anchors the flagellum to the cell, hook is a flexible joint that transmits torque produced by the motor to the filament, and the filament is a rigid helical structure 5-15 μm in length that on counter-clockwise rotation propels the cell forward (Chilcott & Hughes, 2000).

Assembly proceeds in a sequential order beginning with the basal body and concluding at the distal tip of the filament. This order in assembly process is dictated by the genetic logic governing gene expression. Specifically, the flagellar promoters can be divided into three classes (Chilcott & Hughes, 2000). The class 1 promoter, P_{flhDC} , controls expression of the two genes, *flhD* and *flhC*. A large number of regulators feed into the P_{flhDC} promoter and their combinatorial action decides if the cell decides to be motile or not. FlhD and FlhC then form the complex FlhD₄C₂ which is essential for class 2 promoter activation (**Figure 32**) (Ikebe et al., 1999, Wang et al., 2006). Class 2 promoters control expression of hook-basal body (HBB) genes and the class 3 sigma factor, FliA. On successful completion of HBB assembly, FliA activates class 3 promoters which control expression of chemotaxis, motor, and the filament proteins (Kutsukake, 1994, Karlinsey et al., 2000b). Apart from FlhD₄C₂ and FliA, flagellar gene expression is also controlled by a number of regulators encoded in the flagellar network. These regulators include, FlgM, FliT, FlgN, and FliZ (Ohnishi et al., 1992, Yamamoto & Kutsukake, 2006, Kutsukake et al., 1999, Saini et al., 2008, Aldridge et al., 2003). Of particular interest in this report is FliZ, which is encoded in the same operon as FliA and is known to be a positive regulator of flagellar and SPI1 gene expression.

The expression of SPI1-encoded T3SS is controlled in response to specific environmental cues that presumably mimic the conditions in the small intestine. In laboratory, SPI1-including conditions mean those of high-osmolarity and low oxygen. Regulation of the structural genes for the T3SS is primarily controlled by HilA, a member

of ToxR/OmpR family of transcriptional regulators encoded within SPI1 (Bajaj et al., 1995). Expression of HilA in-turn is controlled by three AraC-like regulators – HilD, HilC, and RtsA (**Figure 32**) (Schechter & Lee, 2001, Olekhovich & Kadner, 2002, Akbar *et al.*, 2003, Ellermeier & Slauch, 2003). While HilD and HilC are encoded in SPI1, RtsA is encoded on a 15 kb island inserted near the tRNA^{PheU} gene. All three bind to the P_{hilA} promoter region individually and drive HilA expression. All three – HilD, HilC, and RtsA – independently of each other, also activate the P_{hilD}, P_{hilC}, and P_{rtsA} promoters. SPI1 gene expression is negatively regulated by a *Salmonella*-specific protein, HilE. HilE binds to and prevents HilD-dependent activation of SPI1 promoters (Baxter et al., 2003). The P_{hilE} promoter is not known to be regulated by any SPI1-encoded regulators. In addition, encoded in the same operon as *rtsA* is a gene called *rtsB* (STM4314). RtsB is known to bind the P_{fhDC} promoter and repress motility (Ellermeier & Slauch, 2003).

In *S. typhimurium*, all the genes necessary for Type I fimbriae production are present in the *fim* gene cluster. This gene cluster consists of six structural genes, three regulators, and a tRNA specific for rare arginine codons (AGA and AGG). All six structural genes are transcribed from a single, P_{fimA} promoter (Piknova et al., 2005, Hancox et al., 1997, Purcell et al., 1987, Rossolini et al., 1993). The P_{fimA} promoter is independently activated by FimZ and FimY (**Figure 32**). In addition, FimZ and FimY also activate each other's expression (Saini et al., 2009, Yeh et al., 2002, Tinker & Clegg, 2000). *Fim* gene expression is negatively regulated by FimW. This is done in a negative feedback loop where FimY activates the P_{fimW} and FimW represses P_{fimY} (Saini et al., 2009, Tinker et al.,

2001). In addition, FimZ is known to repress flagellar and SPI1 gene expression. FimZ binds to the P_{fHDC} promoter to repress expression of the flagellar genes (Clegg & Hughes, 2002). It also activates transcription of HliE which negatively regulates SPI1 gene expression (Saini et al., 2009).

While the molecular details of FliZ-, RtsB-, and FimZ-dependent cross-talk interactions have been studied extensively, the significance of these interactions is relatively unknown. Each of the three networks – flagella, SPI1, Type I fimbriae – serve a unique and mutually exclusive cellular function during invasion. Therefore, for successful infection, it is important that the timing of expression and function of these systems is robustly controlled. We hypothesize that the cross-talk between the flagellar, SPI1, and Type I fimbriae in *S. typhimurium* serves to fine-tune the activation and de-activation dynamics to ensure hierarchical expression of the three systems.

To test the hypothesis, we monitored the gene expression dynamics of the flagellar, SPI1, and Type I fimbriae in a number of regulatory mutants. We demonstrate that there is a natural hierarchy of gene expression where flagellar gene expression is followed by SPI1 and then Type I fimbrial gene expression. Our results indicate that the regulatory cross-talk between the three systems ensures the correct timing of activation and de-activation of these circuits, presumably leading to a successful infection process.

Results

Hierarchical Expression of Flagellar, SPI1, and Type I Fimbriae

For a successful infection cycle, multiple processes need to be simultaneously regulated by the bacterium *S. typhimurium*. In this report, we focus on the role of cross-talk between three major systems in the *Salmonella* infection cycle – flagella, SPI1, and Type I fimbriae – in controlling the gene expression dynamics of these three systems. To monitor expression dynamics, we chose the P_{flgA} , P_{hilA} , and the P_{fimA} promoters as representatives of the flagellar, SPI1, and Type I fimbriae gene circuits respectively. The P_{flgA} promoter controls expression of genes that encode structural components of the flagellar P-ring (Nambu & Kutsukake, 2000); the P_{hilA} promoter controls expression of the master regulator HilA in the SPI1 regulatory network (Lostroh & Lee, 2001a); and the P_{fimA} promoter regulates expression of the structural genes of the Type I fimbriae in *S. typhimurium* (Rossolini et al., 1993, Purcell et al., 1987). To track the dynamics of these promoters' activities, in our kinetic experiments we cloned the promoter of interest upstream of the luciferase operon, *luxCDABE*, from *Photobacterium luminescens* on a medium copy plasmid (Goodier & Ahmer, 2001, Saini et al., 2008). Since, luciferase-based reporter system is far more sensitive than fluorescent proteins, particularly at low levels of expression, use of *luxCDABE* allowed us to effectively track promoter activity over time. However, the enzymatic complex in the luciferase system, LuxCD, has a half life of only about 10 minutes and therefore is not suited for end-point measurements (Hakkila et al., 2002). Therefore, for end-point experiments, we used promoter fusions

to a fluorescent gene, *venus*, on an otherwise identical plasmid system (Nagai et al., 2002).

To monitor gene expression dynamics of the three systems (flagella, SPI1, and Type I fimbriae), we first monitored the P_{flgA} , P_{hilA} , and P_{fimA} promoter activity in wild-type cells. Our results show that in wild type *Salmonella*, flagellar, SPI1, and Type I fimbriae systems are expressed sequentially (**Figure 33**). Specifically, the cells first express the flagellar genes, followed by the SPI1, and lastly Type I fimbriae genes. Previous work has established that growth phase plays an important role in the timing of activation of these three systems. In particular, the flagellar genes are known to get expressed during the early log phase, the SPI1 network turns “on” during the late exponential phase, and the Type I fimbriae genes are expressed in the stationary phase of growth.

The Flagellar, SPI1, and Type I Fimbriae Circuits Control Each Other’s Expression Dynamics

Our results in wild type *Salmonella* indicate that, when grown in conditions that mimic those inside the small intestine - the flagellar, SPI1, and Type I fimbriae systems are expressed sequentially. Next, we wanted to study if the three systems control the dynamics of expression of each other or not. Many reports have shown the regulatory links between the flagellar, SPI1, and Type I fimbriae networks. Therefore, we wanted to investigate the impact of this regulation on the timing of expression of these systems.

We studied gene expression dynamics in mutants where one of the three systems was knocked out. Specifically, we monitored the P_{flgA} , P_{hilA} , and P_{fimA} promoter activities in an $\Delta flhDC$ mutant, a $\Delta SPI1$ mutant, and a $\Delta fimYZ$ mutant.

Our results show that absence of one of the three systems has an impact on the timing of expression of all three systems. In particular, we note that in a $\Delta flhDC$ mutant, the P_{flgA} promoter was inactive, the P_{hilA} promoter dynamics were slower, and the P_{fimA} promoter activity “off” to “on” transition was faster as compared to the wild type (**Figure 34A**). In a $\Delta SPI1$ mutant, the P_{flgA} promoter’s “on” to “off” transition was delayed, the P_{hilA} promoter was inactive, and the P_{fimA} promoter activation was delayed (**Figure 34B**). Finally, in a $\Delta fimYZ$ mutant, there was no impact on flagellar gene expression dynamics, the “on” to “off” step for the P_{hilA} promoter activity was delayed, and the P_{fimA} promoter activity was about 70-80% lower than the wild type (**Figure 34C**).

These results clearly demonstrate that apart from being expressed at different times in the growth phase, the timing of expression of the flagellar, SPI1, and Type I fimbriae systems is also controlled by the cross-talk between the three systems. In this report, we focus on the role of FliZ, RtsB, and FimZ in conducting this cross-talk and orchestrating the dynamics of gene expression in the three systems. In addition, we also wanted to test the impact of the three systems on end-point expression of each other.

FliZ-, RtsB-, and FimZ-Mediated Cross-Talk Controls *Fla*, SPI1, and *Fim* Levels

FliZ from the flagellar network is a post-translational activator of the flagellar master regulator FlhD4C2 complex. In addition, FliZ is also known to be a positive regulator of the SPI1-encoded genes via an unknown mechanism. To understand the effect of FliZ on flagellar, SPI1, and fimbrial gene expression, we measured end-point expression levels of the P_{flgA} , P_{hilA} , and P_{fimA} promoter activity in wild type, a $\Delta fliZ$ mutant and a $\Delta fliZ$ mutant constitutively expressing FliZ from an inducible $P_{LTetO-1}$ promoter. Our results indicate that deletion of *fliZ* leads to about a two-fold decrease in P_{flgA} and P_{hilA} promoter activity as compared to the wild type. On the other hand, deletion of *fliZ* leads to an approximately thirty percent increase in P_{fimA} promoter activity. Consistent with these results, over-expression of FliZ from a high-copy plasmid resulted in a roughly two-fold increase in the flagellar and SPI1 network gene expression and about a two-fold decrease in the Type I fimbriae network gene expression (**Figure 35A**).

Next, we studied the impact of RtsB on gene expression of the three systems. RtsB - encoded in the same operon as the SPI1 regulator, RtsA - binds to the flagellar class 1 promoter, $P_{FlhD4C2}$ promoter, and represses activation of the flagellar cascade. The P_{rtsA} promoter, which controls RtsB expression, is activated by SPI1 regulators HilD, HilC, and RtsA. Therefore, cues that turn on SPI1 gene expression also trigger RtsB expression. Deletion of *rtsB* resulted in a roughly 40% increase in the P_{flgA} promoter activity, while over-expression of RtsB lead to about 50% decrease in the P_{flgA} activity.

Interestingly, while knocking out *rtsB* was found to have minimal impact on SPI1 and Type I fimbriae gene expression, over-expression of RtsB resulted in roughly 40% decrease and increase in the SPI1 and Type I fimbriae activity, respectively (**Figure 35B**).

The Type I fimbriae regulator, FimZ, in conjunction with another regulator in the fimbriae network, FimY, activates transcription from the P_{fimA} promoter. The P_{fimA} promoter controls expression of six genes which form the export apparatus and the structural components of the Type I fimbriae. In addition, FimZ is also known to activate the P_{hilE} promoter. The resulting HilE, then, binds to HilD and prevents HilD-dependent activation of SPI1 genes. FimZ is also known to bind to the $P_{FlhD4C2}$ promoter and repress expression of the flagellar genes. Consistent with these previous results, deletion and over-expression of FimZ resulted in an increase and decrease of flagellar and SPI1 gene expression, respectively. In addition, consistent with previous reports, deletion of FimZ leads to an approximately 70% decrease in the P_{fimA} promoter activity (**Figure 35C**).

While the characterization of the molecular interactions of FlhZ, RtsB, and FimZ in these three systems has been a subject of a large number of studies, little is known about the role of these cross-talk interactions in controlling the dynamics of gene expression. With this understanding of the infection process, we hypothesized that FlhZ-, RtsB-, and FimZ-mediated cross-talk interactions serve to fine-tune the timing of activation and deactivation of the three systems. Therefore, we next systematically studied the dynamics of gene expression in the three systems in different regulatory

mutants where the FliZ-, RtsB-, and FimZ-mediated cross-talk elements have been altered.

FliZ Fine-Tunes the Timing of Activation of the Flagellar, SPI1, and Type I Fimbriae Circuits

First, we studied the dynamics of flagellar, SPI1, and fimbriae gene expression in wild type, a $\Delta fliZ$ mutant, and a $\Delta fliZ$ mutant constitutively expressing FliZ from a high copy plasmid. Consistent with the previous reports, in a $\Delta fliZ$ mutant, the peak P_{flgA} (flagellar) and P_{hilA} (SPI1) activity is reduced. Over-expression of FliZ led to about a two-fold increase in the peak promoter activity levels for the P_{flgA} and P_{hilA} promoters. However, in a $\Delta fliZ$ mutant, we also observed slower induction of the SPI1 gene circuit. In addition, a $\Delta fliZ$ mutant also displayed elevated and faster induction of the *fim* circuit as compared to the wild type (**Figure 36A**). Our results also demonstrate that over-expression of FliZ led to delay in the “on” to “off” transition of the flagellar and SPI1 systems (**Figure 36B**) and a delay in the “off” to “on” transition of the Type I fimbriae network.

A number of studies have tried to characterize the mode of action of FliZ-dependent activation of the flagellar and SPI1 genes. However, the precise mechanism is still unknown. We previously reported that FliZ acts as a post-translational activator of the flagellar master regulator complex FlhD4C2. In similar way, we hypothesized that FliZ dependent activation of SPI1 and repression of fimbrial networks is via regulation of

their respective master regulators, HilD and FimZ. Therefore, we next tested the hypothesis whether FliZ activates SPI1 via HilD and represses fimbriae via FimZ.

To understand the mechanism of FliZ regulation of SPI1, we first tested whether FliZ could activate the P_{hilA} promoter in the absence of HilC and RtsA. To do this, we over-expressed FliZ in a $\Delta hilC \Delta rtsA$ mutant, and measured the P_{hilA} promoter activity. Our results show that FliZ is able to activate HilA expression in the absence of HilC and RtsA (data not shown). Next, to test whether FliZ activates SPI1 independent of HilD, we over-expressed FliZ from a $P_{LtetO-1}$ promoter from a medium copy plasmid in a $\Delta hilD \Delta fliZ$ mutant and measured the P_{hilA} promoter activity. Our results show that in the absence of HilD, FliZ was unable to activate SPI1 gene expression (**Figure 37A**).

To investigate if the FliZ-dependent SPI1 activation is P_{hilD} promoter dependent; we replaced the P_{hilD} promoter with a *tetRA* element at its native chromosomal locus. In this construct ($\Delta P_{hilD}::tetRA$), expression of HilD was under a P_{tetA} promoter and expression could be induced by addition of tetracycline. We then measured P_{hilA} promoter activity in the strain ($\Delta P_{hilD}::tetRA \Delta hilC \Delta rtsA \Delta fliZ$) in the presence of tetracycline with and without over-expression of FliZ. The rationale behind the experiment was to test whether FliZ controls HilD transcription or does it control HilD-amount or HilD-activity post-transcriptionally. In this experiment, FliZ was over-expressed from an arabinose-inducible promoter P_{BAD} on a medium copy plasmid. Our results demonstrate that in the strain $\Delta P_{hilD}::tetRA \Delta hilC \Delta rtsA \Delta fliZ$, over-expression of

FliZ was still able to induce the P_{hilA} promoter activity (**Figure 37B**), suggesting that FliZ regulates SPI1 gene expression by its regulation of HilD post-transcriptionally.

A novel observation from this study was FliZ-dependent repression of the Type I fimbriae gene expression. In a $\Delta fliZ$ mutant, the P_{fimA} promoter exhibited faster and stronger induction kinetics as compared to the wild-type. To characterize the mechanism of this FliZ-dependent repression of the fimbrial gene circuit we measured P_{fimA} promoter activity in the strain $\Delta P_{fimZ}::tetRA \Delta fimY \Delta fliZ$, with and without ectopic over-expression of FliZ from a plasmid source. Based on our data, we show that FliZ represses the Type I fimbriae circuit by either controlling FimZ level post-transcriptionally or FimZ-activity inside the cell (**Figure 37C and 37D**). In addition, it is also known that the Type I fimbriae regulator FimY binds to and activates the P_{fimA} promoter. To test the possibility if FliZ also acts through FimY to repress P_{fimA} promoter activity, we did similar experiments in the strain $\Delta P_{fimY}::tetRA \Delta fimY \Delta fliZ$. Our results show that FliZ-dependent regulation of the P_{fimA} promoter activity is independent of FimY (data not shown).

Collectively, our results show that FliZ, in addition of being a positive flagellar regulator, plays an important role in linking the expression of SPI1 and Type I fimbriae with flagellar expression. Despite the fact that the precise mechanism of the FliZ-dependent regulation still eludes us, we demonstrate that FliZ plays an important role in controlling the hierarchy of activation of the processes involved during the infection

cycle. Physiologically, when the cell is motile, FliZ-dependent activation of SPI1 seems to better prepare the cell for the next process in the infection cycle. This seems to be important for rapid “off” to “on” transition of the SPI1 gene circuit. In addition, FliZ also ensures that the genes responsible for persistence in the intestine are not turned “on” prematurely.

RtsB Controls the “On” to “Off” Dynamics of the Flagellar Circuit

Next, we focused on characterizing the role of RtsB in regulating the dynamics of the flagellar, SPI1, and Type I fimbriae gene expression. RtsB is encoded in the same operon as RtsA. While RtsA is a SPI1 activator, RtsB binds to and represses expression from the $P_{FlhD4C2}$ promoter. To understand its role in dictating gene expression dynamics, we measured the P_{flgA} , P_{hilA} , and P_{fimA} promoter activity in wild type, an $\Delta rtsB$ mutant, and an $\Delta rtsB$ mutant where RtsB was over-expressed from a high copy plasmid. Our data shows two important observations. First, deletion of *rtsB* delays shutting down of the flagellar network. In other words, in an *rtsB* mutant, the flagellar system is in the “on” state for longer than in wild type. Secondly, deletion of *rtsB* also delays the induction of the *fim* circuit (**Figure 38A**). Consistent with these observations, over-expression of RtsB led to - the flagellar system being completely turned “off”; SPI1 gene expression was delayed and slower as compared to wild type; and the fimbrial genes were induced faster and to higher levels as compared to the wild type (**Figure 38B**). These results demonstrate that RtsB plays an important role in coupling the dynamics of the SPI1 network with the dynamics of the flagellar and Type I fimbriae system.

While RtsB-dependent repression of the flagellar network has been reported previously, RtsB is not known to regulate the P_{fimA} promoter. To characterize the mechanism of RtsB-dependent activation of the *fim* circuit, we performed experiments where we measured end-point P_{fimA} promoter activity in wild-type and $\Delta fliZ \Delta rtsB$, pRtsB strain. The rationale behind this experiment was to test if RtsB-dependent activation of the Type I fimbriae circuit was via FliZ. Consistent with our hypothesis, we observed that in a $\Delta rtsB$ mutant, the P_{fimA} promoter was upregulated by around 25%. Over-expression of RtsB in the absence of FliZ however, was not able to repress P_{fimA} promoter (**Figure 38C**).

Therefore, we conclude that once the SPI1 genes are “on”, they also activate RtsB expression. RtsB, then, binds to the P_{flhDC} promoter and down-regulates the flagellar gene expression. As indicated by our results, RtsB-dependent repression of the flagellar network is important in the effective shut-down of the flagellar circuit. Secondly, down-regulation of flagellar genes consequently negatively regulates the FliZ levels inside the cell which relieves the FliZ-dependent repression of the Type I fimbrial circuit. Physiologically, this additional regulation likely ensures two things. First, SPI1-activation also turns “on” RtsB expression, which is important to turn “off” the flagellar network. Secondly, by shutting down the flagellar network rapidly, RtsB ensures timely activation of the Type I fimbrial network.

FimZ-Dependent Negative Regulation of FlhD₄C₂ and HilD

Last, we analyzed the role of Type I fimbriae regulator FimZ in dictating dynamics of flagellar, SPI1, and Type I fimbriae gene expression. FimZ binds to and activates transcription from the P_{fimA} promoter. In addition, however, FimZ is also known to repress SPI1 and flagellar networks. FimZ binds to and activates the P_{hilE} promoter. The resultant HilE negatively regulates SPI1 gene expression. FimZ is also known to bind to the $P_{FlhD4C2}$ promoter and repress flagellar gene expression. Therefore, we hypothesized that FimZ controls the dynamics of the three systems under consideration in this study.

To test this hypothesis, we tracked the P_{flgA} , P_{hilA} , and P_{fimA} promoter activity in wild type, a $\Delta fimZ$ mutant, and $\Delta P_{fimZ}::tetRA$, where the P_{fimZ} promoter was replaced by a *tetRA* element. In the strain $\Delta P_{fimZ}::tetRA$, FimZ expression could be induced by addition of tetracycline. Consistent with our hypothesis, we observed that in the absence of FimZ - SPI1 shut-down and Type I fimbriae-induction are both delayed. In addition, we note that in the absence of FimZ, the absolute levels of the P_{fimA} promoter drop considerably (**Figure 39A**). Similarly, we also tested the gene expression dynamics of the three systems in a strain called $\Delta P_{fimZ}::tetRA$. In this strain, we replaced the P_{fimA} promoter with a *tetRA* element. By doing this, FimZ expression was made conditional on the presence of tetracycline in the media. Upon induction, in this strain, the P_{fimA} promoter was induced first followed by the P_{flgA} , and the P_{hilA} promoter (**Figure 39B**). In addition, the flagellar and SPI1 expression levels were also reduced by about 70% in this strain. Therefore, in addition to being a P_{fimA} activator, FimZ-dependent repression of

the flagellar and SPI1 networks leads to a change in the timing of gene expression dynamics.

To demonstrate that FimZ-dependent repression of the SPI1 circuit was because of activation of P_{hilE} promoter, we measured P_{hilA} activity in the strains $\Delta fimZ$ and $\Delta fimZ \Delta hilE$ where FimZ was being over-expressed from a $P_{LtetO-1}$ promoter on a high copy plasmid. Our results indicate that over-expression of FimZ in the absence of HilE did not lead to repression of the P_{hilA} promoter expression levels (data not shown). There was no impact of a $\Delta fimZ$ mutation on flagellar dynamics or absolute levels of flagellar activity. This is probably due the fact that the *fim* system only comes on late in the growth phase and by that time the flagellar network has already been shut down by global regulators and SPI1-activated RtsB. But, FimZ-dependent repression of the flagellar gene expression likely encodes an additional check-point inside the cell to ensure effective shut-down of the flagellar gene expression.

Put together, our results indicate that cross-talk interactions between the flagellar, SPI1, and Type I fimbriae gene circuits serve an important purpose in controlling the timing of activation and deactivation of the systems. Coordinated expression of the three systems is critical for successful infection and long-term persistence of the bacterium in the intestine. We demonstrate that FliZ, RtsB, and FimZ regulators encoded in the flagellar, SPI1, and Type I fimbriae networks respectively, control the level and timing of interaction the three steps.

Discussion

The food-borne pathogen *Salmonella* coordinates a number of cellular functions to cause a successful infection. The three main systems employed by the bacterium in the intestinal phase of the infection are flagella, SPI1 encoded T3SS, and Type I fimbriae. Presumably, the bacteria use flagella to swim to the site of infection (M-cells lining the small intestine), SPI1 encoded T3SS to invade M-cells, and Type I fimbriae to persist in the intestine. In order to ensure that each of these three systems is expressed at the appropriate times in the infection cycle, it is important that *Salmonella* regulates the dynamics of these systems. In this report, we demonstrate that the flagellar, SPI1, and Type I fimbriae networks are expressed sequentially in wild type *Salmonella*. In this hierarchy, the flagellar genes are activated first, followed by the SPI1 and Type I fimbriae genes respectively. As flagellar genes are expressed in the early log-phase, SPI1 genes in the late log-phase, and the Type I fimbriae genes in the stationary phase of growth, this hierarchy in gene expression is enforced by the growth-phase of the bacterium. However, to better control the temporal activation and deactivation of these systems, *Salmonella* utilizes regulatory cross-talk between the flagellar, SPI1, and Type I fimbriae networks. Our results show that in the absence of regulatory cross-talk between these systems, cells are unable to maintain both, wild type hierarchy of activation and also the maximal levels of expression.

In the context of invasion, our results suggest that this dynamic regulation of the flagellar, SPI1, and Type I fimbriae gene circuits is important for the following reason. In the conditions prevailing in the small intestine, the flagellar network is active resulting in the bacterium actively swimming to the site of infection. FlhZ from the flagellar network then: (a) positively regulates HilD, and (b) negatively regulates FimZ. As demonstrated by our results, FlhZ-dependent activation of HilD accelerates SPI1 gene expression, resulting in the cell actively assembling needle complexes for invasion and FlhZ-dependent repression of FimZ likely prevents premature activation of the Type I fimbriae gene network.

Once the SPI1 network is “on”, SPI1-regulators HilD, HilC, and RtsA activate expression of RtsB. As mentioned before, RtsB binds to the P_{flhDC} promoter and represses transcription. This interaction is important for rapid shut-off of the flagellar network. RtsB-dependent repression of the flagellar gene circuit also weakens the FlhZ-dependent repression of the Type I fimbriae network. This secondary interaction allows for the activation of the fimbriae genes if the bacterium is not internalized in the host cell. The activation of the Type I fimbriae gene network is likely important for long-term persistence in the intestine, as has been observed before. Last, once the Type I fimbriae genes are “on”, FimZ represses both flagellar and SPI1 gene circuits leading to effective shut-down of these systems.

Dynamic regulation of multiple systems is widely observed in bacteria. In particular, pathogens are often required to coordinate the expression of multiple systems to accomplish a successful infection process. A number of studies have identified mechanisms employed in different pathogens to exhibit this coordination and dynamic control on expression of multiple systems. Perhaps the most common example of regulatory cross-talk mediating the timing of activation leading to hierarchical expression of systems is sugar transport and utilization in bacteria (Monod, 1966, Desai & Rao, 2010). Simple cross-talk interactions in *E. coli* ensure that the bacterium processes multiple carbon sources sequentially. This cross-talk mediated hierarchy allows the bacterium to utilize its preferred carbon source first before it moves to less desirable carbon sources.

In this study, we demonstrate that using regulatory cross-talk interactions between the flagellar, SPI1, and Type I fimbriae networks, the bacterium *S. typhimurium* controls the hierarchical expression of these systems and ensures a successful infection process. However, *Salmonella* is also known to employ long polar fimbriae (*lpf*), SPI4-encoded non-fimbriae adhesin, and SPI2-encoded T3SS during different stages of the infection process. While *lpf* (van der Velden et al., 1998, Baumler et al., 1997, Ledebauer et al., 2006) and SPI4-encoded (Gerlach et al., 2007b) adhesin are known to coordinate attachment of the bacteria to the epithelial cells, SPI2-encoded T3SS is central for the ability of the cell to cause systemic infections and for intracellular pathogenesis. Consistent with this, the *lpf* and the SPI4 systems are expressed in conditions prevailing

in the small intestine, and are known to be co-regulated with the flagellar and SPI1 networks respectively (Ahmer et al., 1999, De Keersmaecker et al., 2005, Ellermeier & Slauch, 2003, Gerlach et al., 2007b, Main-Hester et al., 2008, Saini & Rao, 2010). The SPI2 system is also known to be activated by SPI1-encoded regulator HilD (Fass & Groisman, 2009, Bustamante *et al.*, 2008), but, the environmental cues that turn “on” SPI2 genes are different from the ones that activate systems involved in the intestinal phase of the infection. More precisely, SPI2 gene expression is known to get activated in response to low Mg^{2+} concentration and low pH (Hensel, 2000). How the cells coordinate the transition from SPI1-activated to SPI2-activated gene expression profile, and what is the significance of HilD-mediated regulatory cross-talk between these two systems is not well understood.

To conclude, in this chapter, we present evidence for role of cross-talk in dynamically coordinating a number of cellular processes in the common food-borne pathogen, *Salmonella*. We show that three important systems in the early phase of the infection cycle – flagella, SPI1, and Type I fimbriae – are expressed hierarchically in wild type *Salmonella* and that regulatory cross-talk between the three systems is an important tool employed by the bacterium to effectively transition from one system to another.

Figures – Coordinated Regulation of the Flagellar, SPI1, and Type I Fimbriae Gene Networks

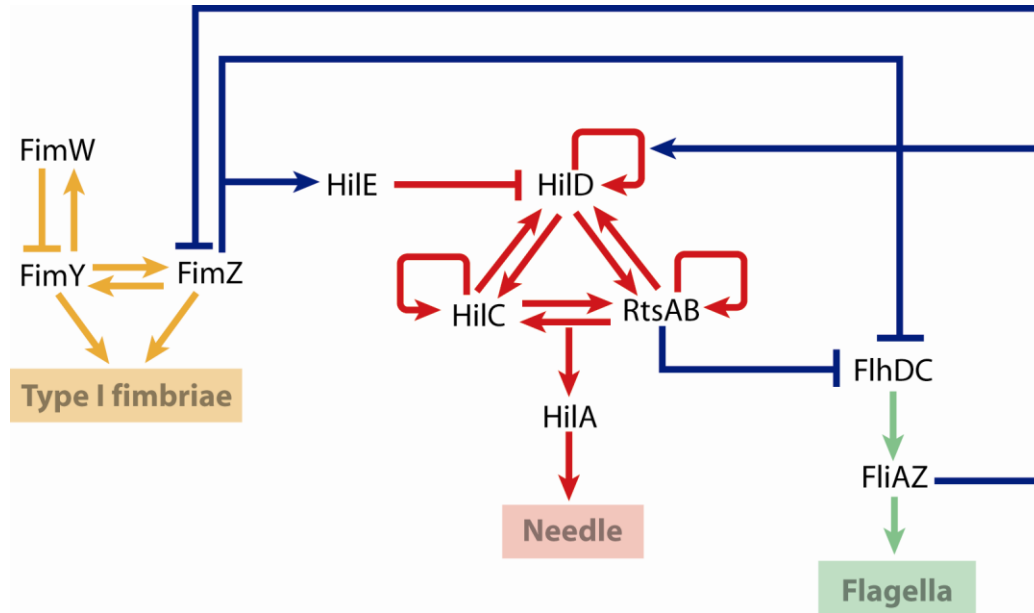


Figure 32. Regulatory cross-talk between the flagellar, SPI1, and Type I fimbriae gene regulatory networks in *S. typhimurium*. FliZ from the flagellar network activates HilD expression post-translationally. FliZ also represses Type I fimbriae network by its action on FimZ post-translationally. FimZ binds to the P_{hilE} promoter to activate transcription. FimZ binds to the P_{flhDC} promoter to repress flagellar expression. RtsB binds to the P_{flhDC} promoter to repress motility.

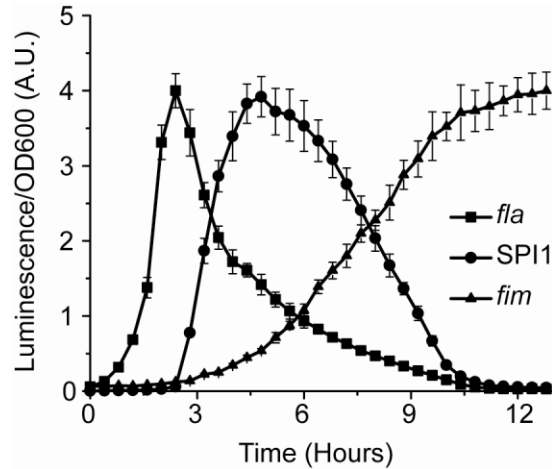


Figure 33. Flagellar, SPI1, and Type I fimbrial gene expression is sequential. Flagellar (P_{flgA} promoter), SPI1 (P_{hilA} promoter), and Type I fimbrial (P_{fimA} promoter) gene expression is hierarchical. Wild-type cells (14028) were grown overnight at 37°C in conditions of high oxygen, no salt, and vigorous shaking. The overnight culture was then sub-cultured 1:500 in fresh LB media (with salt). 100 μ l aliquot of the sub-cultured cells was transferred to a 96-well plate and covered with a breathe-easy membrane to prevent evaporation. Luminescence and optical density (OD600) readings were taken every 20 minutes. All experiments were done in three independent repeats with six samples in each experiment. Error bars denote standard deviations.

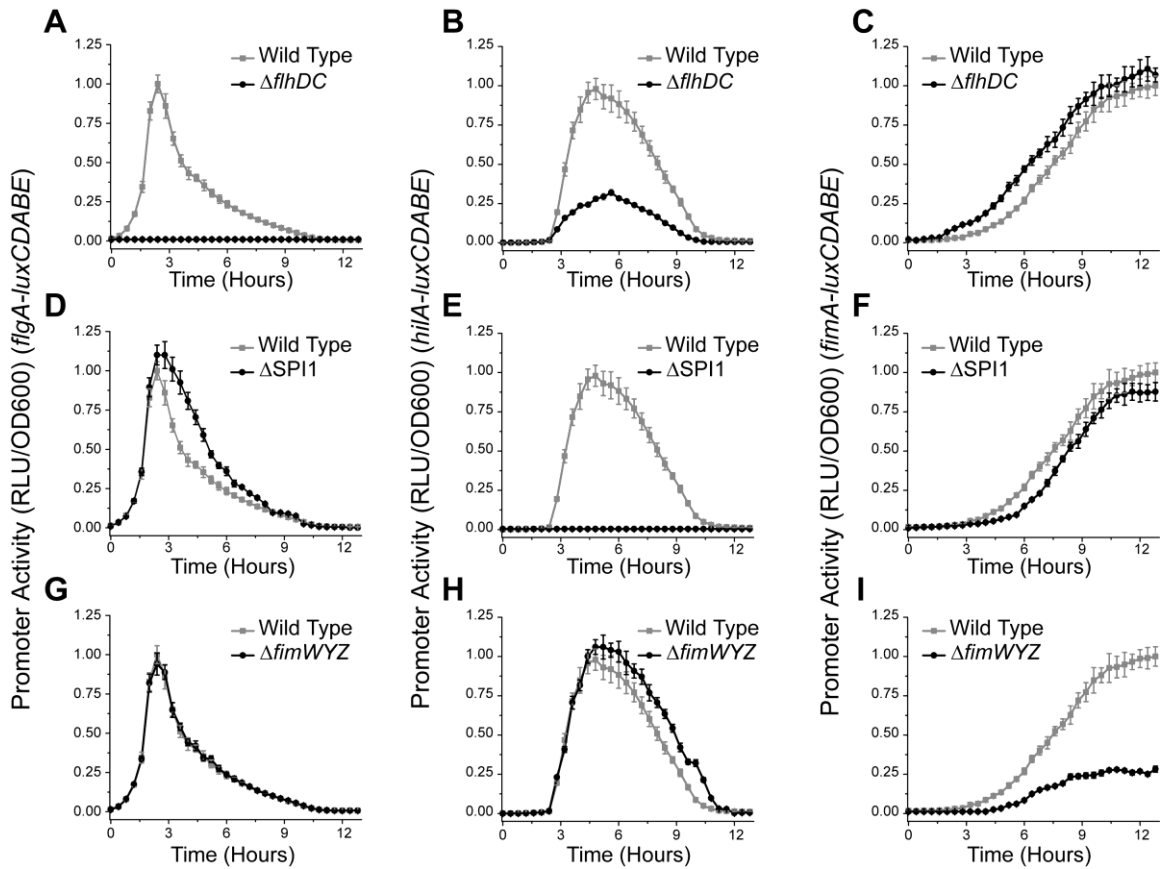


Figure 34. Flagellar, SPI1, and Type I fimbriae gene networks control each other's gene expression dynamics. (A-C) Comparison of the P_{flgA} (A), P_{hilA} (B), and P_{fimA} (C) promoter activity in wild type cells and a $\Delta flhDC$ mutant. (D-F) Comparison of the P_{flgA} (D), P_{hilA} (E), and P_{fimA} (F) promoter activity in wild type cells and a $\Delta SPI1$ mutant. (G-I) Comparison of the P_{flgA} (G), P_{hilA} (H), and P_{fimA} (I) promoter activity in wild type cells and a $\Delta fimWYZ$ mutant. Experiments were done on three different days and average values and standard deviations are repeated. All experiments were performed as described in Figure 33.

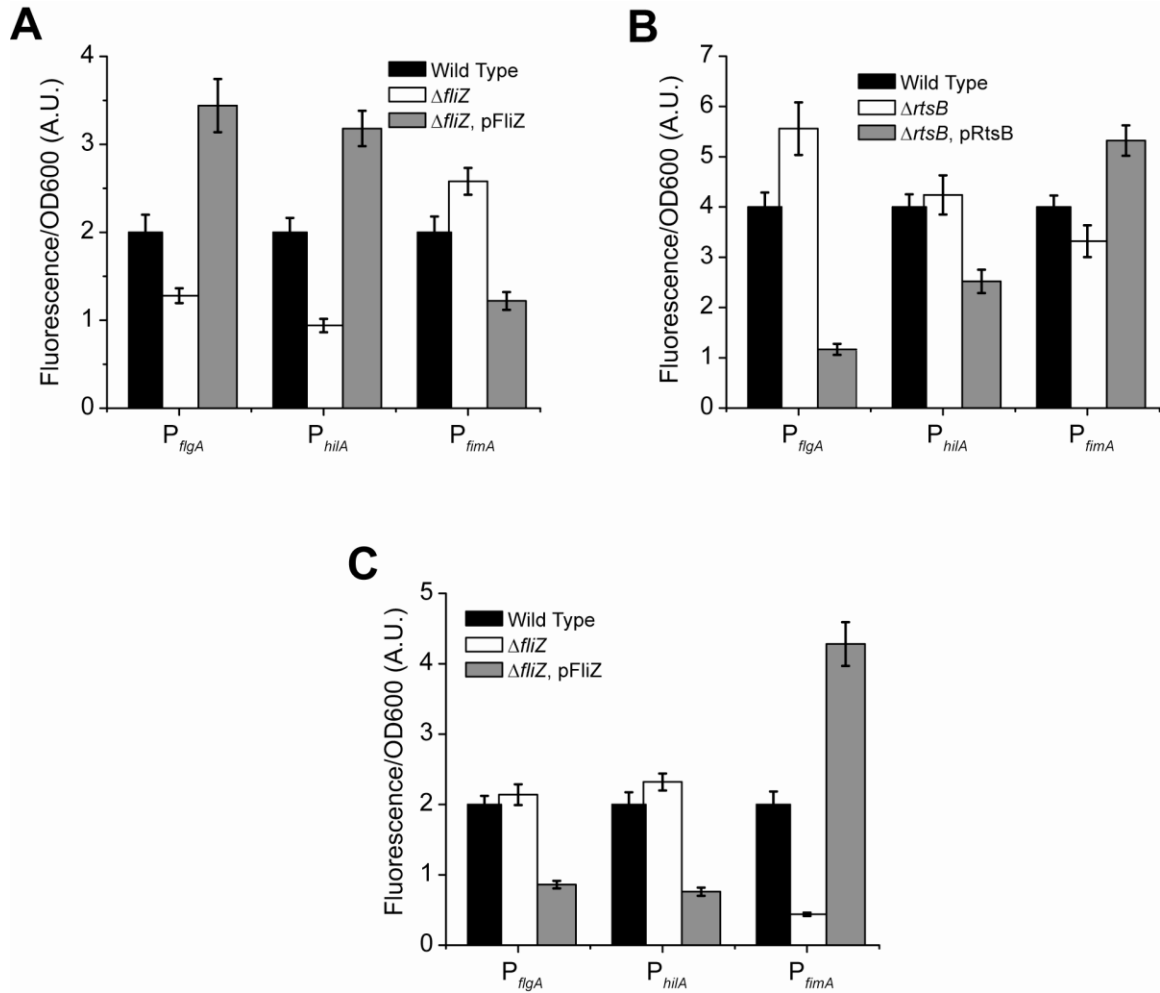


Figure 35. Cross-talk between flagella, SPI1, and Type I fimbriae networks controls the end-point expression levels. **(A)** FliZ is a flagellar and SPI1 activator and a Type I fimbrial repressor. P_{flgA} , P_{hilA} , and P_{fimA} promoter activities in wild-type, $\Delta fliZ$, and $\Delta fliZ$ pFliZ strains. **(B)** RtsB tunes flagellar, SPI1, and Type I fimbriae activities. P_{flgA} , P_{hilA} , and P_{fimA} promoter activities in wild-type, $\Delta rtsB$, and $\Delta rtsB$ pRtsB strains. **(C)** FimZ regulates flagella, SPI1, and fimbrial gene expression. P_{flgA} , P_{hilA} , and P_{fimA} promoter activities in wild-type, $\Delta fimZ$, and $\Delta fimZ$ pRtsB strains.

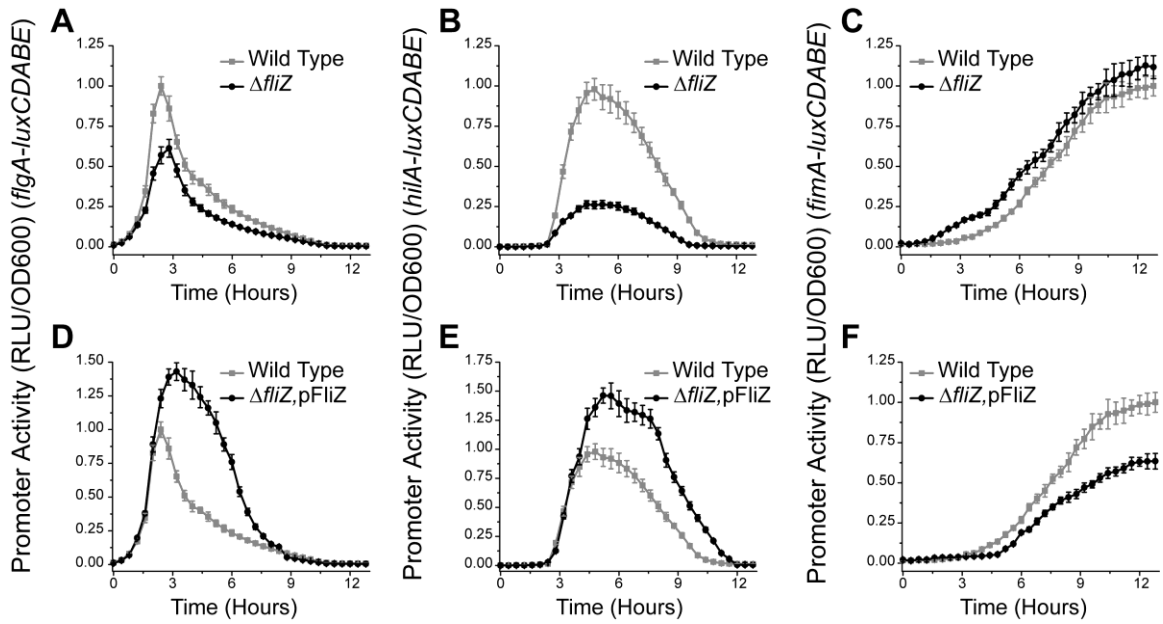


Figure 36. FliZ controls the timing of expression of the flagellar, SPI1, and fimbrial gene expression. (A-C) P_{flgA} (A), P_{hilA} (B), and P_{fimA} (C) promoter activities in wild-type cells and a $\Delta fliZ$ mutant. (D-F) P_{flgA} (D), P_{hilA} (E), and P_{fimA} (F) promoter activities in wild-type and ($\Delta fliZ$ pFliZ) strain where FliZ is constitutively being expressed from a $P_{LTetO-1}$ promoter. All experiments were performed as described in **Figure 33**.

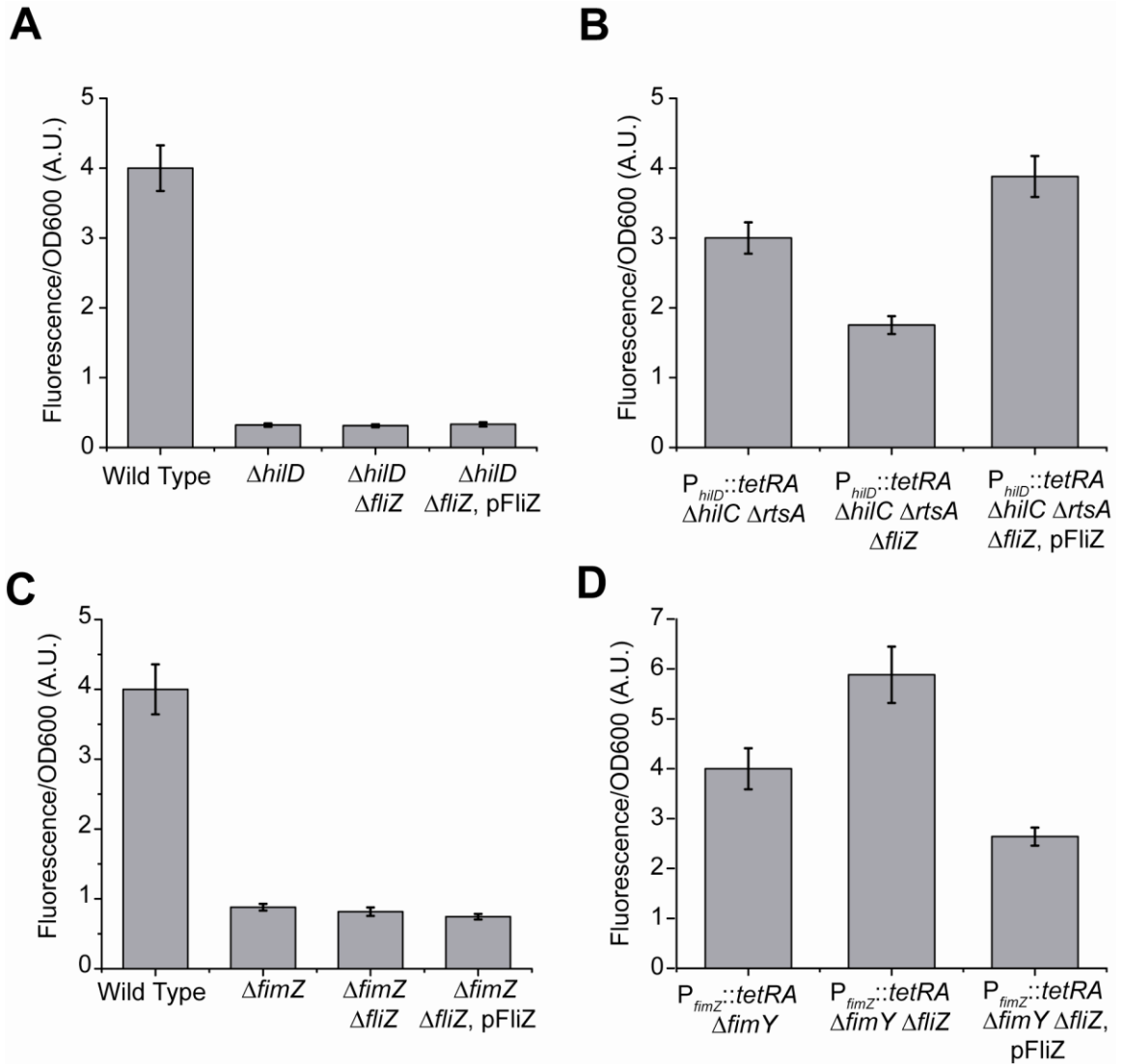


Figure 37. FliZ controls flagellar and Type I fimbriae gene expression by regulating HilD and FliZ post-transcriptionally. (A) FliZ activates SPI1 gene expression via HilD. P_{hilA} promoter activity in wild-type, $\Delta hilD$, $\Delta hilD \Delta fliZ$, and $\Delta hilD \Delta fliZ$ pFliZ. (B) FliZ regulation of SPI1 is independent of HilD transcription. P_{hilA} promoter activity in $P_{hilD}::tetRA \Delta hilC \Delta rtsA$, $P_{hilD}::tetRA \Delta hilC \Delta rtsA \Delta fliZ$, and $P_{hilD}::tetRA \Delta hilC \Delta rtsA \Delta fliZ$ pFliZ. (C) FliZ activation of fimbrial genes is through FimZ. P_{fimA} promoter activity in wild-type, $\Delta fimZ$, $\Delta fimZ \Delta fliZ$, and $\Delta fimZ \Delta fliZ$ pFliZ. (D) FliZ repression of fimbrial network is by post-transcriptional regulation of FimZ. P_{fimA} promoter activity in $P_{fimZ}::tetRA \Delta fimY$, $P_{fimZ}::tetRA \Delta fimY \Delta fliZ$, and $P_{fimZ}::tetRA \Delta fimY \Delta fliZ$ pFliZ. All experiments were performed in triplicate. Average values and standard deviations are reported.

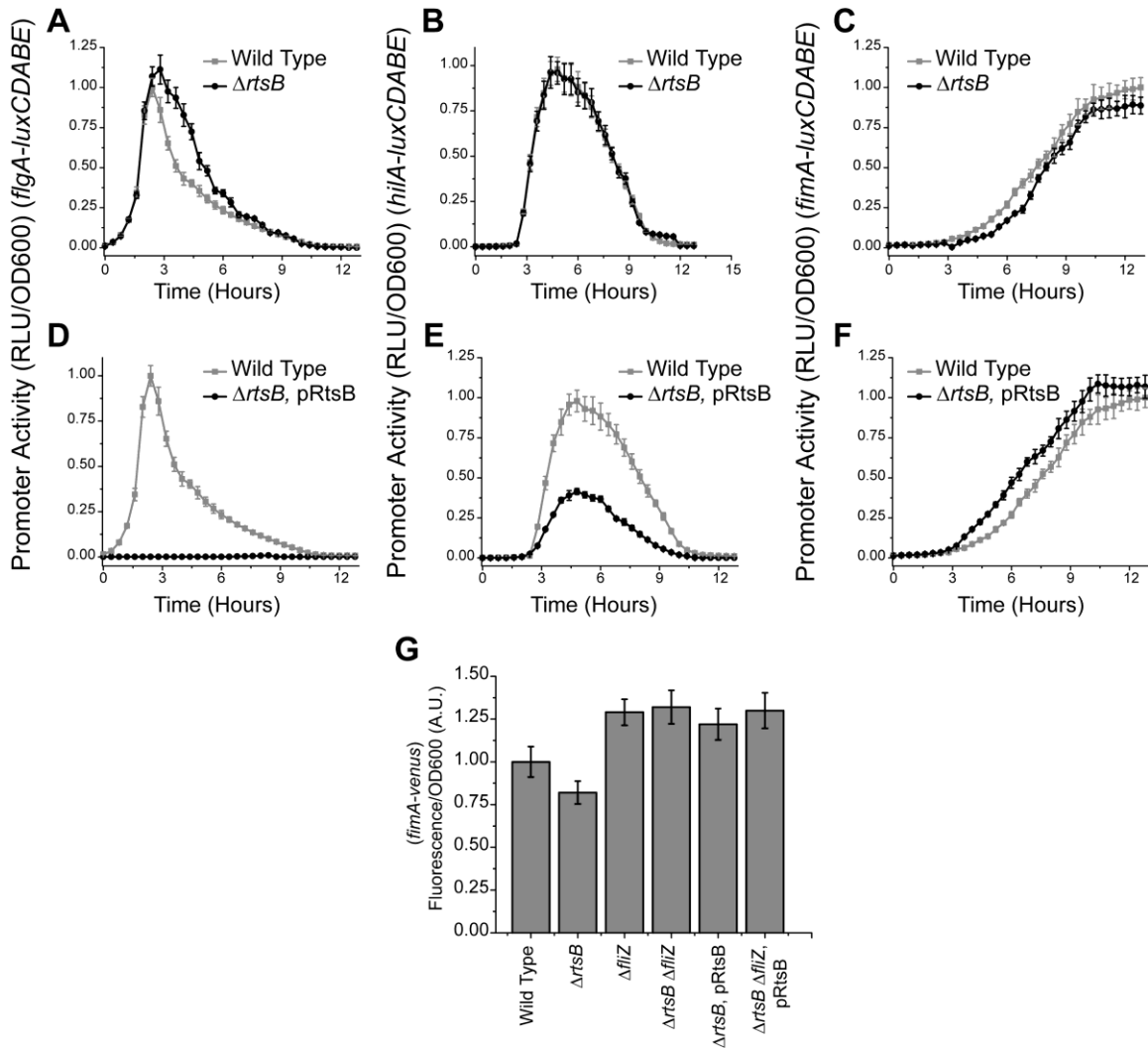


Figure 38. RtsB controls the timing of flagellar and fimbrial gene circuits. (A-C) P_{flgA} (A), P_{hilA} (B), and P_{fimA} (C) promoter activity in wild-type cells and a $\Delta rtsB$ mutant. (D-F) P_{flgA} (D), P_{hilA} (E), and P_{fimA} (F) promoter activity in wild-type cells and a $\Delta rtsB$ mutant constitutively expressing RtsB from a $P_{LTetO-1}$ promoter on a high-copy plasmid (dashed lines with open symbols). The experiments were performed as described in Figure 33. (G) RtsB controls the timing of activation of the *fim* circuit by repression of *FliZ*. P_{fimA} promoter activity in wild-type, $\Delta fliZ$, $\Delta rtsB \Delta fliZ$, and $\Delta rtsB \Delta fliZ$ pRtsB. All experiments were performed in triplicate. Average values and standard deviations are reported.

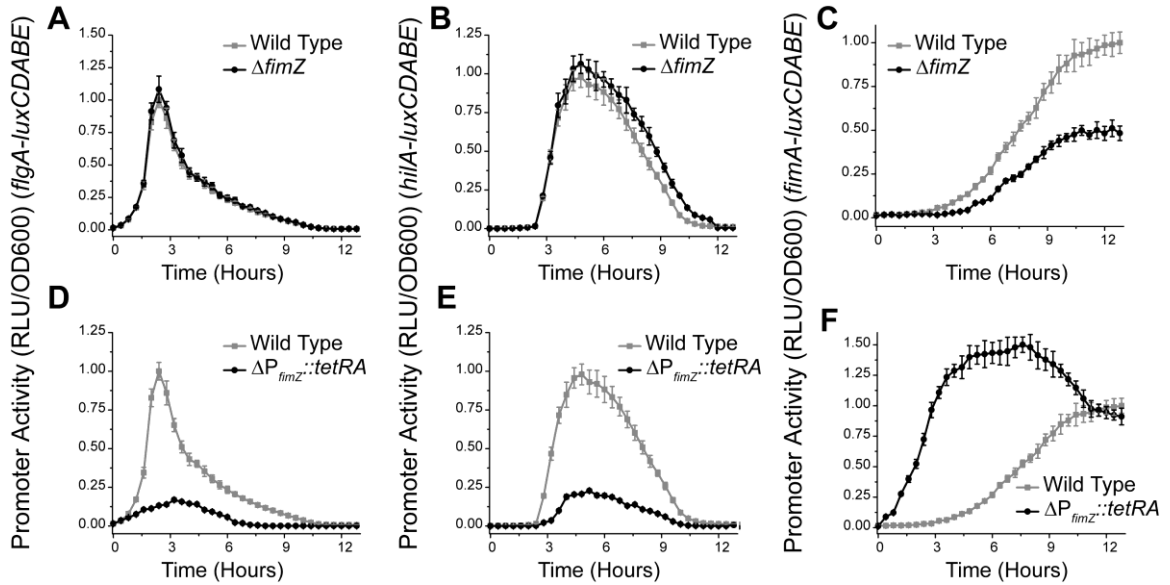


Figure 39. FimZ controls the timing of flagellar, SPI1 and fimbrial gene circuits. FimZ speeds up the “On” to “Off” transition of the SPI1 network and the “Off” to “On” transition of the fim network. **(A-C)** P_{flgA} (A), P_{hilA} (B), and P_{fimA} (C) promoter activities in wild-type cells and a $\Delta fimZ$ mutant. **(D-F)** P_{flgA} (D), P_{hilA} (E), and P_{fimA} (F) promoter activities in wild-type cells and the strain $\Delta P_{fimZ}::tetRA$ where expression of FimZ could be induced by addition of tetracycline. All experiments were performed as described in **Figure 33**. All experiments were performed in triplicate. Average values and standard deviations are reported.

Chapter 8. Other Results

HilE Acts as a Switch Between SPI1 and SPI2

In our previous work, we have demonstrated that the HilD-HilE interplay sets a threshold-mechanism for SPI1 gene expression. In this model, we assumed that HilE is expressed at constant rates inside the cell and sequesters HilD resulting from the step-input. However, as the cell transitions from the intestine to the intracellular environment, it has to make rapid adjustments to its gene expression profile to better survive in the harsh intracellular environment. To accomplish this, the cell requires an effective switching mechanism from one gene expression profile to the other. One example of this switching is shutting the SPI1 T3SS “off” and triggering the SPI2 encoded T3SS “on”. In this work, we try to understand this switching mechanism and the role of HilE and the two-component regulator, PhoPQ.

We first measured P_{hilA} promoter activity in wild type and $\Delta hilE$ mutant in both, SPI1-inducing and SPI2-inducing conditions. Our results indicate that in SPI1-inducing media, absence of HilE is only able to upregulate HilA expression about 2-fold (**Figure 40**). However, in SPI2-inducing media, in a $\Delta hilE$ mutant, HilA expression is upregulated approximately 5 times, indicating that HilE is an important component in the genetic architecture to shut-down SPI1 gene expression after the internalization of the cell.

To test the role of HilE in the switch between SPI1 and SPI2, we also measured P_{hilE} promoter activity in wild-type and a $\Delta hilE$ mutant. Our data demonstrates that in SPI2 inducing media, HilE gene expression is up-regulated 4-5 folds (**Figure 41**). The increase in promoter activity in the SPI2 media is dependent on a large number of factors. Among them is the two-component system, PhoPQ. Consistent with this result, we observe that a P_{hilE} promoter fusion is up-regulated in SPI2-inducing media, however, the up-regulation is significantly lower in a $\Delta phoP$ mutant. Based on this observation, we hypothesize that, PhoPQ-mediated up-regulation of the P_{hilE} promoter serves as a mechanism to switch off SPI1 gene expression.

To monitor the effect of PhoPQ on SPI2 gene expression, we measured P_{sseA} promoter activity in SPI1- and SPI2-inducing media. Our results show that SPI2 is turned “on” specifically in SPI2-inducing conditions. This up-regulation of SPI2 gene expression was, however, not observed in a $\Delta phoP$ mutant (**Figure 42**). Put together, our results indicate that as cells transition from the intestinal to the intracellular phase of infection, PhoPQ and HilE serve to switch the SPI1-encoded T3SS “off” and the SPI2-encoded T3SS “on”.

We do not, as yet, know how PhoPQ system induces P_{hilE} promoter activity. PhoPQ has been reported to induce HilE expression, but the precise mechanism of this activation is not known. But we demonstrate that the interplay between HilE and PhoPQ

encodes a strategy that helps the cell efficiently switch from SPI1- to SPI2-inducing gene expression profile.

Salicylic Acid is a SPI1 Repressor

Salicylic acid is a known activator of the *mar/sox/rob* regulon in both *E. coli* and *S. typhimurium*. Presence of Salicylic acid turns on the interlocked *mar/sox/rob* regulons which are responsible for turning on a large number of downstream genes responsible for survival in the presence of antibiotics. While the role of Salicylic acid as an inducer of the *mar/sox/rob* regulon has been the subject of considerable effort in the related organism *E. coli* (Cherepenko & Hovorun, 2005, Randall & Woodward, 2002, Miller & Sulavik, 1996), its effect on SPI1 gene expression has previously not been looked at. With this intention, we studied SPI1 gene expression in the presence of antibiotics such as Salicylic acid.

As a first experiment, we observed P_{hilA} promoter activity in wild type in the presence and absence of 10 mM Salicylic Acid. Surprisingly, we found that addition of Salicylic Acid completely turns off the P_{hilA} promoter **Figure 43**. This effect on the P_{hilA} promoter activity was independent of SPI1-activators HilC and RtsA and was also independent of the SPI1-repressor, HilE. Salicylic acid was, however, unable to repress SPI1 gene expression in the strain $P_{hilD}::tetRA$, where the P_{hilD} promoter is replaced by a

tetRA element. Therefore, we conclude that Salicylic Acid-dependent repression of SPI1 gene expression is dependent on the P_{hilD} promoter.

Many systems are known to get turned on in response to antibiotics in the surrounding media. Among them is the *mar/sox/rob* regulon in *E. coli*. In particular, *marRAB* system is induced by Salicylic Acid, and is known to induce downstream targets which are responsible for controlling a variety of systems in the cell, for example, porin concentrations, and providing antibiotic resistance (Allen *et al.*, 2008). Therefore, we hypothesized that Salicylic acid-dependent repression of SPI1 gene expression might be through its action on the *mar/sox/rob* regulon. To test this hypothesis, we deleted *marRAB*, *rob*, and *soxRS* from the wild-type and checked P_{hilA} promoter activity in the presence and absence of Salicylic Acid. Contrary to our hypothesis, we observed that even in the absence of *marRAB*, *rob*, and *soxRS*, Salicylic Acid was able to repress SPI1 gene expression **Figure 44**. As an additional test, we over-expressed the regulators *marR*, *rob*, and *soxR* in wild type *Salmonella* and monitored P_{hilA} promoter activity. Over-expression of these regulators did not significantly alter SPI1 gene expression (data not shown).

Next, to identify the target through which Salicylic Acid-dependent repression of SPI1 gene expression is mediated, we developed a screen to carry random transposon mutagenesis in wild type *Salmonella*. In this screen, we integrated a *hilA'-lac* fusion at the lambda attachment site in the *Salmonella* chromosome. When this strain was

streaked on plates containing 20 µg/ml of X-Gal, all colonies were blue in color. However, when the strain was streaked on plates containing 20 µg/ml of X-Gal and 10 mM Salicylic Acid, white colonies were observed. The two plates are as shown in **Figure 45**. To identify the target of Salicylic Acid-dependent repression of SPI1 genes, we did random transposon mutagenesis with this screen. We have screened around 15000 colonies till date. However, we have been unable to isolate mutants where the Salicylic Acid-dependent repression was relieved.

Reprogramming the Type I Fimbriae Network

From a networks perspective, the Type I fimbriae gene network poses an interesting question. As previously discussed in **Figure 31**, Type I fimbriation in *S. typhimurium* is controlled by two-interlocked positive feedback loops. These loops likely encode an AND gate in the network where only when activating signals feed into both P_{fimY} and P_{fimZ} promoters will fimbriation take place. Despite the presence of coupled-positive feedback, we demonstrated that the network does not exhibit switch-like transition from the “off” to the “on” state. Rather, the transition of the P_{fimA} promoter from the “off” to the “on” state was like a rheostat. With this understanding of the network, we were interested in answering the following questions about the fimbriae network.

Firstly, what are the precise signals that are fed into the P_{fimY} and the P_{fimZ} promoters that control fimbriae gene expression in *S. typhimurium*. Type I fimbriae are known to be assembled in static, highly aerobic conditions in liquid media (Duguid et al., 1966a). To investigate which promoter are these signals fed through, we monitored the P_{fimY} and P_{fimZ} promoter activity in several environmental conditions in a $\Delta fimYZ$ mutant. Our results indicate that the two different promoters likely integrate two distinct environmental signals leading to expression of genes responsible for Type I fimbriae. We demonstrate that high oxygen signal is fed through the P_{fimY} promoter as its activity was 3-fold higher in high oxygen conditions than in anaerobic conditions, while there was no appreciable increase in the P_{fimZ} promoter in the presence or absence of oxygen in a $\Delta fimYZ$ mutant. Similarly, we also monitored P_{fimY} and P_{fimZ} promoter activity following growth on solid media vs. liquid cultures. Our results demonstrate that while both, P_{fimY} and P_{fimZ} promoters are upregulated in liquid media as compared to solid media, the increase in P_{fimZ} promoter activity is much more as compared to the increase in the P_{fimY} promoter activity. These results suggest that information about growth on solid/liquid media is fed to the Type I fimbrial circuit primarily at the level of P_{fimZ} promoter (**Figure 46**). Therefore, in this manner, the network integrates different signals leading to fimbriation under the most appropriate conditions.

Secondly, we were also interested in investigating the dynamics of the system at both population average and a single-cell level by changing the architecture of the network. Specifically, we wanted to strengthen the positive feedback in the network

and monitor if that leads to a change in qualitative behavior of the network response at a single-cell level. To reprogram the *fim* system where the positive feedback is strengthened, we switched the P_{fimY} and the P_{fimZ} promoters on the chromosome. The motivation behind doing this was that in wild type arrangement, FimZ primarily activates P_{fimY} promoter and FimY is an activator of the P_{fimZ} promoter. Therefore, in the resulting strain $P_{fimY}::P_{fimZ}$ $P_{fimZ}::P_{fimY}$, both FimY and FimZ will be free to feedback on the respective promoters driving their expression.

We first checked the gene expression dynamics of the P_{fimA} promoter in the $P_{fimY}::P_{fimZ}$ $P_{fimZ}::P_{fimY}$ strain and compared it with wild type and a $\Delta fimW$ mutant (**Figure 47**). Our results show that the P_{fimA} promoter activity in the reprogrammed strain is stronger as compared to the wild type. In fact, the expression levels were very similar to those observed in the $\Delta fimW$ mutant. This demonstrates that our hypothesis of switching the promoters to strengthen the system was correct. Along with strengthening positive feedback in the reprogrammed strain, we note that we are also strengthening the FimY-FimW negative feedback loop. To remove this negative feedback loop, we removed FimW from the reprogrammed strain. The resulting strain was called $P_{fimY}::P_{fimZ}$ $P_{fimZ}::P_{fimY}$ $\Delta fimW$. In this strain, the P_{fimA} promoter activity was about twice as stronger than the wild type and about 50% stronger than the reprogrammed $P_{fimY}::P_{fimZ}$ $P_{fimZ}::P_{fimY}$ strain. Therefore, we demonstrate that the *fim* circuit employs interlocked positive and negative feedback loops to generate the wild type response of the system.

We have previously shown that the Type I fimbrial gene expression, despite encoding coupled feedback loops, does not exhibit transient heterogeneity as cells transition from the “off” to the “on” state. To examine the response of the reprogrammed *fim* network, we monitored P_{fimA} promoter activity in the wild type, the reprogrammed P_{fimY::P_{fimZ}} P_{fimZ::P_{fimY}} mutant, and the P_{fimY::P_{fimZ}} P_{fimZ::P_{fimY}} Δ *fimW* mutant. Our results demonstrate that in wild type and the P_{fimY::P_{fimZ}} P_{fimZ::P_{fimY}} strain, the transition of the cells from the “off” to “on” state was homogeneous and there was no heterogeneity in the population. However, in the P_{fimY::P_{fimZ}} P_{fimZ::P_{fimY}} Δ *fimW* strain, we see a switch-like transition of P_{fimA} gene expression as cells transition from the “off” to “on” state (**Figure 48**). These results demonstrate that the natural Type I fimbrial gene circuit encodes coupled positive and negative feedback loops. The coupled positive feedback loop between FimY and FimZ acts to integrate different environmental and cellular signals and the FimY and FimW negative loop prevents a run-away reaction in terms of P_{fimA} gene expression. By tuning the strength of the positive feedback loops (by reprogramming the network) and by eliminating the negative feedback loop (Δ *fimW*), we demonstrate that we can change the qualitative gene expression pattern across the population, as cells transition from the “off” to the “on” state.

Figures – Other Results

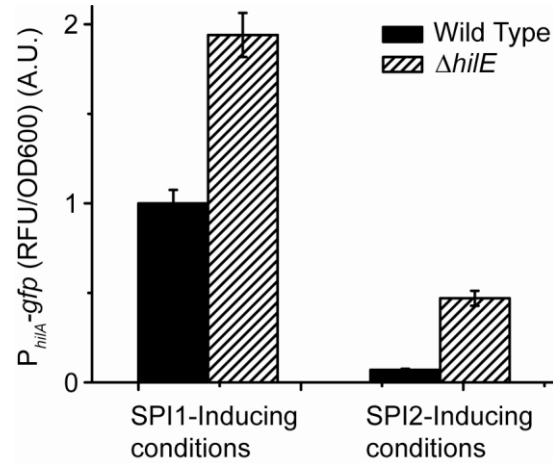


Figure 40. P_{hilA} promoter activity in wild type and $\Delta hilE$ mutant in SPI1- and SPI2-inducing conditions. In the absence of Hile, HilA expression increases 5-fold in SPI2-inducing conditions as compared to 2-fold in SPI1-inducing conditions. Cells were grown for 12 hours before measuring fluorescence and optical density. All experiments were performed in triplicate and average values and standard deviations are reported.

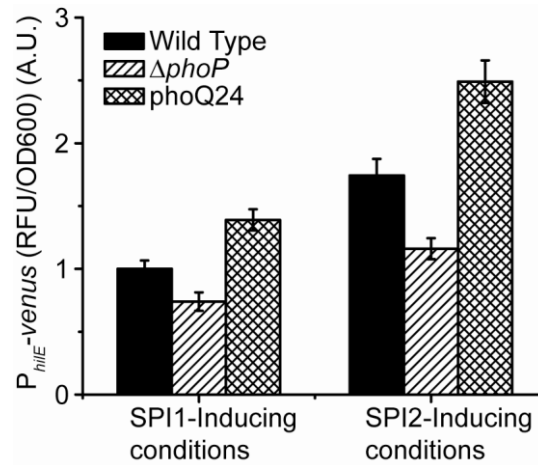


Figure 41. HiE expression is tuned by PhoPQ two-component system. HiE is up-regulated in SPI2-inducing conditions by PhoPQ. P_{hilE} promoter activity in wild type, $\Delta phoP$ mutant, and PhoQ24 mutant where PhoQ is constitutively active. Fluorescence and optical densities were measured after 12 hours of growth. All experiments were performed in triplicate and average values and standard deviations are reported.

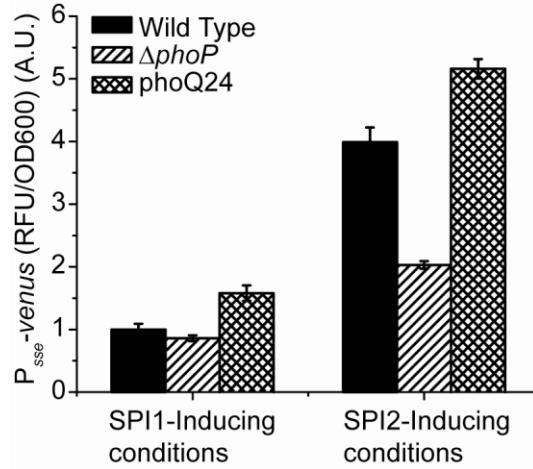


Figure 42. P_{sseA} promoter activity is up-regulated in SPI2-inducing conditions. Induction of the SPI2 promoter is dependent on presence of PhoPQ in SPI2-inducing conditions. All experiments were performed in triplicate with average values and standard deviations reported.

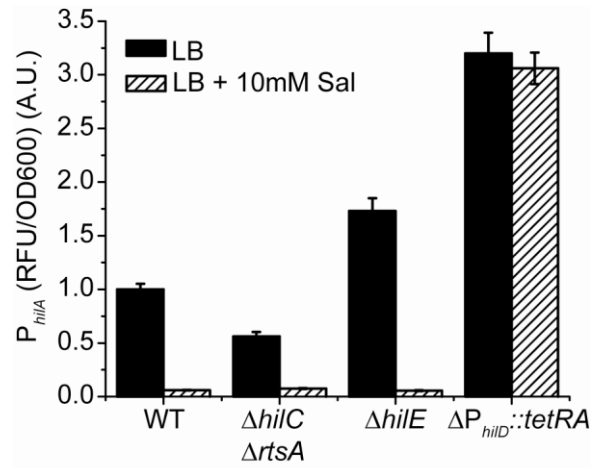


Figure 43. Salicylic Acid shuts down SPI1 gene expression. Repression is independent of SPI1 regulators HilC, RtsA, and HilE; but dependent on P_{hilD} promoter. P_{hilA} promoter activity in wild type, $\Delta hilC \Delta rtsA$, $\Delta hilE$, and $\Delta P_{hilD}::tetRA$. All experiments were done in triplicate. Average values and standard deviations are reported.

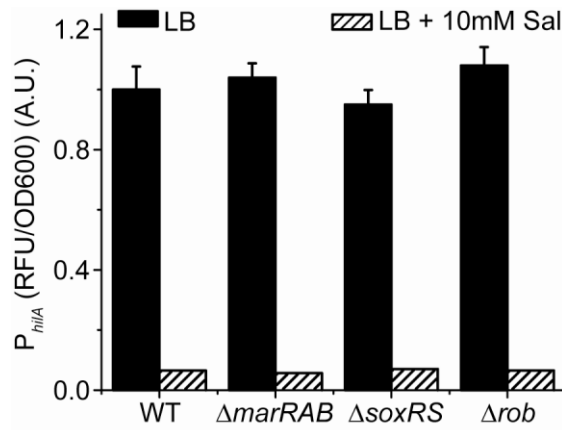


Figure 44. Salicylic Acid- dependent repression of SPI1 gene expression is independent of *marRAB*, *soxRS*, and *rob* regulons. P_{hilA} promoter activity in wild type, $\Delta marRAB$ mutant, $\Delta soxRS$ mutant, and Δrob mutant in LB and LB containing 10mM Salicylic Acid. All experiments were done in triplicate. Average values and standard deviations are as shown above.

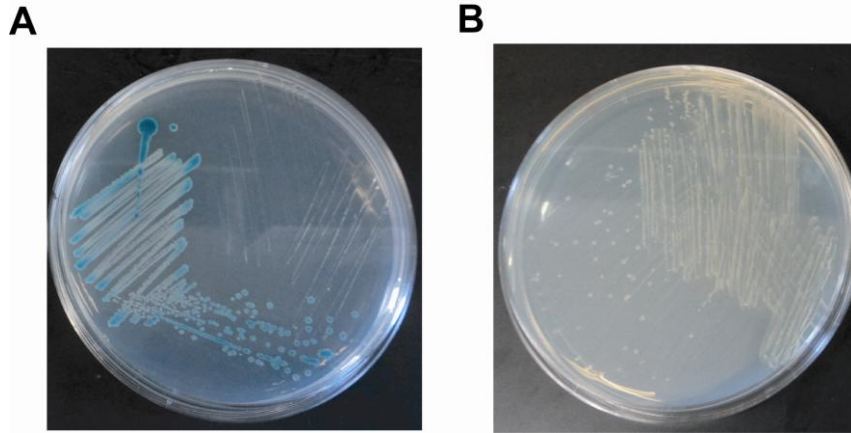


Figure 45. Salicylic Acid & X-Gal screen for SPI1 gene expression. **(A)** Wild type *Salmonella* strain carrying *hilA'*-*lac* fusion streaked on plates with 20 $\mu\text{g}/\text{ml}$ X-Gal. **(B)** Wild type *Salmonella* strain carrying *hilA'*-*lac* fusion streaked on plates with 20 $\mu\text{g}/\text{ml}$ X-Gal and 10 mM Salicylic Acid.

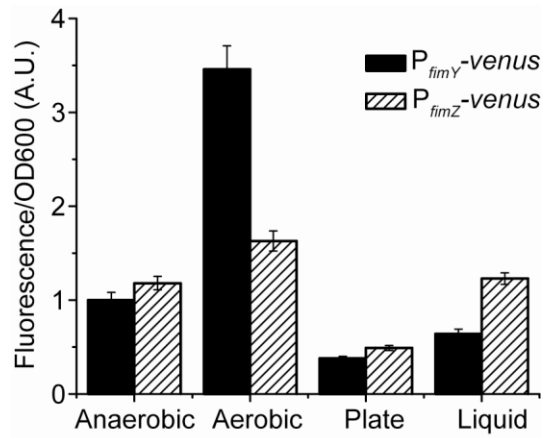


Figure 46. Environmental signals feeding through the P_{fimY} and P_{fimZ} promoters are integrated in the *fim* gene circuit leading to assembly of the Type I fimbriae. P_{fimY} and P_{fimZ} promoter activity in $\Delta fimYZ$ mutant in different environmental conditions. Cells were grown for 24 hours in the respective conditions and then fluorescence and optical density (OD600) measured. The experiments were performed at 37°C. All experiments were performed in triplicate, and average values and standard deviations are reported.

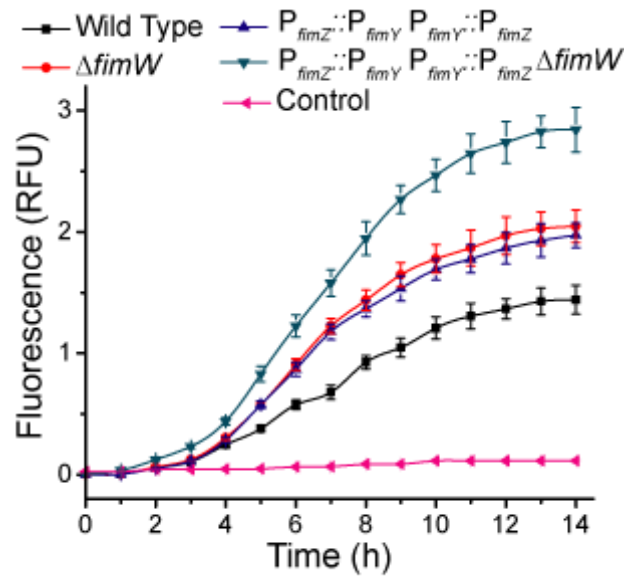


Figure 47. By reprogramming the Type I fimbrial gene circuit, we can tune the dynamic response of the system. P_{fimA} promoter activity in wild type, $\Delta fimW$, $P_{fimY}::P_{fimZ}$ $P_{fimZ}::P_{fimY}$, and $P_{fimY}::P_{fimZ}$ $P_{fimZ}::P_{fimY}$ $\Delta fimW$ mutant. The control is wild type cells with empty pVenus vector integrated at the lambda attachment site. The experiments were performed thrice, and average values with the standard deviations are reported.

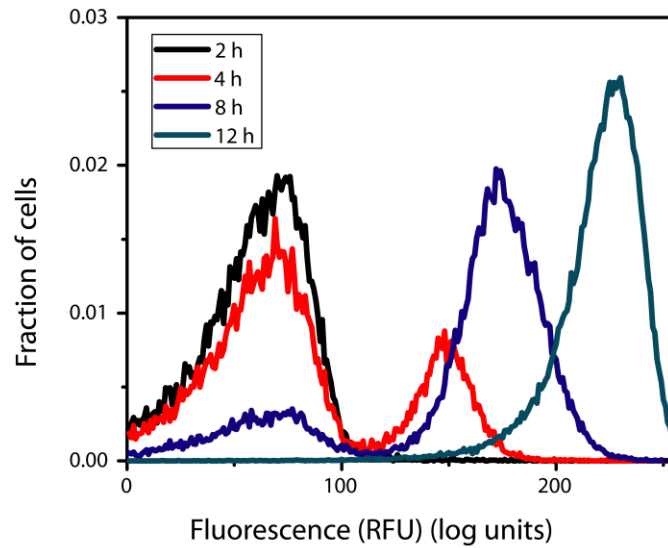


Figure 48. Reprogramming the Type I fimbrial gene circuit and eliminating the negative feedback leads to a switch-like transition of the cells from the “off” to “on” state. P_{fimA} promoter activity in the $P_{fimY}::P_{fimZ} P_{fimZ}::P_{fimY} \Delta fimW$ mutant at a single-cell resolution at the indicated times. Around 30,000 cells were processed for each experiment. The experiments were performed three times with similar behavior observed each time.

Chapter 9. Conclusions and Future Directions

In this work, we demonstrate that multiple systems coordinate in the food-borne pathogen *Salmonella* leading to a successful infection process. We investigated the design of genetic networks controlling the flagellar, SPI1, SPI4, and Type I fimbriae gene networks and demonstrate that the underlying feature in this design is the presence of a logic gate which limits expression to conditions most favorable for invasion. We hypothesize that these logic gates serve as check points which prevent waste of precious cellular responses.

Another result presented in this study is the coordination between the cellular processes. We show that regulatory cross-talk between the flagellar, SPI1, SPI4, and Type I fimbriae gene networks is important for correct timing of activation and de-activation of these networks. These processes serve mutually exclusive roles in the infection process and are expressed sequentially in wild type *Salmonella*. Cross-talk between these systems ensures that for each system, the transition from “off” to “on” and “on” to “off” takes place at the correct time in the infection cycle. These results illustrate that cellular processes do not work in isolation but are closely linked to each other in accomplishing a complex task such as invasion of a mammalian host.

We still do not many things about the infection process gene regulation in *Salmonella*. Some of the questions which might be of interest for future studies are discussed below:

Salicylic Acid-Dependent Repression of SPI1 Gene Expression

To investigate if there is a link between multiple antibiotic resistance (*mar*) locus (Randall & Woodward, 2002, Miller & Sulavik, 1996) and SPI1, we measured SPI1 gene expression in presence of *mar* inducer Salicylic acid (Cohen *et al.*, 1993). Our data suggests that addition of Salicylic acid completely turns off SPI1 gene expression. This effect was found independent of genes involved in multiple antibiotic resistance, *marRAB*, *soxSR*, and *rob*, and SPI1 regulators, *hilC*, *rtsA*, and *hilE*. However, the effect was found to be dependent on the P_{hilD} promoter. Using transposon mutagenesis, we attempted to identify the target of Salicylic Acid-dependent repression of SPI1 gene regulation but no target was identified.

Gene Expression Profile as Cells Switch from SPI1-Inducing to SPI2-Inducing Conditions

Upon internalization in the host cells, the bacteria need to rapidly adapt their gene expression profile. To do this, they need to switch from SPI1-expression to a SPI2-expression state. Hence, they need to encode a strategy where upon internalization,

SPI1 gene expression is repressed and SPI2 gene expression is activated. We speculate that this strategy is encoded by two component systems, PhoPQ and PmrAB, and SPI1-regulator HilE. PhoPQ is known to respond to low pH and Mg²⁺ and activate SPI2 gene expression (Garcia Vescovi *et al.*, 1994, Smith & Maguire, 1998, Prost & Miller, 2008). It also up-regulates HilE expression and likely involved in shutting down SPI1 gene expression. The two-component system PmrAB is also known to respond to low pH and Fe²⁺ in the environment (Gunn, 2008, Kato *et al.*, 2007, Perez & Groisman, 2007, Nishino *et al.*, 2006). However, its role in regulation of SPI1 and SPI2 gene expression has not been studied yet. We hypothesize, that PhoPQ and PmrAB, in conjunction with HilE play the role of the switch. This switch likely helps the cell transition from a SPI1-active gene expression profile to a SPI2-active gene expression profile, thus, helping the cell survive in the harsh environment in the Salmonella-containing vacuoles.

SPI1 Negative Regulation

It has previously been reported that SPI1 gene regulation is subject to negative regulation (De Keersmaecker *et al.*, 2005). It was proposed that this negative regulation is mediated by HilA binding to its own P_{hilA} promoter and repressing transcription. To understand this negative regulation of the SPI1 gene circuit, we studied promoter activity in wild type and a $\Delta hilA$ mutant. In our experiments, we observe that all SPI1 regulators (HilD, HilC, RtsA, and HilA) were up-regulated in a $\Delta hilA$ mutant (data not shown). The source and target for this regulation was not identified. The effect was also

observed in a needle complex mutant where the *prg* operon was knocked out. However, to account for the possibility that disrupting the *prg* operon might have interfered with *hilD* transcription regulation, we also constructed an *invG* mutant. We observed identical results in an $\Delta invG$ mutant. Therefore, we speculate that there is a negative feedback loop in the SPI1 gene network that is linked to the assembly status of the needle complex. We note that this form of regulation is observed in the flagellar network where intra-cellular concentration of regulators is controlled by protein secretion through the growing flagellum.

Appendix A: Strains Used in This Study

Strain No.	Genotype	Genomic Region	Ref.
SS572	$\Delta flhDC::cm$	2021671-2022298	
SS573	$\Delta flgM::cm$	1257046-1257339	
SS684	$\Delta flgM::kan$	1257046-1257339	
SS687-l	$\DeltafliT::cm$	2051201-2051605	
SS687	$\DeltafliT::kan$	2051201-2051605	
SS701	$\DeltafliA::kan$	2044747-2045480	
SS702	$\DeltafliA::cm$	2044747-2045480	
SS699	$\DeltafliZ::cm$	2044068-2044678	
SS700	$\DeltafliZ::kan$	2044068-2044678	
SS703	$\DeltafliAZ::kan$	2044068-2045480	
SS704	$\DeltafliAZ::cm$	2044068-2045480	
SS707	$\Delta flhDC::cm$	2021431-2022298	
SS901	$\Delta P_{fliA}::tetRA$	2045466-2045714	
SS903	$\Delta P_{fliA}:: P_{flhB}$	2045466-2045714:: 2011434-2011994	
SS912	$\Delta P_{fliA}:: P_{flc}$	2045466-2045714:: 2049148-2049654	
SS913	$\Delta P_{fliA}:: P_{flhDC}$	2045466-2045714:: 2023077-2022070	
SS1105	FlgM-Bla		
SS608	$\Delta P_{flhDC}::tetRA \Delta SPI1::frt$		
SS609	$\Delta P_{flhDC}::tetRA \DeltafliAZ::frt$		
SS619	$\Delta SPI1::frt \Delta rtsB::frt$		
SS685	$\DeltafliZ::frt \DeltafliT::cm$		
SS686	$\DeltafliZ::frt \DeltafliT::kan$		
SS695	$\Delta P_{flhDC}::tetRA$	2022440-2022080	
SS696	$\Delta P_{flhDC}::tetRA \DeltafliZ::frt$		
SS697	$\Delta P_{flhDC}::tetRA \DeltafliT::frt$		
SS698	$\Delta P_{flhDC}::tetRA \DeltafliZ::frt \DeltafliT::frt$		
SS708	$\Delta flhDC::frt$	pCP20 (SS707)	
SS717	$\Delta flhDC::cm \DeltafliA::frt$		
SS718	$\Delta flhDC::cm \DeltafliAZ::frt$		
SS719	$\Delta flhDC::cm \DeltafliZ::frt$		
SS720	$\Delta flhDC::frt \DeltafliA::frt$		

SS721	$\Delta flhDC::f rt \Delta fliAZ::f rt$		
SS722	$\Delta flhDC::f rt \Delta fliZ::f rt$		
SS724	$\Delta flhDC::f rt \Delta fliZ::cm$		
SS725	$\Delta flhDC::f rt \Delta fliZ::kan$		
SS917	$\Delta P_{flhDC}::tetRA \Delta P_{fliA}::P_{flhB}$		
SS918	$\Delta P_{flhDC}::tetRA \Delta P_{fliA}::P_{fliC}$		
SS919	$\Delta P_{flhDC}::tetRA \Delta P_{fliA}::P_{flhDC}$		
SS930	$\Delta clpP::cm \Delta fliZ::f rt$		
SS976	$\Delta P_{flhDC}::tetRA \Delta flgM::cm$		
SS977	$\Delta P_{flhDC}::tetRA \Delta flgM::cm \Delta P_{fliA}::P_{flhDC}$		
SS978	$\Delta P_{flhDC}::tetRA \Delta flgM::cm \Delta P_{fliA}::P_{flhB}$		
SS979	$\Delta P_{flhDC}::tetRA \Delta flgM::cm \Delta P_{fliA}::P_{fliC}$		
SS1006	Wild Type $\lambda att::P_{flhD}$ -Venus kan^R		
SS1007	Wild Type $\lambda att::P_{flhB}$ -Venus kan^R		
SS1009	Wild Type $\lambda att::P_{motA}$ -Venus kan^R		
SS1038	$\Delta P_{flhDC}::tetRA \lambda att::P_{flhB}$ -Venus kan^R		
SS1039	$\Delta P_{flhDC}::tetRA \lambda att::P_{motA}$ -Venus kan^R		
SS1040	$\Delta P_{flhDC}::tetRA \Delta fliZ::f rt \lambda att::P_{flhB}$ -Venus kan^R		
SS1041	$\Delta P_{flhDC}::tetRA \Delta fliZ::f rt \lambda att::P_{motA}$ -Venus kan^R		
SS0142	$\Delta P_{flhDC}::tetRA \Delta P_{fliA}::P_{flhB} \lambda att::P_{flhB}$ -Venus kan^R		
SS1043	$\Delta P_{flhDC}::tetRA \Delta P_{fliA}::P_{flhB} \lambda att::P_{motA}$ -Venus kan^R		
SS1044	$\Delta fliZ::f rt \lambda att::P_{flhB}$ -Venus kan^R		
SS1045	$\Delta fliZ::f rt \lambda att::P_{motA}$ -Venus kan^R		
SS1046	$\Delta P_{fliA}::P_{flhB} \lambda att::P_{flhB}$ -Venus kan^R		
SS1047	$\Delta P_{fliA}::P_{flhB} \lambda att::P_{motA}$ -Venus kan^R		
SS1072	Wild Type $\lambda att::P_{fliD}$ -Venus kan^R		
SS1073	Wild Type $\lambda att::P_{fliC}$ -Venus kan^R		
SS1074	Wild Type P22att:: P_{flhDC} -cherry gen ^R		
SS1077	Wild Type P22att:: P_{fliC} -cherry gen ^R		
SS1080	$\Delta P_{flhDC}::tetRA \lambda att::P_{fliD}$ -Venus kan^R		
SS1081	$\Delta P_{flhDC}::tetRA \lambda att::P_{fliC}$ -Venus kan^R		
SS1083	$\Delta P_{flhDC}::tetRA \Delta fliZ::f rt \lambda att::P_{flhD}$ -Venus kan^R		
SS1084	$\Delta P_{flhDC}::tetRA \Delta fliZ::f rt \lambda att::P_{flhB}$ -Venus kan^R		
SS1085	$\Delta P_{flhDC}::tetRA \Delta fliZ::f rt \lambda att::P_{fliD}$ -Venus		

	<i>kan^R</i>		
SS1086	$\Delta P_{flhDC}::tetRA \Delta fliZ::ftr \lambda att::PfliC$ -Venus <i>kan^R</i>		
SS1087	$\Delta P_{flhDC}::tetRA \Delta flgM::ftr \lambda att::PflhD$ - Venus <i>kan^R</i>		
SS1088	$\Delta P_{flhDC}::tetRA \Delta flgM::ftr \lambda att::PflhB$ - Venus <i>kan^R</i>		
SS1089	$\Delta P_{flhDC}::tetRA \Delta flgM::ftr \lambda att::PfliD$ -Venus <i>kan^R</i>		
SS1090	$\Delta P_{flhDC}::tetRA \Delta flgM::ftr \lambda att::PfliC$ -Venus <i>kan^R</i>		
SS1091	$\Delta P_{flhDC}::tetRA \Delta P_{fliA}::P_{flhB} \lambda att::PflhD$ - Venus <i>kan^R</i>		
SS1092	$\Delta P_{flhDC}::tetRA \Delta P_{fliA}::P_{flhB} \lambda att::PflhB$ - Venus <i>kan^R</i>		
SS1093	$\Delta P_{flhDC}::tetRA \Delta P_{fliA}::P_{flhB} \lambda att::PfliD$ - Venus <i>kan^R</i>		
SS1094	$\Delta P_{flhDC}::tetRA \Delta P_{fliA}::P_{flhB} \lambda att::PfliC$ - Venus <i>kan^R</i>		
SS1095	$\Delta P_{flhDC}::tetRA FlgM$ -Bla $\lambda att::PflhD$ -Venus <i>kan^R</i>		
SS1096	$\Delta P_{flhDC}::tetRA FlgM$ -Bla $\lambda att::PflhB$ -Venus <i>kan^R</i>		
SS1097	$\Delta P_{flhDC}::tetRA FlgM$ -Bla $\lambda att::PfliD$ -Venus <i>kan^R</i>		
SS1098	$\Delta P_{flhDC}::tetRA FlgM$ -Bla $\lambda att::PfliC$ -Venus <i>kan^R</i>		
SS1201	$\Delta flgKL::cm$	1265458 - 1268046	
SS1202	$\Delta flgKL::ftr$	1265458 - 1268046	
SS1203	$\Delta P_{flhDC}::tetRA \Delta flgKL::ftr \lambda att::PflhD$ - Venus <i>kan^R</i>		
SS1204	$\Delta P_{flhDC}::tetRA \Delta flgKL::ftr \lambda att::PflhB$ - Venus <i>kan^R</i>		
SS1205	$\Delta P_{flhDC}::tetRA \Delta flgKL::ftr \lambda att::PfliD$ - Venus <i>kan^R</i>		
SS1206	$\Delta P_{flhDC}::tetRA \Delta flgKL::ftr \lambda att::PfliC$ -Venus <i>kan^R</i>		
SS1207	$\Delta P_{flhDC}::tetRA \Delta flgKL::ftr$		
SS1185	$\Delta PfliA::Ptac lacI^q$		
SS1186	$\Delta P_{flhDC}::tetRA \Delta PfliA::Ptac lacI^q$		
SS1187	$\Delta P_{flhDC}::tetRA \Delta PfliA::Ptac lacI^q \lambda att::PflhD$ -		

	Venus <i>kan^R</i>		
SS1188	$\Delta P_{fhlDC}::tetRA \Delta P_{fliA}::Ptac lacI^q \lambda att::P_{fliB}$ - Venus <i>kan^R</i>		
SS1189	$\Delta P_{fhlDC}::tetRA \Delta P_{fliA}::Ptac lacI^q \lambda att::P_{fliD}$ - Venus <i>kan^R</i>		
SS1190	$\Delta P_{fhlDC}::tetRA \Delta P_{fliA}::Ptac lacI^q \lambda att::P_{fliC}$ - Venus <i>kan^R</i>		
SSCR004	$\Delta hilA::cm$	3019859-3021522	
SSCR009	$\Delta hilE::cm$	4763554-4764087	
SSCR097	$\Delta iagB::cm$	3021539-3022037	
REB114			
REB107			
JS252	$\Delta hilC113::cm$		(Ellermeier & Slauch, 2003)
JS253	$\Delta hilD114::cm$		(Ellermeier & Slauch, 2003)
JS248	$\Delta rtsA5$		(Ellermeier & Slauch, 2003)
JS481	$\Delta SPI1::cm$		(Ellermeier et al., 2005)
SS351	$\Delta invF::cm$	3043282-3043932	
SS403	$\Delta SPI1::ftr$		
SS404	$\Delta invF::ftr$	pCP20 on SS351	
SS405	$\Delta hilA::ftr$	pCP20 on SSCR004	
SS413	$\Delta SPI1::ftr \Delta rtsA::ftr$		
SS812	Fur box in <i>hilA</i> by <i>tetRA</i> , 14028	3020955-3020974	
SS813	Fur box in <i>hilC</i> by <i>tetRA</i> , 14028	3012391-3012410	
SS814	Fur box in <i>hilA</i> by <i>tetRA</i> , <i>hilD</i> fur box mut		
SS815	Fur box in <i>hilC</i> by <i>tetRA</i> , <i>hilD</i> fur box mut		
SS891	fur box in <i>hilA</i> mutated, 14028	3020955-3020974	
SS892	fur box in <i>hilC</i> mutated, 14028	3012391-3012410	
SS893	fur box in <i>hilC</i> and <i>hilD</i> mutated, 14028		
SS766	Δfur box in <i>hilD::tetRA</i>	3017894-3017913	
SS883	$\Delta spaPQRS::cm$	3034340-3031522	
SS894	14028 <i>hilD</i> -3XFLAG	3018762- 3018778	
SS895	14028 $\Delta P_{hilD}::tetRA$ <i>hilD</i> -3XFLAG		
SS902	14028 $\Delta fliZ::cm$ <i>hilD</i> -3XFLAG		
SS903	14028 $\Delta P_{hilD}::tetRA \Delta fliZ::cm$ <i>hilD</i> -3XFLAG		
SS914	$\Delta P_{hilC}::tetRA$	3013780-3013010	
SS913	$\Delta P_{hilD}::tetRA$	3017694-3017820	

SS915	$\Delta P_{hilD}::P_{hilC}$	3017694-3017820:: 3013780-3013010	
SS916	$\Delta P_{hilC}::P_{hilD}$	3013780-3013010:: 3017294-3017820	
SS931	$\Delta P_{hilC}::P_{hilD} \Delta hilD::cm$		
SS932	$\Delta P_{hilC}::P_{hilD} \Delta hilD::frt$		
SS933	$\Delta P_{hilC}::tetRA$ (at <i>hilC</i> ATG)	3013780-3013000	
SS938	$\Delta P_{hilC}::P_{hilD}$ (at <i>hilC</i> ATG)	3013780-3013000:: 3017694-3017830	
SS1004	14028 $\lambda att::P_{prgH}$ -venus kan ^R		
SS1005	14028 $\lambda att::P_{hilA}$ -venus kan ^R		
SS1008	14028 $\lambda att::P_{hilD}$ -venus kan ^R		
SS1016	$\Delta sipBC::cm$	3030862-3027844	
SS1017	$\Delta sipBC::kan$	3030862-3027844	
SS1021	$\Delta prg::cm$ (leaving <i>hilD</i> promoter intact)	3017533-3014999	
SS1026	14028 $\Delta rtsA::kan$	4561800-4561402	
SS1027	14028 $\Delta rtsAB::kan$	4561800-4560581	
SS1028	14028 $\Delta rtsA::frt$	4561800-4561402	
SS1029	14028 $\Delta rtsAB::frt$	4561800-4560581	
CR218	14028 FlhC-3XFLAG	2021569-2021500	
CR219	14028 $\Delta fliz::frt$ FlhC-3XFLAG		
CR220	14028 $\Delta P_{flhDC}::tetRA$ FlhC-3XFLAG		
CR221	14028 $\Delta P_{flhDC}::tetRA \Delta fliz$ FlhC-3XFLAG		
	<i>hilD</i> ::frt	pCP20 on JS252	
	<i>hilC</i> ::frt	pCP20 on JS253	
SSCR018	Dh5 α Z1		
SS095	MG1655 att λ ::lac-gfp pAx1 Apra ^R		
SS098	MG1655 att λ ::PBAD-gfp pAx1 Apra ^R		
SS406	CR1 $\Delta fliz::frt$		
SS516	LT2 (John Roth's strain)		
SS536	LT2 $\Delta fliz::kan$		
SS710	BL21		
SS764	14028 $\Delta P_{luxS}::tetRA$	2966810-2966935	
SS780	LT2 $\Delta fliz::frt$		
SS869	1655 <i>rhaT</i> -T1- <i>cm</i> -T1- <i>rhaR</i>		
SS890	14028 <i>sodCI</i> -3XFLAG		
SS906	$\Delta clpP::cm$	503210-503839	
SS907	$\Delta clpP::kan$	503210-503839	
SS920	$\Delta hns::cm$	1847261-1847700	
SS924	M04450 (IGEM)		

SS934	LT2 $\Delta cheRB::cm$	2014610-2012690	
SS935	LT2 $\Delta cheRBY::cm$	2014610-2012283	
SS936	LT2 $\Delta cheV::kan$	2420641-2421660	
SS939	LT2 $\Delta cheRB::frt$	2014610-2012690	
SS940	LT2 $\Delta cheRBY::frt$	2014610-2012283	
SS943	LT2 $\Delta cheRB::frt \Delta cheV::kan$		
SS944	LT2 $\Delta cheRBY::frt \Delta cheV::kan$		
SS953	$\Delta luxS::cm$	2966810-2966270	
SS954	$\Delta ygiXY::cm$	3340782-3342839	
SS955	$\Delta feoAB::cm$	3363883-3666559	
SS956	$\Delta feoAB::kan$	3363883-3666559	
SS973	$\Delta sprB::frt \Delta fliZ::cm$		
SS974	$\Delta sprB::frt \Delta fliZ::kan$		
SS975	$\Delta sprB::kan \Delta fliZ::frt$		
SS1010	$\Delta hfq::cm$	4604571-4604898	
SS1011	$\Delta hfq::kan$	4604571-4604898	
SS1014	BW25142		
SS1018	14028 $\Delta lon::cm$	505592-507856	
SS1019	14028 $\Delta lon::kan$	505592-507856	
SS1023	TH3468		
SS1024	TH3467		
SS1025	TH3466		
SS1030	MG1655 $\lambda att::PrhaBAD-venus kan^R$		
SS1031	MG1655 $\Delta rhaT1::frt \phi 80::pCAH63$ $\lambda att::PrhaBAD-venus kan^R$		
CR362	$\Delta sprB::kan$	3011762-3010927	
	$\Delta sprB::cm$	3011762-3010927	
CR363	$\Delta sprB::frt$	3011762-3010927	
CR365	$\Delta hilC::FRT \Delta sprB::FRT$		
CR366	$\Delta rtsA5 \Delta sprB::kan$		
CR367	$\Delta rtsA5 \Delta sprB::FRT$		
CR369	$P_{hilD}::tetRA \Delta sprB::kan$		
CR370	$P_{hilD}::tetRA \Delta sprB::FRT$		
CR311	$\Delta fimY::cm$	612218-611488	
CR312	$\Delta fimZ::cm$	610886-610251	
CR313	$\Delta fimYZ::cm$	612218-610251	
CR314	$\Delta fimW::cm$	612706-613302	
CR315	$\Delta fimU::cm$	613570-613648	
CR322	$\Delta fimY::frt$	612218-611488	
CR328	$\Delta fimZ::frt$	610886-610251	

CR334	<i>ΔfimYZ:: frt</i>	612218-610251	
CR340	<i>ΔfimW:: frt</i>	612706-613302	
CR316	<i>ΔfimU:: frt</i>	613570-613648	
CR317	14028 attλ:: <i>PfimA-venus kan^R</i>		
CR318	14028 attλ:: <i>PfimY-venus kan^R</i>		
CR319	14028 attλ:: <i>PfimZ-venus kan^R</i>		
CR320	14028 attλ:: <i>PfimW-venus kan^R</i>		
CR321	14028 attλ:: <i>PfimU-venus kan^R</i>		
CR323	<i>ΔfimY::frt attλ::PfimA-venus kan^R</i>		
CR324	<i>ΔfimY::frt attλ::PfimY-venus kan^R</i>		
CR325	<i>ΔfimY::frt attλ::PfimZ-venus kan^R</i>		
CR326	<i>ΔfimY::frt attλ::PfimW-venus kan^R</i>		
CR327	<i>ΔfimY::frt attλ::PfimU-venus kan^R</i>		
CR329	<i>ΔfimZ::frt attλ::PfimA-venus kan^R</i>		
CR330	<i>ΔfimZ::frt attλ::PfimY-venus kan^R</i>		
CR331	<i>ΔfimZ::frt attλ::PfimZ-venus kan^R</i>		
CR332	<i>ΔfimZ::frt attλ::PfimW-venus kan^R</i>		
CR333	<i>ΔfimZ::frt attλ::PfimU-venus kan^R</i>		
CR335	<i>ΔfimYZ::frt attλ::PfimA-venus kan^R</i>		
CR336	<i>ΔfimYZ::frt attλ::PfimY-venus kan^R</i>		
CR337	<i>ΔfimYZ::frt attλ::PfimZ-venus kan^R</i>		
CR338	<i>ΔfimYZ::frt attλ::PfimW-venus kan^R</i>		
CR339	<i>ΔfimYZ::frt attλ::PfimU-venus kan^R</i>		
CR341	<i>ΔfimW::frt attλ::PfimA-venus kan^R</i>		
CR342	<i>ΔfimW::frt attλ::PfimY-venus kan^R</i>		
CR343	<i>ΔfimW::frt attλ::PfimZ-venus kan^R</i>		
CR344	<i>ΔfimW::frt attλ::PfimW-venus kan^R</i>		
CR345	<i>ΔfimW::frt attλ::PfimU-venus kan^R</i>		
	<i>ΔfimU::frt attλ::PfimA-venus kan^R</i>		
	<i>ΔfimU::frt attλ::PfimY-venus kan^R</i>		
	<i>ΔfimU::frt attλ::PfimZ-venus kan^R</i>		
	<i>ΔfimU::frt attλ::PfimW-venus kan^R</i>		
	<i>ΔfimU::frt attλ::PfimU-venus kan^R</i>		
	14028 attλ:: <i>PhilE-venus kan^R</i>		
CR347	<i>ΔfimYZ::frt attλ::PhilE-venus kan^R</i>		
	<i>ΔfimYZ::frt ΔfimW::cm</i>		
CR372	<i>ΔfimYZ::frt ΔfimW::frt</i>		
CR361	<i>ΔrtsB::cm</i>	4560891-4560592	
CR362	<i>ΔrtsB::frt</i>	4560891-4560592	
CR365	<i>ΔfimZ::cm ΔfliZ::FRT</i>		

CR366	$\Delta fimZ::FRT \Delta fliZ::FRT$		
CR367	$\Delta P_{fimZ}::tetRA$	611401-610904	
CR368	$\Delta P_{fimZ}::tetRA \Delta fimY::FRT$		
CR369	$\Delta P_{fimZ}::tetRA \Delta fimYZ::FRT$		
CR370	$\Delta rtsB::cm \Delta fimZ::FRT$		
CR371	$\Delta rtsB::FRT \Delta fimZ::FRT$		
SS1146	$\Delta P_{fimY}::tetRA$	612222-612289	
SS1147	$\Delta P_{fimY}::P_{fimZ}$	612222-612289:: 611401-610904	
SS1148	$\Delta P_{fimY}::P_{fimZ} \Delta P_{fimZ}::tetRA$		
SS1149	$\Delta P_{fimY}::P_{fimZ} \Delta P_{fimZ}::P_{fimY}$	611401-610904:: 612222-612289	
SS1150	$\Delta P_{fimY}::P_{fimZ} \Delta P_{fimZ}::P_{fimY} \Delta fimW::cm$		
SS1151	$\Delta P_{fimY}::P_{fimZ} \Delta P_{fimZ}::P_{fimY} \Delta fimW::frt$		
SS1152	$\Delta marRAB::cm$	1598139-1596185	
SS1153	$\Delta rob::cm$	2916367-2917512	
SS1154	$\Delta soxRS::cm$	4504367-4504869	

a: This study unless specified

b: American Type Culture Collection

Appendix B: Plasmids Used in This Study

Plasmid Number	Plasmid Name	Reference
pSS001	<i>PflgA-gfp</i> , pPROBE	(Saini <i>et al.</i> , 2008)
pSS002	<i>PflgB-GFP</i> pPROBE	(Saini <i>et al.</i> , 2008)
pSS003	<i>PflhB-GFP</i> pPROBE	(Saini <i>et al.</i> , 2008)
pSS004	<i>PfliE-GFP</i> pPROBE	(Saini <i>et al.</i> , 2008)
pSS005	<i>PfliD-GFP</i> pPROBE	(Saini <i>et al.</i> , 2008)
pSS006	<i>PflgK-GFP</i> pPROBE	(Saini <i>et al.</i> , 2008)
pSS007	<i>PfliC-GFP</i> pPROBE	(Saini <i>et al.</i> , 2008)
pSS008	<i>PflhD-GFP</i> pPROBE	(Saini <i>et al.</i> , 2008)
pSS009	pPROBE <i>luxCDABE</i>	(Saini <i>et al.</i> , 2008)
pSS010	<i>PflgA-luxCDABE</i>	(Saini <i>et al.</i> , 2008)
pSS011	<i>PfliC-luxCDABE</i>	(Saini <i>et al.</i> , 2008)
pSS012	pPROTet.E <i>tetR</i>	(Saini <i>et al.</i> , 2008)
pSS013	pFliZ	(Saini <i>et al.</i> , 2008)
pSS014	pFliZ-TetR	(Saini <i>et al.</i> , 2008)
pSS015	pFliZ-native	(Saini <i>et al.</i> , 2008)
pSS016	pFliA-TetR	(Saini <i>et al.</i> , 2008)
pSS017	pFhDC-TetR	(Saini <i>et al.</i> , 2008)
pSS018	<i>PflhDC flhDC-lacZ</i>	(Saini <i>et al.</i> , 2008)
pSS019	PLtetO-1 <i>flhC-lacZ</i>	(Saini <i>et al.</i> , 2008)
pSS020	PLtetO-1 <i>flhDC-lacZ</i>	(Saini <i>et al.</i> , 2008)
SS444	pPROTet.E <i>rtsB</i>	
SS448	pBAD30 <i>rtsB</i>	
SS450	pPROTet.E <i>fliZ</i> (5' His)	
SS451	pPROTet.E <i>fliZ</i> (3' His)	
SS621	pFliAZ – native	
SS672	pBAD30 <i>flhDC</i>	
SS673	pPROTet.E <i>flhDC tetR</i>	
SS675	pPROTet.E <i>fliAZ tetR</i>	
SS676	pPROTet.E <i>fliZ tetR</i>	
SS677	pPROTet.E <i>fliA tetR</i>	
SS679	pPROTet.E <i>fliT tetR</i>	
SS682	pQE80L <i>flhDC</i>	
SS714	pET28a <i>flhC</i>	

SS822	pPROBE <i>fliA-luxCDABE</i>	
SS824	pPROBE <i>flgM-luxCDABE</i>	
SS829	pBAD30 <i>fliD</i>	
SS830	pBAD30 <i>flgM</i>	
SS831	pBAD30 <i>flgKL</i>	
SS832	pBAD30 <i>fliS</i>	
SS833	pBAD30 <i>fliT</i>	
SS834	pSE380 <i>fliD</i>	
SS835	pSE380 <i>flgM</i>	
SS836	pSE380 <i>flgKL</i>	
SS837	pSE380 <i>fliS</i>	
SS838	pSE380 <i>fliZ</i>	
SS839	pSE380 <i>fliT</i>	
SS878	pQE80L <i>flhDC</i>	
SS879	pBAD30 <i>flhDC</i>	
SS908	pPROBE <i>fliB-gfp[tagless]</i>	
SS909	pPROBE <i>fliB-luxCDABE</i>	
SS969	<i>PflhDC-venus kan λatt</i>	
SS970	<i>PfliB-venus kan λatt</i>	
SS1052	pPROBE <i>flgA-cherry</i>	
SS1053	pPROBE <i>motA-cherry</i>	
SS1054	pPROBE <i>flhB-cherry</i>	
SS1055	pPROBE <i>fliD-cherry</i>	
SS1057	(<i>PflgA-cherry kan λatt</i>) BW15142	
SS1058	(<i>PmotA-cherry kan λatt</i>) BW15142	
SS1059	(<i>PfliB-cherry kan λatt</i>) BW15142	
SS1060	(<i>PfliD-cherry kan λatt</i>) BW15142	
SS1062	(<i>PflgA-cherry gen P22</i>) BW15142	
SS1063	(<i>PmotA-cherry gen P22</i>) BW15142	
SS1064	(<i>PfliB-cherry gen P22</i>) BW15142	
SS1065	(<i>PfliD-cherry gen P22</i>) BW15142	
SS1066	(<i>PfliD-venus kan lambda</i>) BW25142	
SS1067	(<i>PmotA-venus kan lambda</i>) BW25142	
SS1068	(<i>PflhDC-cherry kan lambda</i>) BW25142	
SS1069	(<i>PflhDC-cherry gen P22</i>) BW25142	
SS1101	(<i>PflhDC-cherry cmR P22</i>) BW25142	
SS1102	(<i>PfliB-cherry cmR P22</i>) BW25142	
SS1103	(<i>PfliD-cherry cmR P22</i>) BW25142	
TPA30	pRG19(<i>PmotA-luxCDABE TCR</i>)/LT2	
TPA38	pRG38(<i>pflhD-luxCDABE TCR</i>)/LT2	

TPA42	pRG39(<i>pmotA</i> - <i>luxCDABE</i> TCR)/LT2	
TPA46	pRG46(<i>pfliD</i> - <i>luxCDABE</i> TCR)/LT2	
TPA50	pRG51(<i>pflgA</i> - <i>luxCDABE</i> TCR)/LT2	
TPA58	pRG53(<i>pfliE</i> - <i>luxCDABE</i> TCR)/LT2	
TPA74	pRG19::FCF/p(<i>flhDC</i>)5451::Tnd10Tc[del-25]	
TPA82	pRG38::FCF/p(<i>flhDC</i>)5451::Tnd10Tc[del-25]	
TPA86	pRG39::FCF/p(<i>flhDC</i>)5451::Tnd10Tc[del-25]	
TPA90	pRG46::FCF/p(<i>flhDC</i>)5451::Tnd10Tc[del-25]	
TPA94	pRG51::FCF/p(<i>flhDC</i>)5451::Tnd10Tc[del-25]	
TPA102	pRG53::FCF/p(<i>flhDC</i>)5451::Tnd10Tc[del-25]	
TPA1154	pPRO <i>motA</i> /LT2	
TPA1155	pPRO <i>fliD</i> /LT2	
TPA1156	pPRO <i>motA</i> /LT2	
TPA1157	pPRO <i>flgA</i> -3/LT2	
TPA1158	pPRO <i>flgB</i> /LT2	
TPA1159	pPRO <i>flgA</i> -5/LT2	
	pVenus (<i>attλ</i>)	(Saini <i>et al.</i> , 2009)
	<i>PfimA</i> - <i>venus</i> (<i>attλ</i>)	(Saini <i>et al.</i> , 2009)
	<i>PfimY</i> - <i>venus</i> (<i>attλ</i>)	(Saini <i>et al.</i> , 2009)
	<i>PfimZ</i> - <i>venus</i> (<i>attλ</i>)	(Saini <i>et al.</i> , 2009)
	<i>PfimW</i> - <i>venus</i> (<i>attλ</i>)	(Saini <i>et al.</i> , 2009)
	<i>PfimU</i> - <i>venus</i> (<i>attλ</i>)	(Saini <i>et al.</i> , 2009)
	<i>PhilE</i> - <i>venus</i> (<i>attλ</i>)	(Saini <i>et al.</i> , 2009)
	pPROTet.E <i>fimY tetR</i>	(Saini <i>et al.</i> , 2009)
	pPROTet.E <i>fimZ tetR</i>	(Saini <i>et al.</i> , 2009)
	pPROTet.E <i>fimW tetR</i>	(Saini <i>et al.</i> , 2009)
	pPROTet.E <i>fimY* tetR</i>	(Saini <i>et al.</i> , 2009)
SS790	(pPROBE <i>fimZ-gfp</i> [tagless])	
SS791	(pPROTet.E <i>fimY</i>)	
SS801	(pPROBE <i>fimA-gfp</i> [tagless])	
SS802	(pPROBE <i>fimZ-gfp</i> [tagless])	
SS803	(pPROBE <i>fimY-gfp</i> [tagless])	
SS804	(pPROTet.E <i>fimZ</i>)	
SS816	(pPROBE <i>fimA-lux</i>)	
SS817	(pPROBE <i>fimY-lux</i>)	
SS818	(pPROBE <i>fimZ-lux</i>)	
SS927	pBAD30 <i>fimZ</i> (CDC)	
SS929	pPROTET.E <i>fimY fimZ</i> (CDC) <i>tetR</i>	
SS945	pPROBE <i>Venus</i>	
SS946	pPROBE <i>PfimZ Venus</i> (14)	

SS947	pPROBE <i>PfimA Venus</i> (15)	
SS948	pPROBE <i>PfimY Venus</i> (37)	
SS949	pPROBE <i>PfimZ Venus</i> (103)	
SS950	pPROBE <i>PfimW Venus</i>	
SS952	pPROBE <i>PfimW GFP</i> [tagless]	
SS959	pPROBE <i>PfimU GFP</i> [tagless]	
SS960	pPROBE <i>PfimU Venus</i>	
SS961	pPROBE <i>PhilE Venus</i>	
pSS052	pProbe <i>hilD-gfp</i> [tagless]	(Saini, 2010)
pSS053	pProbe <i>hilC-gfp</i> [tagless]	(Saini, 2010)
pSS054	pProbe <i>rtsA-gfp</i> [tagless]	(Saini, 2010)
pSS055	pProbe <i>hilA-gfp</i> [tagless]	(Saini, 2010)
pSS072	pProbe <i>hilD-gfp</i> [asv]	(Saini, 2010)
pSS073	pProbe <i>hilC-gfp</i> [asv]	(Saini, 2010)
pSS074	pProbe <i>hilD-lux</i>	(Saini, 2010)
pSS075	pProbe <i>hilC-lux</i>	(Saini, 2010)
pSS076	pProbe <i>rtsA-lux</i>	(Saini, 2010)
pSS077	pProbe <i>hilA-lux</i>	(Saini, 2010)
	pProbe-Venus	(Saini & Rao, 2010)
	pProbe P_{hilD} -Venus	(Saini & Rao, 2010)
	pProbe P_{hilC} -Venus	(Saini & Rao, 2010)
	pProbe P_{rtsA} -Venus	(Saini & Rao, 2010)
	pProbe P_{hilA} -Venus	(Saini & Rao, 2010)
	pProbe P_{prgH} -Venus	(Saini & Rao, 2010)
	pProbe P_{sicA} -Venus	(Saini & Rao, 2010)
	pProbe P_{sopB} -Venus	(Saini & Rao, 2010)
	pProbe P_{fimA} -Venus	(Saini & Rao, 2010)
	pProbe P_{sprB} -Venus	(Saini & Rao, 2010)
	pProbe P_{siiA} -Venus	(Saini & Rao, 2010)
	pSprB (pPROTet.E <i>sprB tetR</i>)	(Saini & Rao, 2010)
	pHilA	(Saini & Rao, 2010)
	pHilD	(Saini & Rao, 2010)
	pHilC	(Saini & Rao, 2010)
	pRtsA	(Saini & Rao, 2010)
	pSprB-con (pPROTet.E <i>sprB</i>)	(Saini & Rao, 2010)
	pBAD-SprB	(Saini & Rao, 2010)
	pHis-SprB	(Saini & Rao, 2010)
	pHis-HilA	(Saini & Rao, 2010)
SS005	<i>PinvF-gfp</i> (pProbe)	
SS006	<i>PprgH-gfp</i> (pProbe)	

SS009	<i>PsicA-gfp</i> (pProbe)	
SS010	<i>PsopB-gfp</i> (pProbe)	
SS014	<i>PflhDC-gfp</i> (pProbe)	
SS018	<i>PssaB-gfp</i> (pProbe)	
SS019	<i>PhilE-gfp</i> (pProbe)	
SS061	pBAD30 <i>hila</i>	
SS062	pBAD30 <i>hilC</i>	
SS063	pBAD30 <i>hilD</i>	
SS064	pBAD30 <i>rtsA</i>	
SS442	pPROBE <i>PsprB-gfp</i>	
SS490	pPROTet.E <i>hila tetR</i>	
SS491	pPROTet.E <i>hilC tetR</i>	
SS492	pPROTet.E <i>hilD tetR</i>	
SS493	pPROTet.E <i>rtsA tetR</i>	
SS556	(pBAD30 <i>lagB</i>)	
SS674	(pPROTet.E <i>iagB tetR</i>)	
SS713	(pET28a <i>hilD</i>) (86F/34R)	
SS757	(<i>PprgH-lux</i>)	
SS758	(<i>PsicA-lux</i>)	
SS759	(<i>PsopB-lux</i>)	
SS771	(pPROBE <i>hila-gfp</i> [aav])	
SS772	(pPROBE <i>hila-gfp</i> [asv])	
SS773	(pPROBE <i>hila-gfp</i> [lva])	
SS775	(pPROTet.E <i>hilE tetR</i>)	
SS776	(pBAD30 <i>hilE</i>)	
SS778	(pBAD30 <i>hilD fur box mut</i>)	
SS787	(pPROBE <i>hilD-gfp</i> [aav])	
SS788	(pPROBE <i>hilD-gfp</i> [asv])	
SS789	(pPROBE <i>hilD-gfp</i> [lva])	
SS840	(pPROBE <i>hilC-gfp</i> [aav])	
SS841	(pPROBE <i>hilC-gfp</i> [lva])	
SS842	(pPROBE <i>rtsA-gfp</i> [aav])	
SS843	(pPROBE <i>rtsA-gfp</i> [lva])	
SS880	pPROBE <i>hilE-gfp</i> [tagless]	
SS881	pPROBE <i>hilE-lux</i>	
SS967	<i>PprgH Venus</i> (964) in REB114	
SS968	<i>Phila Venus</i> (964) in REB114	
SS969	<i>PflhD Venus</i> (964) in REB114	
SS970	<i>PflhB Venus</i> (964) in REB114	
SS971	<i>PhilD Venus</i> (964) in REB114	

SS972	<i>PflgM Venus</i> (964) in REB114	
SS863	pLA2 <i>rhaBAD-gfp</i> [tagless]	
SS864	pLA2 <i>rhaSR-gfp</i> [tagless]	
SS865	pLA2 <i>rhaT-gfp</i> [tagless]	
SS866	pPROTet.E <i>Venus</i>	
SS867	pPROBE <i>fur-gfp</i> [tagless]	
SS868	pPROBE <i>venus</i>	
SS921	pPROBE <i>clpP-gfp</i> [tagless]	
SS922	pPROBE <i>lon-gfp</i> [tagless]	
SS957	pPROBE <i>PfeoAB GFP</i> [tagless]	
SS958	pPROBE <i>PfeoAB Venus</i>	
SS964	pVenus (<i>kan^R</i> , λ att), Dh5a pir+	
SS980	<i>PlpfA Venus</i> (pProbe) (CDC)	
SS981	<i>PstdA Venus</i> (pProbe) (CDC)	
SS982	<i>PstdB Venus</i> (pProbe) (CDC)	
SS983	<i>PsafA Venus</i> (pProbe) (CDC)	
SS984	<i>PsafB Venus</i> (pProbe) (CDC)	
SS985	<i>PbcfA Venus</i> (pProbe) (Dh5a)	
SS986	<i>PstbA Venus</i> (pProbe) (Dh5a)	
SS987	<i>PstcA Venus</i> (pProbe) (Dh5a)	
SS988	<i>PstfA Venus</i> (pProbe) (Dh5a)	
SS989	<i>PstfC Venus</i> (pProbe) (Dh5a)	
SS990	<i>PsthA Venus</i> (pProbe) (Dh5a)	
SS488	pPROTet.E <i>tetR</i>	(Saini et al., 2008)

a:This study unless specified

Appendix C: Matlab Code for Flagella Gene Network Model

```
function fliA_dynamic()

t0 = linspace(0,200,1001);
x0 = zeros(6,1);
x0(2) = 1;
p = linspace(0,4,60);
b = linspace(0,1,10);

clf
h1 = axes;
set(h1,'FontSize',16)

[t,x] = ode15s(@model,t0,x0,[],3,1.8);
c2 = x(:,4);
c3 = x(:,5);

[t,x] = ode15s(@model,t0,x0,[],3,0);
c2b = x(:,4);
c3b = x(:,5);

figure(1)
h = plot(t,c2,'-k',t,c3,'-r',t,c3b,'--r');
set(h,'LineWidth',4)
axis([0 max(t) 0 max([max(c2),max(c3),max(c3b)])])
xlabel('Time (A.U.)','FontSize',18);
ylabel('Gene Expression (A.U.) ','FontSize',18);
legend('Class 2','Class 3','Class 3 (PfliA::Plac)','Location','SouthEast')

%%%%%%%%%%%%%%%%%%%%%%%%%%%%%%%%%%%%%%%%%%%%%%%%%%%%%%%%%%%%%%%%%%%%%%%%
%%%%%%%%%%%%%%%%%%%%%%%%%%%%%%%%%%%%%%%%%%%%%%%%%%%%%%%%%%%%%%%%%%%%%%%%
function xdot = model(t,x,p,check)
xdot = zeros(size(x));

x(1) = max(x(1),0);
```

```

% doubling time (minutes)
mu = 30;

% half-life of FliA (Barembuch)
ga = 0.4 + log(2)/mu;
% half life of FlgM
gm = 0.4 + log(2)/mu;
% half life of complex
gam = 0.04 + log(2)/mu;

% FlgM-FliA association rate
% 30 /uM/min (0.5e6 /M/sec) (Chadsey and Hughes)
a_am = 30.0;
d_am = 6e-3;

f = gammainc(t/10,6);

% diassociation constants
Ka = 1;
Km = 1;
Kam = 3;

k2m = 1.5;
k3m = 3;
k2a = 0.2;
k3a = 1.8;
sec = 2;

sec = p*x(4);
%k2m = b;

p2m = k2m*f;
%p3m = 3*x(1)/(Km+x(1));
p3m = k3m*x(1)/(Km+x(1));

if check>0
    pa = (k2a*Ka*f + k3a*x(1))/(Ka+x(1));
else
    pa = 0.65;
end

export = sec*x(3)/(Kam+x(3));

```

`% A`

`x(1)dot = pa - ga*x(1) - a_am*x(1)*x(2) + d_am*x(3) + export;`

`% M`

`x(2)dot = 1*(p2m + p3m) - gm*x(2) - a_am*x(1)*x(2) + d_am*x(3);`

`% A-M`

`x(3)dot = a_am*x(1)*x(2) - d_am*x(3) - gam*x(3) - export;`

`% c2`

`x(4)dot = f - x(4);`

`% c3`

`x(5)dot = 2*f*x(1)/(Km+x(1)) - x(5);`

`x(6)dot = sec-x(6);`

Appendix D: Matlab Code for SPI1 Gene Network Model

% Supporting matlab m-file for Chapter 4

```
function SPI1_model_final()
close all
```

% uncomment functions below to generate specific figure

```
%Figure_5ABC(); % wild type
%Figure_5DE(); % mutants
Figure_S5AB(); % continous mutants
%Figure_S5CD(); % more mutants
%Figure_6A(); % alphaD versus kD
%Figure_6B(); % alphaD versus RC
%Figure_6C(); % HiE
%Figure_S6D(); % alphaE versus kD
```

```
%%%%%%%%%%%%%%%%%%%%%%%%%%%%%%%%%%%%%%%%%%%%%%%%%%%%%%%%%%%%%%%%%%%%%%%%
%%%%%%%%%%%%%%%%%%%%%%%%%%%%%%%%%%%%%%%%%%%%%%%%%%%%%%%%%%%%%%%%%%%%%%%%
```

```
function Figure_5ABC()
```

% get parameters

```
p = parameters();
```

% integration time domain

```
t0 = linspace(0,6,40);
```

```
for i=1:p.Ncells
    ti = sum(-log(rand()))*p.lambda;
    x0 = zeros(7,1);
    [t,x] = ode15s(@model,t0,x0,[],p,ti);
    D(:,i) = x(:,6);
    A(:,i) = x(:,7);
    C(:,i) = x(:,4);
    R(:,i) = x(:,5);
end
```

```
figure(1)
```

```

clf
ha = axes;
set(ha,'FontSize',16)
h=plot(t0,mean(D'),t0,mean(A'),t0,mean(C'),t0,mean(R'));
set(h,'LineWidth',3)
xlabel('Time (hr.)')
ylabel('Gene Expression (A.U.)')
legend('HiLD','HiIA','HiIC','RtsA','Location','NorthWest')

```

```

% show Hi1 expression at single-cell resolution

```

```

[pAx,pAy] = parzen_estimation(log(A+1)/max(max(log(A+1))),t0,p.Ncells);

```

```

figure(2)
clf
ha = axes;
set(ha,'FontSize',16)
set(ha,'LineWidth',2)
surf(pAx,t0,pAy)
lighting phong
shading interp
colormap(jet)
view([25 30])
ylabel('Time (hr.)')
xlabel('Gene Expression (A.L.U.)')
zlabel('Density of Events')
axis tight

```

```

figure(3)
clf
ha = axes;
set(ha,'FontSize',16)
set(ha,'LineWidth',2)
surf(pAx,t0,pAy)
lighting phong
shading interp
colormap(jet)
view([90 -90])
ylabel('Time (hr.)')
xlabel('Gene Expression (A.L.U.)')
axis tight
colorbar('FontSize',14)

```

```

%% UNCOMMENT TO SEE OTHER PROTEINS AT SINGLE-CELL RESOLUTION

```

```

% % show HiLD expression at single-cell resolution

```



```

% [pDx,pDy] = parzen_estimation(log(D+1)/max(max(log(D+1))),t0,p.Ncells);

% figure(4)
% clf
% ha = axes;
% set(ha,'FontSize',16)
% set(ha,'LineWidth',2)
% surf(pDx,t0,pDy)
% lighting phong
% shading interp
% colormap(jet)
% view([25 30])
% ylabel('Time (hr.)')
% xlabel('Gene Expression (A.L.U.)')
% zlabel('Density of Events')
% axis tight

%% show HilC expression at single-cell resolution
% [pCx,pCy] = parzen_estimation(log(C+1)/max(max(log(C+1))),t0,p.Ncells);

% figure(5)
% clf
% ha = axes;
% set(ha,'FontSize',16)
% set(ha,'LineWidth',2)
% surf(pCx,t0,pCy)
% lighting phong
% shading interp
% colormap(jet)
% view([25 30])
% ylabel('Time (hr.)')
% xlabel('Gene Expression (A.L.U.)')
% zlabel('Density of Events')
% axis tight

%% show RtsA expression at single-cell resolution
% [pRx,pRy] = parzen_estimation(log(R+1)/max(max(log(R+1))),t0,p.Ncells);

% figure(6)
% clf
% ha = axes;
% set(ha,'FontSize',16)
% set(ha,'LineWidth',2)
% surf(pRx,t0,pRy)

```

```

% lighting phong
% shading interp
% colormap(jet)
% view([25 30])
% ylabel('Time (hr.)')
% xlabel('Gene Expression (A.L.U.)')
% zlabel('Density of Events')
% axis tight

%%%%%%%%%%%%%%%%%%%%%%%%%%%%%%%%%%%%%%%%%%%%%%%%%%%%%%%%%%%%%%%%%%%%%%%%
%%%%%%%%%%%%%%%%%%%%%%%%%%%%%%%%%%%%%%%%%%%%%%%%%%%%%%%%%%%%%%%%%%%%%%%%
function Figure_5DE()

% get parameters
p = parameters();

% integration time domain
t0 = linspace(0,6,40);

% wild type
for i=1:p.Ncells
    ti = sum(-log(rand()))*p.lambda;
    x0 = zeros(7,1);
    [t,x] = ode15s(@model,t0,x0,[],p,ti);
    D(:,i) = x(:,6);
    A(:,i) = x(:,7);
    C(:,i) = x(:,4);
    R(:,i) = x(:,5);
end

% hiLE
p = parameters();
p.KO_E = 0;
for i=1:p.Ncells
    ti = sum(-log(rand()))*p.lambda;
    x0 = zeros(7,1);
    [t,x] = ode15s(@model,t0,x0,[],p,ti);
    D_E(:,i) = x(:,6);
    A_E(:,i) = x(:,7);
    C_E(:,i) = x(:,4);
    R_E(:,i) = x(:,5);
end

```

```

% hilC rtsA
p=parameters();
p.KO_C = 0;
p.KO_R = 0;
for i=1:p.Ncells
    ti = sum(-log(rand()))*p.lambda;
    x0 = zeros(7,1);
    [t,x] = ode15s(@model,t0,x0,[],p,ti);
    D_RC(:,i) = x(:,6);
    A_RC(:,i) = x(:,7);
    C_RC(:,i) = x(:,4);
    R_RC(:,i) = x(:,5);
end

% hilD
p=parameters();
p.KO_D = 0;
for i=1:p.Ncells
    ti = sum(-log(rand()))*p.lambda;
    x0 = zeros(7,1);
    [t,x] = ode15s(@model,t0,x0,[],p,ti);
    D_D(:,i) = x(:,6);
    A_D(:,i) = x(:,7);
    C_D(:,i) = x(:,4);
    R_D(:,i) = x(:,5);
end

figure(1)
clf
ha = axes;
set(ha,'FontSize',16)
h = plot(t0,mean(D),'-b',t0,mean(D_E),'-r',...
    t0,mean(D_RC),'-k',t0,mean(D_D),'-g')
set(h,'LineWidth',3)
xlabel('Time (hours)')
ylabel('HiLD Expression (A.U.)')
legend('Wild Type','\DeltahilE','\DeltahilC\DeltartsA',...
    '\DeltahilD','Location','NorthWest')

figure(2)
clf
ha = axes;
set(ha,'FontSize',16)
h = plot(t0,mean(A),'-b',t0,mean(A_E),'-r',...

```

```

    t0,mean(A_RC),'-k',t0,mean(A_D),'-g')
set(h,'LineWidth',3)
xlabel('Time (hours)')
ylabel('HilA Expression (A.U.)')
legend('Wild Type','\DeltahilE','\DeltahilC\DeltartsA',...
       '\DeltahilD','Location','NorthWest')

```

```

%%%%%%%%%%%%%%%%%%%%%%%%%%%%%%%%%%%%%%%%%%%%%%%%%%%%%%%%%%%%%%%%%%%%%%%%
%%%%%%%%%%%%%%%%%%%%%%%%%%%%%%%%%%%%%%%%%%%%%%%%%%%%%%%%%%%%%%%%%%%%%%%%

```

```
function Figure_S5AB()
```

```
% get parameters
```

```
p = parameters();
```

```
% integration time domain
```

```
t0 = linspace(0,6,100);
```

```
% continuous mutant
```

```
p.flag = 1;
```

```
for i=1:p.Ncells
```

```
    ti = sum(-log(rand()))*p.lambda;
```

```
    x0 = zeros(7,1);
```

```
    [t,x] = ode15s(@model,t0,x0,[],p,ti);
```

```
    D1(:,i) = x(:,6);
```

```
    A1(:,i) = x(:,7);
```

```
    C1(:,i) = x(:,4);
```

```
    R1(:,i) = x(:,5);
```

```
end
```

```
% slow mutant
```

```
t02 = linspace(0,2,100);
```

```
p = parameters();
```

```
% rescale time by factor of ten
```

```
p.lambda = 0.2;
```

```
for i=1:p.Ncells
```

```
    ti = sum(-log(rand()))*p.lambda;
```

```
    x0 = zeros(7,1);
```

```
    [t,x] = ode15s(@model,t02,x0,[],p,ti);
```

```
    D2(:,i) = x(:,6);
```

```

A2(:,i) = x(:,7);
C2(:,i) = x(:,4);
R2(:,i) = x(:,5);

end

t02 = t02*10;

% show HiA expression at single-cell resolution
[pA1x,pA1y] = parzen_estimation(log(A1+1)/max(max(log(A1+1))),t0,p.Ncells);
[pA2x,pA2y] = parzen_estimation(log(A2+1)/max(max(log(A2+1))),t02,p.Ncells);

```

```

figure(1)
clf
ha = axes;
set(ha,'FontSize',16)
set(ha,'LineWidth',2)
surf(pA1x,t0,pA1y)
lighting phong
shading interp
colormap(jet)
view([90 -90])
ylabel('Time (hr.)')
xlabel('Gene Expression (A.L.U.)')
axis tight
colorbar('FontSize',14)

```

```

figure(2)
clf
ha = axes;
set(ha,'FontSize',16)
set(ha,'LineWidth',2)
surf(pA2x,t02,pA2y)
lighting phong
shading interp
colormap(jet)
view([90 -90])
ylabel('Time (hr.)')
xlabel('Gene Expression (A.L.U.)')
axis tight
colorbar('FontSize',14)

```

```

%%%%%%%%%%%%%%%%%%%%%%%%%%%%%%%%%%%%%%%%%%%%%%%%%%%%%%%%%%%%%%%%%%%%%%%%
%%%%%%%%%%%%%%%%%%%%%%%%%%%%%%%%%%%%%%%%%%%%%%%%%%%%%%%%%%%%%%%%%%%%%%%%

```

```

function Figure_S5CD()

% get parameters
p = parameters();

% integration time domain
t0 = linspace(0,6,40);

% wild type
for i=1:p.Ncells
    ti = sum(-log(rand()))*p.lambda;
    x0 = zeros(7,1);
    [t,x] = ode15s(@model,t0,x0,[],p,ti);
    D(:,i) = x(:,6);
    A(:,i) = x(:,7);
    C(:,i) = x(:,4);
    R(:,i) = x(:,5);
end

% hiLE
p = parameters();
p.KO_E = 0;
for i=1:p.Ncells
    ti = sum(-log(rand()))*p.lambda;
    x0 = zeros(7,1);
    [t,x] = ode15s(@model,t0,x0,[],p,ti);
    D_E(:,i) = x(:,6);
    A_E(:,i) = x(:,7);
    C_E(:,i) = x(:,4);
    R_E(:,i) = x(:,5);
end

% hiLD
p=parameters();
p.KO_D = 0;
for i=1:p.Ncells
    ti = sum(-log(rand()))*p.lambda;
    x0 = zeros(7,1);
    [t,x] = ode15s(@model,t0,x0,[],p,ti);
    D_D(:,i) = x(:,6);
    A_D(:,i) = x(:,7);
    C_D(:,i) = x(:,4);
    R_D(:,i) = x(:,5);
end

```

```

% show HiC expression at single-cell resolution in WT versus HiD
[pCx,pCy] = parzen_estimation(log(C+1)/max(max(log(C+1))),t0,p.Ncells);
[pCDx,pCDy] = parzen_estimation(log(C_D+1)/max(max(log(C_D+1))),t0,p.Ncells);

figure(1)
clf
ha = axes;
set(ha,'FontSize',16)
set(ha,'LineWidth',2)
surf(pCx,t0,pCy)
lighting phong
shading interp
colormap(jet)
view([90 -90])
ylabel('Time (hr.)')
xlabel('Gene Expression (A.L.U.)')
axis tight
colorbar('FontSize',14)

figure(2)
clf
ha = axes;
set(ha,'FontSize',16)
set(ha,'LineWidth',2)
surf(pCDx,t0,pCDy)
lighting phong
shading interp
colormap(jet)
view([90 -90])
ylabel('Time (hr.)')
xlabel('Gene Expression (A.L.U.)')
axis tight
colorbar('FontSize',14)

%%%%%%%%%%%%%%%%%%%%%%%%%%%%%%%%%%%%%%%%%%%%%%%%%%%%%%%%%%%%%%%%%%%%%%%%
%%%%%%%%%%%%%%%%%%%%%%%%%%%%%%%%%%%%%%%%%%%%%%%%%%%%%%%%%%%%%%%%%%%%%%%%
function Figure_6A()
% alphaD versus kD
x0 = zeros(7,1);
t0 = linspace(0,500,3);

```

```

p = parameters();

p1 = linspace(0,0.8,45);
p2 = linspace(0,25,45);

for i=1:length(p1);
    for j=1:length(p2)
        p.alphaD = p1(i);
        p.kD = p2(j);
        [t,x] = ode15s(@model,t0,x0,[],p,0);
        D(i,j) = x(end,6);
        A(i,j) = x(end,7);
    end
end

p = parameters();
for i=1:length(p1)
    p.alphaD = p1(i);
    [t,x] = ode15s(@model,t0,x0,[],p,0);
    Dn(i) = x(end,6);
    An(i) = x(end,7);
end

figure(1)
clf
ha = axes;
set(ha,'FontSize',16)
set(ha,'LineWidth',2)
h = mesh(p1,p2,D');
lighting phong
colormap([0 0 0])
set(h,'LineWidth',1)
xlabel('Parameter \alpha_D')
ylabel('Parameter k_D')
zlabel('HiID Expression')
%view([-130 30])
hold on
h1 = plot3(p1,p.kD*ones(size(p1)),Dn,'-k')
set(h1,'LineWidth',6)
hold off
axis tight

```



```

figure(2)
clf
ha = axes;
set(ha,'FontSize',16)
set(ha,'LineWidth',2)
h = mesh(p1,p2,A');
lighting phong
colormap([0 0 0])
set(h,'LineWidth',1)
xlabel('Parameter \alpha_D')
ylabel('Parameter k_D')
zlabel('HilA Expression')
%view([-130 30])
hold on
h1 = plot3(p1,p.kD*ones(size(p1)),An,'-k')
set(h1,'LineWidth',6)
hold off
axis tight

%%%%%%%%%%%%%%%%%%%%%%%%%%%%%%%%%%%%%%%%%%%%%%%%%%%%%%%%%%%%%%%%%%%%%%%%
%%%%%%%%%%%%%%%%%%%%%%%%%%%%%%%%%%%%%%%%%%%%%%%%%%%%%%%%%%%%%%%%%%%%%%%%
function Figure_6B()
% alphaD versus RC
x0 = zeros(7,1);
t0 = linspace(0,500,3);

p = parameters();

p1 = linspace(0,0.8,40);
p2 = linspace(0,20,40);

for i=1:length(p1);
    for j=1:length(p2)
        p.alphaD = p1(i);
        p.kC = p2(j);
        p.kR = p2(j);
        [t,x] = ode15s(@model,t0,x0,[],p,0);
        D(i,j) = x(end,6);
        A(i,j) = x(end,7);
    end
end

p = parameters();
p.kR = p.kC;

```

```

for i=1:length(p1)
    p.alphaD = p1(i);
    [t,x] = ode15s(@model,t0,x0,[],p,0);
    Dn(i) = x(end,6);
    An(i) = x(end,7);
end

figure(1)
clf
ha = axes;
set(ha,'FontSize',16)
set(ha,'LineWidth',2)
h = mesh(p1,p2,D');
lighting phong
colormap([0 0 0])
set(h,'LineWidth',1)
xlabel('Parameter \alpha_D')
ylabel('Parameter k_C/k_R')
zlabel('HilD Expression')
%view([-130 30])
hold on
h1 = plot3(p1,p.kC*ones(size(p1)),Dn,'-k')
set(h1,'LineWidth',6)
hold off
axis tight

figure(2)
clf
ha = axes;
set(ha,'FontSize',16)
set(ha,'LineWidth',2)
h = mesh(p1,p2,A');
lighting phong
colormap([0 0 0])
set(h,'LineWidth',1)
xlabel('Parameter \alpha_D')
ylabel('Parameter k_C/k_R')
zlabel('HilA Expression')
%view([-130 30])
hold on
h1 = plot3(p1,p.kC*ones(size(p1)),An,'-k')
set(h1,'LineWidth',6)
hold off
axis tight

```

```

%%%%%%%%%%%%%%%%%%%%%%%%%%%%%%%%%%%%%%%%%%%%%%%%%%%%%%%%%%%%%%%%%%%%%%%%
%%%%%%%%%%%%%%%%%%%%%%%%%%%%%%%%%%%%%%%%%%%%%%%%%%%%%%%%%%%%%%%%%%%%%%%%
function Figure_6C()
% HiLE plot

x0 = zeros(7,1);
t0 = linspace(0,500,3);

p = parameters();

p1 = linspace(0,0.8,45);
p2 = linspace(0,25,45);

for i=1:length(p1);
    for j=1:length(p2)
        p.alphaD = p1(i);
        p.alphaE = p2(j);
        [t,x] = ode15s(@model,t0,x0,[],p,0);
        D(i,j) = x(end,6);
        A(i,j) = x(end,7);
    end
end

p = parameters();
for i=1:length(p1)
    p.alphaD = p1(i);
    [t,x] = ode15s(@model,t0,x0,[],p,0);
    Dn(i) = x(end,6);
    An(i) = x(end,7);
end

figure(1)
clf
ha = axes;
set(ha,'FontSize',16)
h = mesh(p2,p1,D);
lighting phong
colormap([0 0 0])
set(h,'LineWidth',1)
ylabel('Parameter \alpha_D')
xlabel('Parameter \alpha_E')
zlabel('HiLE Expression')

```

```

view([-15 30]);
hold on
h1 = plot3(p.alphaE*ones(size(p1)),p1,Dn,'-k')
set(h1,'LineWidth',6)
hold off
axis tight

figure(2)
clf
ha = axes;
set(ha,'FontSize',16)
h = mesh(p2,p1,A);
lighting phong
colormap([0 0 0])
set(h,'LineWidth',1)
ylabel('Parameter \alpha_D')
xlabel('Parameter \alpha_E')
zlabel('HilA Expression')
view([-15 30]);
hold on
h1 = plot3(p.alphaE*ones(size(p1)),p1,An,'-k')
set(h1,'LineWidth',6)
hold off
axis tight

%%%%%%%%%%%%%%%%%%%%%%%%%%%%%%%%%%%%%%%%%%%%%%%%%%%%%%%%%%%%%%%%%%%%%%%%
%%%%%%%%%%%%%%%%%%%%%%%%%%%%%%%%%%%%%%%%%%%%%%%%%%%%%%%%%%%%%%%%%%%%%%%%
function Figure_S6D()
% HilE plot

x0 = zeros(7,1);
t0 = linspace(0,500,3);

p = parameters();

p1 = linspace(0,30,45);
p2 = linspace(0,30,45);

for i=1:length(p1);
    for j=1:length(p2)
        p.kD = p1(i);
        p.alphaE = p2(j);
        [t,x] = ode15s(@model,t0,x0,[],p,0);
        D(i,j) = x(end,6);
    end
end

```

```

        A(i,j) = x(end,7);
    end
end

```

```

figure(1)
clf
ha = axes;
set(ha,'FontSize',16)
h = surf(p1,p2,D');
lighting phong
colormap(jet)
set(h,'LineWidth',1)
xlabel('Parameter k_D')
ylabel('Parameter \alpha_E')
zlabel('HilD Expression')
axis tight

```

```

figure(2)
clf
ha = axes;
set(ha,'FontSize',16)
h = surf(p1,p2,A');
lighting phong
colormap(jet)
set(h,'LineWidth',1)
xlabel('Parameter k_D')
ylabel('Parameter \alpha_E')
zlabel('HilA Expression')
axis tight

```

```

%%%%%%%%%%%%%%%%%%%%%%%%%%%%%%%%%%%%%%%%%%%%%%%%%%%%%%%%%%%%%%%%%%%%%%%%
%%%%%%%%%%%%%%%%%%%%%%%%%%%%%%%%%%%%%%%%%%%%%%%%%%%%%%%%%%%%%%%%%%%%%%%%

```

```

function [x,y] = parzen_estimation(xi,t0,m,xmax)

```

```

h = 0.05;
xi_min = min(min(xi));
xi_max = max(max(xi));
x = linspace(xi_min-3*h,xi_max+3*h,100);
n = length(t0);
y=zeros(n,length(x));

```

```

for j=1:n

```

```

for i=1:m
    y(j,:) = y(j,:) + 1/(m*h*sqrt(2*pi))*exp(-0.5*(x-xi(j,i)).^2/h/h);
end
end

%%%%%%%%%%%%%%%%%%%%%%%%%%%%%%%%%%%%%%%%%%%%%%%%%%%%%%%%%%%%%%%%%%%%%%%%
%%%%%%%%%%%%%%%%%%%%%%%%%%%%%%%%%%%%%%%%%%%%%%%%%%%%%%%%%%%%%%%%%%%%%%%%
function xdot = model(t,x,p,ti)
xdot = zeros(size(x));

D = p.KO_D*x(1);
C = p.KO_C*x(4);
R = p.KO_R*x(5);

O1 = (p.KO1D*D + p.KO1C*C + p.KO1R*R)/(1+p.KO1D*D + p.KO1C*C + p.KO1R*R);
O2 = (p.KO2D*D + p.KO2C*C + p.KO2R*R)/(1+p.KO2D*D + p.KO2C*C + p.KO2R*R);
pX = O1*O2;

pX = O1*O2;

% HiID
xdot(1) = p.alphaD*(t>=ti) + p.kD*pX - p.deltaD*x(1) ...
    - p.aE*x(1)*x(2) + p.dE*x(3);

% HiIE
xdot(2) = p.alphaE*p.KO_E - p.deltaE*x(2) - p.aE*x(1)*x(2) + p.dE*x(3);

% HiID-HiIE
xdot(3) = p.aE*x(1)*x(2) - p.dE*x(3) - p.deltaDE*x(3);

% HiIC
xdot(4) = p.alphaC*(1-exp(-t/p.lambda)) + p.kC*pX - p.deltaC*x(4);

% RtsA
xdot(5) = p.kR*pX - p.deltaR*x(5);

% hiID'-reporter
xdot(6) = p.alphaD*(t>=ti) + p.kD*pX - p.deltaG*x(6);

% HiIA
xdot(7) = p.kA*pX - p.deltaA*x(7);

if (p.flag)
    xdot(1) = p.alphaD*(1-exp(-t/p.lambda)) + p.kD*pX - p.deltaD*x(1) ...

```

```
- p.aE*x(1)*x(2) + p.dE*x(3);  
end
```

```
%%%%%%%%%%%%%%%%%%%%%%%%%%%%%%%%%%%%%%%%%%%%%%%%%%%%%%%%%%%%%%%%%%%%%%%%  
%%%%%%%%%%%%%%%%%%%%%%%%%%%%%%%%%%%%%%%%%%%%%%%%%%%%%%%%%%%%%%%%%%%%%%%%
```

```
function p = parameters()
```

```
% number of cells for stochastic simulations  
p.Ncells = 1000;
```

```
% initiation  
p.lambda = 2.0;
```

```
p.alphaD = 1.2;  
p.alphaC = 0.4;  
p.alphaE = 12.0;
```

```
% promoters  
p.kD = 16;  
p.kC = 10;  
p.kR = 8;  
p.kA = 6;
```

```
% promoter binding  
p.KO1D = 10.0;  
p.KO1C = 0.001;  
p.KO1R = 0.001;
```

```
p.KO2D = 1.0;  
p.KO2C = 0.1;  
p.KO2R = 0.1;
```

```
% degradation  
p.deltaD = 4.0;  
p.deltaE = 8.0;  
p.deltaC = 4.0;  
p.deltaR = 4.0;  
p.deltaA = 4.0;  
p.deltaG = 4.0;
```

```
% binding and unbinding of HiE and HiD  
p.aE = 8.0;  
p.dE = 8.0;
```

```
p.deltaDE = 16.0;
```

```
% flags for KO
```

```
p.KO_D = 1;
```

```
p.KO_C = 1;
```

```
p.KO_R = 1;
```

```
p.KO_E = 1;
```

```
% flags for continuous mutant
```

```
p.flag = 0; % continuous
```


References

- Abraham, J. M., C. S. Freitag, J. R. Clements & B. I. Eisenstein, (1985) An invertible element of DNA controls phase variation of type 1 fimbriae of *Escherichia coli*. *Proc Natl Acad Sci U S A* **82**: 5724-5727.
- Ahmer, B. M., J. van Reeuwijk, P. R. Watson, T. S. Wallis & F. Heffron, (1999) *Salmonella* SirA is a global regulator of genes mediating enteropathogenesis. *Mol Microbiol* **31**: 971-982.
- Akbar, S., L. M. Schechter, C. P. Lostroh & C. A. Lee, (2003) AraC/XylS family members, HilD and HilC, directly activate virulence gene expression independently of HilA in *Salmonella typhimurium*. *Mol Microbiol* **47**: 715-728.
- Aldridge, P., J. Karlinsey & K. T. Hughes, (2003) The type III secretion chaperone FlgN regulates flagellar assembly via a negative feedback loop containing its chaperone substrates FlgK and FlgL. *Mol Microbiol* **49**: 1333-1345.
- Allen, K. J., D. Lepp, R. C. McKellar & M. W. Griffiths, (2008) Examination of stress and virulence gene expression in *Escherichia coli* O157:H7 using targeted microarray analysis. *Foodborne Pathog Dis* **5**: 437-447.
- Altier, C., (2005) Genetic and environmental control of salmonella invasion. *J Microbiol* **43 Spec No**: 85-92.
- Asakura, S., G. Eguchi & T. Iino, (1968) Unidirectional growth of *Salmonella* flagella in vitro. *J Mol Biol* **35**: 227-236.
- Bajaj, V., C. Hwang & C. A. Lee, (1995) hilA is a novel ompR/toxR family member that activates the expression of *Salmonella typhimurium* invasion genes. *Mol Microbiol* **18**: 715-727.
- Bajaj, V., R. L. Lucas, C. Hwang & C. A. Lee, (1996) Co-ordinate regulation of *Salmonella typhimurium* invasion genes by environmental and regulatory factors is mediated by control of hilA expression. *Mol Microbiol* **22**: 703-714.
- Batchelor, E., T. J. Silhavy & M. Goulian, (2004) Continuous control in bacterial regulatory circuits. *Journal of bacteriology* **186**: 7618-7625.
- Baumler, A. J., R. M. Tsois & F. Heffron, (1996) Contribution of fimbrial operons to attachment to and invasion of epithelial cell lines by *Salmonella typhimurium*. *Infect Immun* **64**: 1862-1865.
- Baumler, A. J., R. M. Tsois & F. Heffron, (1997) Fimbrial adhesins of *Salmonella typhimurium*. Role in bacterial interactions with epithelial cells. *Adv Exp Med Biol* **412**: 149-158.
- Baxter, M. A., T. F. Fahlen, R. L. Wilson & B. D. Jones, (2003) HilE interacts with HilD and negatively regulates hilA transcription and expression of the *Salmonella enterica* serovar Typhimurium invasive phenotype. *Infect Immun* **71**: 1295-1305.
- Baxter, M. A. & B. D. Jones, (2005) The fimYZ genes regulate *Salmonella enterica* Serovar Typhimurium invasion in addition to type 1 fimbrial expression and bacterial motility. *Infect Immun* **73**: 1377-1385.

- Becker, D., M. Selbach, C. Rollenhagen, M. Ballmaier, T. F. Meyer, M. Mann & D. Bumann, (2006) Robust Salmonella metabolism limits possibilities for new antimicrobials. *Nature* **440**: 303-307.
- Becskei, A., B. Seraphin & L. Serrano, (2001) Positive feedback in eukaryotic gene networks: cell differentiation by graded to binary response conversion. *Embo J* **20**: 2528-2535.
- Behlau, I. & S. I. Miller, (1993) A PhoP-repressed gene promotes Salmonella typhimurium invasion of epithelial cells. *J Bacteriol* **175**: 4475-4484.
- Bennett, J. C., J. Thomas, G. M. Fraser & C. Hughes, (2001) Substrate complexes and domain organization of the Salmonella flagellar export chaperones FlgN and FliT. *Mol Microbiol* **39**: 781-791.
- Berg, H. C., (2003) The rotary motor of bacterial flagella. *Annu Rev Biochem* **72**: 19-54.
- Bischoff, D. S., M. D. Weinreich & G. W. Ordal, (1992) Nucleotide sequences of Bacillus subtilis flagellar biosynthetic genes fliP and fliQ and identification of a novel flagellar gene, fliZ. *J Bacteriol* **174**: 4017-4025.
- Boddicker, J. D., B. M. Knosp & B. D. Jones, (2003) Transcription of the Salmonella invasion gene activator, hilA, requires Hild activation in the absence of negative regulators. *J Bacteriol* **185**: 525-533.
- Bode, U., I. T. Magrath, W. A. Bleyer, D. G. Poplack & D. L. Glaubiger, (1980) Active transport of methotrexate from cerebrospinal fluid in humans. *Cancer Res* **40**: 2184-2187.
- Bowe, F., C. J. Lipps, R. M. Tsois, E. Groisman, F. Heffron & J. G. Kusters, (1998) At least four percent of the Salmonella typhimurium genome is required for fatal infection of mice. *Infect Immun* **66**: 3372-3377.
- Brandman, O., J. E. Ferrell, Jr., R. Li & T. Meyer, (2005) Interlinked fast and slow positive feedback loops drive reliable cell decisions. *Science* **310**: 496-498.
- Brown, J. D., S. Saini, C. Aldridge, J. Herbert, C. V. Rao & P. D. Aldridge, (2008) The rate of protein secretion dictates the temporal dynamics of flagellar gene expression. *Mol Microbiol* **70**: 924-937.
- Buchanan, K., S. Falkow, R. A. Hull & S. I. Hull, (1985) Frequency among Enterobacteriaceae of the DNA sequences encoding type 1 pili. *J Bacteriol* **162**: 799-803.
- Bustamante, V. H., L. C. Martinez, F. J. Santana, L. A. Knodler, O. Steele-Mortimer & J. L. Puente, (2008) Hild-mediated transcriptional cross-talk between SPI-1 and SPI-2. *Proc Natl Acad Sci U S A* **105**: 14591-14596.
- Cain, R. J., R. D. Hayward & V. Koronakis, (2008) Deciphering interplay between Salmonella invasion effectors. *PLoS Pathog* **4**: e1000037.
- Carter, P. B. & F. M. Collins, (1974) The route of enteric infection in normal mice. *J Exp Med* **139**: 1189-1203.
- Chadsey, M. S. & K. T. Hughes, (2001) A multipartite interaction between Salmonella transcription factor sigma28 and its anti-sigma factor FlgM: implications for sigma28 holoenzyme destabilization through stepwise binding. *J Mol Biol* **306**: 915-929.

- Chadsey, M. S., J. E. Karlinsey & K. T. Hughes, (1998) The flagellar anti-sigma factor FlgM actively dissociates *Salmonella typhimurium* sigma28 RNA polymerase holoenzyme. *Genes Dev* **12**: 3123-3136.
- Chang, D. E., S. Leung, M. R. Atkinson, A. Reifler, D. Forger & A. J. Ninfa, (2009) Building biological memory by linking positive feedback loops. *Proc Natl Acad Sci U S A*.
- Cherepanov, P. P. & W. Wackernagel, (1995) Gene disruption in *Escherichia coli*: TcR and KmR cassettes with the option of Flp-catalyzed excision of the antibiotic-resistance determinant. *Gene* **158**: 9-14.
- Cherepenko, Y. & D. M. Hovorun, (2005) Bacterial multidrug resistance unrelated to multidrug exporters: cell biology insight. *Cell Biol Int* **29**: 3-7.
- Chilcott, G. S. & K. T. Hughes, (2000) Coupling of flagellar gene expression to flagellar assembly in *Salmonella enterica* serovar typhimurium and *Escherichia coli*. *Microbiol Mol Biol Rev* **64**: 694-708.
- Clegg, S., L. S. Hancox & K. S. Yeh, (1996) *Salmonella typhimurium* fimbrial phase variation and FimA expression. *Journal of bacteriology* **178**: 542-545.
- Clegg, S. & K. T. Hughes, (2002) FimZ is a molecular link between sticking and swimming in *Salmonella enterica* serovar Typhimurium. *J Bacteriol* **184**: 1209-1213.
- Cohen, S. P., S. B. Levy, J. Foulds & J. L. Rosner, (1993) Salicylate induction of antibiotic resistance in *Escherichia coli*: activation of the mar operon and a mar-independent pathway. *J Bacteriol* **175**: 7856-7862.
- Collazo, C. M. & J. E. Galan, (1996) Requirement for exported proteins in secretion through the invasion-associated type III system of *Salmonella typhimurium*. *Infect Immun* **64**: 3524-3531.
- Collazo, C. M. & J. E. Galan, (1997a) The invasion-associated type-III protein secretion system in *Salmonella*--a review. *Gene* **192**: 51-59.
- Collazo, C. M. & J. E. Galan, (1997b) The invasion-associated type III system of *Salmonella typhimurium* directs the translocation of Sip proteins into the host cell. *Mol Microbiol* **24**: 747-756.
- Cotter, P. A. & J. F. Miller, (1994) BvgAS-mediated signal transduction: analysis of phase-locked regulatory mutants of *Bordetella bronchiseptica* in a rabbit model. *Infect Immun* **62**: 3381-3390.
- Cui, J., C. Chen, H. Lu, T. Sun & P. Shen, (2008) Two independent positive feedbacks and bistability in the Bcl-2 apoptotic switch. *PLoS One* **3**: e1469.
- Daly, R. A. & C. P. Lostroh, (2008) Genetic analysis of the *Salmonella* transcription factor HilA. *Can J Microbiol* **54**: 854-860.
- Darwin, K. H. & V. L. Miller, (1999a) InvF is required for expression of genes encoding proteins secreted by the SPI1 type III secretion apparatus in *Salmonella typhimurium*. *Journal of bacteriology* **181**: 4949-4954.
- Darwin, K. H. & V. L. Miller, (1999b) Molecular basis of the interaction of *Salmonella* with the intestinal mucosa. *Clin Microbiol Rev* **12**: 405-428.
- Darwin, K. H. & V. L. Miller, (2000) The putative invasion protein chaperone SicA acts together with InvF to activate the expression of *Salmonella typhimurium* virulence genes. *Mol Microbiol* **35**: 949-960.

- Darwin, K. H. & V. L. Miller, (2001) Type III secretion chaperone-dependent regulation: activation of virulence genes by SicA and InvF in *Salmonella typhimurium*. *EMBO J* **20**: 1850-1862.
- Datsenko, K. A. & B. L. Wanner, (2000) One-step inactivation of chromosomal genes in *Escherichia coli* K-12 using PCR products. *Proc Natl Acad Sci U S A* **97**: 6640-6645.
- Davis, R. W., D. Botstein, and J. R. Roth, (1980) *Advanced bacterial genetics: a manual for genetic engineering*. Cold Spring Harbor Laboratory Press, Cold Spring Harbor, NY.
- De Keersmaecker, S. C., K. Marchal, T. L. Verhoeven, K. Engelen, J. Vanderleyden & C. S. Detweiler, (2005) Microarray analysis and motif detection reveal new targets of the *Salmonella enterica* serovar Typhimurium HilA regulatory protein, including hilA itself. *J Bacteriol* **187**: 4381-4391.
- Desai, T. A. & C. V. Rao, (2010) Regulation of arabinose and xylose metabolism in *Escherichia coli*. *Appl Environ Microbiol* **76**: 1524-1532.
- Dubnau, D. & R. Losick, (2006) Bistability in bacteria. *Mol Microbiol* **61**: 564-572.
- Duguid, J. P., E. S. Anderson & I. Campbell, (1966a) Fimbriae and adhesive properties in *Salmonellae*. *J Pathol Bacteriol* **92**: 107-138.
- Duguid, J. P., E. S. Anderson & I. Campbell, (1966b) Fimbriae and adhesive properties in *Salmonellae*. *The Journal of pathology and bacteriology* **92**: 107-138.
- Duguid, J. P., M. R. Darekar & D. W. Wheeler, (1976) Fimbriae and infectivity in *Salmonella typhimurium*. *J Med Microbiol* **9**: 459-473.
- Eichelberg, K., W. D. Hardt & J. E. Galan, (1999) Characterization of SprA, an AraC-like transcriptional regulator encoded within the *Salmonella typhimurium* pathogenicity island 1. *Mol Microbiol* **33**: 139-152.
- Ellermeier, C. D., J. R. Ellermeier & J. M. Slauch, (2005) HilD, HilC and RtsA constitute a feed forward loop that controls expression of the SPI1 type three secretion system regulator hilA in *Salmonella enterica* serovar Typhimurium. *Mol Microbiol* **57**: 691-705.
- Ellermeier, C. D., Slauch J.M., (2006) *The genus Salmonella*. In: Dworkin M, Falkow S, Rosenberg E, Schleifer K-H, Stackebrandt E, editors. *The prokaryotes*, 3rd ed. New York, NY.: Springer. pp. 123-158.
- Ellermeier, C. D. & J. M. Slauch, (2003) RtsA and RtsB coordinately regulate expression of the invasion and flagellar genes in *Salmonella enterica* serovar Typhimurium. *J Bacteriol* **185**: 5096-5108.
- Ellermeier, J. R. & J. M. Slauch, (2007) Adaptation to the host environment: regulation of the SPI1 type III secretion system in *Salmonella enterica* serovar Typhimurium. *Curr Opin Microbiol* **10**: 24-29.
- Ellermeier, J. R. & J. M. Slauch, (2008) Fur regulates expression of the *Salmonella* pathogenicity island 1 type III secretion system through HilD. *Journal of bacteriology* **190**: 476-486.
- Fabrega, A., J. Sanchez-Céspedes, S. Soto & J. Vila, (2008) Quinolone resistance in the food chain. *Int J Antimicrob Agents* **31**: 307-315.

- Fahlen, T. F., N. Mathur & B. D. Jones, (2000) Identification and characterization of mutants with increased expression of hilA, the invasion gene transcriptional activator of *Salmonella typhimurium*. *FEMS Immunol Med Microbiol* **28**: 25-35.
- Fass, E. & E. A. Groisman, (2009) Control of *Salmonella* pathogenicity island-2 gene expression. *Curr Opin Microbiol* **12**: 199-204.
- Ferrell, J. E., (2002) Self-perpetuating states in signal transduction: positive feedback, double-negative feedback and bistability. *Curr Opin Cell Biol* **14**: 140-148.
- Francis, C. L., T. A. Ryan, B. D. Jones, S. J. Smith & S. Falkow, (1993) Ruffles induced by *Salmonella* and other stimuli direct macropinocytosis of bacteria. *Nature* **364**: 639-642.
- Fraser, G. M., J. C. Bennett & C. Hughes, (1999) Substrate-specific binding of hook-associated proteins by FlgN and FliT, putative chaperones for flagellum assembly. *Mol Microbiol* **32**: 569-580.
- Fu, Y. & J. E. Galan, (1999) A salmonella protein antagonizes Rac-1 and Cdc42 to mediate host-cell recovery after bacterial invasion. *Nature* **401**: 293-297.
- Galan, J. E. & D. Zhou, (2000) Striking a balance: modulation of the actin cytoskeleton by *Salmonella*. *Proc Natl Acad Sci U S A* **97**: 8754-8761.
- Gally, D. L., J. Leathart & I. C. Blomfield, (1996) Interaction of FimB and FimE with the fim switch that controls the phase variation of type 1 fimbriae in *Escherichia coli* K-12. *Mol Microbiol* **21**: 725-738.
- Ganesh, A. B., H. Rajasingh & S. S. Mande, (2009) Mathematical modeling of regulation of type III secretion system in *Salmonella enterica* serovar Typhimurium by SirA. *In silico biology* **9**: S57-72.
- Garcia Vescovi, E., F. C. Soncini & E. A. Groisman, (1994) The role of the PhoP/PhoQ regulon in *Salmonella* virulence. *Res Microbiol* **145**: 473-480.
- Gerlach, G. F., S. Clegg, N. J. Ness, D. L. Swenson, B. L. Allen & W. A. Nichols, (1989) Expression of type 1 fimbriae and mannose-sensitive hemagglutinin by recombinant plasmids. *Infect Immun* **57**: 764-770.
- Gerlach, R. G., D. Jackel, N. Geymeier & M. Hensel, (2007a) *Salmonella* pathogenicity island 4-mediated adhesion is coregulated with invasion genes in *Salmonella enterica*. *Infect Immun* **75**: 4697-4709.
- Gerlach, R. G., D. Jackel, B. Stecher, C. Wagner, A. Lupas, W. D. Hardt & M. Hensel, (2007b) *Salmonella* Pathogenicity Island 4 encodes a giant non-fimbrial adhesin and the cognate type 1 secretion system. *Cell Microbiol* **9**: 1834-1850.
- Gillen, K. L. & K. T. Hughes, (1991) Molecular characterization of flgM, a gene encoding a negative regulator of flagellin synthesis in *Salmonella typhimurium*. *J Bacteriol* **173**: 6453-6459.
- Ginocchio, C. C., S. B. Olmsted, C. L. Wells & J. E. Galan, (1994) Contact with epithelial cells induces the formation of surface appendages on *Salmonella typhimurium*. *Cell* **76**: 717-724.
- Goodier, R. I. & B. M. Ahmer, (2001) SirA orthologs affect both motility and virulence. *J Bacteriol* **183**: 2249-2258.
- Gunn, J. S., (2008) The *Salmonella* PmrAB regulon: lipopolysaccharide modifications, antimicrobial peptide resistance and more. *Trends Microbiol* **16**: 284-290.

- Guzman, L. M., D. Belin, M. J. Carson & J. Beckwith, (1995) Tight regulation, modulation, and high-level expression by vectors containing the arabinose PBAD promoter. *J Bacteriol* **177**: 4121-4130.
- Hakkila, K., M. Maksimow, M. Karp & M. Virta, (2002) Reporter genes lucFF, luxCDABE, gfp, and dsred have different characteristics in whole-cell bacterial sensors. *Analytical biochemistry* **301**: 235-242.
- Haldimann, A. & B. L. Wanner, (2001) Conditional-replication, integration, excision, and retrieval plasmid-host systems for gene structure-function studies of bacteria. *J Bacteriol* **183**: 6384-6393.
- Hancox, L. S., K. S. Yeh & S. Clegg, (1997) Construction and characterization of type 1 non-fimbriate and non-adhesive mutants of *Salmonella typhimurium*. *FEMS Immunol Med Microbiol* **19**: 289-296.
- Hardt, W. D., L. M. Chen, K. E. Schuebel, X. R. Bustelo & J. E. Galan, (1998) *S. typhimurium* encodes an activator of Rho GTPases that induces membrane ruffling and nuclear responses in host cells. *Cell* **93**: 815-826.
- Harshey, R. M. & T. Matsuyama, (1994) Dimorphic transition in *Escherichia coli* and *Salmonella typhimurium*: surface-induced differentiation into hyperflagellate swarmer cells. *Proc Natl Acad Sci U S A* **91**: 8631-8635.
- Hautefort, I., M. J. Proenca & J. C. Hinton, (2003) Single-copy green fluorescent protein gene fusions allow accurate measurement of *Salmonella* gene expression in vitro and during infection of mammalian cells. *Appl Environ Microbiol* **69**: 7480-7491.
- Hayward, R. D. & V. Koronakis, (2002) Direct modulation of the host cell cytoskeleton by *Salmonella* actin-binding proteins. *Trends Cell Biol* **12**: 15-20.
- Hensel, M., (2000) *Salmonella* pathogenicity island 2. *Mol Microbiol* **36**: 1015-1023.
- Homma, M. & T. Iino, (1985) Locations of hook-associated proteins in flagellar structures of *Salmonella typhimurium*. *J Bacteriol* **162**: 183-189.
- Hughes, K. T., K. L. Gillen, M. J. Semon & J. E. Karlinsey, (1993) Sensing structural intermediates in bacterial flagellar assembly by export of a negative regulator. *Science* **262**: 1277-1280.
- Ikebe, T., S. Iyoda & K. Kutsukake, (1999) Promoter analysis of the class 2 flagellar operons of *Salmonella*. *Genes Genet Syst* **74**: 179-183.
- Iyoda, S., T. Kamidoi, K. Hirose, K. Kutsukake & H. Watanabe, (2001) A flagellar gene *fliZ* regulates the expression of invasion genes and virulence phenotype in *Salmonella enterica* serovar *Typhimurium*. *Microb Pathog* **30**: 81-90.
- Kalir, S., J. McClure, K. Pabbaraju, C. Southward, M. Ronen, S. Leibler, M. G. Surette & U. Alon, (2001) Ordering genes in a flagella pathway by analysis of expression kinetics from living bacteria. *Science* **292**: 2080-2083.
- Karlinsey, J. E., (2007) λ -Red genetic engineering in *Salmonella enterica* serovar *Typhimurium*. *Methods Enzymol* **421**: 199-209.
- Karlinsey, J. E., J. Lonner, K. L. Brown & K. T. Hughes, (2000a) Translation/secretion coupling by type III secretion systems. *Cell* **102**: 487-497.
- Karlinsey, J. E., S. Tanaka, V. Bettenworth, S. Yamaguchi, W. Boos, S. I. Aizawa & K. T. Hughes, (2000b) Completion of the hook-basal body complex of the *Salmonella*

- typhimurium flagellum is coupled to FlgM secretion and fliC transcription. *Mol Microbiol* **37**: 1220-1231.
- Kato, A., A. Y. Mitrophanov & E. A. Groisman, (2007) A connector of two-component regulatory systems promotes signal amplification and persistence of expression. *Proc Natl Acad Sci U S A* **104**: 12063-12068.
- Kim, W. & M. G. Surette, (2004) Metabolic differentiation in actively swarming Salmonella. *Mol Microbiol* **54**: 702-714.
- Kimbrough, T. G. & S. I. Miller, (2000) Contribution of Salmonella typhimurium type III secretion components to needle complex formation. *Proc Natl Acad Sci U S A* **97**: 11008-11013.
- Kimbrough, T. G. & S. I. Miller, (2002) Assembly of the type III secretion needle complex of Salmonella typhimurium. *Microbes Infect* **4**: 75-82.
- Kiss, T., E. Morgan & G. Nagy, (2007) Contribution of SPI-4 genes to the virulence of Salmonella enterica. *FEMS Microbiol Lett* **275**: 153-159.
- Klemm, P., (1984) The fimA gene encoding the type-1 fimbrial subunit of Escherichia coli. Nucleotide sequence and primary structure of the protein. *Eur J Biochem* **143**: 395-399.
- Klemm, P., (1986) Two regulatory fim genes, fimB and fimE, control the phase variation of type 1 fimbriae in Escherichia coli. *EMBO J* **5**: 1389-1393.
- Kovaleva, L. G., (1976) [Determination of life expectancy of patients with acute leukemia]. *Ter Arkh* **48**: 67-73.
- Kubori, T., Y. Matsushima, D. Nakamura, J. Uralil, M. Lara-Tejero, A. Sukhan, J. E. Galan & S. I. Aizawa, (1998) Supramolecular structure of the Salmonella typhimurium type III protein secretion system. *Science* **280**: 602-605.
- Kuo, M. H. & C. D. Allis, (1999) In vivo cross-linking and immunoprecipitation for studying dynamic Protein:DNA associations in a chromatin environment. *Methods* **19**: 425-433.
- Kutsukake, K., (1994) Excretion of the anti-sigma factor through a flagellar substructure couples flagellar gene expression with flagellar assembly in Salmonella typhimurium. *Mol Gen Genet* **243**: 605-612.
- Kutsukake, K., T. Ikebe & S. Yamamoto, (1999) Two novel regulatory genes, fliT and fliZ, in the flagellar regulon of Salmonella. *Genes Genet Syst* **74**: 287-292.
- Labbe, D., J. Garnon & P. C. Lau, (1997) Characterization of the genes encoding a receptor-like histidine kinase and a cognate response regulator from a biphenyl/polychlorobiphenyl-degrading bacterium, Rhodococcus sp. strain M5. *J Bacteriol* **179**: 2772-2776.
- Lanois, A., G. Jubelin & A. Givaudan, (2008) FliZ, a flagellar regulator, is at the crossroads between motility, haemolysin expression and virulence in the insect pathogenic bacterium Xenorhabdus. *Mol Microbiol* **68**: 516-533.
- Lau, P. C., Y. Wang, A. Patel, D. Labbe, H. Bergeron, R. Brousseau, Y. Konishi & M. Rawlings, (1997) A bacterial basic region leucine zipper histidine kinase regulating toluene degradation. *Proc Natl Acad Sci U S A* **94**: 1453-1458.

- Lawley, T. D., K. Chan, L. J. Thompson, C. C. Kim, G. R. Govoni & D. M. Monack, (2006) Genome-wide screen for Salmonella genes required for long-term systemic infection of the mouse. *PLoS Pathog* **2**: e11.
- Ledeboer, N. A., J. G. Frye, M. McClelland & B. D. Jones, (2006) Salmonella enterica serovar Typhimurium requires the Lpf, Pef, and Tafi fimbriae for biofilm formation on HEp-2 tissue culture cells and chicken intestinal epithelium. *Infect Immun* **74**: 3156-3169.
- Lee, C. A., B. D. Jones & S. Falkow, (1992) Identification of a Salmonella typhimurium invasion locus by selection for hyperinvasive mutants. *Proceedings of the National Academy of Sciences of the United States of America* **89**: 1847-1851.
- Letunic, I., R. R. Copley, B. Pils, S. Pinkert, J. Schultz & P. Bork, (2006) SMART 5: domains in the context of genomes and networks. *Nucleic acids research* **34**: 257-260.
- Lim, S., J. Yun, H. Yoon, C. Park, B. Kim, B. Jeon, D. Kim & S. Ryu, (2007) Mlc regulation of Salmonella pathogenicity island I gene expression via hilE repression. *Nucleic acids research* **35**: 1822-1832.
- Lin, A. Y., C. Y. Lin, C. T. Chen & W. L. Chen, (2008a) Host defense against Salmonella and rotaviral gastroenteritis: a serial study of transcriptional factors and cytokines. *J Microbiol Immunol Infect* **41**: 265-271.
- Lin, D., C. V. Rao & J. M. Slauch, (2008b) The Salmonella SPI1 type three secretion system responds to periplasmic disulfide bond status via the flagellar apparatus and the RcsCDB system. *Journal of bacteriology* **190**: 87-97.
- Lostroh, C. P. & C. A. Lee, (2001a) The HilA box and sequences outside it determine the magnitude of HilA-dependent activation of P(prgH) from Salmonella pathogenicity island 1. *J Bacteriol* **183**: 4876-4885.
- Lostroh, C. P. & C. A. Lee, (2001b) The Salmonella pathogenicity island-1 type III secretion system. *Microbes Infect* **3**: 1281-1291.
- Lucas, R. L. & C. A. Lee, (2001) Roles of hilC and hilD in regulation of hilA expression in Salmonella enterica serovar Typhimurium. *J Bacteriol* **183**: 2733-2745.
- Lucas, R. L., C. P. Lostroh, C. C. DiRusso, M. P. Spector, B. L. Wanner & C. A. Lee, (2000) Multiple factors independently regulate hilA and invasion gene expression in Salmonella enterica serovar typhimurium. *Journal of bacteriology* **182**: 1872-1882.
- Macnab, R. M., (1999) The bacterial flagellum: reversible rotary propellor and type III export apparatus. *J Bacteriol* **181**: 7149-7153.
- Macnab, R. M., (2003) How bacteria assemble flagella. *Annu Rev Microbiol* **57**: 77-100.
- Maeda, Y. T. & M. Sano, (2006) Regulatory dynamics of synthetic gene networks with positive feedback. *J Mol Biol* **359**: 1107-1124.
- Main-Hester, K. L., K. M. Colpitts, G. A. Thomas, F. C. Fang & S. J. Libby, (2008) Coordinate regulation of Salmonella pathogenicity island 1 (SPI1) and SPI4 in Salmonella enterica serovar Typhimurium. *Infect Immun* **76**: 1024-1035.
- Maithreye, R. & S. S. Mande, (2007) Modelling of the regulation of the hilA promoter of type three secretion system of Salmonella enterica serovar Typhimurium. *Systems and synthetic biology* **1**: 129-137.

- Meighen, E. A., (1991) Molecular biology of bacterial bioluminescence. *Microbiol Rev* **55**: 123-142.
- Miller, P. F. & M. C. Sulavik, (1996) Overlaps and parallels in the regulation of intrinsic multiple-antibiotic resistance in *Escherichia coli*. *Mol Microbiol* **21**: 441-448.
- Miller SI, P. P., (2000) *Salmonella* species, including *Salmonella typhi*. In: Bennett JE, Dolin R, editors. Principles of infectious diseases. Philadelphia PA: Churchill Livingstone. pp. 2344-2363.
- Miller, W. G., J. H. Leveau & S. E. Lindow, (2000) Improved gfp and inaZ broad-host-range promoter-probe vectors. *Mol Plant Microbe Interact* **13**: 1243-1250.
- Miller, W. G. & S. E. Lindow, (1997) An improved GFP cloning cassette designed for prokaryotic transcriptional fusions. *Gene* **191**: 149-153.
- Mills, D. M., V. Bajaj & C. A. Lee, (1995) A 40 kb chromosomal fragment encoding *Salmonella typhimurium* invasion genes is absent from the corresponding region of the *Escherichia coli* K-12 chromosome. *Mol Microbiol* **15**: 749-759.
- Mitrophanov, A. Y. & E. A. Groisman, (2008) Positive feedback in cellular control systems. *Bioessays* **30**: 542-555.
- Mitrophanov, A. Y., M. W. Jewett, T. J. Hadley & E. A. Groisman, (2008) Evolution and dynamics of regulatory architectures controlling polymyxin B resistance in enteric bacteria. *PLoS Genet* **4**: e1000233.
- Monod, J., (1966) From enzymatic adaptation to allosteric transitions. *Science* **154**: 475-483.
- Morgan, D. G., C. Owen, L. A. Melanson & D. J. DeRosier, (1995) Structure of bacterial flagellar filaments at 11 Å resolution: packing of the alpha-helices. *J Mol Biol* **249**: 88-110.
- Morgan, E., J. D. Campbell, S. C. Rowe, J. Bispham, M. P. Stevens, A. J. Bowen, P. A. Barrow, D. J. Maskell & T. S. Wallis, (2004) Identification of host-specific colonization factors of *Salmonella enterica* serovar Typhimurium. *Mol Microbiol* **54**: 994-1010.
- Nagai, T., K. Ibata, E. S. Park, M. Kubota, K. Mikoshiba & A. Miyawaki, (2002) A variant of yellow fluorescent protein with fast and efficient maturation for cell-biological applications. *Nat Biotechnol* **20**: 87-90.
- Nambu, T. & K. Kutsukake, (2000) The *Salmonella* FlgA protein, a putative periplasmic chaperone essential for flagellar P ring formation. *Microbiology* **146 (Pt 5)**: 1171-1178.
- Nishino, K., F. F. Hsu, J. Turk, M. J. Cromie, M. M. Wosten & E. A. Groisman, (2006) Identification of the lipopolysaccharide modifications controlled by the *Salmonella* PmrA/PmrB system mediating resistance to Fe(III) and Al(III). *Mol Microbiol* **61**: 645-654.
- Ochman, H., F. C. Soncini, F. Solomon & E. A. Groisman, (1996) Identification of a pathogenicity island required for *Salmonella* survival in host cells. *Proc Natl Acad Sci U S A* **93**: 7800-7804.
- Ohnishi, K., K. Kutsukake, H. Suzuki & T. Lino, (1992) A novel transcriptional regulation mechanism in the flagellar regulon of *Salmonella typhimurium*: an antisigma

- factor inhibits the activity of the flagellum-specific sigma factor, sigma F. *Mol Microbiol* **6**: 3149-3157.
- Old, D. C. & J. P. Duguid, (1970) Selective outgrowth of fimbriate bacteria in static liquid medium. *J Bacteriol* **103**: 447-456.
- Olekhnovich, I. N. & R. J. Kadner, (2002) DNA-binding activities of the HilC and HilD virulence regulatory proteins of *Salmonella enterica* serovar Typhimurium. *J Bacteriol* **184**: 4148-4160.
- Pang, T., Z. A. Bhutta, B. B. Finlay & M. Altwegg, (1995) Typhoid fever and other salmonellosis: a continuing challenge. *Trends Microbiol* **3**: 253-255.
- Pegues, D. A., M. J. Hantman, I. Behlau & S. I. Miller, (1995) PhoP/PhoQ transcriptional repression of *Salmonella typhimurium* invasion genes: evidence for a role in protein secretion. *Mol Microbiol* **17**: 169-181.
- Perez, J. C. & E. A. Groisman, (2007) Acid pH activation of the PmrA/PmrB two-component regulatory system of *Salmonella enterica*. *Mol Microbiol* **63**: 283-293.
- Piknova, L., E. Kaclikova, D. Pangallo, B. Polek & T. Kuchta, (2005) Quantification of *Salmonella* by 5'-nuclease real-time polymerase chain reaction targeted to fimC gene. *Curr Microbiol* **50**: 38-42.
- Prost, L. R. & S. I. Miller, (2008) The *Salmonellae* PhoQ sensor: mechanisms of detection of phagosome signals. *Cell Microbiol* **10**: 576-582.
- Pruss, B. M., X. Liu, W. Hendrickson & P. Matsumura, (2001) FlhD/FlhC-regulated promoters analyzed by gene array and lacZ gene fusions. *FEMS Microbiol Lett* **197**: 91-97.
- Purcell, B. K., J. Pruckler & S. Clegg, (1987) Nucleotide sequences of the genes encoding type 1 fimbrial subunits of *Klebsiella pneumoniae* and *Salmonella typhimurium*. *J Bacteriol* **169**: 5831-5834.
- Randall, L. P. & M. J. Woodward, (2002) The multiple antibiotic resistance (mar) locus and its significance. *Res Vet Sci* **72**: 87-93.
- Rossolini, G. M., P. Muscas, A. Chiesurin & G. Satta, (1993) Analysis of the *Salmonella* fim gene cluster: identification of a new gene (fimI) encoding a fimbrin-like protein and located downstream from the fimA gene. *FEMS Microbiol Lett* **114**: 259-265.
- Saini, S., J. D. Brown, P. D. Aldridge & C. V. Rao, (2008) FliZ is a posttranslational activator of FlhD4C2-dependent flagellar gene expression. *J Bacteriol* **190**: 4979-4988.
- Saini, S., J. R. Ellermeier, J. M. Slauch, C. V. Rao, (2010) The role of coupled positive feedback in the expression of the SPI1 type three secretion system in *Salmonella*. *PLoS Pathog* **In Press**.
- Saini, S., J. A. Pearl & C. V. Rao, (2009) Role of FimW, FimY, and FimZ in regulating the expression of type i fimbriae in *Salmonella enterica* serovar Typhimurium. *J Bacteriol* **191**: 3003-3010.
- Saini, S. & C. V. Rao, (2010) SprB is the molecular link between *Salmonella* pathogenicity island 1 (SPI1) and SPI4. *J Bacteriol* **192**: 2459-2462.
- Santos, R. L., R. M. Tsolis, A. J. Baumler & L. G. Adams, (2003) Pathogenesis of *Salmonella*-induced enteritis. *Braz J Med Biol Res* **36**: 3-12.

- Schechter, L. M., S. M. Damrauer & C. A. Lee, (1999) Two AraC/XylS family members can independently counteract the effect of repressing sequences upstream of the hilA promoter. *Molecular microbiology* **32**: 629-642.
- Schechter, L. M. & C. A. Lee, (2001) AraC/XylS family members, HilC and HilD, directly bind and derepress the Salmonella typhimurium hilA promoter. *Molecular microbiology* **40**: 1289-1299.
- Shea, J. E., M. Hensel, C. Gleeson & D. W. Holden, (1996) Identification of a virulence locus encoding a second type III secretion system in Salmonella typhimurium. *Proc Natl Acad Sci U S A* **93**: 2593-2597.
- Shin, D. & E. A. Groisman, (2005) Signal-dependent binding of the response regulators PhoP and PmrA to their target promoters in vivo. *J Biol Chem* **280**: 4089-4094.
- Smith, R. L. & M. E. Maguire, (1998) Microbial magnesium transport: unusual transporters searching for identity. *Mol Microbiol* **28**: 217-226.
- Stebbins, C. E. & J. E. Galan, (2001) Structural mimicry in bacterial virulence. *Nature* **412**: 701-705.
- Stender, S., A. Friebel, S. Linder, M. Rohde, S. Miold & W. D. Hardt, (2000) Identification of SopE2 from Salmonella typhimurium, a conserved guanine nucleotide exchange factor for Cdc42 of the host cell. *Mol Microbiol* **36**: 1206-1221.
- Strogatz, S. H., (2001) *Nonlinear Dynamics And Chaos: With Applications To Physics, Biology, Chemistry, And Engineering (Studies in nonlinearity) (Paperback)*. Westview Press; 1 edition.
- Sukhan, A., T. Kubori, J. Wilson & J. E. Galan, (2001) Genetic analysis of assembly of the Salmonella enterica serovar Typhimurium type III secretion-associated needle complex. *J Bacteriol* **183**: 1159-1167.
- Swenson, D. L., K. J. Kim, E. W. Six & S. Clegg, (1994) The gene fimU affects expression of Salmonella typhimurium type 1 fimbriae and is related to the Escherichia coli tRNA gene argU. *Mol Gen Genet* **244**: 216-218.
- Tavendale, A., C. K. Jardine, D. C. Old & J. P. Duguid, (1983) Haemagglutinins and adhesion of Salmonella typhimurium to HEp2 and HeLa cells. *J Med Microbiol* **16**: 371-380.
- Temme, K., H. Salis, D. Tullman-Ercek, A. Levskaya, S. H. Hong & C. A. Voigt, (2008) Induction and relaxation dynamics of the regulatory network controlling the type III secretion system encoded within Salmonella pathogenicity island 1. *Journal of molecular biology* **377**: 47-61.
- Teplitski, M., R. I. Goodier & B. M. Ahmer, (2003) Pathways leading from BarA/SirA to motility and virulence gene expression in Salmonella. *J Bacteriol* **185**: 7257-7265.
- Thomas, R., D. Thieffry & M. Kaufman, (1995) Dynamical behaviour of biological regulatory networks--I. Biological role of feedback loops and practical use of the concept of the loop-characteristic state. *Bull Math Biol* **57**: 247-276.
- Tian, X. J., X. P. Zhang, F. Liu & W. Wang, (2009) Interlinking positive and negative feedback loops creates a tunable motif in gene regulatory networks. *Phys Rev E Stat Nonlin Soft Matter Phys* **80**: 011926.

- Tinker, J. K. & S. Clegg, (2000) Characterization of FimY as a coactivator of type 1 fimbrial expression in *Salmonella enterica* serovar Typhimurium. *Infect Immun* **68**: 3305-3313.
- Tinker, J. K. & S. Clegg, (2001) Control of FimY translation and type 1 fimbrial production by the arginine tRNA encoded by fimU in *Salmonella enterica* serovar Typhimurium. *Mol Microbiol* **40**: 757-768.
- Tinker, J. K., L. S. Hancox & S. Clegg, (2001) FimW is a negative regulator affecting type 1 fimbrial expression in *Salmonella enterica* serovar typhimurium. *J Bacteriol* **183**: 435-442.
- van der Velden, A. W., A. J. Baumler, R. M. Tsois & F. Heffron, (1998) Multiple fimbrial adhesins are required for full virulence of *Salmonella typhimurium* in mice. *Infect Immun* **66**: 2803-2808.
- Wallis, T. S. & E. E. Galyov, (2000) Molecular basis of *Salmonella*-induced enteritis. *Mol Microbiol* **36**: 997-1005.
- Wang, S., R. T. Fleming, E. M. Westbrook, P. Matsumura & D. B. McKay, (2006) Structure of the *Escherichia coli* FlhDC complex, a prokaryotic heteromeric regulator of transcription. *J Mol Biol* **355**: 798-808.
- WHO, (2005) Drug-resistant *Salmonella*. In.: WHO Media Center, pp.
- Winson, M. K., S. Swift, P. J. Hill, C. M. Sims, G. Griesmayr, B. W. Bycroft, P. Williams & G. S. Stewart, (1998) Engineering the luxCDABE genes from *Photobacterium luminescens* to provide a bioluminescent reporter for constitutive and promoter probe plasmids and mini-Tn5 constructs. *FEMS microbiology letters* **163**: 193-202.
- Wu, K. & C. V. Rao, (2010) The role of configuration and coupling in autoregulatory gene circuits. *Mol Microbiol* **75**: 513-527.
- Yamamoto, S. & K. Kutsukake, (2006) FliT acts as an anti-FlhD2C2 factor in the transcriptional control of the flagellar regulon in *Salmonella enterica* serovar typhimurium. *J Bacteriol* **188**: 6703-6708.
- Yanagihara, S., S. Iyoda, K. Ohnishi, T. Iino & K. Kutsukake, (1999) Structure and transcriptional control of the flagellar master operon of *Salmonella typhimurium*. *Genes Genet Syst* **74**: 105-111.
- Yeh, K. S., L. S. Hancox & S. Clegg, (1995) Construction and characterization of a fimZ mutant of *Salmonella typhimurium*. *J Bacteriol* **177**: 6861-6865.
- Yeh, K. S., J. K. Tinker & S. Clegg, (2002) FimZ binds the *Salmonella typhimurium* fimA promoter region and may regulate its own expression with FimY. *Microbiol Immunol* **46**: 1-10.
- Yokoseki, T., K. Kutsukake, K. Ohnishi & T. Iino, (1995) Functional analysis of the flagellar genes in the fliD operon of *Salmonella typhimurium*. *Microbiology* **141 (Pt 7)**: 1715-1722.
- Yonekura, K., S. Maki-Yonekura & K. Namba, (2003) Complete atomic model of the bacterial flagellar filament by electron cryomicroscopy. *Nature* **424**: 643-650.
- Yonekura, K., S. Maki, D. G. Morgan, D. J. DeRosier, F. Vonderviszt, K. Imada & K. Namba, (2000) The bacterial flagellar cap as the rotary promoter of flagellin self-assembly. *Science* **290**: 2148-2152.

- Zhou, D., L. M. Chen, L. Hernandez, S. B. Shears & J. E. Galan, (2001) A Salmonella inositol polyphosphatase acts in conjunction with other bacterial effectors to promote host cell actin cytoskeleton rearrangements and bacterial internalization. *Mol Microbiol* **39**: 248-259.
- Zhou, D. & J. Galan, (2001) Salmonella entry into host cells: the work in concert of type III secreted effector proteins. *Microbes and infection / Institut Pasteur* **3**: 1293-1298.
- Zhou, D., M. S. Mooseker & J. E. Galan, (1999a) An invasion-associated Salmonella protein modulates the actin-bundling activity of plastrin. *Proc Natl Acad Sci U S A* **96**: 10176-10181.
- Zhou, D., M. S. Mooseker & J. E. Galan, (1999b) Role of the *S. typhimurium* actin-binding protein SipA in bacterial internalization. *Science* **283**: 2092-2095.

Curriculum Vitae

Education	<p>Ph.D., Chemical and Biomolecular Engineering – August 2010 University of Illinois at Urbana-Champaign, Urbana, IL Dissertation: “Coordinated regulation of the flagellar, <i>Salmonella</i> Pathogenicity Island 1 (SPI1) and Type I fimbriae gene circuits in <i>Salmonella enterica</i> serovar Typhimurium”</p> <p>M.S., Chemical and Biomolecular Engineering – October 2008 University of Illinois at Urbana-Champaign, Urbana, IL Thesis: “Characterization of FliZ as an FlhD₄C₂-dependent activator of flagellar genes in <i>Salmonella enterica</i> serovar <i>Typhimurium</i>”</p> <p>B.Tech., Chemical Engineering – May 2005 Indian Institute of Technology, Delhi, India Thesis: “Heat and Pressure drop studies in helical tube-in-tube heat exchangers”</p>
Research experience	<p>Graduate Research Assistant – August 2005 to date University of Illinois at Urbana-Champaign, Urbana, IL Research advisor: Dr. Christopher V. Rao</p> <p>Undergraduate researcher – January 2003 to August 2004 Indian Institute of Technology Delhi, India Research advisor: Dr. Ashok N. Bhaskarwar</p> <p>Undergraduate researcher – 2004 to 2005 Indian Institute of Technology Delhi, India Research advisor: Dr. Krishna D. P. Nigam</p>
Teaching Assistant	<p>Introduction to Chemical Engineering – Spring 2010</p> <p>Hidden World of Engineering – Fall 2009</p> <p>Mass Transfer Operations – Spring 2009, 2008, 2007</p> <p>Process Control and Dynamics – Fall 2008, 2007, 2006</p>

- Publications** Saini, S., Slauch, J.M., Aldridge, P.D., and Rao, C.V., “The role of crosstalk in regulating the dynamic expression of the flagellar, *Salmonella* pathogenicity island 1 (SPI1), and type I fimbrial genes” *Journal of Bacteriology*, *In Review*.
- Aldridge, C., Poonchareon, K., Saini, S., Ewen, T., Soloyva, A., Rao, C.V., Imada, K., Minamino, T., and Aldridge, P.D. “The interaction dynamics of a negative feedback loop regulates flagellar number in *Salmonella enterica* serovar Typhimurium” (2010) *Molecular Microbiology In Review*.
- Saini, S., Ellermeier, J.R., Slauch, J.M., Rao, C.V., “The role of coupled positive feedback in the expression of the SPI1 type three secretion system in *Salmonella*” *PLoS Pathogens In Review*.
- Saini, S., Rao, C.V., “SprB is the molecular link between *Salmonella* Pathogenicity Island 1 (SPI1) and SPI4” *Journal of Bacteriology* (2010) 192(9):2459-62.
- Saini S., Pearl J.A., Rao C.V. “Role of FimW, FimY, and FimZ in regulating the expression of type i fimbriae in *Salmonella enterica* serovar Typhimurium.” *Journal of Bacteriology* (2009) 191(9):3003-10.
- Brown J.D., Saini S., Aldridge C., Herbert J., Rao C.V., Aldridge P.D. “The rate of protein secretion dictates the temporal dynamics of flagellar gene expression.” *Molecular Microbiology* (2008) 70(4):924-37.
- Saini S., Brown J.D., Aldridge P.D., Rao C.V. “FlhZ Is a posttranslational activator of FlhD4C2-dependent flagellar gene expression.” *Journal of Bacteriology* (2008) 190(14):4979-88.
- Kumar V., Saini S., Sharma M., Nigam K.D.P. “Pressure drop and heat transfer study in tube-in-tube helical heat exchanger.” *Chemical Engineering Science* (2006) 61(13): 4403-4416.
- Presentations** Saini, S., Rao C.V., “Coordinated regulation of the flagellar, SPI1, and type I fimbriae networks in *Salmonella*” Poster, American Institute of Chemical Engineers Annual Meeting, Nashville, TN – 2009.
- Chubiz, L.M., Saini, S., Rao, C.V., “Convergent Transcription and Transcriptional Interference as a regulatory mechanism in the rhamnose regulon in *Escherichia coli*” Presentation, American Institute of Chemical Engineers Annual Meeting, Nashville, TN – 2009

Saini, S., Aldridge, P.D., Rao, C.V., "Role of feedback in dictating flagellar gene expression dynamics" Presentation, American Institute of Chemical Engineers Annual Meeting, Nashville, TN – 2009

Saini, S., Aldridge, P.D., Rao, C.V., "Role of positive feedback in dictating flagellar gene expression dynamics in *Salmonella*" Poster, Foundations of Systems Biology and Engineering (FOSBE) – Colorado, DN – 2009

Saini, S., Slauch, J.M., Rao, C.V., "Dynamics of SPI1 gene expression in *Salmonella typhimurium*" Presentation, American Society of Microbiology Annual Meeting, Philadelphia, PA – 2009

Saini, S., Slauch, J.M., Rao, C.V., "Role of positive feedback and stochasticity in dictating SPI1 gene expression in *Salmonella typhimurium*" Poster, American Society of Microbiology Annual Meeting, Philadelphia, PA – 2009

Saini, S., Aldridge, P.D., Rao, C.V., "Characterization of FlhZ as a flagellar and SPI1 gene activator in *Salmonella typhimurium*" Poster, Bacterial Locomotion and Signal Transduction (BLAST), Cuernavaca, Mexico – 2009

Honors

Food and Pharmaceutical Division Poster Award – 2009

American Society of Chemical Engineers (AIChE) General Meeting, Nashville, TN

Drickamer Fellowship – 2009-2010

Chemical & Biomolecular Engineering, University of Illinois at Urbana-Champaign, Urbana, IL

Girdhari Tikku Memorial Award – 2009

Center for South Asian and Middle Eastern Studies (CSAMES), University of Illinois at Urbana-Champaign, Urbana, IL

Hanratty Travel Award – 2009

Chemical & Biomolecular Engineering, University of Illinois at Urbana-Champaign, Urbana, IL

Richard & Mary Finkelstein Travel Award - 2009

American Society of Microbiology (ASM) General Meeting, Philadelphia, PA

Excellence in Teaching Award – 2007-2008

School of Chemical Sciences, University of Illinois at Urbana-Champaign, Urbana, IL